

Beyond Standard Model Physics: A non-SUSY Grand Unification perspective

By

Ram Lal Awasthi

PHYS08200704001

Harish-Chandra Research Institute, Allahabad

*A thesis submitted to the
Board of Studies in Physical Sciences*

*In partial fulfillment of requirements
for the Degree of*

DOCTOR OF PHILOSOPHY

of

HOMI BHABHA NATIONAL INSTITUTE



July, 2014

STATEMENT BY AUTHOR

This dissertation has been submitted in partial fulfillment of requirements for an advanced degree at Homi Bhabha National Institute (HBNI) and is deposited in the Library to be made available to borrowers under rules of the HBNI.

Brief quotations from this dissertation are allowable without special permission, provided that accurate acknowledgement of source is made. Requests for permission for extended quotation from or reproduction of this manuscript in whole or in part may be granted by the Competent Authority of HBNI when in his or her judgment the proposed use of the material is in the interests of scholarship. In all other instances, however, permission must be obtained from the author.

Ram Lal Awasthi

DECLARATION

I, hereby declare that the investigation presented in the thesis has been carried out by me. The work is original and has not been submitted earlier as a whole or in part for a degree/diploma at this or any other Institution/University. Whenever contributions of others are involved, every effort is made to indicate this clearly, with due reference to the literature and acknowledgement of collaborative research and discussions.

This work was done under guidance of Professor Sandhya Choubey at Harish-Chandra Research Institute, Allahabad.

Ram Lal Awasthi

List of Publications arising from the thesis

Journal

1. “Inverse Seesaw Mechanism in Nonsupersymmetric SO(10), Proton Lifetime, Nonunitarity Effects, and a Low-mass Z' Boson”, Ram Lal Awasthi and Mina Ketan Parida, Phys. Rev. D, **2012**, Vol 86, 093004.
2. “Neutrino masses, dominant neutrinoless double beta decay, and observable lepton flavor violation in left-right models and SO(10) grand unification with low mass W_R, Z_R bosons”, Ram Lal Awasthi, Mina Ketan Parida and Sudhanwa Patra, Journal of High Energy Physics, **2013**, Vol 1308, 112.
3. “Proton decay and new contribution to $0\nu\beta\beta$ decay in SO(10) with low-mass Z' boson, observable $n-\bar{n}$ oscillation, lepton flavor violation, and rare kaon decay”, Mina Ketan Parida, Ram Lal Awasthi and Pradip K. Sahu, Journal of High Energy Physics, **2015**, Vol 1501, 045.

Ram Lal Awasthi

To my preceptors

Dr. Virelil J. Menon,

My Father

&

My Friends

ACKNOWLEDGEMENTS

I would like to thank GOD, if any, for being with me in all my happiness and dismay. I thank Prof. Sandhya Choubey for her guidance and continuous support through all these years. I thank Prof. Mina Ketan Parida for his encouragement, enthusiastic discussion and trust on my capabilities and scientific attitude. This thesis is an outcome of the work done in strong collaboration with him. I thank Prof Goran Senjanovic, Prof. Borut Bajc and Prof. Chanranjit Aulakh for teaching the basics of the grand unification, from where large fraction of my understanding developed. Interactions with Prof Anjan Joshipura, Joydeep, Ketan and Sudhanwa on the subject have been wonderful and enlightening.

I express my deep gratitude to Prof. Ashoke Sen, Raj Gandhi, Sudhakar Panda, Rajesh Gopakumar, Dileep Jatkar, Satchidananda Naik, V. Ravindran, Tapas Kumar Das, Sandhya Choubey, Justin David, Asheshkrishna Datta and Andreas Nyfeler for giving me wonderful courses on basic physics. Interactions with Santosh, Manimala, Trilochan, Shailesh, Sanjoy, Nishita, Roji, Utkarsh, Uttam, Krishna, Abhishek, Archana, Karam Dev, Pradeep, Sanjay, Bhavin, Ujjal, Saurabh, Ashutosh, Siddharth, Rishu, Anitha, Charanjit, Ila and other senior and junior fellows on physics, mathematics and beyond played major role in shaping my current state of mind. I thank Prof. A. Raychaudhuri and Prof. J. K. Bhattacharjee for giving me an opportunity to work at one of the premier research institutes in India.

I thank the administration of HRI, for their help and support. The administration here has a distinctive image of a human resource, that is not only helpful and cooperative, it actually gives you a feel of being at home among family. I specially thank Ravindra Singh, P. B. Chakraborty, Yashpal Bhadauriya, Ajay Srivastava, Umakant Dwivedi, Dharmendra Malhotra, Amit Roy, Raj Gulati, Archana Tandon, Seema Agrawal, Amit Kulve, Rachana, Shweta, Chandan, Rajiv, Anoop, Shiv Kumar Pathak, Pradeep, and Saadhu for their help and support.

Staying connected with the social world outside HRI wouldn't have been possi-

ble without Ripunjay, Amit, Dinesh, Manish, Girdhar, Sheshnarayan, Neha, Vijay, Satyendra, Ajay, Rajesh, Devendra, Ankit, Shishir, Amit Goyal, Bala, Yashwant, Shashwat, Uday, Subodh, Bhaskar, Niraj, Mayank, Paritosh, Brajraj, Pawan, Rajnikant and many other friends. I particularly thank to Ripunjay, Amit and Dinesh for their continuous love and support. The unconditional love, care, affection and support of my mother and my wife Minakshi have been the most important ingredient of my life.

I specially thank Rajarshi, Vikas and Jaban for being with me, guiding me to the righteousness and understanding me to the depth of my heart. Without them my survival at HRI wouldn't have been possible. Rajarshi, Vikas and Ripunjay have been the source of my conscience. Jaban have been the monitor and critic on my insolences.

Contents

SYNOPSIS	i
LIST OF FIGURES	vii
LIST OF TABLES	xiii
1 Introduction	1
2 Standard Model and beyond	7
2.1 Standard Model of particle physics	7
2.2 SSB and Higgs Mechanism	11
2.3 Excellencies of Standard Model	13
2.4 Deficiencies of Standard Model	14
2.5 Evolution of gauge couplings and unification	17
2.5.1 SM gauge coupling running	17
2.5.2 MSSM gauge coupling running	20
3 Grand Unified Theory	23
3.1 Motivations and Constraints	23
3.2 $SU(5)$ GUTs	24
3.3 $SO(10)$ GUTs	28
3.4 Majorana neutrinos and seesaw mechanism	33

4	LHC testable inverse seesaw in non-SUSY $SO(10)$	37
4.1	The Model	38
4.2	Gauge coupling unification and proton decay	39
4.2.1	Unification in minimal models	39
4.2.2	Unification in simple model extensions	41
4.3	Inverse seesaw mechanism	42
4.4	Fermion masses and Determination of M_D	46
4.4.1	Determination of M_D	47
4.5	Non-unitarity deviations and constraining M	48
4.6	Estimating CP -violation and Lepton flavor violation	50
4.7	Discussion	56
5	Neutrinoless double beta decay in $SO(10)$ model	61
5.1	Low scale left-right gauge theory and extended seesaw	62
5.1.1	The Model	62
5.1.2	Extended inverse seesaw	63
5.1.3	Neutrino parameters and non-unitarity constraints on M	64
5.1.4	Determination of μ_S from fits to neutrino oscillation data	67
5.2	Amplitudes for $0\nu 2\beta$ decay and effective mass parameters	68
5.2.1	W_L^- - W_L^- mediation	69
5.2.2	W_R^- - W_R^- mediation	71
5.2.3	W_L^- - W_R^- mediation	72
5.2.4	Doubly Charged Higgs contribution	72
5.2.5	Nuclear matrix elements and normalized effective mass parameters	73
5.3	Numerical estimation of effective mass parameters	75
5.3.1	Nearly standard contribution	75
5.3.2	Dominant non-standard contributions	76
5.4	Estimations on lepton flavor violating decays and J_{CP}	78

5.4.1	Branching ratio	79
5.4.2	CP -violation due to non-unitarity	80
5.5	Implementation in $SO(10)$	82
5.5.1	Symmetry breaking chain	82
5.5.2	Gauge coupling unification	83
5.5.3	Physical significance of mass scales	86
5.5.4	Importance of G_{224D} intermediate symmetry	86
5.5.5	Determination of Dirac neutrino mass matrix	87
5.5.6	Suppressed induced contribution to ν - S mixing	98
6	Proton, rare kaon and $0\nu 2\beta$-decays, light Z', n-\bar{n} oscillation, LFV	99
6.1	Precision gauge coupling unification and mass scales	100
6.2	Low mass Z' boson and proton decay	102
6.2.1	Low-mass Z' boson	102
6.2.2	Proton lifetime for $p \rightarrow e^+ \pi^0$ decay	103
6.2.3	GUT scale and proton life-time reduction through bi-triplet scalar	104
6.2.4	Estimation of GUT-threshold effects	105
6.3	Rare kaon decay and n - \bar{n} oscillation	107
6.3.1	Rare kaon decay $K_L \rightarrow \mu \bar{e}$	107
6.3.2	Neutron-antineutron oscillation	110
6.4	Dirac neutrino mass matrix, neutrino parameter fitting and lepton flavor violation	112
6.5	Contributions to neutrinoless double beta decay in $W_L - W_L$ channel	114
6.5.1	Half-life and bound on sterile neutrino mass	119
6.6	Rectifying the large τ_p problem of low energy LR model using light bi-triplet mass	124
7	Conclusion	127

A	Few remarks on $SU(n)$, and $SO(10)$ Algebra	133
A.1	Anomalies	133
A.1.1	Adler Anomalies for a $SU(n)$ representation	133
A.2	Quadratic Casimir and Dynkin index invariants in $SU(n)$	135
A.3	Lorentz group	136
A.3.1	Lorentz scalar and vector constructs	138
A.4	$SO(2n)$ Algebra	138
A.4.1	$SO(2n)$ spinor representation	140
A.4.2	Bilinears and invariant constructs	142
B	Decomposition of representations and beta coefficients	145
B.1	One and two loop beta function coefficients for RG evolution of gauge couplings	145
B.2	Decomposition of $SO(10)$ irreducible representations	147
C	Renormalization group evolution for Model-I	153
D	Neutrino mass and mixings in inverse seesaw	157
D.1	Diagonalization of inverse and extended inverse seesaw	157
D.2	Complete diagonalization and physical neutrino masses	163
E	Estimation of experimental and GUT-threshold uncertainties on the unification scale	165
E.1	Analytic formulas	165
E.2	Uncertainties due to experimental errors in $\sin^2 \theta_W$ and α_s	167
E.3	Uncertainties in M_U with vanishing correction on M_P	168
	Bibliography	169

Synopsis

The quest of a decent quantum field theoretic framework to describe the fundamental behavior of the newly discovered particles and their strange interactions, during the first half of the 20th century, was accomplished with the introduction of Standard Model (SM) of particle physics. The SM is based on the locale gauge symmetry of the Lie algebra $SU(2)_L \otimes U(1)_Y \otimes SU(3)_C$. This has been an extremely successful theory describing three of the four fundamental interactions known so far, namely, weak, electromagnetic and strong interaction. The theory has been experimentally verified to the large accuracy in various collider experiments such as Large Electron Positron Collider (LEP) at CERN in Europe, SLC at Stanford University in USA, Tevatron at Fermilab in USA, HERA at DESY in Germany, PEP-II B-factory at Stanford University, KEKB at Tsukuba in Japan, and Large Hadron Collider (LHC) at CERN. All the particles predicted by the SM, since its birth in 1967–68, namely: τ (1975), c (1974), b (1977), t (1995), gluons (1979), W and Z bosons (1983), ν_τ (2000) and Higgs (2012) scalar, have not only been confirmed but also fit perfectly in the model framework. On top of it, SM is a renormalizable theory. The anomalies generated by the quark sector are cancelled with the anomalies in lepton sector. Hence, though accidentally, SM happens to be an anomaly free theory.

Despite the fact that SM has unravelled the gauge origin of fundamental forces and the structure of universe while successfully confronting numerous experimental tests, it has various limitations. The experimental evidence of tiny neutrino masses compared to charged leptons and quarks, and their peculiar mixing relating flavor to mass basis raises the fundamental issue on the origin of these masses as well as the nature of the neutrinos: Dirac or Majorana. It does not contain any particle which can describe dark matter observed in the universe. The baryonic asymmetry of the universe remains unexplained. The mass of a scalar field receives large radiative corrections due to quadratic divergences. Therefore, the tree-level mass of the Higgs

field and the loop contributions of the cut-off (Planck or GUT) order must cancel to a very high precision in order of the weak scale, known as ‘hierarchy or naturalness’ problem. This problem is often considered as a guideline for BSM physics and has been tried to evade in certain theories like supersymmetry (SUSY). It also does not impose any constraint on the masses or mixing of fermions and they exhibit strong hierarchical pattern, called flavor problem. The peculiar selection of nature to this particular gauge structure and the strange but simple charge quantization still remain unexplained. Also, it does not incorporate the quantum description of gravity. All the above mentioned problems are the open questions to the SM and they lead to a trivial conclusion that the SM is a low energy remnant of a bigger framework at higher energies. Many neutrino, flavor, decay and collider experiments have-been/are-being performed to address these issues, and/or to see any other signature of physics beyond SM.

The smallness of neutrino masses is usually accounted by seesaw mechanism. There are many way to incorporate it in a BSM theory. The three conventional seesaw mechanism namely, type-I, type-II and type-III seesaw are achieved by adding new SM fermionic singlets, a scalar $SU(2)_L$ triplet and fermionic $SU(2)_L$ triplets, respectively. The underlying quark-lepton symmetry in $SO(10)$ forces canonical (type-I) and type-II seesaw scales close to GUT scale, making them inaccessible to any direct test. A number of other interesting neutrino mass generation mechanisms including inverse seesaw, radiative seesaw, double seesaw, linear seesaw, scalar-triplet seesaw, have been suggested and some of them are also experimentally verifiable.

The SUSY extensions of SM, with SUSY restoration at TeV energy scale, solves the gauge hierarchy problem and unifies the gauge couplings around $10^{16.25}$ GeV. The Minimal Supersymmetric Standard Model (MSSM) can be further extended to incorporate the tiny masses of neutrinos and their mixing through seesaw paradigm. In models with R -parity conservation, the lightest SUSY particle (LSP) is stable and weakly interacting massive particle (WIMP) which can be a possible candidate of cold dark matter of universe. Hence, the SUSY grand unification theories (SUSY GUTs) as an extension of these models provide a very attractive framework for representing particles and forces. An evidence of SUSY at the Large Hadron Collider (LHC) would be a land-mark discovery which would certainly change the future course of physics. But, in the absence of any evidence of SUSY so far, it is worth while to explore new physics prospects of non-SUSY GUTs and, particularly, those based upon $SO(10)$ which has grown in popularity as it unifies all fermions of one generation including the right-handed (RH) neutrino into a single spinorial representation. It

provides spontaneous origins of P (= Parity) and CP -violations. Most interestingly, in addition to predicting the right order of tiny neutrino masses, it can explain all fermion masses including large mixing angles in the neutrino sector. In fact neither seesaw mechanism, nor grand unification require SUSY per se. Although gauge couplings automatically unify in the MSSM, and they fail to unify in the minimal standard model in one-step breaking of non-SUSY $SU(5)$ or $SO(10)$, they do unify once intermediate symmetries are included to populate the grand desert in non-SUSY $SO(10)$. In addition, with intermediate gauge symmetries $SO(10)$ also predicts signals of new physics which can be probed at low or accelerator energies.

In the context of non-SUSY $SO(10)$ framework in the work [1] we explored the prospects of inverse seesaw mechanism. This has the potential to be experimentally verified because of the low scale at which it can operate. Its implementation requires additional fermionic $SO(10)$ singlets which introduces a new mass scale μ_S in the theory. The TeV-scale seesaw requires μ_S to be small. Under the consideration of exact lepton number conservation, a global $U(1)$, symmetry $\mu_S \rightarrow 0$. This guarantees left-handed neutrinos to remain massless. The non-SUSY $SO(10)$ breaks to left-right, $SU(2)_L \times SU(2)_R \times U(1)_{(BL)} \times SU(3)_C (\equiv G_{2213})$, symmetry at intermediate scale which further breaks to $SU(2)_L \times U(1)_R \times U(1)_{(BL)} \times SU(3)_C (\equiv G_{2113})$ gauge symmetry at TeV scale. The actual parity restoration scale is high, W_R^\pm are at intermediate scale. The low Z' boson masses and the associated non-unitarity effects of the TeV-scale inverse seesaw are the remnant of high scale left-right symmetry. The model achieves precision gauge coupling unification, and predicts a low mass Z' making them suitable for implementation of TeV-scale inverse seesaw mechanism. The model can be testified through its predictions on observable non-unitarity effects and additional contributions to lepton flavor violations. Another testing ground for the model could be through the $SO(10)$ prediction on gauge boson mediated proton decay on which dedicated search experiments are ongoing at Super-K. The model predicts substantial non-unitarity effects and lepton flavor violating (LFV) decays accessible to ongoing experimental searches for $\tau \rightarrow e\gamma$, $\tau \rightarrow \mu\gamma$, and $\mu \rightarrow e\gamma$. The quark-lepton symmetric origin of the Dirac neutrino mass matrix is found to play a crucial role in enhancing non-unitarity effects leading to enhanced LFV and leptonic CP -violation. The LFV is predicted to be only few order less than the present experimental bound and accessible to ongoing searches.

Regarding other possibilities of inverse seesaw motivated non-SUSY $SO(10)$, we find that the minimal single-step breaking scenario to the TeV scale gauge symmetry, $SO(10) \rightarrow G_{2113}$, is ruled out by renormalization group and coupling uni-

fication constraints. The two-step breaking chains, $SO(10) \rightarrow G_{224D} \rightarrow G_{2113}$, $SO(10) \rightarrow G_{214} \rightarrow G_{2113}$ and $SO(10) \rightarrow G_{224} \rightarrow G_{2113}$ are ruled out by the existing lower bound on proton lifetime $\tau_p = 1.01 \times 10^{34}$ years. Here we have used $SU(2)_L \times U(1)_R \times SU(4)_C \equiv G_{214}$ and $SU(2)_L \times SU(2)_R \times SU(4)_C \equiv G_{224}$. The G_{224D} is the Pati-Salam group (G_{224}) with D -parity.

In the work [2] we have studied a different class of left-right (LR) models having the property of high scale parity restoration but with minimal extension to accommodate experimentally testable extended inverse seesaw mechanism. The light neutrino masses are governed by inverse seesaw formula. The masses of W_R^\pm and Z' gauge bosons, and RH neutrinos could be of $\mathcal{O}(\text{TeV})$ which are also directly accessible to accelerator tests. The model predicts quite dominant contributions to neutrinoless double beta ($0\nu 2\beta$) decay rate in $W_L^- - W_L^-$ channel through relatively light sterile neutrino exchanges. Observation of $0\nu 2\beta$ is expected to determine whether neutrinos are Majorana fermions. The non-unitarity effects and LFV decay predictions are almost same as in the previous study. Finally we show how such a TeV scale LR gauge theory emerges from a non-SUSY $SO(10)$ grand unification framework. Parity is restored at high scales where the D -parity in Pati-Salam symmetry breaks. The grand unified theory also predicts experimentally observable neutron-antineutron ($n - \bar{n}$) oscillation and rare kaon decay branching ratio, $\text{Br}(K_L \rightarrow \mu e)$, mediated by lepto-quark gauge boson of $SU(4)_C$, although proton lifetime is found to be beyond the accessible limit of ongoing experiments. In addition to non-unitarity and LFV, the Dirac neutrino mass matrix is also found to play a crucial role in enhancing $0\nu 2\beta$ decay rate.

The symmetry breaking chain of the model is found to require $SU(2)_L \times SU(2)_R \times SU(4)_C \times D (g_{2L} = g_{2R}) \equiv G_{224D}$ gauge symmetry at the highest intermediate scale which eliminates the possible presence of triangular geometry of gauge couplings around the GUT scale. This in turn determines the unification mass precisely, modulo threshold effects, at the meeting point of two gauge coupling constant lines. The other advantage of this symmetry is that it pushes most of the larger sized sub-multiplets down to the parity restoring intermediate scale reducing the size of GUT-threshold effects on the unification scale and proton lifetime while the GUT-threshold effects on $\sin^2 \theta_W$ or M_P have exactly vanishing contribution.

In the work [3] we show that even though only a TeV scale Z' is detected at LHC, most of the observable predictions of [2] are still applicable except that W_R^\pm boson masses are beyond the currently accessible LHC limit. So effectively follow the strategy which we had adopted in our previous work [1,2]. Low energy signature

of lepto-quark gauge bosons is also predicted through rare kaon decay $K_L \rightarrow \mu\bar{e}$. The model predictions include (i) dominant contribution to $0\nu 2\beta$ rate in the $W_L^- W_L^-$ channel leading to lower bound on the lightest sterile fermion mass $m_{S_1} \geq 14 \pm 4$ GeV, (ii) unitarity-violating contributions to branching ratios for lepton flavor violating (LFV) decays, (iii) leptonic CP -violation due to non-unitarity effects, (iv) experimentally verifiable $|\Delta(B-L)| = 0$ proton decay modes such as $\tau_p(p \rightarrow e^+\pi^0) \simeq 1.05 \times 10^{35 \pm 1.0 \pm 0.35}$ yrs, (v) lepto-quark gauge-boson mediated rare kaon decay with $\text{Br}(K_L \rightarrow \mu\bar{e}) \simeq 10^{-11} - 10^{-12}$, and (vi) observable $n-\bar{n}$ -oscillation mixing time $10^8 - 10^{10}$ seconds. In sharp contrast to the earlier model [2], in the present model we predict proton lifetime to be accessible to ongoing search experiments.

Even though all the grand unifications $SO(10)$ models we studied are non supersymmetric, their LFV branching ratio predictions are of same order as of SUSY $SO(10)$ model with TeV scale LR symmetry. These predictions are not very far from experimental probe. Even for the Dirac phase $\delta = 0, \pi, 2\pi$ of the PMNS matrix, the models predict the CP -violation parameter $J \simeq 10^{-5}$ due to non-unitarity effects. We have explicitly displayed the large effective mass parameter for $0\nu 2\beta$ decay in [2] and [3] due to sterile neutrino exchange in $W_L^- W_L^-$ channel. The prediction of the lightest sterile neutrino mass in [3] can be explained in model [2] as well. The lower bound $m_{S_1} \sim 14 \pm 4$ GeV is imposed by the current experimental limits on the half life. In these models Heidelberg Moscow results can be explained even if light neutrinos are not necessarily quasi-degenerate. The proton-lifetime predictions in the models [1] and [3] are found within the reach of ongoing and future experiments, like Super-K and Hyper-K. While the model studied in [1] claims the recognition of minimal $SO(10)$ GUT; the large $0\nu 2\beta$ decay, $n-\bar{n}$ oscillation and rare kaon decay predictions are additional future prospects of study in [2] and [3] which are different from the popular collider search.

LIST OF FIGURES

2.1	One loop correction to gauge propagator. Dots correspond to ghost and gauge fixing terms.	18
2.2	Standard Model Gauge coupling running.	19
2.3	Minimal Supersymmetric Standard Model Gauge coupling running.	20
3.1	The most popular and physically viable breaking chains of $SO(10)$ down to the SM [52, 58, 126–129].	29
4.1	Gauge coupling unification in Model-I with two loop values $M_{GUT} = 10^{15.53}$ GeV and $M_R^+ = 10^{11.15}$ GeV with low mass Z' gauge boson at $M_R^0 \sim 1$ TeV.	40
4.2	Variation of proton lifetime as a function of color octet mass in simple extensions of Model-I (double dot-dashed line) and Model-I' (dashed line). The horizontal solid line with error band is the prediction of the minimal Model-I while the horizontal dot-dashed line is the experimental lower bound for $p \rightarrow e^+ \pi^0$	42
4.3	The contours of M_1 in the plane of M_2 and M_3 . The solid curves in the diagram represent M_3 dependence of M_2 for fixed values of M_1 using eq. (4.38). The brightest top-right corner suggests that lightest M_1 may exist for largest values of M_2 and M_3	51
4.4	Variation of the third generation RH neutrino mass M_3 as a function of first or second generation neutrino mass M_1 or M_2 in the partially degenerate case for which $M_1 = M_2$	51
4.5	Loop factor vs masses of heavy RH or sterile neutrino.	53

5.1	The contours of M_1 in the plane of M_2 and M_3 . The solid curves in the diagram represent M_3 dependence of M_2 for fixed values of M_1 using eq. (5.13). The brightest top-right corner suggests that lightest M_1 may exist for largest values of M_2 and M_3	66
5.2	Feynman diagrams for neutrinoless double beta decay ($0\nu 2\beta$) contribution with virtual Majorana neutrinos $\hat{\nu}_i$, \hat{S}_i , and \hat{N}_{Ri}^C along with the mediation of two W_L -bosons.	69
5.3	Feynman diagram for neutrinoless double beta decay contribution by W_L^- - W_L^- mediation and by the exchange of virtual sterile neutrinos (S). The Majorana mass insertion has been shown explicitly by a cross.	70
5.4	Same as Fig. 5.2 but with W_R - W_R mediation.	71
5.5	Mixed Feynman diagram with W_L - W_R mediation; left-panel is for λ -mechanism and right-panel is for η -mechanism as defined in ref. [254–256] and discussed in the text.	72
5.6	Variation of effective mass parameters with lightest neutrino mass. The standard contributions are shown by dashed-green (pink) colored lines for NH (IH) case. The non-standard contribution with W_L^- - W_L^- mediation and sterile neutrino exchanges is shown by the upper blue solid line whereas the one with W_L^- - W_R^- mediation and sterile neutrino exchanges is shown by the lower black solid line.	76
5.7	Variation of effective mass parameters with lightest neutrino mass. The standard contributions are shown by dashed-green (pink) colored lines for NH (IH) case. The non-standard contribution with W_L^- - W_L^- mediation and sterile neutrino exchanges is shown by the upper blue solid line whereas the one with W_L^- - W_R^- mediation and sterile neutrino exchanges is shown by the lower black solid line.	77
5.8	Predictions of non-standard contributions to effective mass parameter with W_L^- - W_L^- mediation and sterile neutrino exchange for $M = (120, 250, 1664.9)$ GeV (top solid line), $M = (250, 250, 1663.3)$ GeV (middle solid line), and $M = (250, 400, 1626.1)$ GeV (bottom solid line) keeping $M_N = (5, 5, 10)$ TeV fixed and for M_D as in eq. (5.11).	79
5.9	CP -violation for the full allowed range of leptonic Dirac phase δ_{CP} . The left-panel corresponds to degenerate values of M with $M_1 = M_2 = M_3 \simeq 1604.442$ GeV, and the right panel is due to non-degenerate M with $M_1 = 9.7$ GeV, $M_2 = 115.2$ GeV, and $M_3 = 2776.5$ GeV.	81

5.10	Two loop gauge coupling unification in the $SO(10)$ symmetry breaking chain described in the text. These results are also valid with G_{224D} symmetry near GUT-Planck scale.	85
5.11	Estimations of effective mass parameter for $0\nu 2\beta$ decay in the W_L^- - W_L^- channel with sterile neutrino exchanges shown by top, middle, and bottom horizontal lines. The RH neutrino masses and the Dirac neutrino masses are derived from fermion mass fits and the sterile neutrino masses have been obtained through M values consistent with non-unitarity constraints as described in the text.	93
5.12	Same as Fig. 5.10 but with the scalar sub-multiplet $\xi(2, 2, 15)$ under Pati-Salam group at $M_\xi = 10^{13.2}$ GeV.	96
6.1	The gauge coupling unification for the breaking scheme given in eq. (6.1) and the scalar particle spectrum as given in Tab. B.3.	102
6.2	Same as Fig. 6.1 but with the Higgs scalar bi-triplet acquiring mass $M_{(3,3,1)} = 9 \times 10^{13}$ GeV.	104
6.3	Feynman diagram for rare kaon decays $K_L^0 \rightarrow \mu^\pm e^\mp$ mediated by a heavy lepto-quark gauge boson of $SU(4)_C$ gauge symmetry.	108
6.4	Graphical representation of the method for numerical solution of the lower bound on M_C . The horizontal lines are the RHS of the inequality (6.23) whereas the curve represents the LHS. The colored horizontal bands are due to uncertainties in the input parameters.	110
6.5	Feynman diagrams for neutron-antineutron oscillation mediated by two $\Delta_{u^c d^c}$ and one $\Delta_{d^c d^c}$ di-quark Higgs scalars (left-panel), and two $\Delta_{d^c d^c}$, one $\Delta_{u^c u^c}$ di-quark Higgs scalars (right-panel).	111
6.6	Effective mass as a function of the lightest active neutrino mass. The blue and the red bands correspond to normal and inverted hierarchy, respectively. The vertical bands are from the bounds on the sum of light neutrino masses given by Planck1, Planck2, and KATRIN experiments. The horizontal yellow band in the left panel corresponds to HM claim with $T_{1/2}^{0\nu}(^{76}\text{Ge}) = 2.23_{-0.31}^{+0.44} \times 10^{25}$ yrs at 68% C.L. and that in the right-panel corresponds to the KamLAND-Zen and EXO-200 combined bound $T_{1/2}^{0\nu}(^{136}\text{Xe}) = 3.4 \times 10^{25}$ yrs at 90% C.L. The scattered points are sterile neutrino contributions to the effective mass.	116

6.7	Effective mass as a function of lightest sterile neutrino mass. The green band corresponds to the effective mass corresponding to HM experiment. Horizontal lines are the standard effective masses in the NH, IH, and saturation of Planck1 pattern of light neutrino masses in the absence of any Majorana phase. The solid, dashed, and the dotted curves are for light-neutrino masses corresponding to saturation of Planck1 bound, IH, and NH patterns. We have used $\langle p^2 \rangle = -(130 \text{ MeV})^2$	117
6.8	Predicted variation of combined effective mass parameter for $0\nu\beta\beta$ decay as a function of lightest sterile neutrino mass M_{S1} . The horizontal blue, red and green bands of effective masses are generated for the NH, IH, and the QD type of light neutrinos, respectively when all the Majorana phases are scanned. The horizontal dark-green band, with double-dot line in the middle, represents the HM data. The orange band is quasi-degenerate light + sterile neutrino contribution for fixed $\mathcal{M}'_{0\nu} = 6.64$ and $ p = 130 \text{ MeV}$	118
6.9	Scattered plot of half-life due to NH type light neutrino and heavy sterile neutrino exchange contributions in the $W_L - W_L$ channel as a function of lightest sterile mass. Left (right) panel corresponds to the nuclear matrix elements and phase space factor of ^{76}Ge (^{136}Xe). Details of various parameters is given in the text. The solid horizontal lines indicate the HM evidence.	121
6.10	Same as Fig.6.9 but for inverted hierarchy of light neutrino masses.	122
6.11	Same as Fig.6.9 and Fig.6.10 but for quasi-degenerate light neutrino masses with $m_\nu = 0.23 \text{ eV}$	122
6.12	Predicted variation of half-life as a function of lightest sterile neutrino mass M_{S1} . The blue, red and green bands have been generated taking the normal, inverted and quasi-degenerate patterns of light neutrino masses, respectively when all the Majorana phases are scanned and sterile neutrino contributions are switched off. The orange band is the combined contribution with fixed nuclear matrix element, $\mathcal{M}'_{0\nu} = 6.64$ and $ p = 130 \text{ MeV}$	123

6.13	Mass bounds for the lightest sterile neutrino mass M_{S_1} obtained from scattered plots of half-life for different light-neutrino mass hierarchies and their comparison with experimental data for ^{76}Ge and ^{136}Xe isotopes cited in the text. The horizontal dashed-green line represents the average value $\overline{M}_{S_1} \geq 18.0 \pm 2.9$ GeV. The vertical dashed-red line passing through the average is to guide the eye.	123
6.14	Left panel: Two loop gauge coupling unification for $M_{(3,3,1)} = 10^{7.3}$ GeV. The multiplet $\xi_{(2,2,15)}$ appears at Pati-Salam D -parity breaking scale. The Pati-Salam, left-right and G_{2113} symmetry breaking scales are at $M_C \sim 10^{6.28}$ GeV, $M_R^+ \sim 10$ TeV and $M_R^0 \sim 5$ TeV, respectively. Right panel: The bi-triplet mass dependence of proton life-time. Parameters are same as used for generating the Tab. 6.5.	125

LIST OF TABLES

2.1	The Standard Model particles.	8
2.2	Covariant derivatives of fermionic and Higgs fields under $SU(2)_L \otimes U(1)_Y \otimes SU(3)_C$ gauge structure. $\mathbf{1}$ is 2×2 identity matrix and α, β run over the three color indices.	10
2.3	Latest global best-fit and allowed $1, 2$ and 3σ range analysis of 3ν mass-mixing parameters. The $\Delta m^2 = m_3^2 - (m_1^2 + m_2^2)/2$ for NH and $= -m_3^2 + (m_1^2 + m_2^2)/2$ for IH. The χ^2 for NH and IH are not very different ($\Delta\chi_{I-N}^2 = -0.3$) [97].	15
2.4	One and two loop gauge coupling beta coefficients.	21
3.1	Simple representations of $SU(5)$ and their decomposition in Standard Model.	25
3.2	The multiplets participating in SSB by acquiring VEVs in the invariant direction of the residual symmetry. The bold numbers correspond to dimension of representation of associated non-abelian symmetry and normals are quantum numbers of abelian symmetry. Upper block depicts the $SU(5)$ way of breaking and lower block depicts the Pati-Salam line of breaking.	31
4.1	GUT scale, intermediate scale and proton lifetime predictions for non-SUSY $SO(10)$ models with TeV scale Z' boson and two Higgs doublets as described in the text. The uncertainty in the proton lifetime has been estimated using 3σ uncertainty in $\alpha_S(M_Z)$	41
4.2	Variation of third generation RH neutrino mass M_3 as a function of first or second generation RH neutrino mass in the partially degenerate case $M_1 = M_2$ predicted by non-unitarity through non-SUSY $SO(10)$	52

4.3	Predictions of moduli and phases of non-unitarity parameters as a function of RH neutrino masses.	52
4.4	Mass eigenvalues of μ_S signifying masses of singlet fermions predicted by the inverse seesaw in $SO(10)$	54
4.5	Non-unitarity predictions of leptonic CP -violating parameters for lepton flavor violating decays $\mu \rightarrow e\gamma$, $\tau \rightarrow e\gamma$, and $\tau \rightarrow \mu\gamma$ as a function of RH neutrino masses	55
4.6	Branching ratios for lepton flavor violating decays $\mu \rightarrow e\gamma$, $\tau \rightarrow e\gamma$, and $\tau \rightarrow \mu\gamma$ as a function of RH neutrino masses	55
5.1	Experimental bounds of the non-unitarity matrix elements $ \eta_{\alpha\beta} $ (column $C0$) and their predicted values for degenerate (column $C1$), partially-degenerate (column $C2$), and non-degenerate (column $C3$) values of $M = \text{diag}(M_1, M_2, M_3)$ as described in cases (a), (b) and (c), respectively, in the text.	65
5.2	Structure of μ_S from neutrino oscillation data for NH of light neutrino masses, $m_\nu = (0.00127, 0.008838, 0.04978)$ eV and different mass pattern of M : (a) $M=(1604.44, 1604.44, 1604.44)$ GeV, (b) $M=(100.0, 100.0, 2151.5)$ GeV, and (c) $M=(9.72, 115.12, 2776.57)$ GeV.	67
5.3	Same as Tab. 5.2 but for IH of light neutrino masses $\hat{m}_\nu=(0.04901, 0.04978, 0.00127)$ eV.	67
5.4	Phase space factors and nuclear matrix elements with their allowed ranges as derived in refs. [254–261].	74
5.5	Input values of M , M_N , and \hat{m}_S used for estimating effective mass parameters given in Tab. 5.6.	77
5.6	Rough estimation of effective mass parameters with the allowed model parameters. The results are for the Dirac neutrino mass matrix including RG corrections. The input values of mass matrices allowed by the current data for different columns are presented in Tab. 5.5.	78
5.7	The Heavy mass eigenvalues for the matrices of M and M_N which have been used to evaluate branching ratios.	79
5.8	The three branching ratios in extended inverse seesaw for different values of M and M_N while M_D is same as in eq. (5.11).	80
5.9	The CP -violating effects for (a) degenerate masses $M=(1604.4, 1604.4, 1604.4)$ GeV, (b) partially degenerate masses $M=(100, 100, 2151.6)$ GeV and (c) non degenerate masses $M=(9.7, 115.2, 2776.5)$ GeV, while M_D is same as in eq. (5.11).	81

5.10	Predictions of allowed mass scales and the GUT couplings in the $SO(10)$ symmetry breaking chain with low-mass W_R^\pm, Z' bosons. . . .	83
5.11	Allowed solutions in the $SO(10)$ symmetry breaking chain shown in eq. (5.42) but with the scalar component $\xi(2, 2, 15) \subset 126_H$ lighter than the GUT scale and consistent with the determination of the induced VEV $v_\xi \sim (10 - 100)$ MeV needed to fit charged fermion masses at the GUT scale. For all solutions we have fixed $M_R^0 = 5$ TeV, $M_R^+ = 10$ TeV, and $M_C = 10^6$ GeV.	97
6.1	Proton decay lifetime predictions for different combination of bi-triplet scalar mass $M_{(3,3,1)}$ and the average di-quark scalar mass M_Δ	105
6.2	Predictions for $n-\bar{n}$ oscillation mixing time as a function of allowed couplings and masses of di-quark Higgs scalars in the model described in the text.	112
6.3	Eigenvalues of sterile neutrino mass matrix for different allowed $N - S$ mixing matrix elements.	121
6.4	The one and two loop beta coefficients for $(3, 3, 1)$ and $(2, 2, 15)$ scalar representation under the PS symmetry.	124
6.5	Bi-triplet mass dependence of the unification scale and proton lifetime. The Pati-Salam, left-right and G_{2113} symmetry breaking scales are at $M_C \sim 10^{6.28}$ GeV, $M_R^+ \sim 10$ TeV and $M_R^0 \sim 5$ TeV, respectively. The Pati-Salam D -parity breaking scale remains at $M_P \sim 10^{14.3}$ GeV. The parameter $A_L \sim 1.25$ is used.	125
A.1	Adler anomalies for few simple representations in $SU(n)$ gauge theories. All $SO(n)$, $n \neq 6$, theories are anomaly free. Anomalies for right-handed fermion representations and corresponding complex conjugate representation will change the sign.	134
B.1	One-loop and two-loop beta function coefficients for gauge coupling evolutions in Model-I and Model-I' described in Sec. 4.1. The second Higgs doublet mass assumed at 1 TeV.	145
B.2	One and two loop beta coefficients for different gauge coupling evolutions for the model described in Sec. 5.5. The second Higgs doublet is assumed at $\mu \geq 10$ TeV.	146

B.3	One and two loop beta coefficients for different gauge coupling evolutions for the model described Sec. 6.1. The second Higgs doublet is taken at $\mu \geq 5$ TeV.	147
B.4	Decomposition of the representation 10	148
B.5	Decomposition of the representation 16	148
B.6	Decomposition of the representation 45	148
B.7	Decomposition of the representation 54	149
B.8	Decomposition of the representation 120	149
B.9	Decomposition of the representation $\overline{\mathbf{126}}$	150
B.10	Decomposition of the representation 210	151

CHAPTER 1

Introduction

In the last hundred years of scientific development our understanding about the behavior of nature has evolved from classical to a very neat and clear quantum picture. In the course of this evolution, starting from the discovery of electron, the fundamental constituents of matter (fermions) and the messengers (gauge bosons) of their interaction have been discovered. Like the unification of electricity and magnetism in to electromagnetic theory, the construction of a single mathematical form to explain various distinct phenomena is one of the virtuous paths followed by theoretical scientists. Following the similar guideline it is found that every action of nature can be explained in terms of four fundamental interactions namely gravitational, electromagnetic, weak and strong. The last three of these are nicely expressed in the mathematical formulation of quantum field theory (QFT) under the Poincare symmetry. The gravitational interaction is much weaker compared to other interactions at any reachable energy scale. Therefore, in all micro-scale studies the gravitational interaction is usually ignored. Also, a successful QFT of gravitation is not yet well established. On the other hand, an elegant cocktail of abelian and non-abelian local gauge symmetries (Weyl [1], Yang-Mills [2]) is found to explain the nature at the fundamental scales. A single, coherent theoretical framework which could explain all physical aspects of the universe, known till date, is yet to incarnate.

The attempts to cure the high energy behavior of Fermi theory of beta decay laid the foundation of today's theory of fundamental interactions. Glashow [3] added a $U(1)$ piece to Schwinger's [4] $SU(2)$ local gauge theory of weak and electromagnetic interaction. This addition was necessary to explain the experimental data for non-leptonic decay modes of strange particles, which indicates the existence of neutral, weakly interacting current. In summary, a theory with massive vector bosons is required to explain the short ranged weak interaction. With the implementation of

Higgs mechanism [5,6] in the $SU(2)_L \otimes U(1)_Y$ structure, Salam [7] and Weinberg [8] could successfully explain electro-weak behavior of the fundamental particles. This mathematical construct was further extended by Gross, Wilczek [9] and Politzer [10] to incorporate the explanation of interaction holding the quarks together, called strong interaction. This completes our cocktail of gauge structure of internal symmetries $SU(2)_L \otimes U(1)_Y \otimes SU(3)_C$, known as the Standard Model (SM). A delightful description of ‘The Rise of the Standard Model’ [11] by its pioneers is a science history worth reading. The anomalies generated, due to charge quantization through $U(1)$ symmetry, by quarks fortunately cancel with anomalies generated by leptons. Hence, though accidentally, it is an anomaly free theory. The renormalizability of the SM was shown by G. ’tHooft [12–14]. For a review on renormalization of SM and precision calculations see lectures [15,16].

The SM is a remarkably successful theory of interactions of fundamental particles in low energy regime. The recent discovery of Higgs boson by *A Toroidal LHC Apparatus* (ATLAS) [17] and *Compact Muon Solenoid* (CMS) [18] detectors at Large Hadron Collider (LHC) completes the search of basic ingredients of SM. Despite the fact that the SM has unraveled the gauge origin of fundamental forces and the structure of universe while successfully confronting numerous experimental tests, it has various limitations. In the next chapter we will discuss about its success and failures in more detail. The reliable extensions of the SM to a simple group are considered to be the good candidates for Grand Unification. The aims of Grand Unification Theories (GUTs) include: (i) unification of SM gauge couplings g_{1Y} , g_{2L} , & g_{3C} at some high enough energy, (ii) quarks and leptons are treated under same Lie structure, i.e., the theory must also ensure the coalescence of quarks and leptons in one or at most two irreducible representations of the unifying group. This unification of quarks and leptons would explain the electric charge quantization. The energy scale of gauge coupling unification should be consistent with the current bounds on proton decay lifetime. In addition to the above requirements, the structure should also be anomaly free and able to explain quark, charged lepton, and neutrino masses. The beyond standard model (BSM) predictions such as large flavor violation, baryonic asymmetry of universe, Dirac or Majorana nature of neutrinos, Dark Matter etc. are the premier goals of GUTs. If possible, they should also explain long standing problems like fine-tuning problem, Dirac monopoles, which have disappointed us till date. Models based on $SU(5)$ and $SO(10)$ gauge groups with their minimal and extended structure, in supersymmetric (SUSY) as well as non-SUSY framework have been the most popular, and have partially accomplished the goal.

The SUSY GUTs provide an attractive framework for representing particles and forces of nature as they solve the gauge hierarchy problem, unify three forces of nature, and also explain the tiny neutrino masses through seesaw paradigm. For recent reviews on different neutrino mass generation mechanisms see [19–29]. The type-I and type-II seesaw have natural origin in minimal SUSY $SO(10)$ GUTs [30–35]. This is because minimal left-right (LR) supersymmetric models [36–38] are embedded in it, which have high $B - L$ symmetry breaking scale ($\sim 10^{15}$ GeV) [39, 40], but these GUT models fails to fit the neutrino masses [41, 42] and their extensions were proposed [43, 44]. The minimal LR symmetric models preserve R -parity as gauge discrete symmetry which makes lightest supersymmetric particle (LSP) as a possible cold dark matter candidates of the universe. A particularly fine tuned, simple model of TeV scale LR symmetry breaking was discussed in [45]. An evidence of SUSY at the LHC would be a land-mark discovery, which would certainly change the future course of physics. But, in the absence of any evidence of SUSY so far, it is worth while to explore new physics prospects of non-SUSY GUTs [46–54]. The GUTs based on $SO(10)$ gauge group have particularly grown in popularity compared to $SU(5)$. This is because $SO(10)$ is the smallest, anomaly free group which unifies all fermions of one generation, including the right-handed (RH) neutrino, into a single spinorial representation. It provides spontaneous origins of P (= Parity) and CP (C = Charge conjugation) violations [48, 49, 55–58]. Most interestingly, it predicts the right order of tiny neutrino masses through the canonical (\equiv type-I) [59–64] and type-II [64–67] seesaw mechanism. In addition, it has high potentiality to explain all the fermion masses [32, 68–70] including large neutrino mixings [71] with type-II seesaw dominance [72–76]. Though it was shown in [41, 42, 77] that type-II seesaw dominating scenarios are disfavored.

In fact, neither seesaw mechanism nor grand unification require SUSY per se. The gauge couplings g_{1Y} , g_{2L} , & g_{3C} automatically unify in the Minimal Supersymmetric Standard Model (MSSM) [78–80]. But, they fail to unify through the minimal particle content of the SM. Therefore, in one-step breaking of non-SUSY $SU(5)$ or $SO(10)$ gauge coupling can not predict the right *Weinberg angle*. However, once intermediate symmetries are included to populate the grand desert in case of non-SUSY $SO(10)$ [58, 81–83], gauge couplings may unify. The intermediate gauge symmetries may also occur near the accelerator reachable energies, availing various predictions for BSM signatures at the current or future accelerator based experiments.

In this dissertation we explore the prospects of inverse seesaw mechanism in order to explain neutrino masses and mixings, in the non-SUSY $SO(10)$ framework. The

inverse seesaw mechanism has plausibility to be experimentally verified because of the low scale at which it can operate. The TeV-scale inverse seesaw mechanism can be successfully implemented with a low-mass Z' gauge boson, which can be accessible at LHC and planned accelerators. We call such models ‘LUUC’ for their gauge structure $SU(2)_L \times U(1)_{B-L} \times U(1)_R \times SU(3)_C$. We find that a minimal, single step breaking of $SO(10)$ to TeV scale LUUC is ruled out by gauge coupling unification constraints imposed by existing lower bound on proton lifetime $\tau_p = 1.4 \times 10^{34}$ years [84–87]. We find that there are not many model with two step breaking of $SO(10)$ to TeV scale LUUC, which could fulfill even the minimal requirement of unification. We study two classes of non-SUSY $SO(10)$ GUT models in which the TeV-scale inverse seesaw mechanism can be implemented.

In one class of study we construct a minimal $SO(10)$ model with $10_H, 16_H$ and 45_H scalar multiplets. A $SO(10)$ singlet fermion per flavor generation is required, in addition to 16_F , to construct the inverse seesaw structure. The $SO(10)$ symmetry first breaks to left-right ($SU(2)_L \otimes SU(2)_R \otimes U(1)_{B-L} \otimes SU(3)_C$) symmetry at unification scale. This left-right (LR) symmetry then breaks to LUUC symmetry at intermediate scale. This LUUC symmetry finally breaks to SM at TeV scale. The details of symmetry breaking chain, breaking mechanism and particle mass spectrum are presented in chapter 4.

The precision gauge coupling unification with the predictions of low mass Z' gauge boson makes this GUT model suitable for the implementation of TeV-scale inverse seesaw mechanism. The model can also be verified or falsified through its predictions on observable non-unitarity effects and experimentally reachable contributions to lepton flavor violation (LFV). Another testing ground for the model may come through the $SO(10)$ prediction on gauge boson mediated proton decay, for which dedicated search experiments are ongoing at Super-K [84].

If larger representations like 126_H are absent in such models, the GUT-threshold effects are small. Therefore, the minimal multiplet models can not be easily compatible with the lower limit on proton lifetime unless the splitting among the super-heavy particles is too large. In view of these, the minimal model we studied turns out to be the best among all the possible single and two-step breaking minimal models of $SO(10)$ to TeV scale LUUC gauge symmetry.

In the other class of study, The $SO(10)$ symmetry breaks to SM in multiple stages. The $SO(10)$ symmetry breaks to D -parity preserving Pati-Salam symmetry ($SU(2)_L \otimes SU(2)_R \otimes SU(4)_C$) at the unification scale. The D -preserving Pati-Salam (PSD) symmetry breaks to D -parity violating PS ($PS\cancel{D}$) symmetry at intermediate

scale ($\sim 10^{13}$ GeV). This $PS\mathcal{D}$ symmetry further breaks either to LR or to LUUC at lower intermediate scale ($\sim 10^6$ GeV). Now, if $PS\mathcal{D}$ symmetry breaks to LR symmetry, LR itself break to LUUC and this breaking scale can be as low as few TeV. Thus, in the low left-right parity breaking scale W_R^\pm gauge bosons may be revealed at accelerator energies. This LUUC eventually break to SM at slightly lower energy scale giving Z' gauge boson at the accelerator reachable scales. On the other hand, if $PS\mathcal{D}$ symmetry breaks directly to LUUC, W_R^\pm gauge bosons are unreachable. The high scale of parity breaking in this case manifests only Z' [88–94] gauge boson at low and accelerator energies.

The multi-step breaking schemes and the corresponding particle mass spectrum are discussed in detail in the chapters 5 and 6. The scalar particle content is very rich in these cases due to the presence of various intermediate symmetries. The scalar particle spectrum follows the extended survival hypothesis, unless stated explicitly. The D -parity restoration in PS symmetry at high scale allows the LR gauge symmetry to exist at experimentally reachable scale. It also allows the $PS\mathcal{D}$ symmetry as low as constrained by gauge mediated rare kaon decay experiments. These models therefore also give predictions for observable neutron-antineutron oscillation and lepto-quark gauge boson mediated rare kaon decays.

We investigate in detail the prospects of TeV scale left-right gauge theory with parity restoration scale suitably modified to implement extended inverse seesaw mechanism. This extension predicts large contributions to neutrinoless double beta ($0\nu 2\beta$) decay. The light neutrino masses are still governed by gauged inverse seesaw formula. The dominant contributions to $0\nu 2\beta$ -decay come from the W_L - W_L channel, and are mediated by relatively light sterile neutrinos. Sub-dominating contributions to $0\nu 2\beta$ -decay are also estimated and compared with dominant one. Implementation of TeV scale physics in non-SUSY $SO(10)$ GUT is successfully established. Non-unitarity and LFV effects are also estimated and found to be within the reach of future experiments. In this model proton decay lifetime is very-very large, unreachable to any future experiment.

We extend this study and show that even if only a TeV scale Z' boson is detected at the LHC, a number of these observable predictions will still be applicable. The D -parity violating PS symmetry directly breaks to LUUC symmetry. The W_R^\pm boson masses are part of PS symmetry and far beyond the currently accessible LHC limit. Due to change in the gauge symmetry breaking scheme and the required scalar multiplets, we find that the present model predicts proton lifetime to be accessible at ongoing search experiments. Which is in sharp contrast to the previous model.

New bounds on PS symmetry breaking scale, di-quark scalar and sterile neutrino masses are realized. Extensive study of $0\nu 2\beta$ -decay effective mass and life-time in the model is studied. The possible cancellations among the standard and non-standard contributions to $0\nu 2\beta$ -decay are also elaborated.

In chapter 2, we retrospect the SM and discuss its features and compulsions. In chapter 3, we extend this retrospection to $SU(5)$ and $SO(10)$ GUTs. In chapter 4, we elaborate a two step breaking of $SO(10)$ GUT to SM with minimal representations. The cardinal virtues of this study are (i) LHC reachable Z' gauge boson, (ii) proton lifetime prediction close to Super-K bound, (iii) LHC reachable seesaw, (iv) large LFV and CP-asymmetry etc. In chapter 5, we study a multi step breaking of $SO(10)$ to SM, which preserves D -parity violating PS symmetry until $\sim 10^6$ GeV. The salient features of this study are the predictions for: (i) LHC reachable Z', W_R^\pm gauge bosons, (ii) large CP-asymmetry and LFV, (iii) LHC reachable seesaw, (iv) large $0\nu 2\beta$ decay in W_L-W_L channel, (v) experimentally reachable $n-\bar{n}$ oscillation time, (vi) mass of sterile neutrino, and (vii) rare kaon decays mediated by PS gauge bosons. In this chapter we describe the $0\nu 2\beta$ decay part in detail. In chapter 6, we extend the study of previous chapter and elaborate the details of other predictions of the model. We also found that in case of absence of W_R gauge boson at colliders up to very high energy, the model can predict Hyper-K reachable proton decay. In the seventh chapter we draw our conclusions. We have also appended the relevant supplementary material in five sub categories.

Standard Model and beyond

2.1 Standard Model of particle physics

The Standard Model of particle physics is a theory of electromagnetic, weak and strong interactions, which governs the dynamics of basic building blocks of universe. These building blocks do not possess any sub-structure, therefore are called elementary or fundamental particles. These elementary particles can be categorized into spin-0 scalar (Higgs) bosons, spin-1/2 fermions and spin-1 gauge bosons under the Lorentz symmetry of space-time. The fermions constitute the matter of universe while gauge bosons form force-carriers. Passings the tests of hundreds of scattering experiments in various channels, carried out over a dozen of collider experiments the SM has earned the distinction to the extreme accuracy. The SM has not failed a single test even at very high precision scale.

The SM is a paradigm of QFT constructed on $SU(2)_L \otimes U(1)_Y \otimes SU(3)_C$ group structure of local gauge symmetries, which exposes the underlying action of nature. Quantum field theory is the application of quantum mechanics to the dynamical system of fields physically operating on the continuous symmetry of space-time, namely, the Lorentz symmetry $SO(1, 3)$. For the sake of completeness, the Lorentz symmetry is briefly recapitulated in Appendix A.3. The exotic extensions of SM incorporate additional particles, extra dimensions, elaborated internal and flavor symmetries to explain neutrino oscillations, dark matter etc.

The particle content of the SM is inscribed in Tab. 2.1. The Greek indices on the gauge boson depict their vectorial nature under Lorentz symmetry, while roman indices a and i represent their number which is same as dimension of adjoint representation (rep) of the associated internal symmetry. The matter field is constituted by the fermions belonging to spinorial rep of Lorentz symmetry while Higgs boson is

Spin=1				
Hyperon	B_μ	(1,0,1)	$U(1)_Y$	g'
Weak Bosons	$W_\mu^i, i = 1, 2, 3$	(3,0,1)	$SU(2)_L$	g
Gluons	$G_\mu^a, a = 1, 2 \dots 8$	(1,0,8)	$SU(3)_C$	g_s
Spin=1/2				
Quarks	(2, 1/6, 3)	$\begin{pmatrix} u \\ d \end{pmatrix}_L^\alpha$	$\begin{pmatrix} c \\ s \end{pmatrix}_L^\alpha$	$\begin{pmatrix} t \\ b \end{pmatrix}_L^\alpha$
	(1, 2/3, 3)	u_R^α	c_R^α	t_R^α
	(1, -1/3, 3)	d_R^α	s_R^α	b_R^α
Leptons	(2, -1/2, 1)	$\begin{pmatrix} \nu_e \\ e \end{pmatrix}_L$	$\begin{pmatrix} \nu_\mu \\ \mu \end{pmatrix}_L$	$\begin{pmatrix} \nu_\tau \\ \tau \end{pmatrix}_L$
	(1, -1, 1)	e_R	μ_R	τ_R
Spin=0				
Higgs	(2, 1/2, 1)	$\begin{pmatrix} H^+ \\ H^0 \end{pmatrix}$		

Table 2.1: The Standard Model particles.

the scalar of the symmetry. The alliance of particles under the internal symmetries can be summarized by the set (r_2, Y, r_3) , where r_2 and r_3 are the dimensions of reps of non-abelian internal symmetries $SU(2)_L$ and $SU(3)_C$, and Y is the hypercharge quantum number of the abelian symmetry $U(1)_Y$. All the left handed fermions and the Higgs boson stay in the fundamental rep of $SU(2)_L$, while the right handed fermions are its singlets. Quarks stay in fundamental rep of $SU(3)_C$, while leptons and Higgs stay unexposed to this symmetry. All the flavor generations of fermions under $SU(2)_L$ symmetry are explicitly scripted. The index α on quark sector runs over three colors in the fundamental rep. Coulomb charges of all the particles can be estimated using Gellmann-Nishijima formula

$$Q = T_3 + Y \tag{2.1}$$

where T_3 is the diagonal generators of $SU(2)$ symmetry. This formula appears automatically while generating masses for gauge bosons, and is discussed in next section. The kinetic part of Lagrangian of Gauge (\mathcal{L}_{GK}) and Matter (\mathcal{L}_{MK}) fields can be

written as

$$\mathcal{L}_{GK} = -\frac{1}{4}B_{\mu\nu}B^{\mu\nu} - \frac{1}{4}W_{\mu\nu}^iW^{\mu\nu i} - \frac{1}{4}G_{\mu\nu}^aG^{\mu\nu a} \quad (2.2)$$

$$\begin{aligned} \mathcal{L}_{MK} = & i \sum_{i=1}^3 \left(L_{L_i}^\dagger \sigma^\mu \mathcal{D}_\mu L_{L_i} + e_{R_i}^\dagger \sigma^\mu \mathcal{D}_\mu e_{R_i} + Q_{L_i}^\dagger \sigma^\mu \mathcal{D}_\mu Q_{L_i} \right. \\ & \left. + u_{R_i}^\dagger \sigma^\mu \mathcal{D}_\mu u_{R_i} + d_{R_i}^\dagger \sigma^\mu \mathcal{D}_\mu d_{R_i} \right) \end{aligned} \quad (2.3)$$

where the corresponding field strengths can be expressed as

$$B_{\mu\nu} = \partial_\mu B_\nu - \partial_\nu B_\mu, \quad (2.4)$$

$$W_{\mu\nu}^i = \partial_\mu W_\nu^i - \partial_\nu W_\mu^i - g \epsilon^{ijk} W_\mu^j W_\nu^k, \quad (2.5)$$

$$G_{\mu\nu}^a = \partial_\mu G_\nu^a - \partial_\nu G_\mu^a - g_S f^{abc} G_\mu^b G_\nu^c. \quad (2.6)$$

Here ϵ^{ijk} and f^{abc} are structure functions of $SU(2)_L$ and $SU(3)_C$ groups and $i, j, k = 1, 2, 3$; $a, b, c = 1, 2, \dots, 8$. g_S and g are $SU(3)_C$ and $SU(2)_L$ gauge field coupling strengths. Though non-abelian gauge field do, abelian gauge fields do not self-interact which is clear from eq. (2.4)-eq. (2.6). Abelian field strength appear only in fermion-gauge-fermion and scalar-gauge-scalar interactions, through covariant derivatives present in the fermion kinetic terms and scalar kinetic term, to be introduced later. Covariant derivative operator in general can be expressed as

$$\mathcal{D}_\mu = \partial_\mu 1 + i \sum_p g_p \sum_{l_p}^{n_p^2-1} A_\mu^{l_p} T^{l_p} \prod \delta_{p'}. \quad (2.7)$$

where p is index of internal symmetries present in a theory, l_p are indices over adjoint representation of internal symmetry p , and $\delta_{p'}$ are the Kronecker delta for the internal symmetries other than p . For $U(1)_Y$ symmetry, $l_Y = 1$ and $T^{l_Y} = Y$. The explicit structure of covariant derivatives acting on fermion and Higgs fields are presented in Tab. 2.2.

The collider experiments have tested and confirmed the $SU(2)_L \otimes U(1)_Y$ gauge structure of the theory in the fermion weak boson and triple gauge boson interaction channels. If the gauge symmetry $SU(2)_L \otimes U(1)_Y$ remains unbroken neither the gauge bosons nor the fermions acquire masses. The bare mass terms for fermions and gauge bosons, $m_f \bar{\psi}_f \psi_f$ and $M_A A_\mu A^\mu$, are not $SU(2)_L \otimes U(1)_Y$ invariant hence are forbidden. But, the weak gauge bosons are required to be massive to explain short range weak interaction while quarks and leptons have to be massive to explain the micro structure

Field	Multiplet	Covariant derivatives
Q_L	$(2, 1/6, 3)$	$\mathcal{D}_\mu Q_L = [(\partial_\mu \mathbf{1} + igW_\mu^i \frac{\sigma^i}{2} + i\frac{g'}{6} B_\mu \mathbf{1})\delta_{\alpha\beta} + ig_S G_\mu^a \frac{\lambda_{\alpha\beta}^a}{2} \mathbf{1}] Q_{L\beta}$
L_L	$(2, -1/2, 1)$	$\mathcal{D}_\mu L_L = (\partial_\mu \mathbf{1} + igW_\mu^i \frac{\sigma^i}{2} - i\frac{g'}{2} B_\mu \mathbf{1}) L_L$
u_R	$(1, 2/3, 3)$	$\mathcal{D}_\mu u_R = [(\partial_\mu + i\frac{2g'}{3} B_\mu)\delta_{\alpha\beta} + ig_S G_\mu^a \frac{\lambda_{\alpha\beta}^a}{2}] u_{R\beta}$
d_R	$(1, -1/3, 3)$	$\mathcal{D}_\mu d_R = [(\partial_\mu - i\frac{g'}{3} B_\mu)\delta_{\alpha\beta} + ig_S G_\mu^a \frac{\lambda_{\alpha\beta}^a}{2}] d_{R\beta}$
e_R	$(1, -1, 1)$	$\mathcal{D}_\mu e_R = (\partial_\mu - ig' B_\mu) e_R$
H	$(2, 1/2, 1)$	$\mathcal{D}_\mu H = (\partial_\mu \mathbf{1} + igW_\mu^i \frac{\sigma^i}{2} + i\frac{g'}{2} B_\mu \mathbf{1}) H$

Table 2.2: Covariant derivatives of fermionic and Higgs fields under $SU(2)_L \otimes U(1)_Y \otimes SU(3)_C$ gauge structure. $\mathbf{1}$ is 2×2 identity matrix and α, β run over the three color indices.

of atoms. In fact! all the particles observed till date, except photons, are massive. Therefore the symmetry is broken badly. Thus, under $SU(2)_L \otimes U(1)_Y$ the current is conserved but particle states are not symmetric. This we call spontaneous breaking of symmetry. The novel mechanism to generate the masses for weak gauge bosons and charged fermions won the 2013 noble prize to Prof. Peter Higgs [6] and Prof. Francois Englert [5], and is called ‘Higgs mechanism’.

The masses of the gauge bosons and fermions are generated by the Higgs mechanism via spontaneous symmetry breaking (SSB). To preserve the Lorentz symmetry, the symmetry is spontaneously broken by scalar fields only. A $SU(2)_L$ doublet scalar field with non-zero $U(1)_Y$ charge is required to generate the invariant Yukawa term of fermions and scalar interaction. Hypercharge of left handed particles indoctrinates another symmetry through $Y = (B - L)/2$, while right handed ones seem arbitrary. With the introduction of a Higgs doublet we may write the Yukawa part of the SM Lagrangian as

$$\mathcal{L}_{Yuk} = - \sum_{f_1, f_2=1}^3 \left[Y_{f_1 f_2}^l \bar{L}_{L f_1} H e_{R f_2} + Y_{f_1 f_2}^d \bar{Q}_{L f_1} H d_{R f_2} + Y_{f_1 f_2}^u \bar{Q}_{L f_1} \tilde{H} u_{R f_2} \right] + h.c. \quad (2.8)$$

where

$$\tilde{H} \equiv i\sigma_2 H^\dagger = \begin{pmatrix} H^{0\dagger} \\ -H^- \end{pmatrix}, \quad (2.9)$$

and $Y^{l,d,u}$ are arbitrary 3×3 matrices, eventually determining the fermion masses and flavor mixings. Sum over color and isospin indices have been ignored and f_1, f_2 run over the number of flavor generations.

2.2 SSB and Higgs Mechanism

A vacuum state may or may not be invariant under the symmetry present in the Lagrangian. These modes of symmetry realization are called Wigner-Weyl or Nambu-Goldstone modes respectively. The symmetry realized in nature also depends on the properties of the vacuum state. Wigner-Weyl realization causes all the particles in a single multiplet to have degenerate masses while in Nambu-Goldstone realization the multiplet contains zero-mass particles, known as Nambu-Goldstone boson, equal to the number of broken generators. When the local gauge symmetries are broken spontaneously, the Nambu-Goldstone bosons disappear providing longitudinal modes to gauge fields making them massive. See chapter 3 of [95] for the related details.

The $SU(2)_L$ complex Higgs scalar doublet with SM quantum numbers $(2, 1/2, 1)$ is denoted as,

$$H = \begin{pmatrix} H^+ \\ H^0 \end{pmatrix} \equiv \frac{1}{\sqrt{2}} \begin{pmatrix} H_1 + iH_2 \\ H_3 + iH_4 \end{pmatrix}. \quad (2.10)$$

The scalar part of SM Lagrangian is augmented as

$$\mathcal{L}_H = (\mathcal{D}_\mu H)^\dagger \mathcal{D}_\mu H - \mu^2 H^\dagger H - \lambda (H^\dagger H)^2. \quad (2.11)$$

The scalar potential acquires above structure due to $SU(2)_L \otimes U(1)_Y$ invariance and renormalizability condition. For $\mu^2 < 0$ electroweak symmetry breaks spontaneously, and $\lambda > 0$ is required to keep vacuum stable. Kinetic part of the Lagrangian gives the three and four point interactions between Higgs and gauge bosons, and the λ term describes quartic scalar self-interaction. Re-writing the scalar potential in real basis we get

$$V(H) = \frac{1}{2}\mu \left(\sum_i^4 H_i^2 \right) + \frac{1}{4}\lambda \left(\sum_i^4 H_i^2 \right)^2. \quad (2.12)$$

Without loss of generality we can choose the coordinates in this four dimensional space such that $\langle 0|H_i|0\rangle = 0$ for $i = 1, 2, 4$ and $\langle 0|H_3|0\rangle \geq 0$. Electromagnetic charge neutral component of the scalar field acquires vacuum expectation value (VEV), preserving $U(1)_Q$ symmetry of vacuum. Minimization of potential part yields

$$\langle H^\dagger H \rangle_0 = -\frac{\mu^2}{2\lambda} \equiv \frac{v_{EW}^2}{2} \rightarrow \langle 0|H|0\rangle = \frac{1}{\sqrt{2}} \begin{pmatrix} 0 \\ v_{EW} \end{pmatrix}, \quad (2.13)$$

called the Higgs field acquiring VEV. The complete transformation of Higgs field is

$$H \rightarrow e^{\frac{i}{2}(\alpha^i \sigma^i + i\beta)} H = \frac{1}{\sqrt{2}} \begin{pmatrix} 0 \\ v_{EW} + h \end{pmatrix}. \quad (2.14)$$

Then gauge transformation with, say, $\alpha_{1,2} = 0$ and $\alpha_3 = \beta$ will be a symmetry of VEV. Thus, the generators $\sigma_{1,2}$ and $\frac{1}{2}\sigma_3 - Y\mathbf{1}$ are spontaneously broken since they give non-zero charge to vacuum. But, vacuum carries no quantum number for $Q = \frac{1}{2}\sigma_3 + Y\mathbf{1}$ thus $U(1)_Q$ symmetry stays unbroken. The scalar kinetic term with $H = H' + \langle H \rangle$ gives the relevant mass term

$$\begin{aligned} (\mathcal{D}_\mu \langle H \rangle)^\dagger (\mathcal{D}_\mu \langle H \rangle) &\rightarrow \frac{1}{2}(0, v_{EW}) \left| gW_\mu^i \frac{\sigma^i}{2} + \frac{g'}{2} B_\mu \mathbf{1} \right|^2 \begin{pmatrix} 0 \\ v_{EW} \end{pmatrix} \\ &= \frac{1}{2} \frac{v_{EW}^2}{4} [g^2 W_\mu^+ W_\mu^- + (-gW_\mu^3 + g'B_\mu)^2] \end{aligned} \quad (2.15)$$

where

$$W_\mu^\pm = \frac{1}{\sqrt{2}}(W_\mu^1 \mp iW_\mu^2) \quad \text{with mass } m_W = g \frac{v_{EW}}{2} \quad (2.16)$$

$$Z_\mu = \frac{1}{\sqrt{g^2 + g'^2}}(gW_\mu^3 - g'B_\mu) \quad \text{with mass } m_Z = \sqrt{g^2 + g'^2} \frac{v_{EW}}{2} \quad (2.17)$$

Thus, the field orthogonal to Z_μ is electro-magnetic (EM) field $A_\mu = \frac{1}{\sqrt{g^2 + g'^2}}(g'W_\mu^3 + gB_\mu)$, which remains massless. The EM and neutral weak boson fields are related as

$$\begin{pmatrix} Z_\mu \\ A_\mu \end{pmatrix} = \begin{pmatrix} \cos \theta_W & -\sin \theta_W \\ \sin \theta_W & \cos \theta_W \end{pmatrix} \begin{pmatrix} W_\mu^3 \\ B_\mu \end{pmatrix} \quad (2.18)$$

where $\theta_W = \cos^{-1} \left(\frac{g}{\sqrt{g^2 + g'^2}} \right)$ is called *Weinberg angle*. The relation $M_W^2 = M_Z^2 \cos^2 \theta_W$ confirms the weak doublet nature of the Higgs particle. Fermionic mass terms are acquired trivially as

$$M_\psi = \frac{1}{\sqrt{2}} Y^\psi v_{EW}, \quad (2.19)$$

where $\psi = l, d, u$. The Yukawa couplings are not any special matrices hence can be diagonalized only using bi-unitarity transformation.

This mechanism introduced the nature's complexity through 28 fundamental parameters namely 12 masses, 6 angles and 2 Dirac phases in quark and lepton sector, 2 Majorana phases and in the Bosonic sector $\alpha, m_Z, v_{EW}, m_H, \alpha_S$ and θ_{QCD} . The allowed parameter space for Higgs mass was constrained to very limited region of

parameter space, around 100 GeV, with the help of radiative corrections to gauge bosons due to presence of Higgs in the loop. This was further constrained by LEP, Tevatron direct search experiments and unitarity constraint on WW -scattering, and is eventually discovered at LHC.

The spontaneous symmetry breaking and Higgs mechanism also help in making of a renormalizable theory with massive vector bosons. Breaking of gauge invariance explicitly by adding mass terms for gauge bosons must have culminated the theory into a non-renormalizable one.

2.3 Excellencies of Standard Model

Gauge and fermionic kinetic terms together with Yukawa and Higgs Lagrangian complete the Lagrangian for SM, except the fact that while quantizing SM we need to add gauge fixing and Faddeev-Popov ghost terms. Since its origin the SM has been beautifully confirmed by all the experiments. It has very simple structure and different forces of nature appear in same fashion, i.e., local gauge theories. The 58 objects (45 fermion fields, 12 gauge boson fields and 1 scalar boson field), 118 degrees of freedom (1 for Higgs, 2 for photons, 8×2 for gluons, 3×3 for massive electroweak gauge bosons, 3×4 for charged leptons, 3×2 for neutrinos, $6 \times 3 \times 4$ for quarks) and 28 free parameters (12 for fermion masses, 3 angles and 1 CP phase of Cabibbo-Kobayashi-Maskawa (CKM) matrix, 3 angles and 3 phases in Pontecorvo-Maki-Nakagawa-Sakata (PMNS) matrix, four in electroweak sector of bosons namely α , M_Z , v_{EW} and M_H and 2 in strong sector namely α_S and strong CP phase Θ_{QCD}) constitute the complete model. All these parameters have been experimentally measured except Θ_{QCD} , three phases of PMNS matrix and absolute neutrino mass scale. For a nice summary of SM and beyond see [96].

Few of the world's major collider experiments are LEP (e^+e^-), SLC (e^+e^-), Tevatron ($p\bar{p}$), HERA (e^-p), PEP-II (e^+e^-), KEKB (e^+e^-) and the latest LHC (pp). These experiments have explored the energy scale from 10 GeV to 8 TeV. Leptonic collider experiments give clean signals at fixed energy suitable for detailed study. Hadronic collider experiment signals are messy with unknown/variable energy but are suitable for discovery purposes due to high energy, involved nature and capability of producing large amount of signal. With the above structure, SM fits precisely the experimental findings of above experiments. To test a property of the theory we measure the associated parameter various ways, compare the predicted and measured quantities. Once confirmed, fit the full parameter space of the model and check it's

consistency. All the particles predicted by the SM since its origin, namely τ (1975), ν_τ (2000), c (1974), b (1977), t (1995), gluons (1979), W , Z (1983) and Higgs (2012) scalar, have not only been confirmed but also fit perfectly in the model framework.

2.4 Deficiencies of Standard Model

With the recent discovery of Higgs particle in CMS [18] and ATLAS [17] detectors at LHC our quest for the SM parameters completes. Even ignoring the fact that it does not incorporate gravitational interaction, there are enough reasons for not believing it as a complete story. Few of the most crucial reasons behind the need of BSM physics are listed as follows

- **Neutrino Masses:** The most important and widely discussed experimental evidence of BSM physics is the observed neutrino masses and their peculiar mixings in innumerable oscillation experiments. Solar neutrino experiments (Homestake, Kamiokande, GALLEX/GNO, SAGE, Super-Kamiokande, SNO, BOREXINO) and reactor experiment KamLAND estimated $\Delta m_{sol}^2 \simeq 7.5 \times 10^{-5} \text{ eV}^2$ and angle $\sin^2 \theta_{sol} \simeq 0.3$. Atmospheric experiments (Kamiokande, IMB, Super-Kamiokande, MACRO, Soudan-2, MINOS) and long baseline experiments (K2K, MINOS and T2K) measured $\Delta m_{atm}^2 \simeq 2.4 \times 10^{-3} \text{ eV}^2$ and a mixing angle $\sin^2 \theta_{atm} \simeq 0.5$. The reactor experiments Daya Bay, RENO and Double Chooz recently confirmed non-zero reactor angle $\sin^2 \theta_{rct} \simeq 0.02$. In the standard three generation framework $\Delta m_{sol}^2 = \Delta m_{21}^2$, $\Delta m_{atm}^2 = |\Delta m_{31}^2| \simeq |\Delta m_{32}^2|$ and $\theta_{sol} = \theta_{12}$, $\theta_{atm} = \theta_{23}$, $\theta_{rct} = \theta_{13}$ are chosen for convenience. The latest global fit for these parameters is listed Tab. 2.3 [97]. From a totally different scenario the cosmological bounds coming from WMAP constrain the sum of light neutrino masses to $\sum m_i < 0.19 - 1.19 \text{ eV}$ at 2σ level [98]. Uncertainties in mass hierarchy and CP -phases are expected to be fixed in near future. From SM point of view neutrino masses must vanish if no right handed neutrinos existed, hence no Dirac mass term for neutrinos exist and lepton number is conserved. Charge neutrality of neutrinos leave other doubts like whether neutrinos are Dirac or Majorana type. If they are Dirac kind, Yukawa couplings will have to be $\sim 10^{-12}$, and there will not be any prediction for neutrinoless double beta decay. If they are Majorana type their masses might come through seesaw mechanism quite naturally.

Parameter	Case	Best fit	1σ range	2σ range	3σ range
$\frac{\delta m^2}{10^{-5} \text{ eV}^2}$	NH/IH	7.54	7.32 – 7.80	7.15 – 8.00	6.99 – 8.18
$\frac{\sin^2 \theta_{12}}{0.1}$	NH/IH	3.08	2.91 – 3.25	2.75 – 3.42	2.59 – 3.59
$\frac{\Delta m^2}{10^{-3} \text{ eV}^2}$	NH	2.43	2.37 – 2.49	2.30 – 2.55	2.23 – 2.61
	IH	2.38	2.32 – 2.44	2.25 – 2.50	2.19 – 2.56
$\frac{\sin^2 \theta_{13}}{0.01}$	NH	2.34	2.15 – 2.54	1.95 – 2.74	1.76 – 2.95
	IH	2.40	2.18 – 2.59	1.98 – 2.79	1.78 – 2.98
$\frac{\sin^2 \theta_{23}}{0.1}$	NH	4.37	4.14 – 4.70	3.93 – 5.52	3.74 – 6.26
	IH	4.55	4.24 – 5.94	4.00 – 6.20	3.80 – 6.41
δ/π	NH	1.39	1.12 – 1.77	0.00 – 0.16 \oplus 0.86 – 2.00	—
	IH	1.31	0.98 – 1.60	0.00 – 0.02 \oplus 0.70 – 2.00	—

Table 2.3: Latest global best-fit and allowed 1, 2 and 3σ range analysis of 3ν mass-mixing parameters. The $\Delta m^2 = m_3^2 - (m_1^2 + m_2^2)/2$ for NH and $= -m_3^2 + (m_1^2 + m_2^2)/2$ for IH. The χ^2 for NH and IH are not very different ($\Delta\chi_{I-N}^2 = -0.3$) [97].

- Dark Matter:** There are cosmological and astrophysical evidences that most of the matter in the universe is not SM like, as it does not emit electromagnetic radiation and hence is dark. Neutrinos would also not emit electromagnetic radiation but relic density abundance of neutrinos disfavors its possibility of being Dark Matter. Implication for particle physics are such that there must exist cold dark matter which is non-baryonic. Till date the existence of cold Dark Matter, which is likely to have particle physics origin, is elevated only because of its gravitational interaction. See review by Drees and Gerbier in [99].
- Baryon asymmetry of universe:** The imbalance in baryonic and anti-baryonic matter in the observable universe is known as baryon asymmetry problem. A system outside the thermal equilibrium is required to violate C , CP and B -number, to generate such asymmetry [100]. These conditions are necessary, for theories in which $B = 0$ during the Big Bang, but not sufficient. All of these conditions are satisfied in the SM. B is violated by instantons when kT is of the order of the weak scale (but $B - L$ is conserved). CP is violated by the CKM phase and out of equilibrium conditions could be verified during the electroweak phase transition. A detailed quantitative analysis [101–104] shows that baryogenesis is not possible in the SM because there is not enough CP -violation and the phase transition is not sufficiently strong at first order, unless $m_H < 80$ GeV. Possibility of this mass had been ruled out by LEP ex-

periment. The electroweak Higgs particle has been recently discovered at LHC and found to have $m_H \simeq 126$ GeV.

- **Flavor problem:** Despite the fact that all the SM fermions acquire their masses through a single spontaneous symmetry breaking mechanism, their masses exhibit strong hierarchical pattern. The symmetry of SM does not impose any constraint on the masses or mixings of fermions. Including the tiny but non-zero masses of neutrino, the ratio of heaviest to lightest fermion is $\sim 10^{12}$. There is no explanation of three generations. Even in theories beyond the SM there is no single, justifiable, minimal mechanism to correlate different Yukawa couplings at electroweak scale.
- **Fine tuning:** Once the dependency on the cut-off scale is absorbed in the re-definitions of masses and couplings, SM is a renormalizable theory. Higgs mass is not protected by any symmetry and receives large radiative correction from new-physics scale. This requires order by order fine tuning of extreme orders to make the Higgs mass stable. Best solution out of few is the introduction of SUSY at TeV scale.
- **Gauge symmetry problem:** The gauge structure and pattern of representations once discovered looks simple, but the origin of this structure and three different gauge couplings of totally different nature remains unexplained. A satisfactory theory should be able to explain the origin of these gauge symmetries and couplings. Evolution of these gauge couplings appear to be converging to a single origin, this behavior should also have some convincing explanation.
- **Charge quantization:** Gellmann-Nishijima equation is convincingly acquired while generation masses for gauge bosons, but it does not answer the question why all the particles have integer multiple of $Q_e/3$, where Q_e is charge of electron. More generically, why charges are quantized? From within the SM we do not get hint for Hypercharge quantum numbers.
- **Ultra High energy cosmic rays:** The highest energy cosmic rays observed have macroscopic energies up to several 10^{11} GeV. They may provide a good probe to physics and astrophysics at such a large energies, unattainable in terrestrial lab experiments. The origin of such an energetic cosmic rays is one of the unresolved problem, searching for an explanation in the variety of theories from astrophysical acceleration to BSM physics. For a review see [105].

The motive of our study is two folded: (1) To address some of the above mentioned open problems from grand unification point of view, and (2) to predict some new BSM physics within the reach of ongoing or future experiments. Unfortunately, all the precision data, extensive flavor physics programs at K and B factories, and direct collider searches indicate that there is no new physics at the electroweak scale.

Before we move to next level of our discussion let us have a look at the evolution of gauge couplings of SM and its minimal SUSY extension.

2.5 Evolution of gauge couplings and unification

The high energy behaviors of the three gauge couplings of SM g_s , g and g' point towards the unification of the electro-weak and strong forces. This is one of the main motivation behind studying Grand unification. Aesthetically too, we will prefer all the forces of nature to unify at certain very high energy. Fig. 2.2 and Fig. 2.3 describes the evolution of gauge couplings of SM and MSSM. The group theoretic formulations of one and two loop beta functions coefficients for a general $G_1 \times G_2$ gauge theory are listed in ref. [106, 107] for both non-SUSY and SUSY scenarios. The renormalization group evolution (RGE) of gauge coupling with two loop correction can be expressed as [106, 107]

$$\mu \frac{\partial g_i}{\partial \mu} = \beta_i \equiv \frac{1}{16\pi^2} a_i g_i^3 + \frac{1}{(16\pi^2)^2} \sum_j a_{ij} g_i^3 g_j^2 + \text{Yukawa term} \quad (2.20)$$

where i run over the three symmetries, μ is the energy parameter, and a_i (a_{ij}) are one (two) loop beta function coefficients.

2.5.1 SM gauge coupling running

In the non-SUSY scenario the beta functions coefficients are [107]

$$\begin{aligned} a_i &= -\frac{11}{3}C_2(G_1) + \frac{2}{3}\theta T(R_1)d(R_2) + \frac{1}{6}\delta T(S_1)d(S_2) \\ a_{ii} &= -\frac{34}{3}[C_2(G_1)]^2 + \left[\frac{10}{3}C_2(G_1) + 2C_2(R_1)\right]\theta T(R_1)d(R_2) \\ &\quad + \left[\frac{1}{3}C_2(G_1) + 2C_2(S_1)\right]\delta T(S_1)d(S_2) \\ a_{i \neq j} &= 2\theta C_2(R_2)d(R_2)T(R_1) + 2\delta C_2(S_2)d(S_2)T(S_1) \end{aligned} \quad (2.21)$$

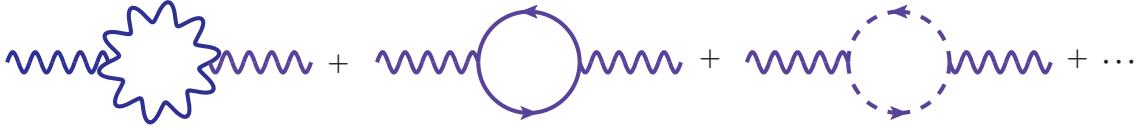


Figure 2.1: One loop correction to gauge propagator. Dots correspond to ghost and gauge fixing terms.

where $\theta = 1(2)$ for Weyl (Dirac) fermions and $\delta = 1(2)$ for real (complex) scalar fields. The fermionic and scalar multiplets transform according to the representations R_i and S_i with respect to the symmetry G_i . For an irreducible representation X we have

$$\begin{aligned} \text{tr}(M_a(X)M_b(X)) &= T(X)\delta_{ab}, \\ [M_a(X)M_a(X)]_{ij} &= C_2(X)\delta_{ij}, \end{aligned} \quad (2.22)$$

where M_a is the matrix representation of the generators of the group. The $T(X)$ and $C_2(X)$ are called Dynkin index invariants and quadratic Casimir invariants, respectively, and are related by $C_2(X)d(X) = T(X)d_G$. Here $d(X)$ is the dimension of the representation X and d_G is the number of generators of the group. We have availed a brief discussion on Quadratic Casimir and Dynkin index invariants in Appendix A.2. If the theory has product of more than two group $d(X_2) = \prod_{i \geq 2} d(X_i)$ is assumed. $C_2(G)$ is the quadratic Casimir for the adjoint representation. For a representation of abelian symmetry $U(1)_z$ we have $C_2(G) = 0$ and $C_2(X) = T(X) = z^2$, where z is the appropriately normalized charge associated to the $U(1)$ symmetry.

We will be frequently estimating these coefficients for various gauge groups under study, hence we have explicitly elaborated the way to calculate those in the following example.

Example: Assume that we have quark doublet $(2, 1/6, 3)$, which is a Weyl fermion above electroweak restoration scale hence $\theta = 1$. This example is as general as required. One loop coefficient corresponding to this representation is

$$a_{(2,1/6,3)} = \frac{2}{3} \left(\frac{1}{2} \times 3, \frac{3}{5} \left(\frac{1}{6} \right)^2 \times 6, \frac{1}{2} \times 2 \right) \times n_g \quad (2.23)$$

In the eq. (2.23) the common factor $2/3$ is the impression of representation being fermionic. There are three terms inside the bracket corresponding to three groups. The first term has a Dynkin index for fundamental of isospin group $SU(2)_L$, i.e.,

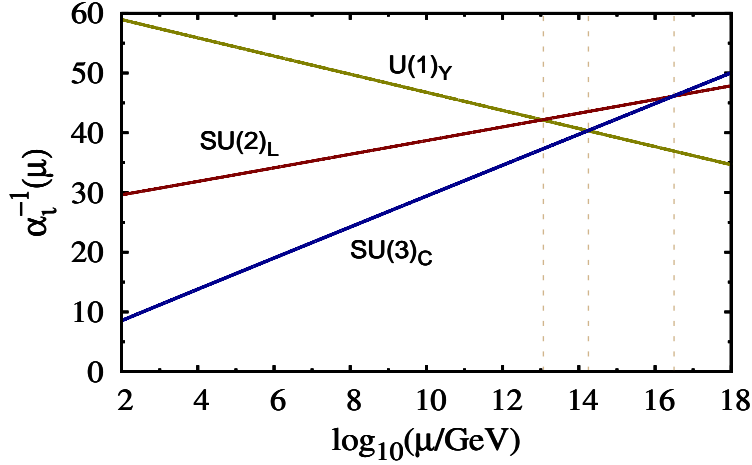


Figure 2.2: Standard Model Gauge coupling running.

$T(R_{SU(2)_L}) = 1/2$ and this isospin fundamental occurs thrice as the dimension of the rest part of the theory, $U(1)_Y \otimes SU(3)_C$, $d_{R_2} = 3$. In the second term the factor $3/5$ is the renormalization factor in redefining the $U(1)_Y$ gauge coupling g' to the new gauge couplings g_1 as $g'Y = g_1T_1$, such that the generator T_1 is normalized to $1/2$ for a fundamental representation of the unifying group. This condition gives $g' = \sqrt{3/5} g_1$. Eventually, the comparison of the RGE of the two gauge couplings g' and g_1 gives $b_1 = (3/5)b_Y$. The term $(1/6)^2$ is the Dynkin index ($T = Y^2$) for $U(1)_Y$ symmetry. This is further multiplied by the dimension ($=6$) coming from remaining symmetry $SU(2)_L \otimes SU(3)_C$. Similarly in the third term we have a $SU(3)_C$ fundamental and the dimension of rest of the theory, $SU(3)_C \otimes U(1)_Y$, $d_R = 3$. At last n_g is the number of flavor generations in the theory for this representation (for SM $n_g = 3$). Similarly we calculate two loop color-color beta coefficient for the above representation, which would be

$$\begin{aligned}
 b_{3C3C} &= \left[\left(\frac{10}{3} C_2(G_1) + 2C_2(R_1) \right) T(R_1) d(R_2) \right] \times n_g \\
 &= \left[\left(\frac{10}{3} \times 3 \times \frac{1}{2} \times 2 \right) + 2 \times \left(\frac{1}{2} \right)^2 \times \frac{8}{3} \times 2 \right] \times 3, \quad (2.24)
 \end{aligned}$$

where $d_{R_1} C_2(R_1) = T(R_1) d_{G_1}$ have been used in the second term. $C_2(G) = 3$, $d_G = 8$ for $SU(3)_C$ and particles are in it's fundamental representation hence $d_{R_1} = 3$ and trivially $d_{R_2} = 2$. Similar calculations will be required for all other representations

present in the theory over all generation of scalars and fermions.

The non-zero contributions of all particles to the gauge couplings at one loop level are depicted in Fig. 2.1. We have listed one and two loop RGE beta coefficient in the first row of the Tab. B.1 in the Sec. A.3.1.

The Fig. 2.2 shows the nature of evolution of gauge couplings assuming the bare SM throughout the range of energy beyond electroweak scale. The meeting of $SU(2)_L$ gauge coupling with $U(1)_Y$ around 10^{13} GeV in Fig. 2.2 is not a viable unification of $SU(2)_L$ and $U(1)_Y$ and is disallowed by proton lifetime constraint.

2.5.2 MSSM gauge coupling running

The SUSY is a symmetry which transforms boson (fermion) in to fermion (boson). SUSY is required in certain kind of theories which integrate gravitation with internal symmetries of Standard Model. Usually, it is introduced at very high energy scales. The emancipation of SM from the fine tuning problem require the SUSY scale at TeV. SUSY pairs fermions and bosons hence every SM fermion is paired with their,

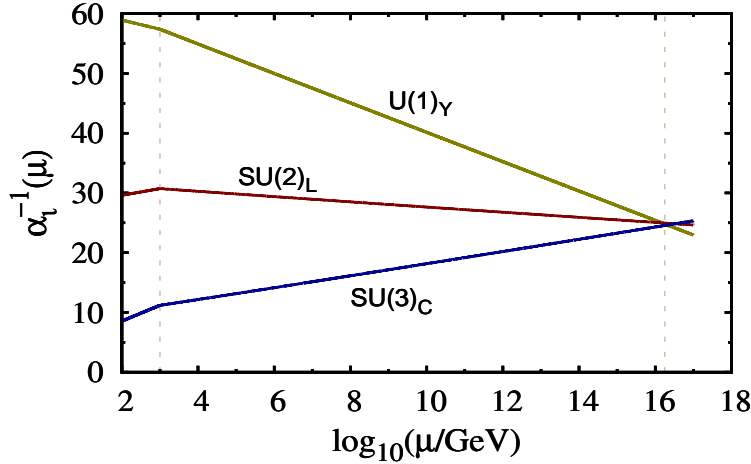


Figure 2.3: Minimal Supersymmetric Standard Model Gauge coupling running.

yet to be discovered, super-partner. Gauge couplings acquire corrections due to super-partners of SM particles present at TeV scale. The gauge coupling meet at a point, around 2×10^{16} GeV. Evolution of gauge couplings is shown in Fig. 2.3 and corresponding one and two loop beta coefficients are listed in Tab. 2.4. Meeting on gauge coupling at a point is a leading motivation for believing the existence of SUSY. To keep the gauge couplings unified beyond the meeting point we need to

MSSM beta coefficients			
b_i	b_{ij}		
$\begin{pmatrix} 33/5 \\ 1 \\ -3 \end{pmatrix}$	$\begin{pmatrix} 199/50 & 27/10 & 44/5 \\ 9/10 & 35/6 & 12 \\ 11/10 & 9/2 & -26 \end{pmatrix}$		

Table 2.4: One and two loop gauge coupling beta coefficients.

embed the MSSM in a higher theory like SUSY $SU(5)$ or $SO(10)$. The ongoing experiments at LHC have constrained the parameter space of MSSM to very limited region [108]. Further extensions in minimal SUSY GUTs will be required to explain neutrino masses.

Grand Unified Theory

3.1 Motivations and Constraints

The plausible convergence of the gauge couplings of SM, Fig. 2.2, is one of the major aesthetic reason to believe in grand unification. Other motivations behind studying the grand unification are: (a) To reduce the number of arbitrary parameters of SM. (b) To address, if not all, some of the deficiencies of SM in a higher symmetry, possibly present at very high energy scale. (c) To find other beyond SM signature of which there have been no experimental evidence, and only bounds are available. The proton decay, LFV, non-unitarity, rare decays, etc. are just few examples from the list.

The basic mathematical requirement for GUT model construction is a simple Lie algebra (G) as the gauge group, similar to SM. This simple group should be large enough to have SM as its subgroup. The total number of commuting generators (\equiv rank of the group) in SM is four. Hence, the G must be a rank ≥ 4 group. All the gauge couplings of theories below GUT symmetry restoration scale become equal to GUT gauge coupling, α_G , and above this scale we have only one gauge coupling α_G . The next requirement is that the reps of GUT model must correctly reproduce the particle content of the observed fermion spectrum of SM. Thus G must posses complex reps, as well as it (or the combination) must be free from anomaly in order not to spoil the renormalizability of GUT by an incompatibility of regularization and gauge invariance. The requirement of complex representation is based on the fact that embedding the known fermions in real representations would require mirror fermions, which must be very heavy making all SM fermions masses close to their scale. The above requirements constrain the possible algebras to $SU(5)$, $SU(6)$, $SO(10)$ and E_6 . The smallest possible unification structure with

rank four is $SU(5)$. The other most popular structure is $SO(10)$ with rank=5. While $SU(5)$ enjoys being smallest and most predictive structure which can give SM after spontaneously breaking it, the $SO(10)$ is the smallest Lie group for which all the SM fermions of one generation can be accommodated in a single anomaly free irreducible representation (16 dimensional spinor), with the natural prediction of right handed neutrino. Having a larger structure $SO(10)$ offers enormous freedom in choosing the symmetry breaking pattern.

The model independent achievements of grand unification theories include: (a) A unique gauge coupling describing nature above the unification scale. (b) Because, quarks and leptons come together in rep(s) of G , the charge quantization is automatically achieved. (c) For the same reason quark-lepton Yukawa couplings get related as a consequence of GUT symmetry constraints. (d) The baryon and lepton number violating super-heavy gauge bosons open the channels for nucleon decay, specifically proton decay. The resolutions of other problems in SM like (i) Fine tuning problem, (ii) Dark matter content of the universe, (iii) Baryonic asymmetry of universe, and (iv) Highly flavored structure of the SM fermions etc. are usually tackled model dependently.

In this report we have focused on $SO(10)$ based models at their variant forms. The subgroups of $SO(10)$ have the simple, $SU(5)$, or direct products of $SU(n)$, $n \geq 2$ and $U(1)$ groups. A short discussions on the properties of $SU(n)$ group is presented in Appendix A.2. The flavor structure of SM fermions is addressed either using the algebra of higher rank symmetry or by introducing additional discrete or continuous symmetries together with above mentioned simple GUT groups.

3.2 $SU(5)$ GUTs

The grand unification theory based on $SU(5)$ was first proposed by Georgi and Glashow in 1974 [50]. The $SU(5)$ group has only four generator in Cartan sub-algebra hence the rank of this group is 4 and the rank of SM is also 4. The adjoint representation is $5^2 - 1 = 24$ dimensional, hence the number of generators and therefore number of gauge bosons is also 24. Because an adjoint representation is a bi-product of fundamental representation and its conjugate representation, $5 \times \bar{5} = 1 + 24$, hence it is an effectively two rank tensor and can be represented in 5×5 matrix form. Only 12 out of 24 gauge bosons belong to SM hence below $SU(5)$ scale only 12, belonging to SM, gauge bosons remain massless while rest acquire GUT scale masses. The fundamental representation, 5, of $SU(5)$ can be

Reps	Origin	Anomaly	SM Decomposition
5	Fund.	1	$(1, -1/3, 3) + (2, 1/2, 1)$
10	$(5 \times 5)_a$	1	$(2, 1/6, 3) + (1, -2/3, \bar{3}) + (1, 1, 1)$
15	$(5 \times 5)_s$	9	$(2, 1/6, 3) + (1, -2/3, 6) + (3, 1, 1)$
24	$(\bar{5} \times 5)_{tr=0}$	0	$(1, 0, 8) + (3, 0, 1) + (2, -5/6, 3) + (2, 5/6, 3) + (1, 0, 1)$

Table 3.1: Simple representations of $SU(5)$ and their decomposition in Standard Model.

decomposed in to $SU(2)_L$ and $SU(3)_C$ like $5 = (2, 1)_{1/2} + (1, 3)_{-1/3}$, where the structures within bracket are fundamental representations of the respective groups and numbers at subscripts are associated hypercharges, such that $\sum Y = 0$ [109], i.e., no hypercharge quantum number in $SU(5)$. Any multiplicative number to the hypercharges is subject to normalization. The 15 Weyl field of each generation of SM can not be put in symmetric representation of $SU(5)$ because Adler anomaly is non-zero for this representation (see Appendix A.1) and this symmetric representation also contains a color sextet of $SU(3)_C$ but, quarks come in color triplet only. The Higgs doublet of SM is put in 5 of $SU(5)$ as $5 = (h_T, H)^T \equiv \Phi$. This whole multiplet has to be charge less hence each colored scalar acquires $Y = Q_{EM} = -1/3$. Weyl field are put in the form

$$\bar{5}_F = \begin{pmatrix} d^C \\ \epsilon_2 L \end{pmatrix}_L, \quad 10_F = \begin{pmatrix} \epsilon_3 u^C & Q \\ -Q^T & \epsilon_2 e^C \end{pmatrix}_L \quad (3.1)$$

Here the superscript C means the charge conjugation, $\epsilon_2 A = \epsilon_{ij} A_j$ and $\epsilon_3 A = \epsilon_{ijk} A_k$. The ϵ_2 and ϵ_3 are the two and three index Levi-Civita antisymmetric tensors in $SU(2)_L$ and $SU(3)_C$ basis, respectively. Expanding the eq. (3.1) we get

$$\epsilon_2 e^C = \begin{pmatrix} 0 & e^C \\ -e^C & 0 \end{pmatrix}, \quad \epsilon_2 L = \begin{pmatrix} e \\ -\nu_e \end{pmatrix} \quad \& \quad \epsilon_3 u^C = \begin{pmatrix} 0 & u_b^C & -u_g^C \\ -u_b^C & 0 & u_r^C \\ u_g^C & -u_r^C & 0 \end{pmatrix} \quad (3.2)$$

$$SU(5) \rightsquigarrow \begin{pmatrix} SU(3) \\ SU(2) \end{pmatrix}, \quad SU(5) \rightsquigarrow \left(\frac{SU(3)_C}{SU(3)_C \otimes SU(2)_L} \middle| \frac{SU(3)_C \otimes SU(2)_L}{SU(2)_L} \right) \quad (3.3)$$

The distribution of $SU(5)$ in to $SU(3)$ and $SU(2)$ substructures for one and two index tensors is symbolically depicted in eq. (3.3), where the $U(1)_Y$ quantum numbers

are ignored. From the Tab. 3.1 we see that decomposition of any of the $SU(5)$ representation smaller than adjoint (24) do not have SM singlet. Therefore, the smallest scalar multiplet which can break $SU(5)$ in to SM has to be the adjoint ($24_H \equiv \Sigma$) representation. Others will simply break the SM as well, or more critically the color symmetry $SU(3)$. A detail analysis of spontaneous symmetry breaking of $SU(n)$ can be found in [110, 111]. The minimal $SU(5)$ is considered as a prototype GUT model to depict the strength and limitations of grand unification and is a text book material today and has been addressed in [112–115] in good detail. Assigning VEV along the off diagonal fields of adjoint representation will again break both $SU(3)_C$ and $SU(2)_L$. Hence, we have the only choice of assigning VEV, which commutes with the generators of $SU(3)$ and $SU(2)$, is

$$\langle \Sigma \rangle \propto \left(\begin{array}{c|c} 2 \times \mathbf{1}_3 & 0 \\ \hline 0 & -3 \times \mathbf{1}_2 \end{array} \right) v_\Sigma. \quad (3.4)$$

Hence leaving the symmetry $SU(3)_C \otimes SU(2)_L$ preserved. Given the correct normalization factor, this VEV mimics exactly the hypercharge quantum numbers, hence also leaving the $U(1)_Y$ symmetry intact.

The most general potential, with additional simplifying Z_2 symmetry $\Sigma = -\Sigma$, which plays the role in the breaking of $SU(5)$ is

$$V(\Sigma) = -\frac{\mu^2}{2} \text{Tr} \Sigma^2 + \frac{\lambda}{4} \text{Tr} \Sigma^4 + \frac{\lambda'}{4} (\text{Tr} \Sigma^2)^2. \quad (3.5)$$

where Σ can be also expanded as

$$\Sigma = \left(\begin{array}{c|c} \Sigma_O(1, 0, 8) & \Sigma_X(2, -5/6, 3) \\ \hline \Sigma_{\bar{X}}(2, 5/6, \bar{3}) & \Sigma_T(3, 0, 1) \end{array} \right) + \Sigma_S \langle \Sigma \rangle. \quad (3.6)$$

Putting the VEV $\langle \Sigma \rangle$ in the eq. (3.5) and estimating the mass term, we get scalar masses

$$m_O^2 = \frac{\lambda}{6} v_\Sigma^2, \quad m_T^2 = \frac{2\lambda}{3} v_\Sigma^2, \quad m_S^2 = 2\mu^2, \quad m_{X, \bar{X}} = 0. \quad (3.7)$$

Therefore, $\lambda > 0$ is required to get an stable and viable solution. These twelve massless scalar bosons $\Sigma_{X, \bar{X}}$ are the Goldstone modes of the theory, which must be swallowed by twelve gauge bosons. The kinetic part of the Higgs under investigation will contribute to the masses of gauge bosons. The covariant derivative for Σ particles is

$$D_\mu \Sigma = \partial_\mu \Sigma + ig_5 [A_\mu, \Sigma] \quad (3.8)$$

where

$$A_\mu = \left(\begin{array}{c|c} G(1, 0, 8) & (X, Y)(2, -5/6, 3) \\ \hline (\bar{X}, \bar{Y})(2, 5/6, \bar{3}) & W(3, 0, 1) \end{array} \right)_\mu + B_\mu, \quad (3.9)$$

and $A_\mu = \sum_{a=1}^{24} A_\mu^a T^a$ is assumed. As per design, $\langle \Sigma \rangle$ commutes with the generators belonging to SM. Hence, the gluons G_μ , weak bosons W_μ , and Hyper gauge boson B_μ stay massless at the $SU(5)$ breaking scale. However, the generators associated with twelve heavy gauge bosons, $(X, Y)_\mu \equiv (2, -5/6, 3)$ and their conjugates, do not commute with the VEV $\langle \Sigma \rangle$ and therefore acquire the GUT scale, $\mathcal{O}(v_\Sigma)$, masses. These gauge bosons were required to be very heavy because they couple quarks with leptons through fermion–gauge boson–fermion interactions, violating baryon (B) and lepton (L) numbers (though accidentally preserving $B - L$) at the vertices. Therefore they mediate the nucleon decay processes. To satisfy the present bound on proton decay life time, masses of these gauge bosons must be $\geq 10^{15.5}$ GeV.

The possible scalar multiplets which can generate the fermion masses can be found from the decompositions of matter bilinears

$$\bar{5} \times \bar{5} = \bar{10} + \bar{15}, \quad \bar{5} \times 10 = 5 + \bar{45}, \quad 10 \times 10 = \bar{5} + 45 + 50. \quad (3.10)$$

Not all the multiplets in the right hand side are allowed because $\bar{5}_F$ contains only one chiral component of the matter field hence Dirac mass term are not permitted. Hence, only $5_H, 45_H$ and 50_H are the possible candidates for generating masses of SM fermions. On the other hand 10_H and 15_H may give Majorana term, helpful for seesaw mechanism. In the minimal model, with only 5 as the Higgs boson, the Yukawa Lagrangian is

$$\mathcal{L}_Y = Y_{\bar{5}_F}^i C 10_{Fij} \bar{5}_H^j + \epsilon^{ijklm} 10_{Fij} C Y_{10} 10_{Fkl} 5_{Hm}. \quad (3.11)$$

Here we have ignored the generation index over the fermions. With three generations known in nature the Yukawa matrices $Y_{\bar{5},10}$ are 3×3 complex matrices. With $\langle \Phi \rangle = (0, 0, 0, 0, v_{EW})^T$, we get the masses of fermions. But, $\langle \Phi \rangle$ preserves the $SU(4)$ symmetry so down quark and lepton masses are related at GUT scale. Also using the properties of antisymmetry of Levi-Civita tensor we get

$$Y_d = Y_e^T \quad \text{and} \quad Y_u = Y_\nu^T. \quad (3.12)$$

The above relations do not fit with the experimental findings. The model also fails in predicting the Weinberg angle, i.e. gauge couplings do not unify at any energy.

On the other hand, the quantization of electric charge finds trivial explanation from the group algebra.

The minimal $SU(5)$ is an extremely predictive model with failed promises. Various extensions of minimal $SU(5)$ model have been popular to explain both experimental as well as philosophical questions. The gauge coupling unification is achieved in its SUSY extensions [116,117], together with the solution to hierarchy problem and the possibility of dark matter candidate. But this extension solicits the incorporation of neutrino mass generating extensions. On the other hand, the adjoint fermionic extension to the minimal $SU(5)$ model gives few-hundred GeV scale type-I+III see-saw, called Adjoint $SU(5)$ model [118,119]. Major problem with such extensions of $SU(5)$ models is that very often we need to make additional fine tuning to generate different mass scales for the particle with different SM quantum numbers but sitting in the same $SU(5)$ multiplet (For example: the triplet color Higgs, h_T , can mediate the proton decay hence has to be very heavy closer to GUT scale). This is either done by adding extra multiplets [120] in the theory or by introducing higher dimensional operators [118,119]. The discussion on minimal $SU(5)$ teaches us about the implementation of some crucial checks on GUT models to confirm its viability.

Any unification model based on $SU(5)$ does not satisfactorily predict the family structure of fermions. There is no chiral symmetry in $SU(5)$ at any scale. There is no prediction for RH neutrinos. Also, $SU(5)$ does not explain nature favoring $(V - A)$ current over $(V + A)$.

3.3 $SO(10)$ GUTs

The next, most popular, candidate gauge group for grand unification is $SO(10)$, first proposed by Fritzsch and Minkowski [54] and Georgi [52]. With one unit larger rank ($=5$), the theory is phenomenologically more attractive due to larger degrees of freedom. All the SM fermions, together with an additional SM singlet, of one generation are beautifully accommodated in a single 16 dimensional, irreducible, spinor representation. The additional SM singlet is identified as the right handed neutrino. This is where $SO(10)$ fits perfectly, for it unifies matter besides the interaction. The theory also suggest the LR symmetry of universe prior to any symmetry breakdown, which may give platform to explain the favor of $(V - A)$ current over $(V + A)$ at low energies.

The special orthogonal group $SO(10)$ is a group of 10×10 real orthogonal matrices, O obeying $OO^T = O^T O = 1$, with $\text{Det}(O) = 1$. The algebra of $SO(N)$ has been

extensive discussed in text books [112–114]. For the sake of completeness, a small recapitulation of the properties of special orthogonal groups is given in Appendix A.4. Since the low energy theory is based on unitary gauge groups, the $SO(10)$ invariants must be re-casted in to the unitary maximal subgroups. The two maximal subgroups of $SO(10)$ are $SU(5) \times U(1)$ and $SU(2)_L \times SU(2)_R \times SU(4)_C \cong SO(4) \times SO(6)$. The decomposition of $SO(10)$ algebra in the basis of $SU(5) \times U(1)$ and $SU(2)_L \times SU(2)_R \times SU(4)_C$ have been extensively discussed in [121,122] and [123], respectively. For the sake of completeness we have listed the table of decompositions of $SO(10)$ irreducible representations up to 210 in to various subgroups, from [124], in the Appendix B.2. The decomposition of $SO(10)$ invariants in to Pati-Salam symmetry has been extensively studied in [124, 125].

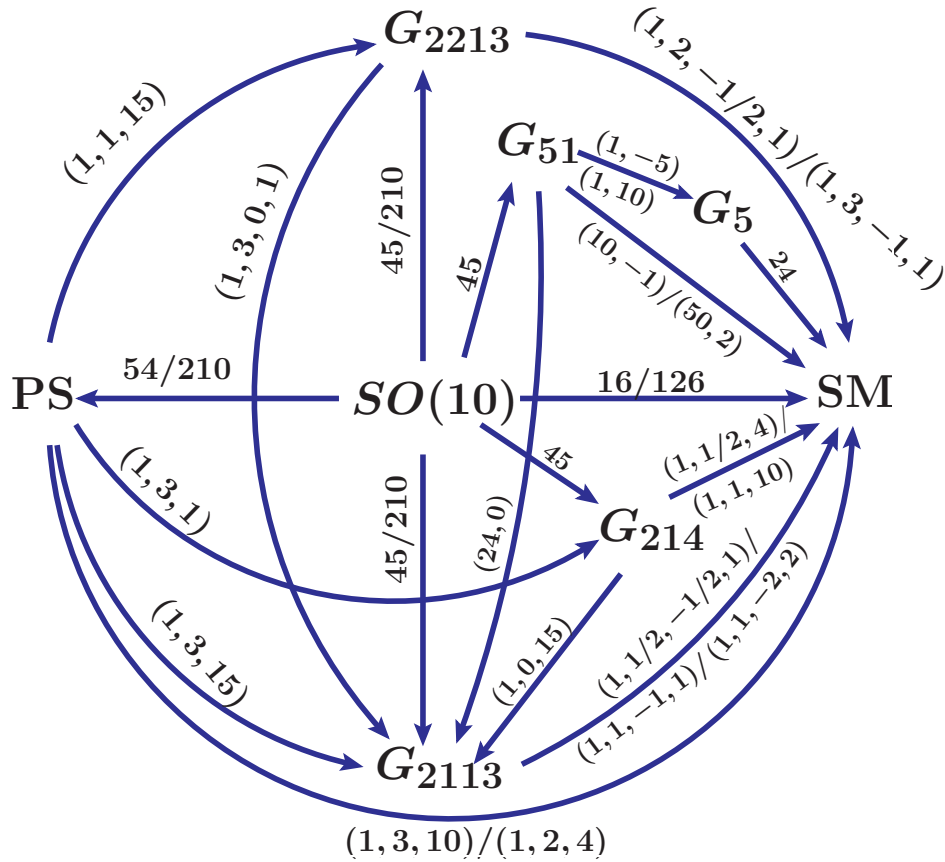


Figure 3.1: The most popular and physically viable breaking chains of $SO(10)$ down to the SM [52, 58, 126–129].

Forty five dimensional adjoint representation are orthogonal matrices with unity determinant. Because $SO(10)$ is a large symmetry, there can be many subgroups which are larger than SM and accommodate the structure of SM. The symmetries of

these subgroups may appear at intermediate energy scales, unlike the $SU(5)$ GUT where we had one and only one way to reach SM. The most popular breaking schemes of $SO(10)$ to SM are depicted in Fig. 3.1, where

$$\begin{aligned}
G_{13} &= U(1)_Q \otimes SU(3)_C \\
G_{5/51} &= SU(5)/SU(5) \otimes U(1)_X \\
G_{213} &= SU(2)_L \otimes U(1)_Y \otimes SU(3)_C \quad (\text{SM}) \\
G_{214} &= SU(2)_L \otimes U(1)_X \otimes SU(4)_C \\
G_{224} &= SU(2)_L \otimes SU(2)_R \otimes SU(4)_C \quad (\text{PS}) \\
G_{2113} &= SU(2)_L \otimes U(1)_{B-L} \otimes U(1)_R \otimes SU(3)_C \\
G_{2213} &= SU(2)_L \otimes SU(2)_R \otimes U(1)_{B-L} \otimes SU(3)_C \quad (\text{LR}) \\
G_{2213D} &= G_{2213} \otimes D \quad (\text{LRD}), \quad G_{224D} = G_{224} \otimes D(\text{PSD}), \quad (3.13)
\end{aligned}$$

and the scalar multiplets sitting near the arrows if given VEV will break the symmetries at the tail in to symmetries at the head. The $SO(10)$ origin of these multiplets can be found from the decomposition tables and are re-listed in Tab. 3.2 The SSB of $SO(10)$ to G_{224D} can be achieved by D -even PS singlet residing in 54 [58, 130, 131], while breaking to G_{224} is achieved by D -odd PS singlet residing in 210 [56, 57]. Also, the SSB of $SO(10)/\text{PS}$ D -even symmetry to G_{2213D} is achieved by D -even LR singlet residing in $210/(1, 1, 15)$ [132], while breaking of $SO(10)$ or PS symmetry (D -odd or even) to G_{2213} is achieved by D -odd LR singlet residing in $45/(1, 1, 15)$ [130, 131, 133]. Rest of the sub-algebras are D -parity broken, and the scalar multiplets breaking these sub-algebras are depicted in Fig. 3.1 and their $SO(10)$ origin can be read from the Tab. 3.2. Under the assumption of *extended survival hypothesis*, particles residing only in these representation acquire the masses of the order of symmetry breaking scale. For example 54 scalar breaks $SO(10)$ in to G_{224D} at GUT scale and does not participate in any breaking further hence all the scalars in 54 get the masses of $\mathcal{O}(M_{GUT})$. Similarly when $(1,3,1)$ of 45 breaks PS symmetry to G_{214} or $(1,3,15)$ of 210 breaks PS symmetry to G_{2113} the scalar particles residing in these multiplets $(1,3,1)$ and $(1,3,15)$ acquire the masses of PS (whether D -odd or even) breaking scale.

Once the additional symmetries are included to populate the grand desert, SUSY is not necessarily required for unification of gauge couplings. In addition, with intermediate gauge symmetries $SO(10)$ also predicts signals of new physics which can be probed at low or accelerator energies. The left-right (LR) [48, 55] symmetry is a finite gauge transformation under charge conjugation. Through Pati-Salam [46]

$(\mathbf{1}, -5)_{G_{51}} \subset \mathbf{16}$
$(\mathbf{1}, 10)_{G_{51}} \subset \overline{\mathbf{126}}$
$(\mathbf{24}, 0)_{G_{51}} \subset \mathbf{45}, \mathbf{210}$
$(\mathbf{1}, \mathbf{1}, -2, 2)_{G_{2113}} \subset (\mathbf{50}, 2)_{G_{51}} \subset \overline{\mathbf{126}}$
$(\mathbf{1}, \mathbf{1}, 1, -1)_{G_{2113}} \subset (\mathbf{10}, -1)_{G_{51}} \subset \mathbf{16}$
$(\mathbf{1}, \mathbf{1}, \mathbf{15})_{G_{224}} \subset \mathbf{45}, \mathbf{210}$
$(\mathbf{1}, \mathbf{3}, 0, \mathbf{1})_{G_{2213}} \subset (\mathbf{1}, \mathbf{3}, \mathbf{1})_{G_{224}} \subset \mathbf{45}$
$(\mathbf{1}, 0, \mathbf{15})_{G_{214}} \subset (\mathbf{1}, \mathbf{3}, \mathbf{15})_{G_{224}} \subset \mathbf{210}$
$(\mathbf{1}, \mathbf{3}, 0, \mathbf{1})_{G_{2213}} \subset (\mathbf{1}, \mathbf{3}, \mathbf{15})_{G_{224}} \subset \mathbf{210}$
$(\mathbf{1}, \mathbf{1}, -1, \mathbf{1})_{G_{2113}} \subset (\mathbf{1}, \mathbf{1}, \mathbf{10})_{G_{214}} \subset (\mathbf{1}, \mathbf{3}, \mathbf{10})_{G_{224}} \subset \overline{\mathbf{126}}$
$(\mathbf{1}, \mathbf{1}, -1, \mathbf{1})_{G_{2113}} \subset (\mathbf{1}, \mathbf{3}, -1, \mathbf{1})_{G_{2213}} \subset (\mathbf{1}, \mathbf{3}, \mathbf{10})_{G_{224}} \subset \overline{\mathbf{126}}$
$(\mathbf{1}, 1/2, -1/2, \mathbf{1})_{G_{2113}} \subset (\mathbf{1}, 1/2, \mathbf{4})_{G_{214}} \subset (\mathbf{1}, \mathbf{2}, \mathbf{4})_{G_{224}} \subset \overline{\mathbf{16}}$
$(\mathbf{1}, 1/2, -1/2, \mathbf{1})_{G_{2113}} \subset (\mathbf{1}, \mathbf{2}, -1/2, \mathbf{1})_{G_{2213}} \subset (\mathbf{1}, \mathbf{2}, \mathbf{4})_{G_{224}} \subset \overline{\mathbf{16}}$

Table 3.2: The multiplets participating in SSB by acquiring VEVs in the invariant direction of the residual symmetry. The bold numbers correspond to dimension of representation of associated non-abelian symmetry and normals are quantum numbers of abelian symmetry. Upper block depicts the $SU(5)$ way of breaking and lower block depicts the Pati-Salam line of breaking.

intermediate symmetry left-right symmetry is realized and the parity violation at low energy is understood as an artifact of the breaking of the left-right symmetry.

We note from the Tab. B.4 to Tab. B.10 that all representations except 10 and 120 contain SM singlets, but not all of them break $SO(10) \rightarrow \text{SM}$ in a single step. The SM singlets of representations 45, 54 and 210 are also singlets of higher symmetry, so assigning VEV to the scalar fields in these representations will break $SO(10)$ to the corresponding higher symmetry. On the other hand, if SM singlets of $\overline{\mathbf{16}}$ and $\overline{\mathbf{126}}$ are assigned a VEV the symmetry of $SO(10)$ will spontaneously break to SM. If an intermediate symmetry is at work then sub-multiplets of $\overline{\mathbf{16}}$ and $\overline{\mathbf{126}}$ under the intermediate symmetry having SM singlets will do the job. The gauge coupling

unification in non-SUSY $SO(10)$ grand unification desperately demands the presence of intermediate symmetries. Hence we require a combination of the appropriately chosen multiplets to generate the breaking mechanism under study.

In the SUSY version of $SO(10)$, if $R [= (-1)^{3(B-L)+2S}]$ parity remains an exact symmetry at all scales the lightest SUSY partner will be stable, which may be an ideal candidate for the dark matter of the universe. Under R -parity $p \rightarrow p$ and $\tilde{p} \rightarrow \tilde{p}$, where p stands for particle and \tilde{p} for its super-partner. The matter parity $M = (-1)^{3(B-L)}$ is obviously equivalent to the R -parity, because $(-1)^{2S} = 1$ for the physical Hamiltonians and only scalars with $S = 0$ are allowed to have non vanishing VEVs. Under matter parity $16 \rightarrow -16$ and $10 \rightarrow 10$. All other relations build out of 10, such as 45, 54, 120, 126, 210 etc., are even. Only representations with spinor content like 16, 144 etc. will be odd.

The decomposition of $SO(10)$ spinor multiplet 16_F in to SM fermions plus additional RH neutrino is expressed as as

$$16_F = \left(2, \frac{1}{6}, 3\right) + \left(2, -\frac{1}{2}, 1\right) + \left(1, -\frac{2}{3}, \bar{3}\right) + \left(1, \frac{1}{3}, \bar{3}\right) + (1, 1, 1) + (1, 0, 1)$$

$$Q_L \quad L_L \quad u_L^C \quad d_L^C \quad e_L^C \quad \nu_L^C. \quad (3.14)$$

In the $SU(5)$ and PS basis this can be equivalently written as

$$16_F \equiv \bar{5}_F \oplus 10_F \oplus 1; \quad SU(5)$$

$$\equiv (2, 1, 4) \oplus (1, 2, \bar{4}); \quad \text{PS}. \quad (3.15)$$

The interesting features of $SO(10)$ GUTs is that the Majorana masses are dictated by Yukawa couplings and the SSB pattern implemented for gauge coupling unification. Since, the $SO(10)$ symmetry does not distinguish among the components of the decomposition, see eq. (3.15), the Yukawa couplings for neutrinos are closely related to charged fermions. The Yukawa Lagrangian which generates masses to the 16_F fermions of the model must have scalars in 10, 120 and $\overline{126}$ representations, in general, because

$$16 \otimes 16 = 10_s \oplus 120_{as} \oplus 126_s. \quad (3.16)$$

We can see that SM Higgs doublets are also present in these representations which further break SM in to $U(1)_Q \times SU(3)_C$. A realistic $SO(10)$ GUT framework allows proper SSB of $SO(10)$ down to SM, and gauge and Yukawa interactions must be compatible with the current experimental results on quark and lepton masses and mixings. In (non-)SUSY case, at least (two)three Higgs representations are required

to break $SO(10)$ down to $U(1)_Q \times SU(3)_C$, the low energy theory. The two multiplets which can break $SO(10)$ down to SM directly are 16_H and 126_H , but SM singlets of these representations are incapable of breaking the $SU(5)$ symmetry. It is easy to see in the decomposition of 16_H in $SU(5)$ basis that the only singlet of SM is also singlet of $SU(5)$. Therefore, we need additional representations. If we demand the $SU(2)_L \times SU(2)_R$ as an intermediate symmetry we need a real representations, 45_H , 54_H or 210_H etc. which have invariants of the handedness. If the BSM models are SUSY preserving the 45_H together with only 16_H or 126_H is not a good choice because vacuum aligns in $SU(5) \times U(1)$ direction [134–136]. Even in non-SUSY $SO(10)$ scenario this is true at tree level [130,131,133,137,138], but has been rectified in radiative corrections [139].

The scalar multiplets which couple to fermionic bilinears $10_H, 120_H$ and $\overline{126}_H$ contain the SM like Higgs doublets. There can be $SU(2)_L$ Higgs doublets coming from the representations which do not directly couple to fermionic bilinears. Their superposition gives effective SM light Higgs doublet which can acquire electroweak VEV. A nice and detail description can be found in [124].

Advantages of using $SO(10)$ over $SU(5)$ are: a) A single family of fermions are accommodated in a single 16-dimensional spinorial representation of $SO(10)$, with a prediction of right-handed neutrino. b) Both left and right handed fermions reside in a single representation, hence, left-right symmetry can be achieved through a finite gauge transformation in the form of charge conjugation. Thus the parity symmetry is a part of continuous symmetry. c) Besides $SU(5) \times U(1)$, its other maximal subgroup is Pati-Salam symmetry, which explains the mysterious relation $m_d = m_e/3$, up to certain extent. d) The gauge coupling unification can be achieved through intermediate symmetry even if the SUSY is absent. e) In the SUSY version, matter parity $M = (-1)^{B-L}$ is equivalent to the R -parity, $R = M(-1)^{2S}$ is a gauge transformation. It is possible to keep R intact if $SO(10)$ symmetry is broken appropriately.

3.4 Majorana neutrinos and seesaw mechanism

Since, the neutrinos are electrically neutral they can be Dirac or Majorana fermions. If they are complex four component Dirac fields, as charge fermions, then neutrinos (ν) and antineutrinos ($\bar{\nu}$) would have same mass but opposite lepton number therefore ν -mass Lagrangian would be lepton number conserving. There is no lepton number preserving symmetry in the SM. Violation of this accidental symmetry

will allow the Majorana mass term in the Lagrangian, and neutrinos would be two component Majorana fields.

Extending the SM with three right handed singlet field ν_R we write Dirac mass Lagrangian

$$\mathcal{L}^D = -\bar{\nu}_L M_D \nu_R + h.c. \quad (3.17)$$

where $M_D = Y_\nu v_{EW}$, and v_{EW} is electroweak VEV. For neutrinos to be as light as 1 eV, $Y_\nu \sim \mathcal{O}(10^{-12})$, which is extremely tiny and leads to fine tuning problem in the theory. On the other hand Majorana mass term can be written as

$$\mathcal{L}^M = -\frac{1}{2}\bar{\nu}_L M_L^M \nu_L^C + h.c. \quad (3.18)$$

The smallness of M_L has also to be explained. With two lepton doublets, we need to make this term gauge and Lorentz invariant. The most elegant way to explain this is the seesaw mechanism [59]. From within the SM, Yukawa interactions augmented by higher dimensional terms are written like dimension-5 Weinberg operator [140]

$$\mathcal{L}_Y(d=5) = \lambda_{ij} \frac{(l_L^T i \sigma_2 H) C (H^T i \sigma_2 l_L j)}{M_\Lambda} \quad (3.19)$$

where M_Λ is the cut-off scale of the theory, λ is couplings strength and i, j are flavour indices. When H acquires VEV we get

$$M_L^M = \lambda \frac{v_{EW}^2}{M_\Lambda}. \quad (3.20)$$

The other non-vanishing contributions, ignoring Lorentz index, can be

$$(l_L^T \sigma_2 \vec{\sigma} l_L) (H^T \sigma_2 \vec{\sigma} H) \quad (3.21)$$

$$(l_L^T \sigma_2 \vec{\sigma} H) (H^T \sigma_2 \vec{\sigma} l_L) \quad (3.22)$$

Closer look at the eq. (3.19), eq. (3.21) and eq. (3.22) suggests that the renormalizable Yukawa term with extended particle structure can reproduce the dim=5 invariants if heavy modes are integrated out of

$$(l_L^T \sigma_2 H) \nu_R, (l_L^T \sigma_2 \vec{\sigma} l_L) \vec{\Delta}, \text{ \& } (l_L^T \sigma_2 \vec{\sigma} H) \vec{\rho}, \quad (3.23)$$

where ν_R , Δ and ρ are SM singlet fermion, $SU(2)_L$ triplet (3,1,1) scalar and $SU(2)_L$ triplet (3,0,1) fermion, respectively, under $SU(2)_L \times U(1)_Y \times SU(3)_C$. The masses of these BSM particles are the cut-off scale. Integrating out the heavy modes generates

the non-zero masses for light neutrinos and this mechanism to generate the masses for neutrinos is known as seesaw mechanism. These three types of generating masses of neutrinos are called type-I [59–63], type-II [118, 119, 141] and type-III [64–67] seesaw, respectively.

With a gauge singlet chiral fermion per generation, the renormalizable Yukawa coupling follows

$$\Delta\mathcal{L} = Y_\nu \bar{l}_L \sigma_2 H^* \nu_R + \frac{M_R}{2} \nu_R^T C \nu_R + h.c. \quad (3.24)$$

with $\nu \equiv \nu_L + C\bar{\nu}_L^T$ and $N \equiv \nu_R + C\bar{\nu}_R^T$ we get the total mass matrix of neutral Lagrangian

$$M_\nu = \begin{pmatrix} 0 & M_D^T \\ M_D & M_R \end{pmatrix} \equiv U_\nu \begin{pmatrix} m_\nu & 0 \\ 0 & M_h \end{pmatrix} U_\nu^T, \quad (3.25)$$

where M_ν, U_ν are 6×6 matrices and rest of the matrices in eq. (3.25) are 3×3 . For $M_D \ll M_R$ we have predominantly Majorana case such that the block diagonalized matrices are

$$m_\nu \simeq -M_D \frac{1}{M_R} M_D^T \quad \& \quad M_N \simeq M_R. \quad (3.26)$$

This is the canonical or type-I seesaw.

Now, if instead of fermionic singlet we have a scalar triplet, the relevant Yukawa part of Lagrangian is

$$\Delta\mathcal{L} = Y_\Delta^{ij} l_{L_i}^T C \sigma_2 \Delta_L l_{L_j} + h.c. \quad (3.27)$$

and the associated scalar potential term is

$$\Delta V = \mu_\Delta H^T \sigma_2 \Delta_L^* H + M_\Delta^2 \text{Tr} \Delta_L^\dagger \Delta_L + .. \quad (3.28)$$

where $\mu_\Delta \sim \mathcal{O}(M_\Delta)$ and $\Delta = \vec{\sigma} \cdot \vec{\Delta}$. The VEV $\langle \Delta \rangle$ results from cubic scalar part of the Lagrangian. Neutrinos get the mass

$$m_\nu = Y_\Delta \langle \Delta \rangle \quad (3.29)$$

with $\langle \Delta \rangle \simeq \frac{\mu_\Delta v_{EW}^2}{M_\Delta^2}$. This is known as type-II seesaw mechanism.

Similarly, addition of a triplet fermion gives the Lagrangian

$$\Delta\mathcal{L} = Y_\rho l_L^T C \sigma_2 \rho H + M_\rho \vec{\rho}^T C \vec{\rho} \quad (3.30)$$

where $\rho = \vec{\sigma} \cdot \vec{\rho}$ and the mass M_ρ is the scale of new physics. Similar to type-I

seesaw for $M_\rho \gg v_{EW}$

$$m_\nu = -Y_\rho \frac{1}{M_\rho} Y_\rho^T v_{EW}^2. \quad (3.31)$$

This mechanism to generate light neutrino masses is called type-III seesaw. While in type-II seesaw only one Δ is enough to get the general neutrino mass matrix, in type-I (III) seesaw the number of required singlet (triplet) is same as required number of non-zero light masses, i.e. at least two.

In the GUT framework, the multiplets giving type-II and type-III seesaw are part of larger representations. For example in $SU(5)$ GUTs the triplet scalar of SM giving type-II seesaw is a part of the symmetric representation of $SU(5)$, the triplet SM fermion giving type-III seesaw is a part of adjoint of $SU(5)$, as we can see in Tab. 3.1. The singlet fermion giving type-I may be part of some GUT multiplet or it may stay singlet of GUT as well. In $SO(10)$ we already have the additional fermion singlet as part of the fermionic family. The triplet scalars (vectors) giving type-II (III) seesaw come from $\overline{126}_H$ and 45_F multiplets. The advantage of $SO(10)$ over $SU(5)$ is that since extra fermion is part of the same multiplet as other SM fermions, the neutrino Dirac mass matrix is strongly correlated with the mass matrices of other fermions.

LHC testable inverse seesaw in non-SUSY $SO(10)$

An evidence of SUSY at the LHC would be a land-mark discovery which would certainly change the future course of physics. In this context, recently realization of TeV scale inverse seesaw mechanism in SUSY $SO(10)$ framework has led to a number of experimentally verifiable predictions including low-mass W_R^\pm and Z' gauge bosons and non-unitarity effects. But, in the absence of any evidence of SUSY so far, it is worth while to explore new physics prospects of non-SUSY GUTs, specially based upon $SO(10)$ for the reasons discussed in the previous chapter. In fact neither seesaw mechanism, nor grand unification require SUSY per se.

In this chapter our purpose is to explore how a TeV scale inverse seesaw mechanism for neutrino masses which is different from conventional seesaw mechanisms in implemented in $SO(10)$ based model. This inverse seesaw also has the potential to be experimentally verified because of the low scale at which it can operate. The residual of symmetry $SO(10)$ is a low-mass Z' boson accessible to LHC. We estimate leptonic non-unitarity effects measurable at neutrino factories and lepton flavor violating decays expected to be probed in near future. Other predictions on branching ratios and CP -violating parameters are discussed. The best identified minimal model is accessible to ongoing search experiments for the decay $p \rightarrow e^+\pi^0$.

This chapter is organized in the following manner. In Sec. 4.1 we briefly discuss the model and carry out gauge coupling unification and proton lifetime predictions in Sec. 4.2. A brief explanation of inverse seesaw mechanism in Sec. 4.3. In Sec. 4.4 we discuss RGE of fermion masses and mixings to the GUT scale in the presence of non-SUSY gauge theories G_{2113} and G_{2213} at intermediate scales. In this section we also show how fermion masses are fitted at the GUT scale and information on the Dirac neutrino mass matrix is obtained. Non-unitarity effects are discussed in Sec. 4.5 with

predictions on the moduli of relevant matrix elements. In Sec. 4.6 we give predictions on CP -violating parameters and LFV where we also discuss possible limitations of the present models. In Sec. 4.7 we provide a brief summary and discussion. In the Tab. B.1 of Appendix B we have also provided beta function coefficients for gauge coupling unification while in Appendix C we summarize derivations of RGEs for fermion masses and mixings.

4.1 The Model

There has been extensive investigation on physically appealing intermediate scale models [56–58, 81, 83, 127] in non-SUSY $SO(10)$. Although in the minimal two step-breaking of non-SUSY $SO(10)$ models [83] we found no suitable chain with a sufficiently low scale to implement the inverse seesaw, the following chain with two intermediate gauge symmetries appears to be quite suitable,

$$SO(10) \xrightarrow[45_H/210_H]{M_{GUT}} G_{2213}/G_{2213D} \xrightarrow[45_H]{M_R^+} G_{2113} \xrightarrow[16_H]{M_R^0} \text{SM} \\ \xrightarrow[10_H]{M_Z} U(1)_Q \times SU(3)_C (G_{13}). \quad (4.1)$$

Model-I: G_{2213} ($g_{2L} \neq g_{2R}$) is realized by breaking the GUT-symmetry and by assigning VEV to the D -Parity odd singlet in 45_H [56, 139].

$$(1, 1, 0, 1) \subset (1, 1, 15) \subset 45$$

where convention is taken as $G_{2213} \subset G_{224} \subset SO(10)$ and first two are named as left-right and Pati-Salam symmetries. As the left-right discrete symmetry is spontaneously broken at the GUT scale, the Higgs sector becomes asymmetric below $\mu = M_{GUT}$ causing inequality between the gauge couplings g_{2L} and g_{2R} . The second step of symmetry breaking takes place by the right-handed Higgs triplet $\sigma_R^0(1, 0, 0, 1) \subset \sigma_R(1, 3, 0, 1) \subset (1, 3, 1) \subset 45_H$. The third step of breaking to SM takes place by $\chi^0(1, 0, 1) \subset \chi(1, -1/2, 1/2, 1) \subset (1, 2, 1/2, 1) \subset (1, 2, \bar{4})$. The well known SM breaking to low energy symmetry by the SM Higgs doublet contained in the bi-doublet $(2, 2, 0, 1)$ under G_{2213} originates from 10_H of $SO(10)$. We assume these doublets to originate from two separate bi-doublets contained in 10_H^a ($a = 1, 2$) [45, 142]. Implementation of inverse seesaw also requires the minimal extension by adding three $SO(10)$ -singlet fermions S_i ($i = 1, 2, 3$), one for each generation [143, 144].

Model-I': G_{2213D} ($g_{2L} = g_{2R}$) is realized by breaking the GUT symmetry by the

VEV of the G_{2213} -singlet $(1, 1, 0, 1) \subset 210_H$ which is even under D -parity [56]. For the sake of simplicity we treat the rest of the symmetry breaking patterns of Model-I' similar to Model-I.

4.2 Gauge coupling unification and proton decay

In this section we examine gauge coupling unification in the minimal Model-I and the minimal Model-I' and make predictions on proton lifetimes while we also predict the corresponding quantities in their simple extensions.

4.2.1 Unification in minimal models

It was shown in [57] that with G_{2113} gauge symmetry at the lowest intermediate scale in $SO(10)$ there is substantial impact of two-loop effects on mass scale predictions in a number of cases. The one-loop and the two-loop beta-function coefficients for the evolution of gauge couplings [51, 107] for Model-I and Model-I' with two Higgs doublets for each case are given in Tab. B.1 of Appendix B. We have also included small mixing effects [127, 145–148] due to two abelian gauge factors $U(1)_R \times U(1)_{(B-L)}$ in both the models below the M_R^+ scale. Using [149, 150]

$$\begin{aligned} \sin^2 \theta_W(M_Z) &= 0.23116 \pm 0.00013, \\ \alpha^{-1}(M_Z) &= 127.9 \text{ and } \alpha_S(M_Z) = 0.1184 \pm 0.0007, \end{aligned} \quad (4.2)$$

we find that with $M_{Z'} \sim M_{R^0} \sim 1$ TeV precision unification of gauge couplings occurs for the following values of masses at one-loop and two-loop levels for the Model-I,

$$\begin{aligned} \mathbf{1 - loop} : \quad & M_{GUT}^{ol} = 10^{15.98} \text{ GeV}, \quad M_{R^+}^{ol} = 10^{10.79} \text{ GeV}, \quad \alpha_G^{ol} = 0.02253 \\ \mathbf{2 - loop} : \quad & M_{GUT} = 10^{15.53} \text{ GeV}, \quad M_R^+ = 10^{11.15} \text{ GeV}, \quad \alpha_G = 0.02290 \end{aligned} \quad (4.3)$$

The RG evolution of gauge couplings at two-loop level is shown in Fig. 4.2.1 exhibiting precision unification at $M_{GUT} = 10^{15.53}$ GeV. In Model-I' coupling unification occurs with similar precision but at $M_{GUT} = 10^{15.17}$ GeV.

The decay width of the proton for $p \rightarrow e^+ \pi^0$ is [109, 151]

$$\Gamma(p \rightarrow e^+ \pi^0) = \frac{m_p}{64\pi f_\pi^2} \left(\frac{g_G^4}{M_{GUT}^4} \right) |A_L|^2 |\bar{\alpha}_H|^2 (1 + D + F)^2 \times R. \quad (4.4)$$

where $R = [(A_{SR}^2 + A_{SL}^2)(1 + |V_{ud}|^2)^2]$ for $SO(10)$, $V_{ud} = 0.974$ = the $(1, 1)$ element

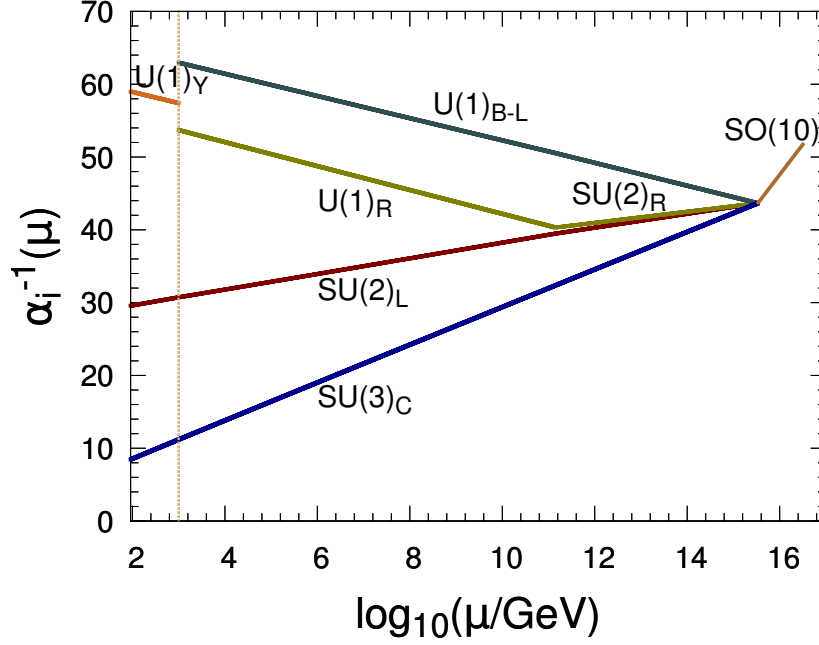


Figure 4.1: Gauge coupling unification in Model-I with two loop values $M_{GUT} = 10^{15.53}$ GeV and $M_R^+ = 10^{11.15}$ GeV with low mass Z' gauge boson at $M_R^0 \sim 1$ TeV.

of V_{CKM} for quark mixings, $A_{SL}(A_{SR})$ is the short-distance renormalization factor in the left (right) sectors and $A_L = 1.25$ = long distance renormalization factor. M_{GUT} = degenerate mass of 24 super-heavy gauge bosons in $SO(10)$, $\bar{\alpha}_H$ = hadronic matrix element, m_p = proton mass = 938.3 MeV, f_π = pion decay constant = 139 MeV, and the chiral Lagrangian parameters are $D = 0.81$ and $F = 0.47$. With $\alpha_H = \bar{\alpha}_H(1+D+F) = 0.012$ GeV³ estimated from lattice gauge theory computations, we obtain $A_R \simeq A_L A_{SL} \simeq A_L A_{SR} \simeq 2.726$ for Model-I. The expression for the inverse decay rates for both the minimal models is expressed as,

$$\begin{aligned} \Gamma^{-1}(p \rightarrow e^+ \pi^0) &= (1.01 \times 10^{34} \text{Yrs}) \left(\frac{0.012 \text{GeV}^3}{\alpha_H} \right)^2 \left(\frac{2.726}{A_R} \right)^2 \left(\frac{1/43.6}{\alpha_G} \right)^2 \\ &\times \left(\frac{7.6}{F_q} \right) \left(\frac{M_{GUT}}{2.98 \times 10^{15} \text{GeV}} \right)^4, \end{aligned} \quad (4.5)$$

where the factor $F_q = 2(1+|V_{ud}|^2)^2 \simeq 7.6$ for $SO(10)$. Now using the estimated values of the model parameters in each case the predictions on proton lifetimes for both models are given in Tab. 4.1 where the uncertainties in unification scale and proton lifetime have been estimated by enhancing the error in α_S to 3σ level. The reduction

of lifetime by nearly two-orders compared to one-loop lifetime (τ_p^{ol}) predictions in both cases is due to the corresponding reduction in the unification scale by a factor of $\simeq 1/3$. It is clear that with maximal value $(\tau_p)_{max.} = 5 \times 10^{34}$ Yrs., Model-I predicts the proton lifetime closer to the SuperKamiokande limit $(\tau_p)_{expt.} (p \rightarrow e^+\pi^0) \geq 1.4 \times 10^{34}$ years [84, 87, 152] which is accessible to ongoing proton decay searches in near future [153]. On the other hand Model-I' is ruled out at two-loop level as it predicts lifetime nearly two orders smaller.

Parameter	Model-I	Model-I'
M_{GUT}^{ol} (GeV)	$10^{15.978}$	$10^{15.56 \pm 0.08}$
$M_{R^+}^{ol}$ (GeV)	$10^{10.787}$	$10^{11.475}$
M_{GUT} (GeV)	$10^{15.530}$	$10^{15.17 \pm 0.08}$
M_{R^+} (GeV)	$10^{11.150}$	$10^{11.750}$
α_G^{-1}	43.67	42.738
A_R	2.726	2.670
τ_p^{ol} (Years)	$1.08 \times 10^{36 \pm 0.32}$	$2.44 \times 10^{34 \pm 0.32}$
τ_p (years)	$2 \times 10^{34 \pm 0.32}$	$6.3 \times 10^{32 \pm 0.32}$

Table 4.1: GUT scale, intermediate scale and proton lifetime predictions for non-SUSY $SO(10)$ models with TeV scale Z' boson and two Higgs doublets as described in the text. The uncertainty in the proton lifetime has been estimated using 3σ uncertainty in $\alpha_S(M_Z)$.

The fact that the Model-I admits a low $B - L$ breaking scale corresponding to a light Z' accessible to accelerator searches makes this non-SUSY model suitable to accommodate inverse seesaw mechanism. Unlike the SUSY $SO(10)$ model [45] here the W_R^\pm bosons are far beyond the LHC accessible range.

4.2.2 Unification in simple model extensions

Although the minimal Model-I clearly satisfies the proton decay constraint to accommodate TeV scale seesaw, we study simple extensions of both models to show that they can evade proton lifetime constraint in case future experiments show τ_p to be substantially longer than 10^{35} Yrs. We use an additional real color octet scalar $C_8(1, 0, 8) \subset 45_H$ where the quantum numbers are under the SM gauge group and allow its mass to vary between 1 TeV and the GUT scale. Making it light would require additional fine tuning of parameters. Recently such a light scalar has been used in models with interesting phenomenological consequences and if the particle mass is in the accessible range, it may be produced at LHC with new physics signatures beyond the SM [73, 154–157].

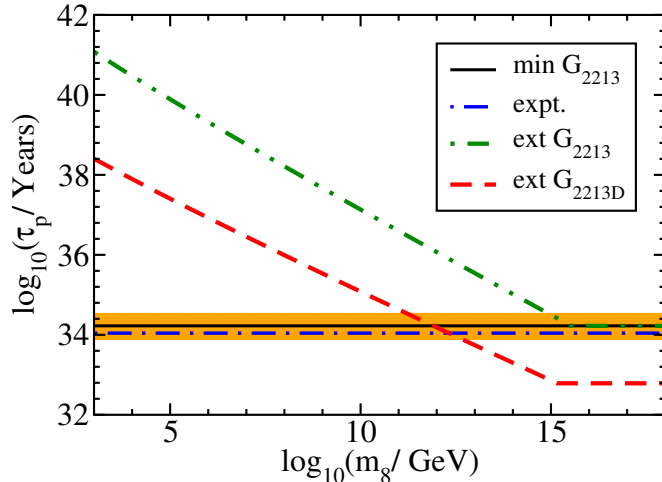


Figure 4.2: Variation of proton lifetime as a function of color octet mass in simple extensions of Model-I (double dot-dashed line) and Model-I' (dashed line). The horizontal solid line with error band is the prediction of the minimal Model-I while the horizontal dot-dashed line is the experimental lower bound for $p \rightarrow e^+\pi^0$.

The presence of this scalar octet with lower mass makes the evolution of $\alpha_{3c}^{-1}(\mu)$ flatter thereby pushing the GUT scale to higher values. In Fig. 4.2 we plot predicted proton lifetimes in the extended G_{2213} and G_{2213D} models as a function of the octet mass m_8 . It is clear that such a simple extension of the two models can easily satisfy proton lifetime requirements in future experimental measurements even if they are found to be much longer than the current limit.

Then while the minimal Model-I can be easily chosen for inverse seesaw, both the models with such simple extension and possessing TeV scale $U(1)_{(B-L)}$ breaking scale qualify for the same purpose. For the phenomenological study of non-unitarity effects we confine to the Model-I and all our analyses are similar for Model-I'.

4.3 Inverse seesaw mechanism

A hallmark of $SO(10)$ grand unification is its underlying quark-lepton symmetry [46] because of which the canonical seesaw scale is pushed closer to the GUT scale making it naturally inaccessible to direct tests by low-energy experiments or collider searches. The energy scale of type-II seesaw mechanism in $SO(10)$ is also too high for direct experimental tests. In contrast to these high scale seesaw mechanisms, an experimentally verifiable and attractive mechanism is the radiative seesaw [22, 157] where the quark-lepton unification has no role to play and additional suppression

to light neutrino mass prediction occurs by loop mediation proportional to a small Higgs quartic coupling that naturally emerges from a Plank-scale induced term in the GUT Lagrangian. The model predicts a rich structure of prospective dark matter candidates also verifiable by ongoing search experiments. It has been further noted that this embedding of the radiative seesaw in $SO(10)$ may have a promising prospect for representing all fermion masses. A number of other interesting neutrino mass generation mechanisms including type-III seesaw, double seesaw, linear seesaw, scalar-triplet seesaw have been suggested and some of them are also experimentally verifiable. For reviews on different neutrino mass generation mechanisms with or without GUTs, SUSY, or flavor symmetry see [19–29].

Here we explore the prospects of inverse seesaw [143, 144] mechanism, which is experimentally verifiable because of the low scale it operate although higher scale inverse seesaw models have been suggested [158–163]. In a large class of models [164–181], the implementation of inverse seesaw requires the introduction of fermionic singlets (S) under the gauge group of the model. Likewise, its implementation in $SO(10)$ introduces a new mass scale μ_S into the Lagrangian corresponding to the mass matrix of the additional singlet fermions of three generations and the TeV-scale seesaw requires this parameter to be small. There is an interesting naturalness argument in favor of its smallness based upon exact lepton number conservation symmetry [45, 164–175].

The Yukawa Lagrangian at the GUT scale gives rise to the effective Lagrangian near the second intermediate scale $\mu = M_R^0 \sim 1$ TeV,

$$\begin{aligned} \mathcal{L}_{\text{Yuk}} &= Y^a 16 \cdot 16 \cdot 10_H^a + y_\chi 16 \cdot 1 \cdot 16_H^\dagger + \mu_S 1 \cdot 1 \\ &\supset (Y^a \bar{\psi}_L \psi_R \Phi^a + y_\chi \bar{\psi}_R S \chi_R^0 + H.c.) + S^T \mu_S S, \end{aligned} \quad (4.6)$$

where the first (second) equation is invariant under $SO(10)$ (G_{2113}) gauge symmetry. The left-handed (LH) and the RH fermion fields $\psi_L(2, 0, -1/2, 1)$, $\psi_R(1, 1/2, -1/2, 1)$ with their respective quantum numbers under G_{2113} are contained in $16_F \subset SO(10)$ and the two Higgs doublets in $10_H \subset SO(10)$. Denoting the heavy Dirac mass matrix relating N_R and S_L as $M = y_\chi v_\chi$ where $v_\chi = \langle \chi_R^0 \rangle$ and the Dirac mass matrix for the neutrinos as $M_D = Y_\nu v_u$, where v_u is the VEV of up-type Higgs doublet, eq. (4.6) gives mass matrix of the neutrino sector in flavor basis after symmetry breaking $G_{2113} \rightarrow \text{SM}$

$$\mathcal{L}_{\text{mass}} = (\bar{\nu} M_D N + \bar{N} M S + H.c.) + S^T \mu_S S, \quad (4.7)$$

which in $|\nu\rangle_f = (\nu, N_R^C, S)^T$ basis gives the mass matrix

$$\mathcal{M}_\nu = \begin{pmatrix} 0 & M_D & 0 \\ M_D^T & 0 & M^T \\ 0 & M & \mu_S \end{pmatrix}. \quad (4.8)$$

The neutrino mass matrices M_D and M are in general 3×3 complex matrices in flavor space whereas the μ_S is 3×3 complex symmetric matrix. Transformation from flavor to mass basis through

$$|\nu\rangle_f = \mathcal{V}^* |\nu\rangle_m \quad (4.9)$$

leads the diagonalization of the above matrix as

$$\mathcal{V}^\dagger \mathcal{M}_\nu \mathcal{V}^* = \hat{\mathcal{M}}_\nu = \text{Diag}\{m_{\nu_i}; M_{\zeta_j}\} \quad (4.10)$$

where $|\nu\rangle_m = (\tilde{\nu}_i, \zeta_j)^T$ represents the three light and six heavy mass states, and i and j run over the light and heavy mass eigenstates respectively. With $\mu_S, M_D \ll M$, the matrix \mathcal{M}_ν can be block diagonalized in to light and heavy sectors as

$$\begin{aligned} m_\nu &\simeq \left(\frac{M_D}{M}\right) \mu_S \left(\frac{M_D}{M}\right)^T, \\ M_H &\simeq \begin{pmatrix} 0 & M^T \\ M & \mu_S \end{pmatrix} \end{aligned} \quad (4.11)$$

With the convention that $\frac{A}{B} = AB^{-1}$.

$$m_\nu \equiv X \mu_S X^T. \quad (4.12)$$

where m_ν is the well known inverse seesaw formula refer for light neutrinos and the other one is the mass matrix for heavy pseudo-Dirac pairs of comparable masses with splitting of the order of μ_S . The μ_S term in the Lagrangian breaks the leptonic global symmetry, $U(1)_{Lepton}$, which is otherwise preserved in the SM, rendering all the LH neutrinos to be massless. Hence the small μ_S should be the natural possibility in the 'tHooft sense [182] even though there is no dynamical understanding for such a small parameter, and can be viewed as slight breaking of the global $U(1)$ symmetry. The above block diagonalized matrices are further diagonalized through the PMNS

matrix, U_ν , and a 6×6 unitary matrix U_H respectively so that

$$\mathcal{V} \simeq \begin{pmatrix} 1 - \frac{1}{2}B^*B^T & B^* \\ -B^T & 1 - \frac{1}{2}B^TB^* \end{pmatrix} \begin{pmatrix} U_\nu & 0 \\ 0 & U_H \end{pmatrix} \quad (4.13)$$

where

$$B^T \simeq \begin{pmatrix} -M^{*-1}\mu_S^*(M_D M^{-1})^\dagger \\ (M_D M^{-1})^\dagger \end{pmatrix} \simeq \begin{pmatrix} 0 \\ X^\dagger \end{pmatrix} \quad (4.14)$$

hence, \mathcal{V} in the leading order approximation can be written as

$$\mathcal{V} \simeq \begin{pmatrix} 1 - \frac{1}{2}XX^\dagger & 0 & X \\ 0 & 1 & 0 \\ -X^\dagger & 0 & 1 - \frac{1}{2}X^\dagger X \end{pmatrix} \begin{pmatrix} (U_\nu)_{3 \times 3} & 0_{3 \times 6} \\ 0_{6 \times 3} & (U_H)_{6 \times 6} \end{pmatrix}, \quad (4.15)$$

where $X = (M_D M^{-1})$, and all the elements in the first block are 3×3 dimensional matrices. The procedure to obtain this result has been discussed in the Appendix D in great detail.

It is clear that the TeV-scale inverse seesaw formula is tenable and appropriate to fit the light neutrino masses provided μ_S is the smallest of the three mass scales occurring in eq. (4.8). The view for the naturally small parameter μ_S being followed in the present work has been adopted in [45, 142] and by a number authors earlier pursuing inverse seesaw mechanism [164–175] although its interpretation through Higgs mechanism has been discussed in a model with extended gauge, fermion and Higgs sectors [183, 184] and possibility of its radiative origin has been explored [185].

The major obstacle in predictions in this mechanism at low energy is that it has too many parameters. Neither of the three matrices M_D , M and μ_S are known. The M_D matrix is determined from $SO(10)$ constraints, and a choice of eigen basis may give diagonal mass matrix M . Elements of M are constrained by non-unitarity bounds. The remaining matrix, μ_S , is determined in the optimistic way from the observed neutrino oscillation data such that

$$\mu_S = \frac{M}{M_D} m_\nu \left(\frac{M}{M_D} \right)^T. \quad (4.16)$$

4.4 Fermion masses and Determination of M_D

The determination of the Dirac neutrino mass matrix M_D (M_R^0) at the TeV seesaw scale is done in five steps [45, 142]:

1. Derivation of RGEs in the presence of G_{2113} and G_{2213} symmetry.
2. Extrapolation of masses to the GUT-scale using low energy data.
3. Fitting the masses at the GUT scale and determination of M_D at M_{GUT} .
4. Determination of M_D by top-down approach.
5. Repeat 2 – 4 with the updated M_D at low energy, till the required accuracy in the SM fermion masses is achieved at M_R^0 scale.

The RGEs for gauge and Yukawa couplings have been derived in non-SUSY scenario and are given in the Appendix C.

Denoting $\Phi_{1,2}$ as the corresponding bi-doublets under G_{2213} they acquire VEVs

$$\langle \Phi_1 \rangle = \begin{pmatrix} v_u & 0 \\ 0 & 0 \end{pmatrix}, \quad \langle \Phi_2 \rangle = \begin{pmatrix} 0 & 0 \\ 0 & v_u \end{pmatrix}, \quad (4.17)$$

Defining the mass matrices

$$\begin{aligned} M_u &= Y_u v_u, & M_D &= Y_\nu v_u, & M_d &= Y_d v_d \\ M_e &= Y_e v_d, & M &= y_\chi v_\chi \end{aligned} \quad (4.18)$$

We use the input values of running masses and quark mixings at the electroweak scale as in refs. [149, 150, 186]

$$\begin{aligned} m_e &= 0.48684727 \pm 0.00000014 \text{ MeV}, \\ m_\mu &= 102.75138 \pm 0.00033 \text{ MeV}, \\ m_\tau &= 1.74669_{-0.00027}^{+0.00030} \text{ GeV}, & m_d &= 4.69_{-0.0.66}^{+0.60} \text{ MeV}, \\ m_s &= 93.4_{-13.0}^{+11.8} \text{ MeV}, & m_b &= 3.00 \pm 0.11 \text{ GeV}, \\ m_u &= 2.33_{-0.45}^{+0.42} \text{ MeV}, & m_c &= 677_{-51}^{+56} \text{ MeV}, \\ m_t &= 181 \pm 1.3 \text{ GeV}, \\ \theta_{12}^q &= 13.04^\circ \pm 0.05^\circ, & \theta_{13}^q &= 0.201^\circ \pm 0.201^\circ, \\ \theta_{23}^q &= 2.38^\circ \pm 0.06^\circ, \end{aligned} \quad (4.19)$$

and the resulting CKM matrix with the CKM Dirac phase $\delta_q = 1.20 \pm 0.08$.

$$V_{\text{CKM}} = \begin{pmatrix} 0.9742 & 0.2256 & 0.0013 - 0.0033i \\ -0.2255 + 0.0001i & 0.9734 & 0.04155 \\ 0.0081 - 0.0032i & -0.0407 - 0.0007i & 0.9991 \end{pmatrix}. \quad (4.20)$$

We use RGEs of the SM for $\mu = M_Z$ to $M_R^0 = 1$ TeV. With two Higgs doublets at $\mu \geq M_R^0$ we use the starting value of $\tan \beta = v_u/v_d = 10$ at $\mu = 1$ TeV which evolves to reach the value $\tan \beta \simeq 6.9$ at the GUT scale. Using the bottom-up approach discussed earlier [186] and the RGEs of Appendix C, the resulting quantities at $\mu = M_{GUT}$

$$\begin{aligned} m_e &= 0.48 \text{ MeV}, & m_\mu &= 97.47 \text{ MeV}, & m_\tau &= 1.8814 \text{ GeV}, \\ m_d &= 1.9 \text{ MeV}, & m_s &= 38.9 \text{ MeV}, & m_b &= 1.4398 \text{ GeV}, \\ m_u &= 1.2 \text{ MeV}, & m_c &= 0.264 \text{ GeV}, & m_t &= 83.04 \text{ GeV}, \end{aligned} \quad (4.21)$$

$$V_{\text{CKM}} = \begin{pmatrix} 0.9748 & 0.2229 & -0.0003 - 0.0034i \\ -0.2227 - 0.0001i & 0.9742 & 0.0364 \\ 0.0084 - 0.0033i & -0.0354 + 0.0008i & 0.9993 \end{pmatrix}. \quad (4.22)$$

We have ignored the running of neutrino masses as the corrections are expected to be insignificant.

4.4.1 Determination of M_D

With Higgs representations $45_H, 16_H, 10_H$, the dim.6 operator [45,142]

$$\frac{f_{ij}}{M^2} 16_i 16_j 10_H 45_H 45_H, \quad (4.23)$$

with $M \simeq M_{Pl}$ or $M \simeq M_{string}$, is suppressed by $(M_{GUT}/M)^2 \simeq 10^{-3} - 10^{-5}$ for GUT-scale VEV of 45_H and acts as an effective 126_H operator to fit the fermion masses at the GUT scale where the formulas for mass matrices are

$$\begin{aligned} M_u &= G_u + F, & M_d &= G_d + F, \\ M_e &= G_d - 3F, & M_D &= G_u - 3F. \end{aligned} \quad (4.24)$$

$$M_u(M_{GUT}) = \begin{pmatrix} 0.0153 & 0.0615 - 0.0112i & 0.1028 - 0.2706i \\ 0.0615 + 0.0112i & 0.3933 & 3.4270 + 0.0002i \\ 0.1028 + 0.2706i & 3.4270 - 0.0002 & 82.90 \end{pmatrix} \text{ GeV}, \quad (4.25)$$

Now using eq. (4.22) and eq. (4.25) in eq. (4.24) gives the Dirac neutrino mass matrix M_D at the GUT scale

$$M_D(M_{GUT}) = \begin{pmatrix} 0.0139 & 0.0615 - 0.0112i & 0.1029 - 0.2707i \\ 0.0615 + 0.0112i & 0.4519 & 3.4280 + 0.0002i \\ 0.1029 + 0.2707i & 3.4280 - 0.0002i & 83.340 \end{pmatrix} \text{ GeV}. \quad (4.26)$$

We then use the RGE for M_D given in Appendix C to evolve $M_D(M_{GUT})$ to $M_D(M_{R^+})$ and then from $M_D(M_{R^+})$ to $M_D(M_{R^0})$ in two steps and obtain,

$$M_D(M_{R^0}) = \begin{pmatrix} 0.0151 & 0.0674 - 0.0113i & 0.1030 - 0.2718i \\ 0.0674 + 0.0113i & 0.4758 & 3.4410 + 0.0002i \\ 0.1030 + 0.2718i & 3.4410 - 0.0002i & 83.450 \end{pmatrix} \text{ GeV}. \quad (4.27)$$

4.5 Non-unitarity deviations and constraining M

The physics underlying non-unitarity effects in lepton sector have been discussed at length in several recent papers [187–198] where relevant formulas have been utilized. Although the PMNS matrix U_ν diagonalizes the light neutrino mass matrix of three generations where

$$U_\nu^\dagger m_\nu U_\nu^* = \text{diag}(m_1, m_2, m_3) \equiv \hat{m}_\nu, \quad (4.28)$$

the appropriate diagonalizing mixing matrix for the inverse seesaw matrix of eq. (4.12) is a 9×9 matrix V ,

$$\mathcal{V}^\dagger \mathcal{M}_\nu \mathcal{V}^* = \hat{M} = \text{diag}(m_i, M_{\zeta_j}) \quad (4.29)$$

where i and j run over light and heavy mass eigenstates and this can be expressed in block partitions, Light neutrino flavor eigenstates as linear combination of light and heavy mass eigenstates is

$$\nu_\alpha = \mathcal{N}_{\alpha i} \hat{\nu}_i + \mathcal{K}_{\alpha j} \zeta_j \quad (4.30)$$

where $\mathcal{K} \simeq (0, X)U_H$ and

$$\mathcal{N} \simeq (1 - \frac{1}{2}XX^\dagger)U_\nu \simeq (1 - \eta)U_\nu. \quad (4.31)$$

The charged current in the mass eigenstates, assuming charged leptons in mass basis, is written as

$$\begin{aligned} \mathcal{L}_{CC} &= -\frac{g_{2L}}{\sqrt{2}}\bar{l}_L\gamma^\mu\nu W_\mu^- + h.c. \\ &\simeq -\frac{g_{2L}}{\sqrt{2}}\bar{l}_L\gamma^\mu(\mathcal{N}\hat{\nu} + \mathcal{K}\zeta)W_\mu^- + h.c. \end{aligned} \quad (4.32)$$

Any non-vanishing value of η is a measure of deviation from the unitarity of the PMNS matrix. Using the TeV scale mass matrix for M_D from eq. (4.27) and assuming

$$M = \text{diag}(M_1, M_2, M_3) \quad (4.33)$$

results in

$$\eta_{\alpha\beta} = \frac{1}{2} \sum_{k=1,2,3} \frac{M_{D\alpha k} M_{D\beta k}^*}{M_k^2} \quad (4.34)$$

For the sake of simplicity assuming degeneracy of RH neutrinos masses $M_R = M_i$ ($i = 1, 2, 3$) gives,

$$\eta = \frac{1\text{GeV}^2}{M_R^2} \begin{pmatrix} 0.0447 & 0.1937 - 0.4704i & 4.4140 - 11.360i \\ 0.1937 + 0.4704i & 6.036 & 144.40 - 0.0002i \\ 4.4140 + 11.360i & 144.40 + 0.0002i & 3488.0 \end{pmatrix}. \quad (4.35)$$

The deviations from unitarity in the leptonic mixing is constrained, for example, by deviations from universality tests in weak interactions, rare leptonic decays, invisible width of Z boson and neutrino oscillation data. The bounds derived at 90% confidence level from the current data on the elements of the symmetric matrix are summarized in [187–190],

$$\begin{aligned} |\eta_{ee}| &\leq 2.0 \times 10^{-3}, & |\eta_{e\mu}| &\leq 3.5 \times 10^{-5}, \\ |\eta_{e\tau}| &\leq 8.0 \times 10^{-3}, & |\eta_{\mu\mu}| &\leq 8.0 \times 10^{-4}, \\ |\eta_{\mu\tau}| &\leq 5.1 \times 10^{-3}, & |\eta_{\tau\tau}| &\leq 2.7 \times 10^{-3}. \end{aligned} \quad (4.36)$$

In the degenerate case the largest element in eq. (4.35) when compared with $|\eta_{\tau\tau}|$ of eq. (4.36) gives the lower bound on the RH neutrino mass, $M_R \geq 1.1366$ TeV, which

is only 7% higher than the SUSY $SO(10)$ bound $(M_R)_{SUSY} \geq 1.06$ TeV [45]. Using this lower bound for other elements in eq. (4.36) yields

$$\begin{aligned}
|\eta_{\mu\mu}| &\leq 4.672 \times 10^{-6}, \\
|\eta_{ee}| &\leq 3.460 \times 10^{-8}, \quad |\eta_{e\mu}| \leq 3.938 \times 10^{-7}, \\
|\eta_{e\tau}| &\leq 9.436 \times 10^{-6}, \quad |\eta_{\mu\tau}| \leq 1.1178 \times 10^{-4}.
\end{aligned}
\tag{4.37}$$

These predicted bounds are several orders lower than the current experimental bounds and they might be reached provided corresponding lepton flavor violating decays are probed with much higher precision. But compared to SUSY $SO(10)$, in this model the upper bound is nearly 2 times larger for $|\eta_{\tau\tau}|$, 3 times larger for $|\eta_{\mu\mu}|$, and nearly 40% smaller in the case of $|\eta_{e\tau}|$. It is interesting to note that in the the present non-SUSY $SO(10)$ model while some of the non-unitarity effects are comparable to the results of [45], others are distinctly different as shown in the next section.

We note in this model that when RH neutrino masses are non-degenerate, they are also constrained by the experimental lower bound on $\eta_{\tau\tau}$ and the corresponding relation obtained by saturating the bound is

$$\frac{1}{2} \left[\frac{0.0845}{M_1^2} + \frac{11.8405}{M_2^2} + \frac{6963.9}{M_3^2} \right] = 2.7 \times 10^{-3},
\tag{4.38}$$

where the numerators inside the square bracket are in GeV^2 . Using partial degeneracy, $M_1 = M_2 = M_3$ leads to the relation between the RH neutrino masses as given in Tab. 4.2. A plot of M_3 vs. M_i ($i = 1, 2$) is shown in Fig. 4.4 exhibiting increase of M_3 with decrease of M_i . The two asymptotes in the hyperbolic curve are at $M_1 = M_2 \simeq 47$ GeV and $M_3 \simeq 1136.6$ GeV.

4.6 Estimating CP -violation and Lepton flavor violation

Two important physical applications of inverse seesaw are leptonic CP and flavor violation effects reflected through the elements. The inverse seesaw formula of eq. (4.12) has three matrices out of which M_D has been determined by fitting the charged fermion masses and mixings, but since the other two matrices, M and μ_S , can not be completely determined using the neutrino oscillation data alone, we make plausible

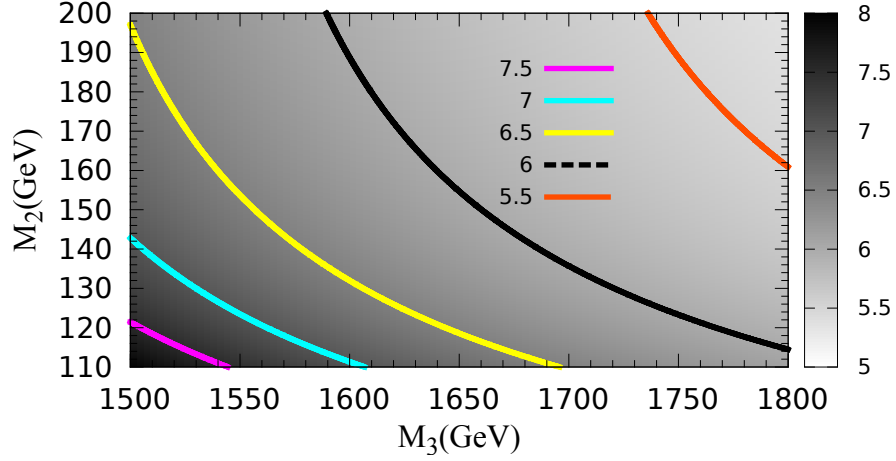


Figure 4.3: The contours of M_1 in the plane of M_2 and M_3 . The solid curves in the diagram represent M_3 dependence of M_2 for fixed values of M_1 using eq. (4.38). The brightest top-right corner suggests that lightest M_1 may exist for largest values of M_2 and M_3 .

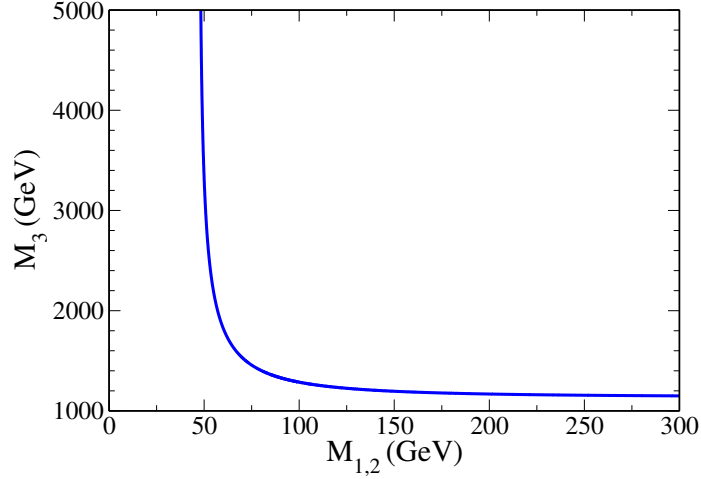


Figure 4.4: Variation of the third generation RH neutrino mass M_3 as a function of first or second generation neutrino mass M_1 or M_2 in the partially degenerate case for which $M_1 = M_2$.

assumptions. In addition to the fully degenerate case we also examine consequences of partial degeneracy with $M_1 = M_2$. From eq. (4.12) and using PMNS matrix to diagonalize m_ν we get

$$\mu_S = X^{-1}U_\nu\hat{m}_\nu U_\nu^T(X^T)^{-1} \quad (4.39)$$

$M_{1,2}$ (GeV)	M_3 (GeV)	$M_{1,2}$ (GeV)	M_3 (GeV)
48.0	5572.83	500.0	1140.66
50.0	3324.69	600.0	1139.11
100.0	1286.51	700.0	1138.18
150.0	1195.81	800.0	1137.57
200.0	1168.32	900.0	1137.16
300.0	1149.80	1000.0	1136.87
400.0	1143.53	1136.58	1136.58

Table 4.2: Variation of third generation RH neutrino mass M_3 as a function of first or second generation RH neutrino mass in the partially degenerate case $M_1 = M_2$ predicted by non-unitarity through non-SUSY $SO(10)$.

$M_1 = M_2$ (GeV)	M_3 (GeV)	$ \eta_{e\mu} $ (10^{-6})	$\delta_{e\mu}$	$ \eta_{e\tau} $ (10^{-5})	$\delta_{e\tau}$	$ \eta_{\mu\tau} $ (10^{-4})	$\delta_{\mu\tau}$
1136	1136	0.394	1.180	0.944	1.200	1.118	1.3×10^{-6}
500	1141	0.422	1.071	0.958	1.166	1.136	2.0×10^{-4}
100	1286	1.848	0.308	1.687	0.563	1.691	5.0×10^{-3}
50	3325	6.733	0.172	4.806	0.202	3.424	1.0×10^{-2}

Table 4.3: Predictions of moduli and phases of non-unitarity parameters as a function of RH neutrino masses.

We construct the unitary matrix U_ν using standard parametrization

$$U_\nu = \begin{pmatrix} c_{13}c_{12} & c_{13}s_{12} & s_{13}e^{-i\delta} \\ -c_{23}s_{12} - c_{12}s_{13}s_{23}e^{i\delta} & c_{23}c_{12} - s_{12}s_{13}s_{23}e^{i\delta} & c_{13}s_{23} \\ s_{23}s_{12} - c_{12}s_{13}c_{23}e^{i\delta} & -c_{12}s_{23} - c_{23}s_{13}s_{12}e^{i\delta} & c_{13}c_{23} \end{pmatrix} \quad (4.40)$$

and neutrino oscillation data at 3σ level [97, 199–205] as listed in Tab. 2.3, and assume hierarchical neutrino masses. We take the leptonic Dirac phase δ in the U_ν matrix to be zero for which the predicted CP -violation from unitarity vanishes irrespective of the values of θ_{13} . We have also checked that inclusion of larger values of $\theta_{13} \simeq 8^\circ - 9^\circ$ [199–202] do not alter our results significantly. Similar results are obtained with $\delta = \pi$.

The parameter $\eta = XX^\dagger/2$ characterizing non-unitarity of the neutrino mixing matrix can have dramatic impact on leptonic CP -violation and branching ratios for

processes with LFV,

$$\begin{aligned}\mathcal{J}_{\alpha\beta}^{ij} &= \text{Im}(\mathcal{N}_{\alpha i}\mathcal{N}_{\beta j}\mathcal{N}_{\alpha j}^*\mathcal{N}_{\beta i}^*), \\ &\simeq \mathcal{J} + \Delta\mathcal{J}_{\alpha\beta}^{ij},\end{aligned}\tag{4.41}$$

where \mathcal{J} is the well known CP -violating parameter due to unitary PMNS matrix U

$$\begin{aligned}\mathcal{J} &\equiv \text{Im}(U_{\alpha i}U_{\beta j}U_{\alpha j}^*U_{\beta i}^*) \\ &= \cos\theta_{12}\cos^2\theta_{13}\cos\theta_{23}\sin\theta_{12}\sin\theta_{13}\sin\theta_{23}\sin\delta,\end{aligned}\tag{4.42}$$

and the non-unitarity contributions are,

$$\begin{aligned}\Delta\mathcal{J}_{\alpha\beta}^{ij} &\simeq - \sum_{\gamma=e,\mu,\tau} \text{Im}(\eta_{\alpha\gamma}U_{\gamma i}U_{\beta j}U_{\alpha j}^*U_{\beta i}^* + \eta_{\beta\gamma}U_{\alpha i}U_{\gamma j}U_{\alpha j}^*U_{\beta i}^* \\ &\quad + \eta_{\alpha\gamma}^*U_{\alpha i}U_{\beta j}U_{\gamma j}^*U_{\beta i}^* + \eta_{\beta\gamma}^*U_{\alpha i}U_{\beta j}U_{\alpha j}^*U_{\gamma i}^*).\end{aligned}\tag{4.43}$$

Very recently $\sin\theta_{13}$ has been measured [199–202] to be small and non-vanishing although no experimental information is available on the leptonic CP -phase δ . Even in the limiting case of vanishing unitarity CP -violation corresponding to $\sin\theta_{13} \rightarrow 0$, or $\delta \rightarrow 0, \pi$ for non-vanishing θ_{13} non-unitarity effects caused due to η may not vanish. In the modified charged current interaction in eq. (4.32), the heavy neutrinos contribute to lepton flavor violating decays with branching ratios [206]

$$\begin{aligned}\text{Br}(l_\alpha \rightarrow l_\beta\gamma) &= \frac{\alpha_w^3 s_w^2 m_{l_\alpha}^5}{256\pi^2 M_w^4 \Gamma_\alpha} \times \left| \sum_{i=1}^6 \mathcal{K}_{\alpha i} \mathcal{K}_{\beta i}^* I\left(\frac{M_i^2}{M_w^2}\right) \right|^2, \\ I(x) &= -\frac{2x^3 + 5x^2 - x}{4(1-x)^3} - \frac{3x^3 \ln x}{2(1-x)^4}.\end{aligned}\tag{4.44}$$

Also the contribution of loop factor for various range of masses allowed in this ex-

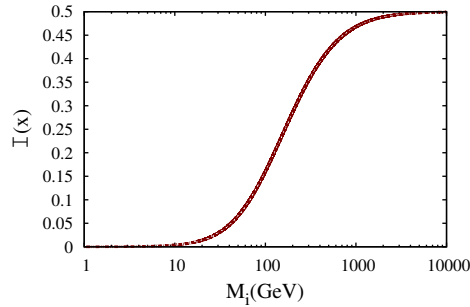


Figure 4.5: Loop factor vs masses of heavy RH or sterile neutrino.

tended seesaw mechanism is shown in Fig. 4.5. Taking into account the contribution of the non-unitarity matrix, it is clear that out of diagonal elements of M_N and M , mostly the latter contributes to the branching ratios. In eq. (4.44) the total decay width Γ_α for lepton species l_α with lifetime τ_α is evaluated using $\Gamma_\alpha = \frac{\hbar}{\tau_\alpha}$ where $\tau_\mu = (2.197019 \pm 0.000021) \times 10^{-6}$ sec and $\tau_\tau = (290.6 \pm 1.0) \times 10^{-15}$ sec.

The matrix element $(\mathcal{K}\mathcal{K}^\dagger)_{\alpha\beta} \propto \eta_{\alpha\beta}$ may lead to significant lepton flavor violating decays in the TeV scale seesaw whereas lepton flavor violating decays are drastically suppressed in Type-I seesaw in $SO(10)$. The procedure for estimating these effects has been outlined in [45, 142] which we follow. The Dirac neutrino mass matrix at the TeV scale which we derive in the next section is central to the determination of non-unitarity effects.

Taking the light neutrino mass eigenvalues $m_1 = 0.001$ eV, $m_2 = 0.0088$ eV, $m_3 = 0.049$ eV, and the constructed U matrix, we utilize the η matrix of eq. (4.35) for the degenerate case and eq. (4.31) to obtain the non-unitary matrix \mathcal{N} . Using eq. (4.39) we also get the μ_S matrix. Once the matrices η and U_ν are determined as discussed above and in Sec. 4.5, the CP -violating parameters are computed using eq. (4.43). Even though U_ν has no imaginary part because of assumed vanishing value of θ_{13} or its vanishing phase, CP -violation would arise from the imaginary parts of the corresponding components of η matrix. We also estimate branching ratios for different lepton flavor violating decay modes using eq. (4.44). For the degenerate case with $M_R = 1.1366$ TeV we get

$M_{1,2}$ (GeV)	M_3 (GeV)	Mass eigenvalues μ_{S_i} (MeV)
50	3324.7	(2.4583, 3.23×10^{-3} , 1.18×10^{-6})
100	1286.5	(8.0423, 2.60×10^{-3} , 1.07×10^{-6})
500	1140.7	(199.37, 5.29×10^{-2} , 1.05×10^{-6})
1136.6	1136.6	(1030.0, 2.72×10^{-1} , 1.04×10^{-6})

Table 4.4: Mass eigenvalues of μ_S signifying masses of singlet fermions predicted by the inverse seesaw in $SO(10)$.

$$\mu_S = \begin{pmatrix} 0.9932 - 0.0124i & -0.1908 + 0.0022i & 0.0066 - 0.0033i \\ -0.1908 + 0.0022i & 0.0370 - 0.0004i & -0.0013 + 0.0006i \\ 0.0066 - 0.0033i & -0.0013 + 0.0006i & 0.00003 - 0.00004i \end{pmatrix} \text{ GeV},$$

and

$$\begin{aligned} \mathcal{J}_{e\mu}^{12} &= -1.31 \times 10^{-6}, \quad \mathcal{J}_{e\mu}^{23} = -1.56 \times 10^{-6}, \\ \mathcal{J}_{\mu\tau}^{23} &= 1.56 \times 10^{-6}, \quad \mathcal{J}_{\mu\tau}^{31} = 1.56 \times 10^{-6}, \quad \mathcal{J}_{\tau e}^{12} = 4.01 \times 10^{-6}, \end{aligned} \quad (4.45)$$

and the branching ratios

$$\begin{aligned} \text{Br}(\mu \rightarrow e\gamma) &= 4.4 \times 10^{-16}, \\ \text{Br}(\tau \rightarrow e\gamma) &= 4.7 \times 10^{-14}, \\ \text{Br}(\tau \rightarrow \mu\gamma) &= 6.6 \times 10^{-12}. \end{aligned} \quad (4.46)$$

For $\theta_{13} = 6^\circ - 9^\circ$, no substantial change is noted in any of the predicted values as long as the Dirac phase in the unitary matrix is assumed to be $\delta \sim 0$ or π .

$M_{1,2}$ (GeV)	M_3 (GeV)	$\Delta\mathcal{J}_{e\mu}^{12}$ ($\times 10^{-6}$)	$\Delta\mathcal{J}_{e\mu}^{23}$ ($\times 10^{-6}$)	$\Delta\mathcal{J}_{\mu\tau}^{23}$ ($\times 10^{-6}$)	$\Delta\mathcal{J}_{\mu\tau}^{31}$ ($\times 10^{-6}$)	$\Delta\mathcal{J}_{\tau e}^{12}$ ($\times 10^{-6}$)
1136	1136	-1.3	-1.6	1.6	1.6	4.0
500	1140	-1.3	-1.6	1.6	1.6	4.0
100	1286	-1.2	-1.6	2.2	1.3	4.1
50	3325	-1.0	-1.8	4.1	0.7	4.3

Table 4.5: Non-unitarity predictions of leptonic CP -violating parameters for lepton flavor violating decays $\mu \rightarrow e\gamma$, $\tau \rightarrow e\gamma$, and $\tau \rightarrow \mu\gamma$ as a function RH neutrino masses

$M_{1,2}$ (GeV)	M_3 (GeV)	$\text{Br}(\mu \rightarrow e\gamma)$	$\text{Br}(\tau \rightarrow e\gamma)$	$\text{Br}(\tau \rightarrow \mu\gamma)$
1136	1136	4.4×10^{-16}	4.7×10^{-14}	6.6×10^{-12}
500	1140	4.9×10^{-16}	4.8×10^{-14}	6.8×10^{-12}
100	1286	1.7×10^{-15}	5.4×10^{-14}	7.0×10^{-12}
50	3325	2.6×10^{-15}	2.8×10^{-14}	1.9×10^{-12}

Table 4.6: Branching ratios for lepton flavor violating decays $\mu \rightarrow e\gamma$, $\tau \rightarrow e\gamma$, and $\tau \rightarrow \mu\gamma$ as a function RH neutrino masses

Thus we find that in this non-SUSY $SO(10)$ model for the degenerate case and with $\theta_{13} = 0.0$, like the SUSY $SO(10)$ prediction [45, 142], although all the five CP -violating parameters are just one order smaller than the corresponding parameter in the quark sector with $\Delta\mathcal{J}_{CKM} = (3.05^{+0.19}_{-0.20}) \times 10^{-5}$, there are certain quantitative differences. The magnitudes of predicted CP -violations for all the five parameters

in the non-SUSY $SO(10)$ model are reduced by nearly 50% compared to their corresponding SUSY $SO(10)$ values.

When compared with the predicted values in SUSY $SO(10)$ [45, 142] the present results on branching ratios satisfy,

$$\begin{aligned}\frac{\text{Br}(\mu \rightarrow e\gamma)_{\text{non-susy}}}{\text{Br}(\mu \rightarrow e\gamma)_{\text{susy}}} &\simeq 1.3, \\ \frac{\text{Br}(\tau \rightarrow e\gamma)_{\text{non-susy}}}{\text{Br}(\tau \rightarrow e\gamma)_{\text{susy}}} &\simeq 0.4, \\ \frac{\text{Br}(\tau \rightarrow \mu\gamma)_{\text{non-susy}}}{\text{Br}(\tau \rightarrow \mu\gamma)_{\text{susy}}} &\simeq 3.3.\end{aligned}\tag{4.47}$$

which can be tested by next generation experiments on lepton flavor violating decays.

Our predictions for the partially degenerate cases for $\theta_{13} = 0$ on different elements $\eta_{\alpha\beta}$ and their phases are given in Tab. 4.3 and those for CP -violating parameters $\mathcal{J}_{\alpha\beta}^{ij}$ and branching ratios are summarized in Tab. 4.5 and Tab. 4.6.

4.7 Discussion

Compared to the predictions in the degenerate case, $|\eta_{\mu\tau}| \simeq 10^{-4}$, $\delta_{\mu\tau} \simeq 10^{-6}$, for the partially degenerate case we find that while $|\eta_{\mu\tau}|$ is of the same order, $\delta_{\mu\tau} \simeq 10^{-2}, 10^{-3}$ and 10^{-4} for $M_{1,2} = 50$ GeV, 100 GeV, and 500 GeV respectively. These parameters enter into the neutrino oscillation probability in the ‘‘golden channel’’ [191],

$$\begin{aligned}P_{\mu\tau} &\simeq 4|\eta_{\mu\tau}|^2 + 4s_{23}^2 c_{23}^2 \sin^2\left(\frac{\Delta m_{31}^2 L}{4E}\right) \\ &\quad - 4|\eta_{\mu\tau}| \sin \delta_{\mu\tau} \sin 2\theta_{23} \sin\left(\frac{\Delta m_{31}^2 L}{4E}\right).\end{aligned}\tag{4.48}$$

leading to the CP -asymmetry,

$$\begin{aligned}\mathcal{A}_{\mu\tau}^{CP} &= \frac{P_{\mu\tau} - P_{\bar{\mu}\bar{\tau}}}{P_{\mu\tau} + P_{\bar{\mu}\bar{\tau}}} \\ &\simeq \frac{-4|\eta_{\mu\tau}| \sin \delta_{\mu\tau}}{\sin 2\theta_{23} \sin\left(\frac{\Delta m_{31}^2 L}{4E}\right)}.\end{aligned}\tag{4.49}$$

when the first term in eq. (4.48) is much smaller compared to the other two terms. Our results in the partial degenerate case satisfies the condition that gives eq. (4.49)

from eq. (4.48). The non-unitarity CP -violating effects are predicted to be much more pronounced by noting that the strength of the third term in eq. (4.48) is enhanced by 100 – 10,000 times compared to the prediction in the degenerate case. Crucial to this prediction is our constraint eq. (4.38) between RH neutrino masses which plays an important role in estimating the phase of $\eta_{\mu\tau}$ in the partially degenerate case that takes into account the increasing behavior of M_3 for decreasing values of $M_1 = M_2$.

Among other significant differences in the model predictions are $\text{Br}(\mu \rightarrow e\gamma)$ values higher by almost one orders for $M_1 = M_2 = 50$ GeV while $\text{Br}(\tau \rightarrow e\gamma)$ hardly changes. On the other hand $\text{Br}(\tau \rightarrow \mu\gamma)$ reduces by a factor of 3.5 for $M_1 = M_2 = 50$ GeV compared to degenerate case. Presently the experimental limits on branching ratios are $\text{Br}(\mu \rightarrow e\gamma) \leq 5.7 \times 10^{-13}$ [207], $\text{Br}(\tau \rightarrow e\gamma) \leq 3.3 \times 10^{-8}$ [208], and $\text{Br}(\tau \rightarrow \mu\gamma) \leq 4.4 \times 10^{-8}$ [208]. The projected reach of future sensitivities are up to $\text{Br}(\tau \rightarrow e\gamma) \sim 10^{-9}$, $\text{Br}(\tau \rightarrow \mu\gamma) \sim 10^{-9}$, but $\text{Br}(\mu \rightarrow e\gamma) \sim 10^{-14}$ [209, 210].

In Tab. 4.4 we show predictions of mass eigenvalues of the μ_S matrix that signifies masses of three fermion singlets S_i ($i = 1, 2, 3$) for degenerate and partially degenerate cases of RH neutrino masses. These mass eigenvalues are noted to vary starting from the lightest ~ 1 eV to the heaviest ~ 1 GeV which may have interesting phenomenological consequences that needs further investigation. It is to be noted that the smallest mass eigenvalue is also predicted directly by the inverse seesaw formula from the TeV scale value of $(M_D)_{33} \sim 100$ GeV in a manner similar to the Type-I seesaw case.

We have also examined the consequences of quasi-degenerate light neutrino masses expected to manifest through tritium beta decay or neutrinoless double beta decay searches. For example with $m_1 = 0.09923$ eV, $m_2 = 0.1$ eV, and $m_3 = 0.1239$ eV, which are consistent with neutrino oscillation data, the three eigenvalues of the resulting μ_S matrix are $\mu_S^{(i)} = (30.110 \text{ GeV}, 1.2 \text{ MeV}, 20.6 \text{ eV})$ with three pairs of heavy pseudo Dirac neutrinos having almost degenerate masses (1151.7, 1121.6) GeV, (1139.5, 1139.5) GeV, and (1136.5, 1136.5) GeV. The predictions for lepton flavor violating decays, CP -violating parameters and the non-unitarity effects are similar to the case of the degenerate pseudo Dirac neutrinos with hierarchical light neutrino masses as discussed above. However, the heaviest eigenvalue of the fermion singlet mass matrix increases to $\mu_S^{(1)} \simeq 30$ GeV compared to the corresponding value of $\mu_S^{(1)} \simeq 1$ GeV in the hierarchical case of light neutrinos as shown in Tab. 4.4.

The introduction of three additional fermion singlets under $SO(10)$ needed for the implementation of inverse seesaw mechanism may be argued to point towards

a deficiency of the related GUT models. For that matter, the $SO(10)$ models of refs. [45, 142, 158–163, 211–215] have utilized these singlets. More recently, the superpartners of two out of these three fermion singlets have been demonstrated to be acting as components of inelastic dark matter [200]. There is another $SO(10)$ based radiative inverse seesaw model [185] which has been designed to explain the smallness of the μ_S parameter with the symmetry breaking chain $SO(10) \rightarrow SU(5) \times U(1)_\chi \rightarrow \text{SM} \times U(1)_\chi$ where more nonstandard fermions and singlets have been found to be necessary. Also noting that a large number of other models have also utilized them as the necessary ingredients of the inverse seesaw mechanism, the merits of results obtained overshadow the presence of fermion singlets which, ultimately, can be justified or falsified by experiments.

In this respect the E_6 GUT [216, 217] or $SU(3)^3$ [218–222] type GUT models contain necessary fermion singlets within their non-trivial representations but they also contain a number of additional nonstandard fermions and extra assumptions on their masses are necessary to implement the present mechanism. The E_6 fermion representation $27 = 16 + 10 + 1$ under $SO(10)$ which is a subgroup of E_6 along with all other intermediate gauge groups including the SM. Also all the $SO(10)$ Higgs representations used so far in Model-I and Model-I' are also contained in the corresponding higher representations of E_6 [56, 57]. Thus, the spontaneous symmetry breaking chains of eq. (4.1) can be implemented starting directly from E_6 GUT instead of $SO(10)$. The fermion mass fit at the GUT scale adopted here can also be repeated by imposing the condition that the additional 10-plet of fermions have masses at the GUT scale. Then all other results obtained would be identical to those achieved here.

It has been also argued that because of large size of Higgs representations such as 210_H and 126_H needed in $SO(10)$ models employing type-I and type-II seesaw mechanisms, GUT-threshold corrections may give rise to larger uncertainties in $\sin^2 \theta_W$ predictions and associated mass scale(s) [223]. Counter examples of this result in $SO(10)$ having Pati-Salam intermediate symmetry (G_{224D}) with unbroken D -Parity have been derived with exactly vanishing GUT-threshold corrections on $\sin^2 \theta_W$ as well as on the intermediate scale [224–226]. Also, in other $SO(10)$ models [82, 158], with D -parity broken at GUT scale, threshold corrections were shown to be smaller if the complete super-heavy $SO(10)$ multiplet acquires mass of the same order. Note that the Higgs representation 126_H is needed for the implementation of the type-I and type-II seesaw mechanisms, and the inverse seesaw needs comparatively much smaller Higgs representation like 16_H . Thus, the possibilities of threshold uncer-

tainties are expected to be correspondingly reduced in our models. In particular our minimal Model-I contains neither of the larger Higgs representations 210_H and 126_H ; it requires only the smaller representations $45_H, 16_H$ and $10_{H_1}, 10_{H_2}$. Also, in case of the Model-I' and its extension, the GUT-threshold effects due to super-heavy components of Higgs representations $210_H, 16_H$ and $10_{H_1}, 10_{H_2}$ are expected to be substantially reduced compared to the $SO(10)$ model of ref. [158] with G_{2213D} intermediate symmetry because of the absence of the large representation 126_H . The maximal value of proton lifetime is found to increase by a factor 2(4) due to GUT threshold effects in our Model-I (Model-I') over the two-loop predictions.

Regarding other possibilities of inverse seesaw motivated non-SUSY $SO(10)$, we find that the minimal single-step breaking scenario to the TeV scale gauge symmetry, $SO(10) \rightarrow G_{2113}$, is ruled out by renormalization group and coupling unification constraints. One of the two-step breaking chains, $SO(10) \rightarrow G_{224D} \rightarrow G_{2113}$ gives a low value of the unification scale $M_{GUT} = 10^{14.7}$ GeV, whereas $SO(10) \rightarrow G_{214} \rightarrow G_{2113}$ also yields almost similar value, $M_{GUT} = 10^{14.8}$ GeV. The third remaining chain, $SO(10) \rightarrow G_{224} \rightarrow G_{2113}$, where D -parity is broken at the GUT scale, gives $M_{GUT} = 10^{15.15}$ GeV. Thus all the three minimal chains at two-loop level are ruled out by the existing lower bound on proton lifetime [84, 152]. As the large representation 126_H is absent in these models, the GUT-threshold effects [158] are smaller in the corresponding minimal models than the required values to make them compatible with the lower limit on proton lifetime unless the splitting among the super-heavy components is too large. In view of these, the minimal Model-I turns out to be the best among all possible single and two-step breaking minimal models of $SO(10)$ with the TeV scale G_{2113} gauge symmetry.

One of the appealing features which have been noted [56, 57] in $SO(10)$ breaking chains under the category of Model-I is that they do not have the cosmological domain wall problem [227] because of spontaneous breaking of D -parity along with the gauge symmetry at the GUT scale. When this criteria is included while searching for equally good models, there are only two possible chains with three step breaking and only one chain with four step breaking to the TeV-scale symmetry G_{2113} . However, if utilization of large Higgs representations is excluded, the minimal Model-I emerges to be unique from among all possible $SO(10)$ breaking chains. Investigation of prospects for these longer symmetry breaking chains along with others will be addressed in the forthcoming chapters.

Neutrinoless double beta decay in $SO(10)$ model

The left-right symmetric gauge theories based on G_{224D} [46, 47] and G_{2213D} [48, 49, 55] with $g_{2L} = g_{2R}$ may suggest the origin of parity restoration [228]. The detection of W_R boson at LHC is likely to resolve the mystery of parity violation in weak interaction. With this possibility we work on a class of LR model with TeV scale W_R, Z' but having parity restoration at high scale where they originate from well known Pati-Salam symmetry or $SO(10)$ GUT [52, 54]. The canonical and type-II seesaw [59–67] emerge naturally from $SO(10)$, G_{224D} and G_{2213D} gauge theories provided both LH and RH neutrinos are Majorana fermions. Usually the scale of operation of conventional seesaw is far beyond the experimental reach. Therefore, we minimally extended the model under study to accommodate TeV scale inverse seesaw frame work for neutrino masses.

Currently a number of dedicated experiments on $0\nu 2\beta$ -decay are in progress [229–239] while a part of the Heidelberg-Moscow experiment [229, 236–239] has already claimed to have measured the effective mass parameter $|m_{ee}^{\text{eff}}| \simeq (0.23 - 0.56)$ eV. This observation might be hinting towards the Majorana nature of the light neutrinos [240]. Its worthwhile to study such prospects under GUT framework. The Dirac mass matrix M_D predicted using underlying quark-lepton symmetry G_{224D} of $SO(10)$ would play crucial role in determining above and other results on non-unitarity and LFV.

The chapter is organized as follows: in Sec. 5.1 we briefly discuss the TeV scale left-right gauge theory with low-mass W_R, Z' bosons, light neutrino masses and associated non-unitarity effects. In Sec. 5.2, we present various Feynman amplitudes for neutrinoless double beta decay; in Sec. 5.3, we give a detailed discussion for

standard and non-standard contributions to the effective mass parameter for $0\nu 2\beta$ decay rate and in Sec. 5.4, we have discussed the branching ratios for lepton flavor violating decays. In Sec. 5.5, we implement the idea in a $SO(10)$ grand unified theory and derive Dirac neutrino mass matrix at the TeV scale.

5.1 Low scale left-right gauge theory and extended seesaw

5.1.1 The Model

Besides the standard 16-fermions per generation including the RH neutrino, we add one additional sterile fermion singlet for each generation, as in inverse seesaw. We start with parity conserving left-right symmetric gauge theory, G_{224D} [46, 47] or G_{2213D} [48, 49, 55], with equal gauge couplings ($g_{2L} = g_{2R}$) at high scales. In the Higgs sector we need both LH and RH triplets (Δ_L, Δ_R) as well as the LH and RH doublets (χ_L, χ_R) in addition to bi-doublet (Φ) and D -parity odd singlet (σ) [56, 57]. Their transformation properties, can be checked in tables given in the Tab. B.10, under $G_{224D} \supset G_{2213D}$ are

$$\begin{aligned}
\sigma(1, 1, 1) &\supset \sigma(1, 1, 0, 1), & \Phi(2, 2, 1) &\supset \Phi(2, 2, 0, 1), \\
\Delta_L(3, 1, 10) &\supset \Delta_L(3, 1, -1, 1), & \Delta_R(1, 3, \bar{10}) &\supset \Delta_R(1, 3, -1, 1), \\
\chi_L(2, 1, 4) &\supset \chi_L(2, 1, -1/2, 1), & \chi_R(1, 2, \bar{4}) &\supset \chi_R(1, 2, -1/2, 1).
\end{aligned} \tag{5.1}$$

When D -parity odd singlet σ acquires a VEV $\langle \sigma \rangle \sim M_P$, the LR discrete symmetry is spontaneously broken but the gauge symmetry G_{2213} remains unbroken leading to $M_{\Delta_R}^2 = (M_\Delta^2 - \lambda_\Delta \langle \sigma \rangle M')$, $M_{\chi_R}^2 = (M_\chi^2 - \lambda_\chi \langle \sigma \rangle M')$, where $\lambda_\Delta, \lambda_\chi$ are trilinear couplings and $\langle \sigma \rangle, M', M_\Delta, M_\chi$ are all $\sim \mathcal{O}(M_P)$, the RH Higgs scalar masses are made lighter depending upon the degree of fine tuning in λ_Δ and λ_χ . The asymmetry in the Higgs sector causes asymmetry in the $SU(2)_L$ and $SU(2)_R$ gauge couplings with $g_{2L}(\mu) > g_{2R}(\mu)$ for $\mu < M_P$. If one wishes to have W_R, Z' mass predictions at nearly the same scales and generate Majorana neutrino masses, it is customary to break $G_{2213} \rightarrow \text{SM}$ by the VEV of the right handed triplet $\langle \Delta_R^0 \rangle \sim v_R$. We rather suggest a more appealing phenomenological scenario with $M_{W_R} > M_{Z'}$ for which two step breaking of the asymmetric gauge theory to the SM is preferable : $G_{2213} \xrightarrow{M_R^+} \text{SM}$

$G_{2113} \xrightarrow{M_R^0}$ SM, where the first step of breaking that generates massive W_R bosons is implemented through the VEV of the heavier triplet $\sigma(1, 3, 0, 1)$ carrying $B - L = 0$ and the second step of breaking is carried out by $\langle \Delta_R^0 \rangle \sim v_R$. At this stage the RH neutral gauge boson gets mass which is kept closer to the current experimental lower bound $M_{Z'} \geq 1.162$ TeV for its visibility by high energy accelerators. We further gauge the extended seesaw mechanism at the TeV scale for which the VEV of the RH-doublet $\langle \chi_R^0 \rangle = v_\chi$ provides the N - S mixing. The G_{2113} symmetric low-scale Yukawa Lagrangian is

$$\mathcal{L}_{\text{Yuk}} = Y^l \bar{\psi}_L \psi_R \Phi + f \psi_R^C \psi_R \Delta_R + F \bar{\psi}_R S \chi_R + S^T \mu S + h.c. \quad (5.2)$$

which gives rise to the 9×9 neutral fermion mass matrix after electroweak symmetry breaking, discussed in the next subsection.

5.1.2 Extended inverse seesaw

The effective neutrino mass matrix in $|\nu\rangle = (\nu, S, N_R^C)^T$ basis is expressed as

$$\mathcal{M}_\nu = \begin{pmatrix} 0 & 0 & M_D \\ 0 & \mu_S & M \\ M_D^T & M^T & M_N \end{pmatrix} \quad (5.3)$$

where $M_D = Y^l \langle \Phi \rangle$, $M_N = f \langle \Delta_R^0 \rangle$ and $M = F \langle \chi_R^0 \rangle$. The neutrino mass matrix M_D and the S - N mass matrix M are in general 3×3 complex matrices in flavor space while μ_S and M_N are 3×3 complex symmetric. In the limit $\mu_S, M_D \ll M \ll M_N$, the heaviest right handed neutrinos can be integrated out from the Lagrangian so that the effective Lagrangian becomes [159, 160]

$$\begin{aligned} -\mathcal{L}_{\text{eff}} &= (M_D M_N^{-1} M_D^T)_{\alpha\beta} \nu_\alpha^T \nu_\beta + (M_D M_N^{-1} M)_{\alpha m} (\bar{\nu}_\alpha S_m + \bar{S}_m \nu_\alpha) \\ &+ (M^T M_N^{-1} M)_{mn} S_m^T S_n - \mu_S S_m^T S_n. \end{aligned} \quad (5.4)$$

The effective mass term of the above Lagrangian

$$\mathcal{M}_{\text{eff}} = - \begin{pmatrix} M_D M_N^{-1} M_D^T & M_D M_N^{-1} M \\ M^T M_N^{-1} M_D^T & M^T M_N^{-1} M - \mu_S \end{pmatrix}, \quad (5.5)$$

can be block diagonalized giving the light and sterile neutrino masses

$$m_\nu \sim M_D M^{-1} \mu_S (M_D M^{-1})^T, \quad (5.6)$$

$$m_S \sim \mu_S - M M_N^{-1} M^T, \quad (5.7)$$

to the leading approximation. Note that type-I seesaw like terms $M_D M_N^{-1} M_D^T$ cancelled out and the inverse seesaw formula [143, 144, 241] emerges. This was possible only under assumption $m_{\nu_S} \ll M M_N^{-1} M^T$. On the other hand if $\mu_S \gg M M_N^{-1} M^T$, type-I seesaw dominates. The complete block diagonalization procedure of the matrix \mathcal{M}_ν is given in Appendix D.

In the third step, m_ν , m_S and $m_N \sim M_N$ are further diagonalized by the respective unitary matrices to give their corresponding eigenvalues

$$\begin{aligned} U_\nu^\dagger m_\nu U_\nu^* &= \hat{m}_\nu = \text{diag}(m_{\nu_1}, m_{\nu_2}, m_{\nu_3}), \\ U_S^\dagger m_S U_S^* &= \hat{m}_S = \text{diag}(m_{S_1}, m_{S_2}, m_{S_3}), \\ U_N^\dagger m_N U_N^* &= \hat{m}_N = \text{diag}(m_{N_1}, m_{N_2}, m_{N_3}). \end{aligned} \quad (5.8)$$

The complete mixing matrix [242–244] diagonalizing the matrix $(\mathcal{M}_\nu)_{9 \times 9}$, given in eq. (5.3), can be expressed as

$$\begin{aligned} \mathcal{V} &\equiv \begin{pmatrix} \mathcal{V}_{\alpha i}^{\nu\hat{\nu}} & \mathcal{V}_{\alpha j}^{\nu\hat{S}} & \mathcal{V}_{\alpha k}^{\nu\hat{N}} \\ \mathcal{V}_{\beta i}^{S\hat{\nu}} & \mathcal{V}_{\beta j}^{S\hat{S}} & \mathcal{V}_{\beta k}^{S\hat{N}} \\ \mathcal{V}_{\gamma i}^{N\hat{\nu}} & \mathcal{V}_{\gamma j}^{N\hat{S}} & \mathcal{V}_{\gamma k}^{N\hat{N}} \end{pmatrix} \\ &= \begin{pmatrix} (1 - \frac{1}{2} X X^\dagger) U_\nu & (X - \frac{1}{2} Z Y^\dagger) U_S & Z U_N \\ -X^\dagger U_\nu & (1 - \frac{1}{2} (X^\dagger X + Y Y^\dagger)) U_S & (Y - \frac{1}{2} X^\dagger Z) U_N \\ y^* X^\dagger U_\nu & -Y^\dagger U_S & (1 - \frac{1}{2} Y^\dagger Y) U_N \end{pmatrix} \end{aligned} \quad (5.9)$$

where $X = M_D M^{-1}$, $Y = M M_N^{-1}$, $Z = M_D M_N^{-1}$ and $y = M^{-1} \mu_S$.

5.1.3 Neutrino parameters and non-unitarity constraints on M

Using the constrained diagonal form of M as mentioned above, the mass matrix μ_S is determined using the gauged inverse seesaw formula and neutrino oscillation data provided that the Dirac neutrino mass matrix M_D is also known. The determination of M_D at the TeV scale, basically originating from high-scale quark-lepton symmetry G_{224D} or $SO(10)$ GUT, is carried out by predicting its value at the high scale from

measure of non-unitarity	Expt. bound [187–190]	C1	C2	C3
	C0			
$ \eta_{ee} $	2.0×10^{-3}	3.5×10^{-8}	2.7×10^{-7}	3.1×10^{-6}
$ \eta_{e\mu} $	3.5×10^{-5}	3.9×10^{-7}	3.4×10^{-6}	1.5×10^{-5}
$ \eta_{e\tau} $	8.0×10^{-3}	9.4×10^{-6}	2.8×10^{-5}	6.4×10^{-5}
$ \eta_{\mu\mu} $	8.0×10^{-4}	4.7×10^{-6}	2.3×10^{-5}	6.9×10^{-5}
$ \eta_{\mu\tau} $	5.1×10^{-3}	1.1×10^{-4}	2.2×10^{-4}	3.2×10^{-4}
$ \eta_{\tau\tau} $	2.7×10^{-3}	2.7×10^{-3}	2.7×10^{-3}	2.7×10^{-3}

Table 5.1: Experimental bounds of the non-unitarity matrix elements $|\eta_{\alpha\beta}|$ (column C0) and their predicted values for degenerate (column C1), partially-degenerate (column C2), and non-degenerate (column C3) values of $M = \text{diag}(M_1, M_2, M_3)$ as described in cases (a), (b) and (c), respectively, in the text.

fits to the charged fermion masses of three generations and then running down to the lower scales using the corresponding RGEs in the top-down approach. It is to be noted that for fits to the fermion masses at the GUT scale, their experimental values at low energies are transported to the GUT scale using RGEs and the bottom-up approach. This procedure has been carried out in Sec. 5.5.5 by successfully embedding the LR gauge theory in a suitable non-SUSY G_{224} and $SO(10)$ framework and the result is

$$M_D = \begin{pmatrix} 0.0227 & 0.0989 - 0.0160i & 0.1462 - 0.3859i \\ 0.0989 + 0.0160i & 0.6319 & 4.884 + 0.0003i \\ 0.1462 + 0.3859i & 4.884 - 0.0003i & 117.8 \end{pmatrix} \text{ GeV.} \quad (5.11)$$

This value of M_D will be utilized for all applications discussed subsequently in this work including the fit to the neutrino oscillation data through the inverse seesaw formula, predictions of effective mass parameters in $0\nu 2\beta$, computation of non-unitarity and CP -violating effects, and lepton flavor violating decay branching ratios.

The light active Majorana neutrino mass matrix is diagonalized by the PMNS mixing matrix U_ν such that $U_\nu^\dagger m_\nu U_\nu^* = \hat{m}_\nu = \text{diag}(m_{\nu_1}, m_{\nu_2}, m_{\nu_3})$. The non-unitarity matrix at the leading order is still $\mathcal{N} \simeq (1 - \eta)U_\nu$, see Appendix D for details.

Thus η is a measure of deviation from unitarity in the lepton sector on which there has been extensive investigations in different models [45, 187–197, 245, 246]. Assuming M to be diagonal for the sake of simplicity, $M \equiv \text{diag}(M_1, M_2, M_3)$, gives $\eta_{\alpha\beta} = \frac{1}{2} \sum_k M_{D\alpha k} M_k^{-2} M_{D\beta k}^*$, but it can be written explicitly for the degenerate case

$$(M_1 = M_2 = M_3 = M_R)$$

$$\eta = \frac{1 \text{ GeV}^2}{M_R^2(\text{GeV}^2)} \begin{pmatrix} 0.0904 & 0.3894 - 0.9476i & 8.8544 - 22.7730i \\ 0.3894 + 0.9476i & 12.1314 & 289.22 + 0.00005i \\ 8.8544 + 22.7730i & 289.22 - 0.00005i & 6950.43 \end{pmatrix} \quad (5.12)$$

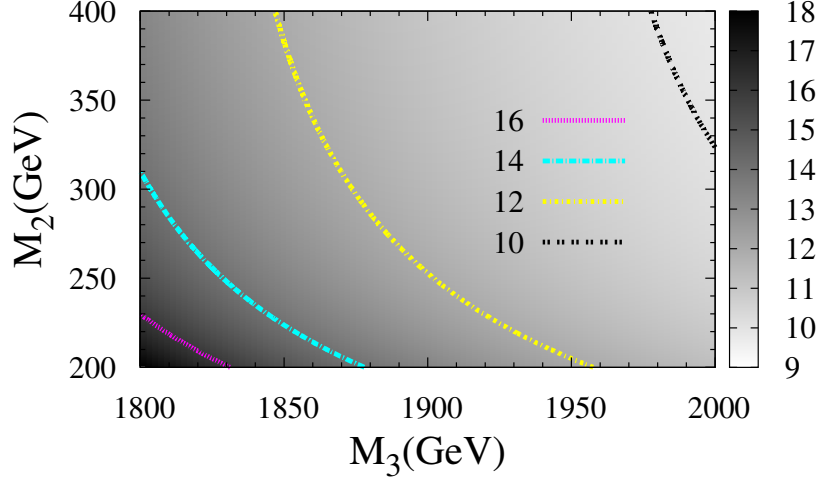


Figure 5.1: The contours of M_1 in the plane of M_2 and M_3 . The solid curves in the diagram represent M_3 dependence of M_2 for fixed values of M_1 using eq. (5.13). The brightest top-right corner suggests that lightest M_1 may exist for largest values of M_2 and M_3 .

For the non-degenerate diagonal matrix M , saturating the experimental bound for $|\eta_{\tau\tau}| < 2.7 \times 10^{-3}$ [245, 246] gives

$$\frac{1}{2} \left[\frac{0.170293}{M_1^2} + \frac{23.8535}{M_2^2} + \frac{13876}{M_3^2} \right] = 2.7 \times 10^{-3}, \quad (5.13)$$

where the three numbers inside the square bracket are in GeV^2 . The correlation between M_2 and M_3 is shown in Fig. 5.1 where the allowed region in the brightest top right corner suggests the possibility of lightest M_1 for large values of M_2 and M_3 . It is clear from eq. (5.13) that M_i can not be arbitrary. Rather they are ordered with $M_3 > M_2 > M_1$ and also they are bounded from below with $M_1 > 5.6 \text{ GeV}$, $M_2 > 66.4 \text{ GeV}$, $M_3 > 1.6 \text{ TeV}$. In the degenerate case $M_1 = M_2 = M_3 = 1604.4 \text{ GeV}$. If we assume equal contribution to non-unitarity from all three terms in the left hand side of eq. (5.13), we get $M = \text{diag}(9.7, 115.1, 2776.6) \text{ GeV}$. Besides these constraints, we have used the primary criteria $M_N > M \gg M_D, \mu_S$ where $M_N \leq O(v_R)$, the G_{2113} breaking scale in choosing the elements of M .

The elements of η have been listed in the Tab. 5.1 for (a) degenerate $M = \text{diag}(1604.4,$

m_ν	M	μ_S
NH	(a)	$\begin{pmatrix} 9.457 + 4.114i & -2.073 - 0.904i & 0.087 - 0.001i \\ \cdot & 0.455 + 0.198i & -0.019 - 0.0003i \\ \cdot & \cdot & 0.00069 - 0.000027i \end{pmatrix} \text{ GeV}$
	(b)	$\begin{pmatrix} 0.037 + 0.016i & -0.008 - 0.003i & 0.007 - 0.0001i \\ \cdot & 0.001 + 0.0007i & -0.001 + 0.00002i \\ \cdot & \cdot & 0.001 - 0.0004i \end{pmatrix} \text{ GeV}$
	(c)	$\begin{pmatrix} 3.476 + 1.512i & -9.018 - 3.933i & 9.180 + 0.141i \\ \cdot & 23.410 + 10.230i & -23.840 - 0.385i \\ \cdot & \cdot & 20.670 - 8.246i \end{pmatrix} \times 10^{-4} \text{ GeV}$

Table 5.2: Structure of μ_S from neutrino oscillation data for NH of light neutrino masses, $m_\nu = (0.00127, 0.008838, 0.04978)$ eV and different mass pattern of M : (a) $M=(1604.44, 1604.44, 1604.44)$ GeV, (b) $M=(100.0, 100.0, 2151.5)$ GeV, and (c) $M=(9.72, 115.12, 2776.57)$ GeV.

1604.4, 1604.4) GeV, (b) partially degenerate $M=\text{diag}(100, 100, 2151.58)$ GeV, and (c) non degenerate $M=\text{diag}(9.73, 115.12, 2776.6)$ GeV in columns $C1, C2$ and $C3$, respectively, where in column $C0$, experimental bounds are presented [187–190].

5.1.4 Determination of μ_S from fits to neutrino oscillation data

We utilize the central values of parameters obtained from recent global fit to the neutrino oscillation data [204, 205, 247] and ignore Majorana phases ($\alpha_1 = \alpha_2 = 0$). Then using the $m_\nu = U_\nu \hat{m}_\nu U_\nu^T$ and inverting eq. (5.6) we get

m_ν	M	μ_S
IH	(a)	$\begin{pmatrix} 82.04 + 2.261i & -17.75 - 0.508i & 0.642 - 0.251i \\ \cdot & 3.842 + 0.114i & -0.138 + 0.054i \\ \cdot & \cdot & 0.0042 - 0.0040i \end{pmatrix} \text{ GeV}$
	(b)	$\begin{pmatrix} 0.318 + 0.0088i & -0.0689 - 0.0019i & +0.0536 - 0.0209i \\ \cdot & +0.0149 + 0.00044i & -0.0116 - 0.0045i \\ \cdot & \cdot & 0.0075 - 0.0073i \end{pmatrix} \text{ GeV}$
	(c)	$\begin{pmatrix} 3.015 + 0.083i & -7.72 - 0.221i & 6.73 - 2.62i \\ \cdot & 19.78 + 0.58i & -17.25 + 6.714i \\ \cdot & \cdot & 12.41 - 12.08i \end{pmatrix} \times 10^{-3} \text{ GeV}$

Table 5.3: Same as Tab. 5.2 but for IH of light neutrino masses $\hat{m}_\nu=(0.04901, 0.04978, 0.00127)$ eV.

$$\begin{aligned}
\mu_S &= X^{-1} U_\nu \hat{m}_\nu U_\nu^T (X^T)^{-1} \\
&= \begin{pmatrix} 3.48 + 1.51i & -9.02 - 3.93i & 9.18 + 0.14i \\ . & 23.41 + 10.23i & -23.84 - 0.38i \\ . & . & 20.67 - 8.25i \end{pmatrix} \times 10^{-4} \text{ GeV}, \quad (5.14)
\end{aligned}$$

where we have used normal hierarchy (NH) for light neutrino masses, $\hat{m}_\nu=(0.00127, 0.00885, 0.0495)$ eV in the non-degenerate case of $M = \text{diag}(9.72, 115.12, 2776.6)$ GeV. For the sake of completeness, we have presented few solutions of μ_S matrix for degenerate, partially-degenerate and non-degenerate values of M as shown in the Tab. 5.2 and Tab. 5.3 corresponding to NH and inverted hierarchy (IH) light neutrino masses, respectively. For the quasi-degenerate (QD) pattern of light neutrino masses the matrix μ_S can be easily derived and all our analyses carried out in Sec. 5.2 to Sec. 5.4 can be repeated.

5.2 Amplitudes for $0\nu 2\beta$ decay and effective mass parameters

In this section we discuss analytically the contributions of various Feynman diagrams in $W_L^- - W_L^-$ channel (with two LH currents), $W_R^- - W_R^-$ channel (with two RH currents), and $W_L^- - W_R^-$ channel (with one LH and one RH current) and estimate the corresponding amplitudes in the TeV scale asymmetric LR gauge theory with extended seesaw mechanism.

The charged current interaction Lagrangian for leptons in this model in the flavor basis is

$$\mathcal{L}_{CC} = \frac{g}{\sqrt{2}} \sum_{\alpha=e,\mu,\tau} \left[\bar{\ell}_{\alpha L} \gamma_\mu \nu_{\alpha L} W_L^\mu + \bar{\ell}_{\alpha R} \gamma_\mu N_{\alpha R}^C W_R^\mu \right] + \text{h.c.} \quad (5.15)$$

Following the masses and mixing for neutrinos in the extended seesaw scheme discussed in Sec. 5.1.2, LH and RH neutrino flavor states are expressed in terms of mass eigenstates ($\hat{\nu}_i, \hat{S}_i, \hat{N}_{Ri}^C$)

$$\nu_{\alpha L} \sim \mathcal{V}_{\alpha i}^{\nu \hat{\nu}} \hat{\nu}_i + \mathcal{V}_{\alpha i}^{\nu \hat{S}} \hat{S}_i + \mathcal{V}_{\alpha i}^{\nu \hat{N}} \hat{N}_{Ri}^C, \quad (5.16)$$

$$N_{R\alpha}^C \sim \mathcal{V}_{\alpha i}^{N \hat{\nu}} \hat{\nu}_i + \mathcal{V}_{\alpha i}^{N \hat{S}} \hat{S}_i + \mathcal{V}_{\alpha i}^{N \hat{N}} \hat{N}_{Ri}^C. \quad (5.17)$$

In addition, there is a possibility where left-handed and right-handed gauge bosons mix with each other and, hence, the physical gauge bosons are linear combinations

of W_L and W_R as

$$\begin{cases} W_1 = \cos \zeta_{LR} W_L + \sin \zeta_{LR} W_R \\ W_2 = -\sin \zeta_{LR} W_L + \cos \zeta_{LR} W_R \end{cases} \quad (5.18)$$

with

$$|\tan 2\zeta_{LR}| \sim \frac{v_u v_d}{v_R^2} \sim \frac{v_d g_{2R}^2}{v_u g_{2L}^2} \left(\frac{M_{W_L}^2}{M_{W_R}^2} \right) \leq 10^{-4}. \quad (5.19)$$

As it is evident from the charged-current interaction given in eq. (5.15) and taking left- and right-handed gauge boson mixings into account given in eq. (5.18), there can be several Feynman diagrams which contribute to neutrinoless double beta decay transition in the TeV scale left-right gauge theory. They can be broadly classified as due to W_L^- - W_L^- mediation purely due to two left-handed currents, W_R^- - W_R^- mediation purely due to two right-handed currents, and W_L^- - W_R^- mediations due to one left-handed current and one right-handed current which are denoted by LL, RR, and LR in the superscripts of the corresponding amplitudes. These diagrams are shown in Fig. 5.2 - Fig. 5.5.

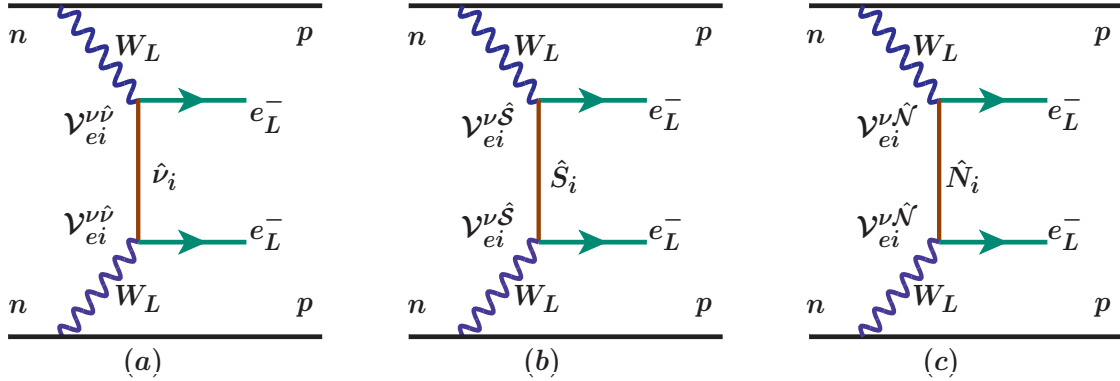


Figure 5.2: Feynman diagrams for neutrinoless double beta decay ($0\nu 2\beta$) contribution with virtual Majorana neutrinos $\hat{\nu}_i$, \hat{S}_i , and \hat{N}_{Ri}^C along with the mediation of two W_L -bosons.

5.2.1 W_L^- - W_L^- mediation

The most popular standard contribution is due to W_L^- - W_L^- mediation by light neutrino exchanges. But one of our major contribution in this work is that even with W_L^- - W_L^- mediation, the sterile neutrino exchange allowed within the extended see-saw mechanism of the model can yield much more dominant contribution to $0\nu 2\beta$ decay rate than the standard one. With the exchange of left-handed light neutrinos ($\hat{\nu}_i$), sterile neutrinos (\hat{S}_j), and RH heavy Majorana neutrinos (\hat{N}_{Rk}^C), the diagrams

shown in Fig. 5.2.(a), Fig. 5.2.(b), and Fig. 5.2.(c) contribute

$$\mathcal{A}_\nu^{LL} \propto \frac{1}{M_{W_L}^4} \sum_{i=1,2,3} \frac{(\mathcal{V}_{ei}^{\nu\hat{\nu}})^2 m_{\nu_i}}{p^2}, \quad (5.20)$$

$$\mathcal{A}_S^{LL} \propto \frac{1}{M_{W_L}^4} \sum_{j=1,2,3} \frac{(\mathcal{V}_{ej}^{\nu\hat{S}})^2}{m_{S_j}}, \quad (5.21)$$

$$\mathcal{A}_N^{LL} \propto \frac{1}{M_{W_L}^4} \sum_{k=1,2,3} \frac{(\mathcal{V}_{ek}^{\nu\hat{N}})^2}{m_{N_k}}, \quad (5.22)$$

where $|p^2| \simeq (190 \text{ MeV})^2$ represents neutrino virtuality momentum [248–253].

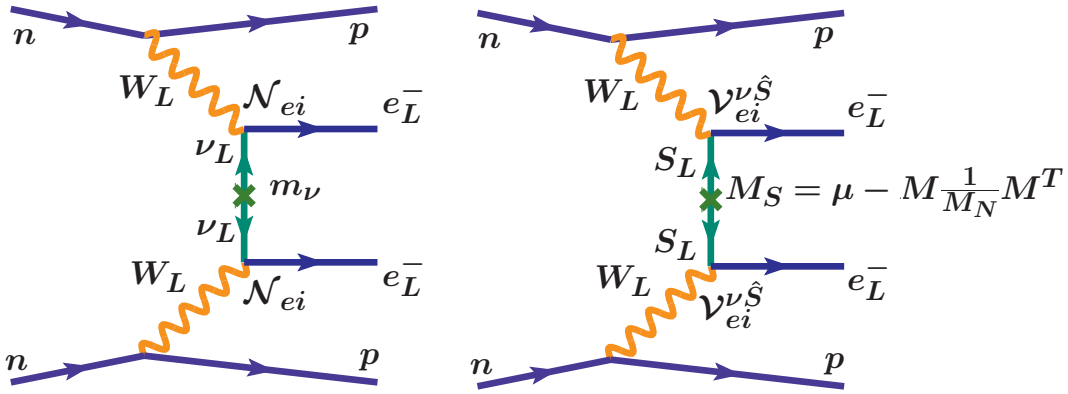


Figure 5.3: Feynman diagram for neutrinoless double beta decay contribution by $W_L^- - W_L^-$ mediation and by the exchange of virtual sterile neutrinos (S). The Majorana mass insertion has been shown explicitly by a cross.

To understand the origin and the role of the relevant Majorana mass insertion terms as source of $|\Delta L| = 2$ lepton number violation in the new contribution to $0\nu 2\beta$ process, we briefly discuss the example of sterile fermion (S) exchange corresponding to Fig. 5.2.(b) and Fig. 5.3. At first we note that, in contrast to the inverse seesaw framework with pseudo-Dirac type RH neutrinos [45, 246] where the only source of $|\Delta L| = 2$ lepton number violation is μ_S , in the present case of extended seesaw the Majorana mass for S gets an additional dominant contribution $MM_N^{-1}M^T$ as shown explicitly in eq. (5.4) and eq. (5.7). The expanded form of the Feynman diagram with both the mass insertion terms is shown in Fig. 5.3 which gives

$$\mathcal{A}_S^{LL} \propto \frac{1}{M_{W_L}^4} P_L \left[\mathcal{V}^{\nu\hat{S}} \frac{1}{\not{p} - \hat{m}_S} \hat{m}_S \frac{1}{\not{p} - \hat{m}_S} \mathcal{V}^{\nu\hat{S}T} \right]_{ee} P_L, \quad (5.23)$$

where we have used $m_S = \mu_S - M M_N^{-1} M^T$. Within the model approximation and allowed values of parameters, $|m_S| \simeq |M M_N^{-1} M^T| \gg |p| \gg |\mu_S|$ resulting in

$$\mathcal{A}_S^{LL} \propto \frac{1}{M_{W_L}^4} \left[\mathcal{V}^{\nu\hat{S}} \left(\frac{\mu_S}{\hat{m}_S^2} + \frac{1}{\hat{m}_S} \right) \mathcal{V}^{\nu\hat{S}T} \right]_{ee}, \quad (5.24)$$

where the first term is negligible compared to the second term, and we get eq. (5.21). On the other hand, in the case of pseudo-Dirac RH neutrinos corresponding to $M_N = 0$ in eq. (5.3), the only Majorana mass insertion term in Fig. 5.3 is through $m_S = \mu_S$ with $|\mu_S| \ll |p|$. Then eq. (5.24) gives $\mathcal{A}_S^{LL} \propto \frac{1}{M_{W_L}^4} \frac{(\mathcal{V}^{\nu\hat{S}})^2 \mu_S}{p^2} \simeq \frac{1}{M_{W_L}^4} \frac{m_\nu}{p^2}$ which is similar to the standard contribution. This latter situation is never encountered in the parameter space of the present models.

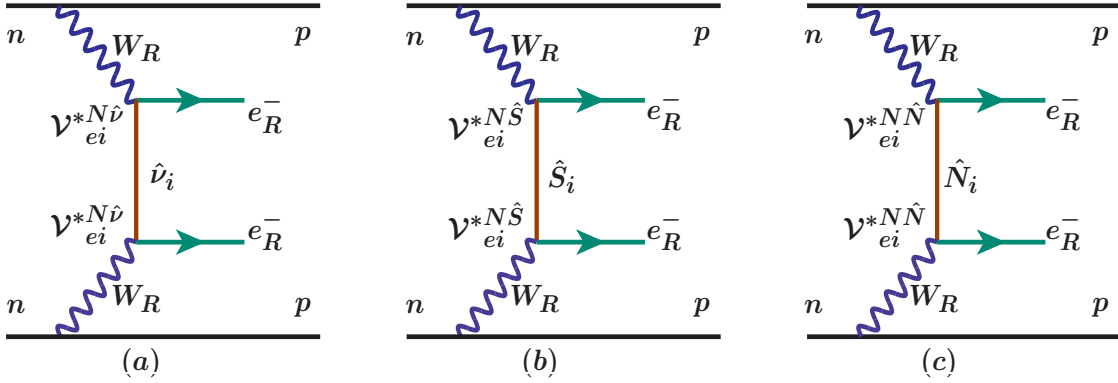


Figure 5.4: Same as Fig. 5.2 but with W_R - W_R mediation.

5.2.2 W_R^- - W_R^- mediation

This contribution arising purely out of right-handed weak currents can also occur by the exchanges of $\hat{\nu}_i$, \hat{S}_i , and \hat{N}_{Ri}^C and the corresponding diagrams are shown in Fig. 5.4.(a), Fig. 5.4.(b), and Fig. 5.4.(c) leading to the amplitudes

$$\mathcal{A}_\nu^{RR} \propto \frac{1}{M_{W_R}^4} \frac{(\mathcal{V}_{ei}^{N\hat{\nu}})^2 m_{\nu_i}}{p^2}, \quad (5.25)$$

$$\mathcal{A}_S^{RR} \propto \frac{1}{M_{W_R}^4} \frac{(\mathcal{V}_{ej}^{N\hat{S}})^2}{m_{S_j}}, \quad (5.26)$$

$$\mathcal{A}_N^{RR} \propto \frac{1}{M_{W_R}^4} \frac{(\mathcal{V}_{ej}^{N\hat{N}})^2}{m_{N_k}}. \quad (5.27)$$

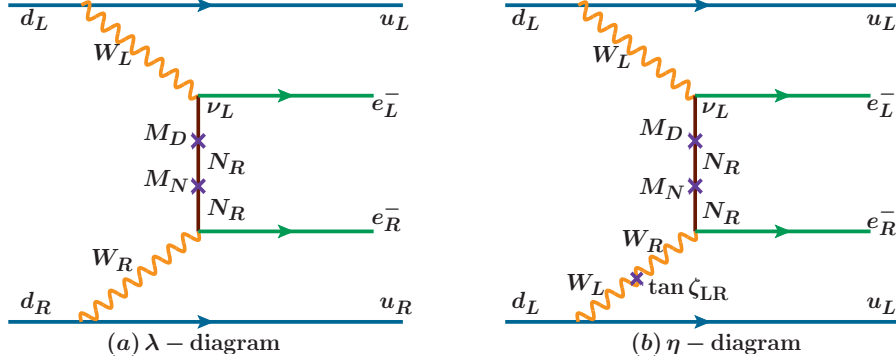


Figure 5.5: Mixed Feynman diagram with W_L - W_R mediation; left-panel is for λ -mechanism and right-panel is for η -mechanism as defined in ref. [254–256] and discussed in the text.

5.2.3 W_L^- - W_R^- mediation

According to our observation, although these contributions arising out of mixed effects by the exchanges of light LH and heavy RH neutrinos and also by the exchange of sterile neutrinos are not so dominant compared to those due to W_L^- - W_L^- mediation with sterile neutrino exchanges, as discussed in Sec. 5.2.1, the amplitudes are stronger than the standard one. The two types of mixed helicity Feynman diagrams are (i) λ -mechanism: coming from one left-handed and one right-handed current (W_L - W_R mediation) shown in Fig. 5.5.(a), (ii) η -mechanism: arising because of additional possibility of W_L - W_R mixing even though two hadronic currents are left-handed, as shown in Fig. 5.5.(b), leading to a suppression factor $\tan \zeta_{LR}$. The corresponding Feynman amplitudes for these mixed helicity diagrams are given below

$$\mathcal{A}_\lambda^{LR} \propto \frac{1}{M_{W_L}^2 M_{W_R}^2} (U_\nu)_{ei} \left(\frac{M_D}{M_N} \right)_{ei} \frac{1}{|p|}, \quad (5.28)$$

$$\mathcal{A}_\eta^{LR} \propto \frac{\tan \zeta_{LR}}{M_{W_L}^4} (U_\nu)_{ei} \left(\frac{M_D}{M_N} \right)_{ei} \frac{1}{|p|} \quad (5.29)$$

5.2.4 Doubly Charged Higgs contribution

Although we have ignored contributions due to exchanges of LH (RH) doubly charged Higgs bosons Δ_L^{--} (Δ_R^{--}) in this work, we present the corresponding amplitudes for the sake of completeness,

$$(i) \quad \mathcal{A}_{\Delta_L}^{LL} \propto \frac{1}{M_{W_L}^4} \frac{1}{M_{\Delta_L}^2} f_L \nu_L \quad ,$$

$$(ii) \quad \mathcal{A}_{\Delta_R}^{RR} \propto \frac{1}{M_{W_R}^4} \frac{1}{M_{\Delta_R}^2} f_R \nu_R \quad .$$

As stated in Sec. 5.1, the masses of Δ_L^- and Δ_L^{++} are of the order of the large parity restoration scale which damps out the induced VEV v_L and the corresponding amplitude. The amplitude due to Δ_R^- exchange is damped out compared to the standard amplitude as it is $\propto \frac{1}{M_{WR}^5}$.

5.2.5 Nuclear matrix elements and normalized effective mass parameters

By now it is well known that different particle exchange contributions for $0\nu 2\beta$ decay discussed above are also modified by the corresponding nuclear matrix elements which depend upon the chirality of the hadronic currents involved [254–261]. Including all relevant contributions except those due to doubly charged Higgs exchanges, and using eq. (5.20) - eq. (5.29), we express the inverse half-life in terms of effective mass parameters with proper normalization factors taking into account the nuclear matrix elements [254–261] leading to the half-life prediction

$$\begin{aligned} [T_{1/2}^{0\nu}]^{-1} &= G_{01}^{0\nu} \{ |\mathcal{M}_\nu^{0\nu}|^2 |\eta_\nu|^2 + |\mathcal{M}_N^{0\nu}|^2 |\eta_{N_R}^L|^2 + |\mathcal{M}_N^{0\nu}|^2 |\eta_{N_R}^R|^2 \\ &+ |\mathcal{M}_\lambda^{0\nu}|^2 |\eta_\lambda|^2 + |\mathcal{M}_\eta^{0\nu}|^2 |\eta_\eta|^2 \} + \text{interference terms.} \end{aligned} \quad (5.30)$$

where the dimensionless particle physics parameters are

$$\begin{aligned} |\eta_\nu| &= \left| \frac{\sum_i \mathcal{V}_{ei}^{\nu\hat{\nu}^2} m_{\nu i}}{m_e} \right| \\ |\eta_{N_R}^R| &= m_p \left(\frac{M_{WL}}{M_{WR}} \right)^4 \left| \frac{\mathcal{V}_{ei}^{N\hat{N}^2}}{m_{N_i}} \right| \\ |\eta_{N_R}^L| &= m_p \left| \frac{V_{ei}^{N\hat{\nu}}}{m_{N_i}} + \frac{V_{ei}^{S\hat{\nu}}}{m_{S_i}} \right| \\ |\eta_\lambda| &= \left(\frac{M_{WL}}{M_{WR}} \right)^2 \left| U_{ei} \left(\frac{M_D}{M_N} \right)_{ei} \right| \\ |\eta_\eta| &= \tan \zeta_{LR} \left| U_{ei} \left(\frac{M_D}{M_N} \right)_{ei} \right| \end{aligned} \quad (5.31)$$

In eq. (5.31), m_e (m_i) = mass of electron (light neutrino), and m_p = proton mass. In eq. (5.30), $G_{01}^{0\nu}$ is the phase space factor and besides different particle parameters, it contains the nuclear matrix elements due different chiralities of the hadronic weak currents such as $(\mathcal{M}_\nu^{0\nu})$ involving left-left chirality in the standard contribution, and due to heavy neutrino exchanges $(\mathcal{M}_\nu^{0\nu})$ involving right-right chirality arising out of

heavy neutrino exchange, $(\mathcal{M}_\lambda^{0\nu})$ for the λ -diagram, and $(\mathcal{M}_\eta^{0\nu})$ for the η -diagram. Explicit numerical values of these nuclear matrix elements discussed in ref. [254–261] are given in Tab. 5.4.

Isotope	$G_{01}^{0\nu}$ [10^{-14} yrs $^{-1}$] refs. [254–260]	$\mathcal{M}_\nu^{0\nu}$	$\mathcal{M}_N^{0\nu}$	$\mathcal{M}_\lambda^{0\nu}$	$\mathcal{M}_\eta^{0\nu}$
^{76}Ge	0.686	2.58–6.64	233–412	1.75–3.76	235–637
^{82}Se	2.95	2.42–5.92	226–408	2.54–3.69	209–234
^{130}Te	4.13	2.43–5.04	234–384	2.85–3.67	414–540
^{136}Xe	4.24	1.57–3.85	160–172	1.96–2.49	370–419

Table 5.4: Phase space factors and nuclear matrix elements with their allowed ranges as derived in refs. [254–261].

In order to arrive at a common normalization factor for all types of contributions, at first we use the expression for inverse half-life for $0\nu 2\beta$ decay process due to only light active Majorana neutrinos, $[T_{1/2}^{0\nu}]^{-1} = G_{01}^{0\nu} |\mathcal{M}_\nu^{0\nu}|^2 |\eta_\nu|^2$. Using the numerical values given in Tab. 5.4, we rewrite the inverse half-life in terms of effective mass parameter

$$[T_{1/2}^{0\nu}]^{-1} = G_{01}^{0\nu} \left| \frac{\mathcal{M}_\nu^{0\nu}}{m_e} \right|^2 |m_\nu^{\text{ee}}|^2 = 1.57 \times 10^{-25} \text{ yrs}^{-1} \text{ eV}^{-2} |m_\nu^{\text{ee}}|^2 = \mathcal{K}_{0\nu} |m_\nu^{\text{ee}}|^2$$

where $m_\nu^{\text{ee}} = \sum_i (\mathcal{V}_{ei}^{\nu\hat{\nu}})^2 m_{\nu_i}$. Then the analytic expression for all relevant contributions to effective mass parameters taking into account the respective nuclear matrix elements turns out to be

$$[T_{1/2}^{0\nu}]^{-1} = \mathcal{K}_{0\nu} \left[|m_\nu^{\text{ee}}|^2 + |m_N^{\text{ee,R}}|^2 + |m_S^{\text{ee,L}}|^2 + |m_\lambda^{\text{ee}}|^2 + |m_\eta^{\text{ee}}|^2 \right] + \dots \quad (5.32)$$

where the ellipses denote interference terms and all other sub-dominant contributions. In eq. (5.32), the new effective mass parameters are

$$m_N^{\text{ee,R}} = \sum_i \left(\frac{M_{W_L}}{M_{W_R}} \right)^4 \left(\mathcal{V}_{ei}^{N\hat{N}} \right)^2 \frac{|p|^2}{m_{N_i}} \quad (5.33)$$

$$m_S^{\text{ee,L}} = \sum_i \left(\mathcal{V}_{ei}^{\nu\hat{S}} \right)^2 \frac{|p|^2}{m_{S_i}} \quad (5.34)$$

$$m_\lambda^{\text{ee}} = 10^{-2} \left(\frac{M_{W_L}}{M_{W_R}} \right)^2 \left| U_{ei} \left(\frac{M_D}{M_N} \dots \right)_{ei} \right| |p| \quad (5.35)$$

$$m_\eta^{\text{ee}} = \tan \zeta_{LR} \left| U_{ei} \left(\frac{M_D}{M_N} \dots \right)_{ei} \right| |p| \quad (5.36)$$

where $|p|^2 = m_e m_p \mathcal{M}_N^{0\nu} / \mathcal{M}_\nu^{0\nu} \simeq (200 \text{ MeV})^2$. It is to be noted that the suppression factor 10^{-2} arises in the λ -diagram as pointed out in refs. [254–261].

5.3 Numerical estimation of effective mass parameters

Using analytic expression for relevant effective mass parameters given in eq. (5.30)-eq. (5.36) and our model parameters discussed in Sec. 5.1.1, we now estimate the relevant individual contributions numerically.

5.3.1 Nearly standard contribution

In our model the new mixing matrix $\mathcal{N}_{ei} \equiv \mathcal{V}_{ei}^{\nu\hat{\nu}} = (1 - \eta) U_\nu$ contains additional non-unitarity effect due to non-vanishing η where

$$\begin{aligned} \mathcal{N}_{e1} &= (1 - \eta_{e1}) U_{11} - \eta_{e2} U_{21} - \eta_{e3} U_{31} \\ \mathcal{N}_{e2} &= (1 - \eta_{e1}) U_{12} - \eta_{e2} U_{22} - \eta_{e3} U_{32} \\ \mathcal{N}_{e3} &= (1 - \eta_{e1}) U_{13} - \eta_{e2} U_{23} - \eta_{e3} U_{33} \end{aligned} \quad (5.37)$$

We estimate numerical values of \mathcal{N}_{ei} using all allowed values of η discussed in Sec. 5.1 and also by using $U_\nu \equiv U_{\text{PMNS}}$. Then the effective mass parameter for the W_L - W_L mediation with light neutrino exchanges is found to be almost similar to the standard prediction

$$|m_\nu^{\text{ee}}| \simeq \begin{cases} 0.004 \text{ eV} & \text{NH,} \\ 0.048 \text{ eV} & \text{IH,} \\ 0.23 \text{ eV} & \text{QD.} \end{cases} \quad (5.38)$$

This nearly standard contribution on effective mass parameter is presented by the dashed-green colored lines of Fig. 5.6 and Fig. 5.7 for NH neutrino masses, but it is presented by the dashed-pink colored lines of the same figures for IH neutrino masses. In our numerical estimations presented in Fig. 5.6 we have used M_D values

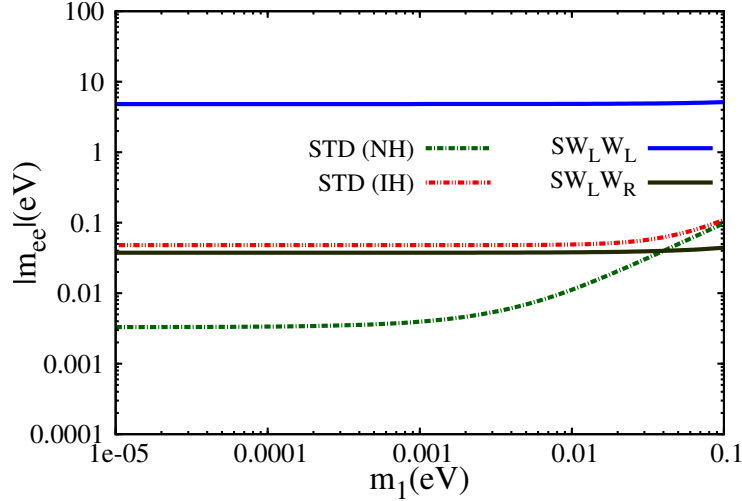


Figure 5.6: Variation of effective mass parameters with lightest neutrino mass. The standard contributions are shown by dashed-green (pink) colored lines for NH (IH) case. The non-standard contribution with W_L^- - W_L^- mediation and sterile neutrino exchanges is shown by the upper blue solid line whereas the one with W_L^- - W_R^- mediation and sterile neutrino exchanges is shown by the lower black solid line.

including RG corrections as given in eq. (5.11) but with $M = (50, 200, 1712)$ GeV, $M_N = (1250, 3000, 5000)$ GeV, and $\hat{m}_S = (2, 13, 532)$ GeV. Similarly, in Fig. 5.7 we have utilized M_D values including RG corrections from eq. (5.11) but with $M = (100, 100, 2151.6)$ GeV, $M_N = (5000, 5000, 5000)$ GeV, and $\hat{m}_S = (2, 2, 800)$ GeV.

5.3.2 Dominant non-standard contributions

Before estimating the non-standard effective mass parameters, we present the mixing matrices numerically. As discussed in eq. (5.10) of Sec. 5.1.2, the mixing matrices $X = M_D M^{-1}$, $Y = M M_N^{-1}$, $Z = M_D M_N^{-1}$, and $y = \mu_S M^{-1}$ all contribute to non-standard predictions of $0\nu 2\beta$ amplitude in the extended seesaw scheme.

Using eq. (5.10) and the diagonal structures of the RH Majorana neutrino mass matrix $M_N = \text{diag}(M_{N_1}, M_{N_2}, M_{N_3})$ as well as N - S mixing matrix $M = \text{diag}(M_1, M_2, M_3)$, and the Dirac neutrino mass matrix M_D with RG corrections given in eq. (5.11), we derive the relevant elements of the mixing matrices \mathcal{N} , $\mathcal{V}^{\nu\hat{N}}$, $\mathcal{V}^{\nu\hat{S}}$, $\mathcal{V}^{S\hat{\nu}}$, $\mathcal{V}^{S\hat{S}}$, $\mathcal{V}^{S\hat{N}}$, $\mathcal{V}^{N\hat{\nu}}$, $\mathcal{V}^{N\hat{S}}$ and $\mathcal{V}^{N\hat{N}}$ for which one example is

$$\begin{aligned} \mathcal{N}_{ei} &= \{0.8135, 0.5597, 0.1278\} \\ \mathcal{V}_{ei}^{\nu\hat{S}} &= \{4.5398 \times 10^{-4}, 4.93 \times 10^{-4}, 2.148 \times 10^{-4}\}, \\ \mathcal{V}_{ei}^{\nu\hat{N}} &= \{1.8 \times 10^{-5}, 3.3 \times 10^{-5}, 6.7 \times 10^{-5}\}, \end{aligned}$$

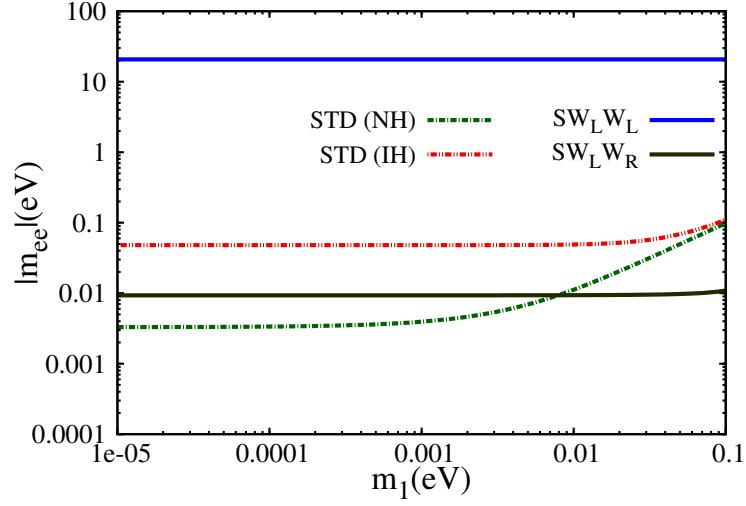


Figure 5.7: Variation of effective mass parameters with lightest neutrino mass. The standard contributions are shown by dashed-green (pink) colored lines for NH (IH) case. The non-standard contribution with W_L^- - W_L^- mediation and sterile neutrino exchanges is shown by the upper blue solid line whereas the one with W_L^- - W_R^- mediation and sterile neutrino exchanges is shown by the lower black solid line.

$$\begin{aligned}
\mathcal{V}_{ei}^{S\hat{\nu}} &= \{3.6 \times 10^{-3}, 3.3 \times 10^{-3}, 6.0 \times 10^{-3}\}, \\
\mathcal{V}_{ei}^{S\hat{S}} &= \{0.999, 0.0002, 5.0 \times 10^{-6}\}, \\
\mathcal{V}_{ei}^{S\hat{N}} &= \{0.04, 0.0, 0.0\}, \\
\mathcal{V}_{ei}^{N\hat{N}} &= \{1.0, 0.0, 0.0\}, \\
\mathcal{V}_{ei}^{N\hat{\nu}} &= \{9.33 \times 10^{-10}, 2.97 \times 10^{-9}, 1.0 \times 10^{-8}\}, \\
\mathcal{V}_{ei}^{N\hat{S}} &= \{0.04, 0.0, 0.0\}.
\end{aligned} \tag{5.39}$$

For evaluating these mixing matrix elements we have taken the input values, M ,

C1: (GeV)	C2: (GeV)
$M = \text{diag}(50.0, 200.0, 1711)$	$M = \text{diag}(100.0, 100.0, 2151.6)$
$M_N = \text{diag}(1250.0, 3000.0, 5000.0)$	$M_N = \text{diag}(5000.0, 5000.0, 5000.0)$
$\hat{m}_S = \text{diag}(2.0, 13.0, 532)$	$\hat{m}_S = \text{diag}(2.0, 2.0, 800)$

Table 5.5: Input values of M , M_N , and \hat{m}_S used for estimating effective mass parameters given in Tab. 5.6.

M_N , and \hat{m}_S presented under column C1 of Tab. 5.5. These lead to the numerical results for effective mass parameter contributing to $0\nu 2\beta$ decay rate presented under column C1 of Tab. 5.6. Similarly when we use the M , M_N , and \hat{m}_S values from column C2 of Tab. 5.5 we obtain effective mass parameters given in column C2 of

Tab. 5.6.

Effective mass parameter	C1 (eV)	C2 (eV)
m_ν^{ee}	0.004	0.004
$m_N^{ee,R}$	0.0085	0.0085
$m_S^{ee,L}$	20.75	188.48
$m_{\lambda,\eta}^{ee}$	0.0093	0.0274

Table 5.6: Rough estimation of effective mass parameters with the allowed model parameters. The results are for the Dirac neutrino mass matrix including RG corrections. The input values of mass matrices allowed by the current data for different columns are presented in Tab. 5.5.

The most dominant and new contribution to the effective mass parameters is found to emerge from the amplitude A_S^{LL} of eq. (5.20) due to W_L^- - W_L^- mediation and sterile neutrino exchanges. This has been shown in Fig. 5.8 for various combinations of sterile neutrino mass eigenvalues and for M_D values including RG corrections given in eq. (5.11). In Fig. 5.8 our estimated values range from 0.2 – 1.0 eV. Looking to the results given in Tab. 5.6 and Fig. 5.6, Fig. 5.7, and Fig. 5.8, it is clear that the actual enhanced rate of $0\nu\beta\beta$ decay in this model depends primarily upon the sterile neutrino mass eigenvalues m_{S_1} and m_{S_2} . If the decay rate corresponds to $|m_{\text{eff}}| \simeq 0.21 - 0.53$ eV as claimed by the Heidelberg-Moscow experiment using ^{76}Ge [229, 236–239], our new finding is that the light neutrino masses could be still of NH or IH pattern, instead of necessarily being of QD pattern, but with $m_{S_1} \sim 10$ GeV and $m_{S_2} \sim 30$ GeV. Of course the the Dirac neutrino mass matrix having its high scale quark-lepton symmetric origin also contributes to the magnification of the effective mass parameter. The next dominant contributions coming from the Feynman amplitude A_S^{LR} of eq. (5.29) due to W_L^- - W_R^- mediation and sterile neutrino exchanges with $m_{\lambda,\eta}^{ee,LR} = 0.04$ eV (0.01 eV) have been shown in Fig. 5.6 (Fig. 5.7).

5.4 Estimations on lepton flavor violating decays and J_{CP}

Besides the neutrinoless double beta decay process, the sterile and heavy neutrinos in this model can predominantly mediate different lepton flavor violating decays, $\mu \rightarrow e + \gamma$, $\tau \rightarrow e + \gamma$, and $\tau \rightarrow \mu + \gamma$. Since $\ell_\alpha \rightarrow \ell_\beta + \gamma$ ($\alpha \neq \beta$) is lepton flavor changing process, it is strictly forbidden in the SM when $m_\nu = 0$ and lepton number is conserved. In our model the underlying lepton flavor violating interactions and

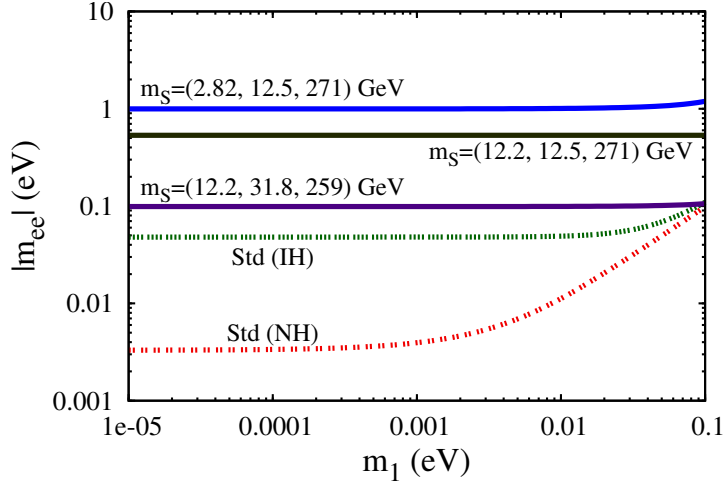


Figure 5.8: Predictions of non-standard contributions to effective mass parameter with W_L^- - W_L^- mediation and sterile neutrino exchange for $M = (120, 250, 1664.9)$ GeV (top solid line), $M = (250, 250, 1663.3)$ GeV (middle solid line), and $M = (250, 400, 1626.1)$ GeV (bottom solid line) keeping $M_N = (5, 5, 10)$ TeV fixed and for M_D as in eq. (5.11).

non-unitarity effects contribute to lepton flavor violating decays by the mediation of heavy RH Majorana and sterile Majorana fermions.

$M(\text{GeV})$	$M_N(\text{TeV})$	Heavy Mass Eigen Values(GeV)
(9.7, 115.2, 2776.5)	(5, 5, 5)	(0.018, 2.65, 1238, 5000, 5002, 6238)
(100, 100, 2151.57)	(5, 5, 5)	(1.99, 2.00, 800.5, 5001, 5002, 5800)
(100, 200, 1702.67)	(5, 5, 5)	(1.99, 8.00, 527.5, 5001, 5007, 5527)
(50, 200, 1711)	(1.5, 2, 5)	(1.67, 19.8, 532.2, 1501, 2019, 5532)
(1604.4, 1604.4, 1604.4)	(5, 5, 10)	(252.4, 461.5, 470.6, 5471.6, 5471.4, 10252.4)

Table 5.7: The Heavy mass eigenvalues for the matrices of M and M_N which have been used to evaluate branching ratios.

5.4.1 Branching ratio

Keeping in mind the charged-current interaction in the neutrino mass basis for extended seesaw scheme given in eq. (5.15) - eq. (5.17), the dominant contributions are mainly through the exchange of the sterile and heavy RH neutrinos. The decomposition of eq. (4.44) in to heavy and sterile parts gives [45, 165, 167, 170, 171, 206, 262]

$$\text{Br}(\ell_\alpha \rightarrow \ell_\beta + \gamma) = \frac{\alpha_w^3 s_w^2 m_{\ell_\alpha}^5}{256 \pi^2 M_W^4 \Gamma_\alpha} |\mathcal{G}_{\alpha\beta}^N + \mathcal{G}_{\alpha\beta}^S|^2, \quad (5.40)$$

$$\begin{aligned}
\text{where } \mathcal{G}_{\alpha\beta}^N &= \sum_k \left(\nu^{\nu\hat{N}} \right)_{\alpha k} \left(\nu^{\nu\hat{N}} \right)_{\beta k}^* \mathcal{I} \left(\frac{m_{N_k}^2}{M_{W_L}^2} \right), \\
\mathcal{G}_{\alpha\beta}^S &= \sum_j \left(\nu^{\nu\hat{S}} \right)_{\alpha j} \left(\nu^{\nu\hat{S}} \right)_{\beta j}^* \mathcal{I} \left(\frac{m_{S_j}^2}{M_{W_L}^2} \right), \tag{5.41}
\end{aligned}$$

and $I(x)$ has already been defined in eq. (4.44). It is clear from the above equation and within the model parameter range, $M_N \gg M \gg M_D$, that the first term in eq. (5.40) is negligible while second term involving the the heavy sterile neutrinos gives dominant contribution which is proportional to $\sum_j \left(\nu_{\alpha j}^{\nu\hat{S}} \right) \left(\nu_{\beta j}^{\nu\hat{S}} \right)^* \simeq 2\eta_{\alpha\beta}$.

$M(\text{GeV})$	$M_N(\text{TeV})$	$\text{Br}(\mu \rightarrow e\gamma)$ (10^{-16})	$\text{Br}(\tau \rightarrow e\gamma)$ (10^{-14})	$\text{Br}(\tau \rightarrow \mu\gamma)$ (10^{-12})
(50, 200, 1711.8)	(1.5, 2, 5)	3.05	3.11	4.36
(100, 100, 2151.57)	(5, 5, 5)	1.28	1.39	1.95
(100, 200, 1702.67)	(5, 5, 5)	2.85	3.1	4.3
(1604.4, 1604.4, 1604.4)	(5, 5, 10)	2.18	2.32	3.25

Table 5.8: The three branching ratios in extended inverse seesaw for different values of M and M_N while M_D is same as in eq. (5.11).

Using the numerically computed mixing matrix, and using allowed mass scales presented in Tab. 5.7, our model estimations on branching ratios are given in Tab. 5.8. Recent experimental data gives the best limit on these branching ratios for lepton flavor violating decays coming from the MEG collaboration [208–210, 263]. Out of these $\text{Br}(\mu \rightarrow e + \gamma) \leq 1.2 \times 10^{-11}$ [208–210, 263]. is almost three orders of magnitude stronger than the limit $\text{Br}(\tau \rightarrow e + \gamma) \leq 3.3 \times 10^{-8}$ or $\text{Br}(\tau \rightarrow \mu + \gamma) \leq 4.4 \times 10^{-8}$ at 90% C.L. However, projected reach of future sensitivities of ongoing searches are $\text{Br}(\tau \rightarrow e + \gamma) \leq 10^{-9}$, $\text{Br}(\tau \rightarrow \mu + \gamma) \leq 10^{-9}$, and $\text{Br}(\mu \rightarrow e + \gamma) \leq 10^{-18}$ [208–210, 263] which might play crucial role in verifying or falsifying the discussed scenario.

5.4.2 CP -violation due to non-unitarity

There are attempts taken in long baseline experiments [199–202] with accelerator neutrinos ν_μ and anti-neutrinos $\bar{\nu}_\mu$ to search for CP -violating effects in neutrino oscillations. In the usual notation, the standard contribution to these effects is determined by the re-phasing invariant J_{CP} associated with the Dirac phase δ_{CP} and matrix elements of the PMNS matrix is given in eq. (4.42). In this extended seesaw mechanism, the leptonic CP -violation can be written as in eq. (4.41), where

[45, 187–197, 246] $\Delta J_{\alpha\beta}^{ij}$ is expanded in eq. (4.43). The extra contribution arises because of the non-unitarity mixing matrix which depends on both M_D and M . Thus the new contribution to CP -violation is larger for larger M_D which is generated with quark-lepton symmetry and for smaller M while safeguarding the constraint $M_N \gg M > M_D, \mu_S$. It is noteworthy that in our model even if the leptonic Dirac phase $\delta_{CP} \simeq 0, \pi, 2\pi$, and/or $\sin\theta_{13} \rightarrow 0$, there is substantial contribution to CP -violation which might arise out of the imaginary parts of the non-unitarity matrix elements $\eta_{\alpha\beta}$.

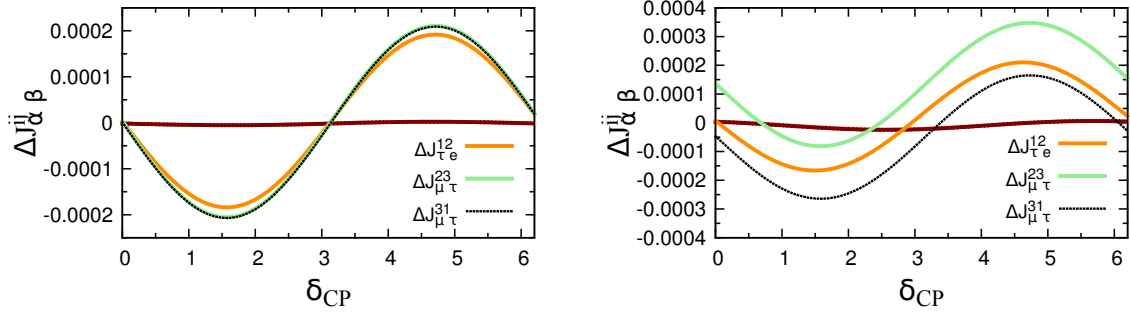


Figure 5.9: CP -violation for the full allowed range of leptonic Dirac phase δ_{CP} . The left-panel corresponds to degenerate values of M with $M_1 = M_2 = M_3 \simeq 1604.442$ GeV, and the right panel is due to non-degenerate M with $M_1 = 9.7$ GeV, $M_2 = 115.2$ GeV, and $M_3 = 2776.5$ GeV.

M	$\Delta \mathcal{J}_{e\mu}^{12}$	$\Delta \mathcal{J}_{e\mu}^{23}$	$\Delta \mathcal{J}_{\mu\tau}^{23}$	$\Delta \mathcal{J}_{\mu\tau}^{31}$	$\Delta \mathcal{J}_{\tau e}^{12}$
(a)	-2.0×10^{-6}	-2.3×10^{-6}	-1.2×10^{-4}	-1.2×10^{-4}	-1.1×10^{-4}
(b)	-2.7×10^{-6}	-3.2×10^{-6}	-1.2×10^{-4}	-1.2×10^{-4}	-1.1×10^{-4}
(c)	-2.1×10^{-5}	-2.4×10^{-5}	1.1×10^{-7}	-1.8×10^{-4}	-7.9×10^{-5}

Table 5.9: The CP -violating effects for (a) degenerate masses $M=(1604.4, 1604.4, 1604.4)$ GeV, (b) partially degenerate masses $M=(100, 100, 2151.6)$ GeV and (c) non degenerate masses $M=(9.7, 115.2, 2776.5)$ GeV, while M_D is same as in eq. (5.11).

Our estimations using RGE corrected Dirac neutrino mass matrix and both degenerate and non-degenerate matrix M are shown in the left-panel and right-panel of Fig. 5.9. If the leptonic Dirac phase $\delta_{CP} \neq 0, \pi, 2\pi$, significant CP -violation up to $|\Delta \mathcal{J}|_{\max} \simeq 1.5 \times 10^{-4}$ is found to occur for degenerate M , but when M is non-degenerate we obtain $|\Delta \mathcal{J}|_{\max} \simeq (2-4) \times 10^{-4}$. Also even if $\delta_{CP} \simeq 0, \pi, 2\pi$, non-vanishing CP -violation to the extent of $|\Delta \mathcal{J}| \simeq (1-2) \times 10^{-4}$ is noted to emerge for non-degenerate M . These results may be compared with CP -violation in the quark

sector where $\mathcal{J}_{\text{CKM}} \simeq 3.05_{-0.20}^{+0.19} \times 10^{-5}$ [149, 150] which is nearly one order lower than the leptonic case. The horizontal lines in Fig. 5.9 represent absence of non-unitarity effects on CP -violation. In Fig. 5.9 we have plotted the δ_{CP} dependence of $\Delta\mathcal{J}_{\alpha\beta}^{ij}$ and found that estimation of $\Delta\mathcal{J}_{\alpha\beta}^{ij}$ in different channel would give the amount of non-degeneracy together with non-unitarity.

5.5 Implementation in $SO(10)$

Our main goal in this section is to examine whether the TeV scale LR gauge model that has been shown to give rise to dominant contribution to $0\nu 2\beta$ decay and LFV in Sec. 5.1 - Sec. 5.4 can emerge from a non-SUSY $SO(10)$ grand unified theory. Although the search for low mass W_R^\pm bosons in non-SUSY GUTs has been attempted initially without [90–92, 264, 265] precision CERN-LEP data on $\alpha_S(M_Z)$ and $\sin^2\theta_W(M_Z)$ [149, 150], there are more recent results on physically appealing intermediate scales [58, 81, 83, 127, 145]. But the analyses in non-SUSY cases where the $B-L$ breaking scale synonymous to W_R gauge boson mass much lower than 10^{10} GeV are ruled out because of the associated large contributions to light neutrino masses via type-I seesaw mechanism. In view of the rich phenomenological consequences of the extended seesaw mechanism that evades the discordance between dominant $0\nu 2\beta$ decay and small neutrino mass predictions as discussed in Sec. 5.1 - Sec. 5.4, we explore the possibility of such low scale LR gauge theory in the minimally extended $SO(10)$ grand unification model.

5.5.1 Symmetry breaking chain

We consider the symmetry breaking chain discussed in ref. [58]. Although this model, as such, is ruled out because of the TeV scale canonical seesaw that operates to give large neutrino masses in contravention of the oscillation data, here we modify this model by including the additional doublets $(\chi_L, \chi_R) \subset 16_H$ of $SO(10)$ and extending the minimal fermion content in 16_F with the addition of one $SO(10)$ singlet neutral fermion per generation in order to implement the extended seesaw mechanism

$$\begin{aligned}
 SO(10) & \xrightarrow[\ 54_H]{M_{GUT}} G_{224D} \xrightarrow[\ 210_H]{M_P} G_{224} \xrightarrow[\ 210_H]{M_C} G_{2213} \\
 & \xrightarrow[\ 210_H]{M_R^+} G_{2113} \xrightarrow[\ 126_H+16_H]{M_R^0} G_{213} \xrightarrow[\ 10_H]{M_Z} G_{13}
 \end{aligned} \tag{5.42}$$

Above the energy scale M_P , the D -parity is restored therefore above this energy $g_{2L} = g_{2R}$. It was found in refs. [56–58] that the G_{224} -singlets in 54_H and 210_H of $SO(10)$ are D -parity even and odd, respectively. Also it was noted that the neutral components of the G_{224} multiplet $(1, 1, 15)$ contained in 210_H and 45_H of $SO(10)$ have D -parity even and odd, respectively. In the first step, VEV is assigned along the $\langle(1, 1, 1)\rangle \subset 54_H$ which has even D -Parity to guarantee the LR symmetric Pati-Salam group to survive while at the second step D -parity is broken by assigning $\langle(1, 1, 1)\rangle \subset 210_H$ to obtain asymmetric G_{224} with $g_{2L} \neq g_{2R}$. The spontaneous breaking $G_{224} \rightarrow G_{2213}$ is achieved by the VEV $\langle(1, 1, 15)_H^0\rangle \subset 210_H$. The symmetry breaking $G_{2213} \rightarrow G_{2113}$ is implemented by assigning $O(M_R^+)$ VEV to the neutral component of the submultiplet $\langle(1, 3, 15)_H^0\rangle \subset 210_H$, and the breaking $U(1)_R \times U(1)_{B-L} \rightarrow U(1)_Y$ is achieved by $\langle\Delta_R^0(3, 1, \bar{10})\rangle \subset 126_H$ while the VEV $\langle\chi_R^0(1, 2, 4)\rangle \subset 16_H$ provides the N - S mixing. As usual, the breaking of SM to low energy symmetry $U(1)_Q \times SU(3)_C$ is carried out by the SM doublet contained in the bi-doublet $\Phi(2, 2, 1) \subset 10_H$.

5.5.2 Gauge coupling unification

While SM is the symmetry of fundamental interactions near the M_Z scale, in the conventional approach to investigation of gauge coupling unification, usually the semi simple gauge symmetry to which the GUT gauge theory breaks is a product of three or more groups. As a result the symmetry below the GUT-breaking scale involves three or more gauge couplings. The renormalization group (RG) evolution of gauge couplings thus may creates a triangular region around the projected unification scale (Similar to SM) making the determination of the scale more or less uncertain. Even though the region of uncertainty is reduced in the presence of intermediate scales, it exists in principle. Only in the case when $G_I = SU(2)_L \times SU(2)_R \times SU(4)_C \times D$, the Pati-Salam symmetry with LR discrete symmetry [47] ($\equiv D$ -Parity) [56, 266], there are two gauge couplings $g_{2L} = g_{2R}$ and g_{4C} , and the meeting point of the two

M_R^0 (TeV)	M_R^+ (TeV)	M_C (TeV)	M_P (GeV)	M_G (GeV)	α_G
5	10	10^3	$10^{14.2}$	$10^{17.64}$	0.03884
5	10	$10^{3.5}$	$10^{14.42}$	$10^{17.61}$	0.03675
5	20	10^3	$10^{14.08}$	$10^{17.54}$	0.03915
5	10	100	$10^{13.72}$	$10^{17.67}$	0.0443
5	20	500	$10^{13.93}$	$10^{17.55}$	0.0406

Table 5.10: Predictions of allowed mass scales and the GUT couplings in the $SO(10)$ symmetry breaking chain with low-mass W_R^\pm, Z' bosons.

RG-evolved coupling lines determines the unification point exactly. Several interesting consequences of this intermediate symmetry have been derived earlier including vanishing corrections to GUT-threshold effects on $\sin^2 \theta_W$ and the intermediate scale [82, 224–226]. We find this symmetry to be essentially required at the highest intermediate scale in the present model to guarantee several observable phenomena as $SO(10)$ model predictions while safeguarding precision unification. We have evaluated the one-loop and two-loop coefficients of β -functions of renormalization group equations for the gauge couplings [51, 107], as given in eq. (2.20). The one and two loop β -coefficients are given in Tab. B.2 of Appendix B.

The Higgs spectrum used in different ranges of mass scales under respective gauge symmetries (G) are

$$\begin{aligned}
\text{(i)} \quad \mu = M_Z - M_R^0 : G = \text{SM} = G_{213}, \quad & \Phi(2, 1/2, 1); \\
\text{(ii)} \quad \mu = M_R^0 - M_R^+ : G = G_{2113}, \quad & \Phi_1(2, 1/2, 0, 1) \oplus \Phi_2(2, -1/2, 0, 1) \oplus \\
& \chi_R(1, 1/2, -1, 1) \oplus \Delta_R(1, 1, -2, 1); \\
\text{(iii)} \quad \mu = M_R^+ - M_C : G = G_{2213}, \quad & \Phi_1(2, 2, 0, 1) \oplus \Phi_2(2, 2, 0, 1) \oplus \\
& \chi_R(1, 2, -1, 1) \oplus \Delta_R(1, 3, -2, 1) \\
& \oplus \Sigma_R(1, 3, 0, 1); \\
\text{(iv)} \quad \mu = M_C - M_P : G = G_{224}, \quad & \Phi_1(2, 2, 1) \oplus \Phi_2(2, 2, 1) \oplus \\
& \chi_R(1, 2, \bar{4}) \oplus \Delta_R(1, 3, \bar{10}) \\
& \oplus \Sigma_R(1, 3, 15); \\
\text{(v)} \quad \mu = M_P - M_U : G = G_{224D}, \quad & \Phi_1(2, 2, 1) \oplus \Phi_2(2, 2, 1) \oplus \\
& \chi_L(2, 1, 4) \oplus \chi_R(1, 2, \bar{4}) \oplus \\
& \Delta_L(3, 1, 10) \oplus \Delta_R(1, 3, \bar{10}) \oplus \\
& \Sigma_L(3, 1, 15) \oplus \Sigma_R(1, 3, 15). \tag{5.43}
\end{aligned}$$

Recently bounds on the masses of the charged and neutral components of the second Higgs doublet in the left-right symmetric model has been estimated to be

$\mathcal{O}(20)$ TeV [267]. While searching for possible mass scales we have used the second Higgs doublet Φ_2 only for $\mu \geq 10$ TeV.

We have used extended survival hypothesis in implementing spontaneous symmetry breaking of $SO(10)$ and intermediate gauge symmetries leading to the SM gauge theory [268, 269]. In addition to D -Parity breaking models [56–58], the importance of the Higgs representation 210_H has been emphasized in the construction of a minimal SUSY $SO(10)$ GUT model [30–35]. But the present non-SUSY $SO(10)$ symmetry breaking chain shows a departure in that the G_{224D} symmetry essentially required at the highest intermediate scale has unbroken D -Parity which is possible by breaking the GUT symmetry through the Higgs representation $54_H \subset SO(10)$ that acquires GUT-scale VEV in the direction of its D -parity even G_{224D} -singlet. The importance of this G_{224D} symmetry in stabilizing the values of M_P and $\sin^2 \theta_W(M_Z)$ against GUT-Planck scale threshold effects has been discussed in refs. [224–226] and Sec. 5.5.4 below.

Using precision CERN-LEP data [149, 150] $\alpha_S(M_Z) = 0.1184$, $\sin^2 \theta_W(M_Z) = 0.2311$ and $\alpha^{-1}(M_Z) = 127.9$, different allowed solutions presented in Tab. 5.10. One set of solutions corresponding to low mass W_R^\pm and Z' gauge bosons is

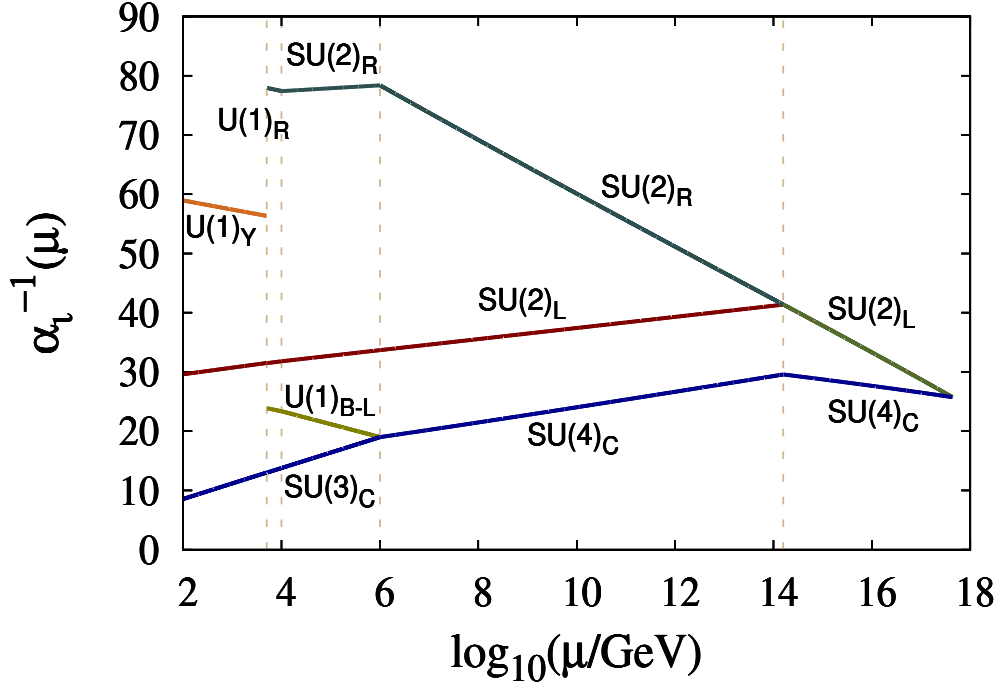


Figure 5.10: Two loop gauge coupling unification in the $SO(10)$ symmetry breaking chain described in the text. These results are also valid with G_{224D} symmetry near GUT-Planck scale.

$$\begin{aligned}
M_R^0 &= 3 - 5 \text{ TeV}, \quad M_R^+ = 10 \text{ TeV}, \quad M_C = 10^2 \text{ TeV} - 10^3 \text{ TeV}, \\
M_P &\simeq 10^{14.17} \text{ GeV} \text{ and } M_{GUT} \simeq 10^{17.8} \text{ GeV}.
\end{aligned}
\tag{5.44}$$

For these mass scales the emerging pattern of gauge coupling unification is shown in Fig. 5.10 with GUT fine structure constant $\alpha_G = 0.0388$.

5.5.3 Physical significance of mass scales

The presence of G_{224D} symmetry above the highest intermediate scale plays a crucial role in lowering down the values of M_R^+ while achieving high scale gauge coupling unification. With the gauge couplings allowed in the region $\mu \simeq 3 \text{ TeV} - 10 \text{ TeV}$ in the grand unified scenario with $g_{B-L} \simeq 0.725$, $g_{2R} \simeq 0.4$, we have estimated the predicted W_R and Z' masses to be $M_{W_R} \simeq 4 \text{ TeV}$, $M_{Z'} \simeq (2.3 - 3.6) \text{ TeV}$ for the allowed mass scales $M_R^0 \simeq (3 - 5) \text{ TeV}$, and $M_R^+ \simeq 10 \text{ TeV}$ of Tab. 5.10. These low mass W_R and Z' bosons have interesting RH current effects at low energies including K_L - K_S mass difference and dominant $0\nu 2\beta$ rates as discussed in Sec. 5.2 - Sec. 5.4. The predicted low mass W_R^\pm and Z' bosons are also expected to be testified at the LHC and future accelerators for which the current bounds are $M_{W_R} \geq 2.5 \text{ TeV}$ [270–275] and $M_{Z'} \geq 1.162 \text{ TeV}$ [276, 277]. The predicted mass scale $M_C \sim (10^5 - 10^6) \text{ GeV}$ leads to experimentally verifiable branching ratios for rare kaon decay with $\text{Br}(K_L^0 \rightarrow \mu \bar{e}) \simeq (10^{-9} - 10^{-11})$ [278] via leptoquark gauge boson mediation [279–281]. Because of the presence of \mathcal{G}_{224} symmetry for $\mu \geq M_C (10^5 - 10^6) \text{ GeV}$, all the components of di-quark Higgs scalars in $\Delta_R (3, 1, \bar{10})$ mediating n - \bar{n} and H - \bar{H} oscillations also acquire masses at that scale whereas the di-lepton Higgs scalar carrying $B - L = -2$ is at the $\simeq 1 \text{ TeV}$ scale. This gives rise to observable n - \bar{n} oscillation with mixing time $\tau_{n\bar{n}} \simeq (10^8 - 10^{11}) \text{ secs}$ [282–284]. However because of the large value of the GUT scale $M_{GUT} \simeq 10^{18} \text{ GeV}$, which is close to the Planck scale, the predicted proton life time for $p \rightarrow e^+ \pi^0$ is large, i.e. $\tau_p \geq 10^{40} \text{ yrs}$ which is beyond the accessible range of ongoing search experiments that have set the lower limit $(\tau_p)|_{\text{expt.}} \geq 1.1 \times 10^{34} \text{ yrs}$. [152].

5.5.4 Importance of G_{224D} intermediate symmetry

Near Planck scale unification of this model exposes an interesting possibility that grand unification can be also achieved by the Pati-Salam symmetry G_{224D} even without the help of the GUT-gauge group $SO(10)$ since, above this scale, gravity effects are expected to take over [285].

The most interesting role of G_{224D} gauge symmetry at the highest intermediate scale has been pointed out in ref. [224–226]. Normally super-heavy Higgs scalars contained in larger representations like 210_H and 126_H introduce uncertainties into GUT predictions of $\sin^2 \theta_W(M_Z)$ on which CERN-LEP data and others have precise experimental results. But the presence of G_{224D} at the highest scale achieves the most desired objective that the GUT scale corrections to $\sin^2 \theta_W(M_Z)$ vanish due to such sources as super-heavy particles or higher dimensional operators signifying the effect of gravity.

5.5.5 Determination of Dirac neutrino mass matrix

It is well known that within Pati-Salam gauge symmetry G_{224D} , the presence of $SU(4)_C$ unifies quarks and leptons treating the latter as fourth color and this relates the up-quark mass matrix (M_u^0) to the Dirac neutrino mass matrix M_D^0 at the unification scale. Such relations are also valid in $SO(10)$ at the GUT scale since G_{224D} is its maximal subgroup. Over the recent years it has been shown that in a large class of $SO(10)$ model the fermion mass fits at the GUT scale gives $M_D^0 \sim \mathcal{O}(M_u^0)$ [45, 72, 246, 286, 287]. Since the predictions of lepton number and LFVs carried out in this work are sensitive to the Dirac neutrino mass matrix, it is important to derive M_D at the TeV scale given in eq. (5.11). This question has been answered in non-SUSY $SO(10)$ [246] and SUSY $SO(10)$ [45] while utilizing renormalization group running of fermion masses analogous to ref. [186] and using their low energy data but in the presence of intermediate symmetries G_{2113} , G_{2213} , and G_{2213D} . In this analysis we will also use additional RGEs for Yukawa coupling and fermion masses in the presence of G_{224} and G_{224D} symmetries operating between $M_C \simeq 10^5$ GeV to $M_{GUT} \simeq 10^{17.5}$ GeV [288–290].

The determination of the Dirac neutrino mass matrix $M_D(M_{R^0})$ at the TeV seesaw scale is done in three steps [246]: (A.) Extrapolation of masses to the GUT-scale using low-energy data on fermion masses and CKM mixings through corresponding RGEs in the bottom-up approach, (B.) Fitting the fermion masses at the GUT scale and determination of $M_D(M_{GUT})$, (C.) Determination of $M_D(M_{R^0})$ by top-down approach.

5.5.5.1 Extrapolation of fermion masses to the GUT scale

At first RGEs for Yukawa coupling matrices and fermion mass matrices are set up from which RGEs for mass eigenvalues and CKM mixings are derived in the presence

of G_{2113} , G_{2213} , G_{224} , and G_{224D} symmetries.

Denoting $\Phi_{1,2}$ as the corresponding bidoublets under G_{2213} their VEVs are taken as

$$\begin{aligned}\langle\Phi_1\rangle &= \begin{pmatrix} v_u & 0 \\ 0 & 0 \end{pmatrix}, \\ \langle\Phi_2\rangle &= \begin{pmatrix} 0 & 0 \\ 0 & v_d \end{pmatrix}.\end{aligned}\tag{5.45}$$

For mass scales $\mu \ll M_G$, ignoring the contribution of the super-heavy bi-doublet in 126_H , the bi-doublet $\Phi_1 \subset 10_{H_1}$ is assumed to give dominant contribution to up quark and Dirac neutrino masses M_u and M_D whereas $\Phi_2 \subset 10_{H_2}$ is used to generate masses for down quarks and charged leptons, M_d and M_ℓ

$$\begin{aligned}M_u &= Y_u v_u, & M_D &= Y_\nu v_u, & M_d &= Y_d v_d, \\ M_e &= Y_e v_d, & M_R &= y_\chi v_\chi,\end{aligned}\tag{5.46}$$

At $\mu = M_Z$ we use the input values of running masses and quark mixings as in eq. (4.19) [186] with the CKM Dirac phase $\delta^q = 1.20 \pm 0.08$. This results in the CKM matrix at $\mu = M_Z$ as given in eq. (4.20). We use RGEs of the SM [186] to evolve all charged fermion masses and CKM mixings from $\mu = M_Z$ to $M_R^0 \simeq 10$ TeV. With two Higgs doublets at $\mu > 10$ TeV consistent with the current experimental lower bound on the second Higgs doublet [267], we use the starting value of $\tan\beta = v_u/v_d = 10$ and evolve the masses up to $\mu = M_C$ using RGEs derived in the presence of non-SUSY $SO(10)$ and intermediate symmetries G_{2113} and G_{2213} [246] with two Higgs bi-doublets. For $\mu \geq M_C$, we use the fermion mass RGEs in the presence of G_{224} and G_{224D} [288–290] modified including the corresponding RGEs of v_u and v_d . The fermion mass eigen values m_i and the V_{CKM} at the GUT scale turn out to be

At $\mu = M_{GUT}$ scale:

$$\begin{aligned}m_e^0 &= 0.2168 \text{ MeV}, m_\mu^0 = 38.846 \text{ MeV}, m_\tau^0 = 0.9620 \text{ GeV}, \\ m_d^0 &= 1.163 \text{ MeV}, m_s^0 = 23.352 \text{ MeV}, m_b^0 = 1.0256 \text{ GeV}, \\ m_u^0 &= 1.301 \text{ MeV}, m_c^0 = 0.1686 \text{ GeV}, m_t^0 = 51.504 \text{ GeV},\end{aligned}\tag{5.47}$$

$$V_{\text{CKM}}^0 = \begin{pmatrix} 0.9764 & 0.216 & -0.0017 - 0.0036i \\ -0.2159 - 0.0001i & 0.9759 - 0.00002i & 0.0310 \\ 0.0084 - 0.0035i & -0.0299 - 0.0008i & 0.9995 \end{pmatrix}, \quad (5.48)$$

where, in deriving eq. (5.47), we have used “run and diagonalize” procedure. Then using eq. (5.47) and eq. (5.48), the RG extrapolated value of the up-quark mass matrix at the GUT scale is determined

$$M_u^0(M_{\text{GUT}}) = \begin{pmatrix} 0.0097 & 0.0379 - 0.0069i & 0.0635 - 0.167i \\ 0.0379 + 0.0069i & 0.2482 & 2.117 + 0.0001i \\ 0.0635 + 0.167i & 2.117 - 0.0001i & 51.38 \end{pmatrix} \text{ GeV}. \quad (5.49)$$

5.5.5.2 Determination of M_D at GUT scale

In order to fit the fermion masses at the GUT scale, in addition to the two bi-doublets originating from two different Higgs representations 10_{H_1} and 10_{H_2} , we utilize the super-heavy bi-doublet in $\xi(2, 2, 15) \subset 126_H$. We will show that even if ξ has to be at the intermediate scale ($10^{13} - 10^{14}$) GeV to generate the desired value of induced VEV needed for quark-lepton mass splitting, the precision gauge coupling unification is unaffected. This fermion mass requires the predicted Majorana coupling f to be diagonal and the model predicts experimentally testable RH neutrino masses. In the presence of inverse seesaw formula taking into account the small masses and large mixings in the LH neutrino sector in the way of fitting the neutrino oscillation data, this diagonal structure of f causes no problem. However we show that when we treat the intermediate scale for sub-multiplet to be $\xi'(2, 2, 15)$ replacing $\xi(2, 2, 15)$ but originating from a second Higgs representation $126'_H$ which has coupling f' to the fermions and all other scalar components at the GUT scale, the coupling f and hence M_N can have a general texture, not necessarily diagonal, although fermion mass fit needs only f' to be diagonal.

The VEV of $\xi(2, 2, 15)$ is well known for its role in to splitting the quark and lepton masses through the Yukawa interaction $f 16.16.126_H^\dagger$ [32]. It is sometimes apprehended, as happens in the presence of only one 10_H , that this new contribution may also upset the near equality of $M_u^0 \simeq M_D^0$ at the GUT scale. But in the presence of the two different 10_{H_1} and 10_{H_2} producing the up and down type doublets, the effective theory from the $\mu \geq 10$ TeV acts like a non-SUSY two-Higgs doublet model with available large value of $\tan\beta = v_u/v_d$ that causes the most desired splitting between the up and down quark mass matrices but ensures $M_u^0 \sim M_D^0$. After having achieved this splitting a smaller value of of the VEV v_ξ is needed to implement fitting

of charged fermion mass matrices without substantially upsetting the near equality of $M_u^0 \simeq M_D^0$ at the GUT scale ^a.

The formulas for mass matrices at the GUT scale are [45, 246]

$$\begin{aligned} M_u &= G_u + F, & M_d &= G_d + F, \\ M_e &= G_d - 3F, & M_D &= G_u - 3F. \end{aligned} \quad (5.50)$$

where $G_k = Y_k \langle 10_H^k \rangle$, $k = u, d$ and $F = f v_\xi$ leading to

$$f = \frac{(M_d - M_e)}{4v_\xi}. \quad (5.51)$$

Using a charged-lepton diagonal mass basis and eq. (5.47) and eq. (5.50) we have

$$\begin{aligned} M_e(M_{GUT}) &= \text{diag}(0.000216, 0.0388, 0.9620) \text{ GeV}, \\ G_{d,ij} &= 3F_{ij}, \quad (i \neq j). \end{aligned} \quad (5.52)$$

(i) Diagonal structure of RH neutrino mass matrix:

In refs. [45, 246] dealing with TeV scale pseudo-Dirac RH neutrinos, a diagonal structure of F was assumed with the help of higher dimensional non-renormalizable operators in order to fit the charged fermion masses and mixings at the GUT scale. In the present model renormalizable interaction of 126_H is available the diagonal structure of F is a result of utilization of diagonal basis of down quarks as well.

This diagonal structure of f would have caused serious problem in fitting the neutrino oscillation data if we had a dominant type-II seesaw formula [65, 66], but it causes no problem in our present model where type-II seesaw contribution to light neutrino mass matrix is severely damped out compared to inverse seesaw contribution which fits the neutrino oscillation data. Further, the resulting diagonal structure of RH neutrino mass matrix that emerges in this model has been widely used in SUSY and non-SUSY $SO(10)$ by a large number of authors, and this model creates no anomaly as there are no experimental data or constraints which are violated by this diagonal structure.

The quark mixings reflected through the CKM mixing matrix $V_{CKM} = U_L^\dagger D_L = U_L$ has been parametrized at $\mu = M_Z$ in the down-quark diagonal basis and this

^aIt is to be noted that the validity of our estimations of $0\nu 2\beta$ decay and non-unitarity and lepton flavor violating effects do not require exact equality of M_u and M_D and a relation between them within less than an order of magnitude deviation would suffice to make dominant contributions at the TeV scale. But the present models, either with G_{224D} or $SO(10)$ symmetry at the high GUT scale, give the high scale prediction $M_u^0 \sim M_D^0$ up to a good approximation.

mixing matrix has been extrapolated to the GUT scale resulting in $V_{CKM}^0 \equiv U_L^0$ in eq. (5.48) provided $D_L^0 = I$ which can hold even at the GUT scale if we use down quark diagonal basis. In that case $M_d(M_{GUT}) = M_d^0 = \text{diag}(m_d^0, m_s^0, m_b^0)$ which is completely determined by the respective mass eigen values determined by the bottom-up approach. Then the second mass relation of eq. (5.50) gives,

$$G_{d_{ij}} = -F_{ij}, \quad (i \neq j). \quad (5.53)$$

Now eq. (5.52) and eq. (5.53) are satisfied only if $F_{ij} = 0$, ($i \neq j$) i.e, if F is diagonal. This is also reflected directly through the eq. (5.51). In other words the diagonality of F used in earlier applications of inverse seesaw mechanism in $SO(10)$ [45, 246] is a consequence of utilization of down quark and charged lepton diagonal bases and vice-versa, although through non-renormalizable Yukawa interaction. In the present model it shows that even by restricting F to its diagonal structure which eliminates at least six additional parameters which would have otherwise existed via its non-diagonal elements, the model successfully fits all the charged fermion masses and mixings including the Dirac phase of the CKM matrix at the GUT scale. Besides, as shown below, the model predicts the RH neutrino masses accessible to high energy accelerators including LHC. We have relations between the diagonal elements which, in turn, determine the diagonal matrices F and G_d completely.

$$\begin{aligned} G_{d,ii} + F_{ii} &= m_i^0, \quad (i = d, s, b), \\ G_{d,jj} - 3F_{jj} &= m_j^0, \quad (j = e, \mu, \tau). \end{aligned} \quad (5.54)$$

$$\begin{aligned} F &= \text{diag} \frac{1}{4}(m_d^0 - m_e^0, m_s^0 - m_\mu^0, m_b^0 - m_\tau^0), \\ &= \text{diag}(2.365 \times 10^{-4}, -0.0038, +0.015) \text{ GeV}, \\ G_d &= \text{diag} \frac{1}{4}(3m_d^0 + m_e^0, 3m_s^0 + m_\mu^0, 3m_b^0 + m_\tau^0), \\ &= \text{diag}(9.2645 \times 10^{-4}, 0.027224, 1.00975) \text{ GeV}, \end{aligned} \quad (5.55)$$

where we have used the RG extrapolated values of eq. (5.47). It is clear from the value of the mass matrix F in eq. (5.55) that we need as small a VEV as $v_\xi \sim 10$ MeV to carry out the fermion mass fits at the GUT scale. In the Sec. 5.5.5.4 below we show how the $SO(10)$ structure and the Higgs representations given for the symmetry breaking chain of eq. (5.42) clearly predicts a VEV $v_\xi \sim (10 - 100)$ MeV consistent with precision gauge coupling unification and the fermion mass values discussed in

this subsection.

The model ansatz for CKM mixings at the GUT scale matches successfully with those given by V_{CKM}^0 of eq. (5.48) and, similarly, the model predictions for up quark masses can match with those given in eq. (5.47) provided we can identify M_u of eq. (5.50) with M_u^0 of eq. (5.49). This is done by fixing $G_u = M_u^0 - F$ leading to

$$G_u(M_{GUT}) = \begin{pmatrix} 0.00950 & 0.0379 - 0.00693i & 0.0635 - 0.1671i \\ 0.0379 + 0.00693i & 0.2637 & 2.117 + 0.000116i \\ 0.0635 + 0.1672i & 2.117 - 0.000116i & 51.4436 \end{pmatrix} \text{ GeV.} \quad (5.56)$$

Now using eq. (5.55) and eq. (5.56) in eq. (5.50) gives the Dirac neutrino mass matrix M_D at the GUT scale

$$M_D^0(M_{GUT}) = \begin{pmatrix} 0.00876 & 0.0380 - 0.00693i & 0.0635 - 0.1672i \\ 0.0380 + 0.00693i & 0.3102 & 2.118 + 0.000116i \\ 0.0635 + 0.1672i & 2.118 - 0.000116i & 51.6344 \end{pmatrix} \text{ GeV.} \quad (5.57)$$

The relation $F = f v_\xi = \text{diag}(f_1, f_2, f_3) v_\xi$ in eq. (5.53) with $v_\xi = 10 \text{ MeV}$ gives $(f_1, f_2, f_3) = (0.0236, -0.38, 1.5)$ ^b. Then the allowed solution to RGEs for gauge coupling unification with $M_R^0 = v_R = 5 \text{ TeV}$ determines the RH neutrino masses.

$$M_{N_1} = 115 \text{ GeV}, \quad M_{N_2} = 1.785 \text{ TeV}, \quad M_{N_3} = 7.5 \text{ TeV.} \quad (5.58)$$

Here we note that M_N in general is not a diagonal matrix. But, complete RGE analysis gives that the off-diagonal elements of M_N are very small compared to the diagonal elements. Therefore, for simplicity we will use the eigenvalues of M_N given in eq. (5.58) with the right phase (i.e. $M_{N_2} = -1.785 \text{ TeV}$) instead of complete M_N matrix, for simplicity and intuitive predictions.

While the first RH neutrino is lighter than the current experimental limit on Z' boson mass, the second one is in-between the Z' and W_R boson mass limits, but the heaviest one is larger than the W_R mass limit. These are expected to provide interesting collider signatures at LHC and future accelerators. This hierarchy of the RH neutrino masses has been found to be consistent with lepton-number and LFVs discussed in Sec. 5.1, Sec. 5.3, and Sec. 5.4.

We estimate effective mass parameters for $0\nu 2\beta$ decay using this predicted di-

^bIn the context of observable $n - \bar{n}$ oscillation, the value of $f_1 \sim 0.01$ and quartic coupling $\lambda \sim 1$ need the degenerate mass of di-quark Higgs scalars $M_\Delta = 5 \times 10^4 \text{ GeV}$. We have checked that precision gauge coupling unification in the symmetry breaking chain remains unaltered with such mildly tuned value of di-quark Higgs scalars contained in $\Delta_R(1, 3, \overline{10}) \subset 126_H$.

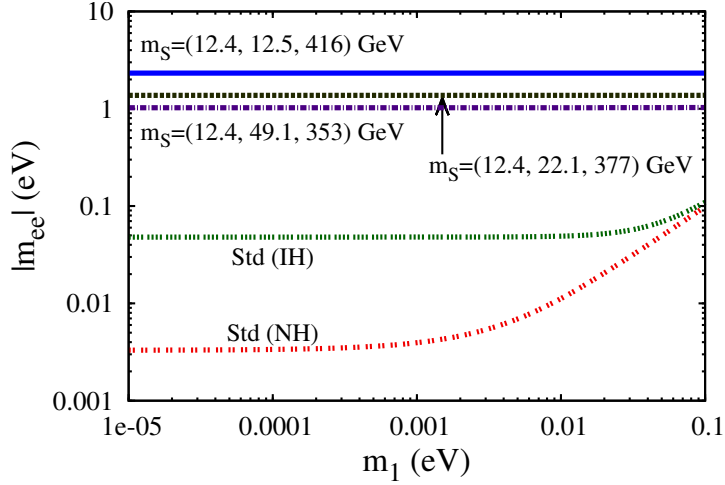


Figure 5.11: Estimations of effective mass parameter for $0\nu 2\beta$ decay in the $W_L^- - W_L^-$ channel with sterile neutrino exchanges shown by top, middle, and bottom horizontal lines. The RH neutrino masses and the Dirac neutrino masses are derived from fermion mass fits and the sterile neutrino masses have been obtained through M values consistent with non-unitarity constraints as described in the text.

agonal structure of M_N and three sets of constrained N - S mixing matrix $M_i = (40, 150, 1810)$ GeV, $M_i = (40, 200, 1720)$ GeV, and $M_i = (40, 300, 1660)$ GeV corresponding to the three sets of sterile neutrino mass eigenvalues $\hat{m}_S = (12.4, 12.5, 416)$ GeV, $\hat{m}_S = (12.5, 22.1, 377)$ GeV, and $\hat{m}_S = (12.4, 49, 350)$ GeV, respectively. The estimated values of the effective mass parameters in the $W_L - W_L$ channel due to sterile neutrino exchanges have been shown in Fig. 5.11 where the top, middle and the bottom horizontal lines represent $m_S^{\text{ee,L}} = 2.1$ eV, 1.3 eV, and 1.0 eV corresponding to the first, second and the third set, respectively. Thus the new values are found to be much more dominant compared to the standard predictions in this channel. Clearly the Heidelberg-Moscow results can be easily accommodated even for normally hierarchical or inverted hierarchical light neutrino masses.

(ii) General form of RH neutrino mass matrix:-

Although we have shown the emergence of diagonal structure of M_N from the successful fermion mass fits at the GUT scale, it is worthwhile to explore as to how this approach may also allow a general structure for the Yukawa coupling f of 126_H and hence the RH neutrino mass matrix while giving a successful fit to charged fermion masses at the GUT scale. It is clear from the above discussions that this is not possible via renormalizable interaction if the model has only a single 126_H . We introduce a second $126'_H$ with its coupling f' and all its scalar sub-multiplets at the GUT-Plank scale except for the component $\xi'(2, 2, 15)$ which is tuned to have its mass at the in-

intermediate scale $M_{\xi'} \sim 10^{13} \text{ GeV} - 10^{14} \text{ GeV}$. Also, as before, the VEV of the neutral component of $\Delta_R(1, 3, \bar{10}) \subset 126_H$ is used to contribute to the spontaneous breaking of $G_{2113} \rightarrow \text{SM}$, but the component $\xi(2, 2, 15)$ assumes its natural GUT scale mass without the necessity of being at the intermediate scale. All our results go through by redefining $F = f'v_{\xi'}$ and $v_{\xi'} = (10 - 100) \text{ MeV}$ is realized in the same way as discussed below in Sec. 5.5.5.4. In this case the diagonal structure of f' gives the same successful fit to charged fermion masses and mixings at the GUT scale without affecting the allowed general structure of f and M_N . Unlike the case (i) with single 126_H discussed above, as f_1 is not constrained to be small, observable $n-\bar{n}$ oscillation is possible in this case for all di-quark Higgs scalar masses $M_\Delta \sim M_C \sim 10^5 - 10^6 \text{ GeV}$ already permitted by RGE solutions to precision gauge coupling unification.

So far we have discussed emergence of dominant $0\nu 2\beta$ decay rates subject to non-unitarity constraints with either a purely diagonal or nearly diagonal M_N matrix with small mixing. To test whether such results exist for a general structure, we consider a mass matrix,

$$M_N = \begin{pmatrix} 1853.6 + 320.5i & -2165.2 - 47.98i & 2064.69 + 364.44i \\ -2165.24 - 47.98i & 2818.92 - 210.57i & -2030.45 + 245.8i \\ 2064.69 + 364.436i & -2030.45 + 245.82i & 4610.57 - 2.68i \end{pmatrix} \text{ GeV} \quad (5.59)$$

which has the eigenvalues $M_{N_i} = (115, 1750, 7500) \text{ GeV}$ with the same mixings as the LH neutrinos. Using eq. (5.59), the non-unitarity constrained N - S mixing matrix $M = \text{diag}(40, 150, 1810) \text{ GeV}$, and the derived value of the Dirac neutrino mass matrix from eq. (5.61) leads to the sterile neutrino mass eigenvalues $m_{S_i} \simeq (0.77, 51, 878) \text{ GeV}$ and the resulting effective mass parameters in the notations of Sec. 5.3- Sec. 5.5 are found to be

$$m_S^{\text{ee,L}} = 6.3 \text{ eV}, \quad m_N^{\text{ee,L}} = 0.02 \text{ eV}, \quad m_S^{\text{ee,LR}} = 0.08 \text{ eV}. \quad (5.60)$$

and all other contributions are relatively insignificant. Thus, we see that the dominant contribution in the W_L - W_L channel due to sterile neutrino exchanges dominates over all other contributions. The difference of $\mathcal{O}(10^2)$ in the leading and next to leading contributions to effective mass resemble the results of diagonal structure of M_N , if m_{S_i} are of same order, as presented in Sec. 5.3, Fig. 5.6 - Fig. 5.8 and Tab. 5.5 - Tab. 5.6. A general M_N , such as in eq. (5.59), is not restricted by GUT-scale fermion mass fits. Henceforth, we will use the diagonal form of M_N , eq. (5.58), as in Fig. 5.11.

5.5.5.3 Determination of $M_D(M_{R^0})$ by top-down approach

. We use the RGEs in the top-down approach [186, 246, 288–290] for M_D in the presence of G_{224D} , G_{224} , G_{2213} , and G_{2113} to evolve $M_D(M_{GUT})$ to $M_D(M_{R^0})$ through $M_D(M_{M_P})$, $M_D(M_{M_C})$ and $M_D(M_{M_R^+})$ and obtain the ansatz given in eq. (5.11) as

$$M_D = \begin{pmatrix} 0.02274 & 0.09891 - 0.01603i & 0.1462 - 0.3859i \\ 0.09891 + 0.01603i & 0.6319 & 4.884 + 0.0003034i \\ 0.1462 + 0.3859i & 4.884 - 0.0003034i & 117.8 \end{pmatrix} \text{ GeV}. \quad (5.61)$$

As can be noted from the determination of running mass eigenvalues at the high GUT scale of the model shown in eq. (5.47), b - τ unification is almost perfect, although $m_\mu^0 \simeq 2m_s^0$ ^c. In view of the fact that G_{224} symmetry with unbroken $SU(4)_C$ gauge symmetry is present in this model right from $M_C \simeq 10^6$ GeV up to the high GUT scale $M_{GUT} \sim 10^{17.5}$ GeV, the dominance of quark lepton symmetry has manifested in the fermion mass relations like $m_b^0 \simeq m_\tau^0 \simeq 1.06$ and $M_u^0 \simeq M_D^0$ at the GUT scale while making the $SU(4)_C$ -breaking effects sub-dominant. The bi-doublet $\xi(2, 2, 15) \subset 126_H$ has been found to make a small contribution resulting in the mass matrix F in eq. (5.55) which plays an important role in our present model. The impressive manner in which the underlying quark-lepton symmetry manifests in exhibiting $M_u(M_{GUT}) \simeq M_D(M_{GUT})$ can be noted from the explicit forms of the two mass matrices derived at the GUT scale and shown in eq. (5.49) and eq. (5.57).

Thus, the present non-SUSY $SO(10)$ model, having predicted M_D value given in eq. (5.11), all our discussions using TeV scale inverse see-saw mechanism including neutrinoless double beta decay, non-unitarity effects leading to LFVs, and new CP -violating effects discussed in Sec. 5.1 - Sec. 5.4, where this mass matrix has been used, are also applicable in this GUT model.

5.5.5.4 Determination of induced vacuum expectation value of $\xi(2, 2, 15)$

Now we show how a small induced VEV $v_\xi \sim 10$ MeV of the sub-multiplet $\xi(2, 2, 15) \subset 126_H$, which has been found to be necessary for fitting the charged fermion masses at the GUT scale, originates from the the present $SO(10)$ model. The Higgs representations needed for the symmetry breaking chain permits the following term in

^cWhile running mass eigenvalues are extrapolated up to the non-SUSY $SO(10)$ unification scale in the presence of G_{2113} and G_{2213} intermediate scales [246], it has been noted that at the GUT scale $m_b^0/m_\tau^0 \simeq 1.3$, $m_\mu^0/m_s^0 \simeq 2.5$, and $m_d^0/m_e^0 \simeq 4$. Compared to refs. [45, 246] where a non-renormalizable $dim. 6$ operator has also been used for fermion mass fits at the GUT scale, all the interactions used in this work are renormalizable.

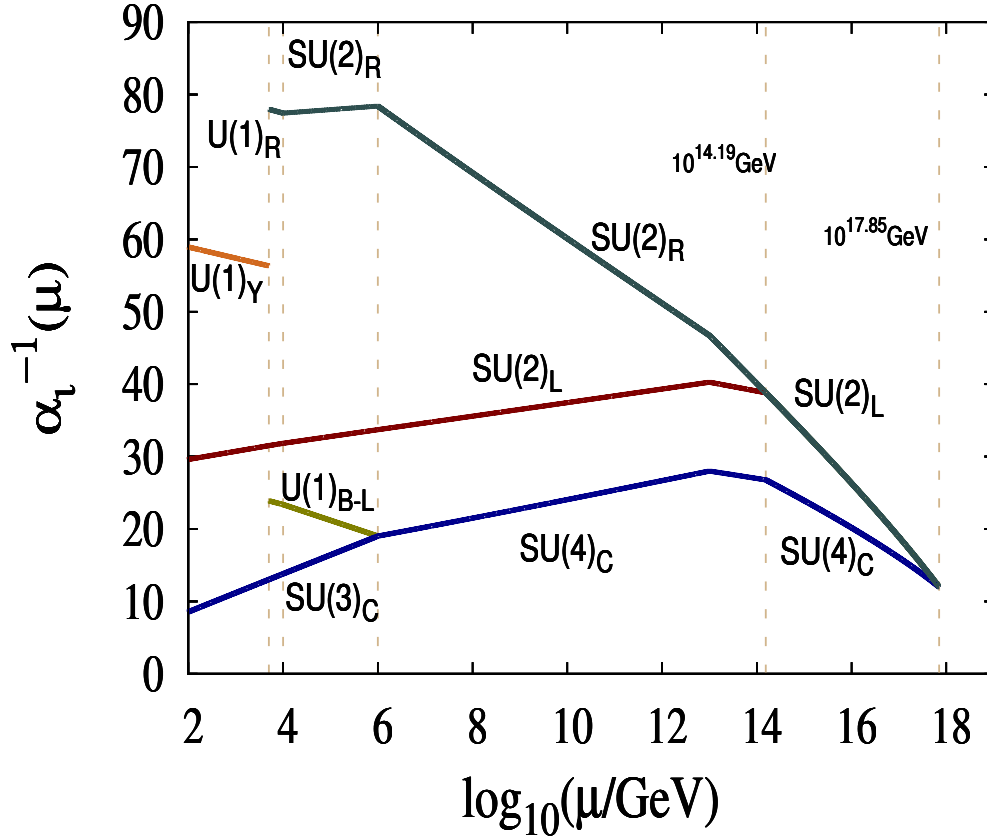


Figure 5.12: Same as Fig. 5.10 but with the scalar sub-multiplet $\xi(2, 2, 15)$ under Pati-Salam group at $M_\xi = 10^{13.2}$ GeV.

the Higgs potential

$$\lambda_\xi M' 210_H 126_H^\dagger 10_H \supset \lambda_\xi M' (2, 2, 15)_{126} (1, 1, 15)_{210} (2, 2, 1)_{10} \quad (5.62)$$

where M' is a mass parameter appropriate for trilinear scalar coupling which is naturally of the order of the GUT scale $\sim \mathcal{O}(10^{18})$ GeV. For allowed solutions of the mass scales in our model, we have found $\langle (1, 1, 15) \rangle = M_C \simeq 10^6$ GeV, a criteria necessary for observable $n-\bar{n}$ oscillation and rare kaon decay. The induced v_ξ then turns out to be

$$v_\xi = \lambda_\xi M' M_C v_{ew} / M_\xi^2 \quad (5.63)$$

Using $M_C \simeq 10^6$ GeV which is required as model predictions for observable $n-\bar{n}$ oscillation and rare kaon decay, and $v_{ew} \sim 100$ GeV, we find that for $\lambda_\xi = 0.1 - 1.0$, the eq. (5.63) gives the induced VEV $v_\xi \simeq (10 - 100)$ MeV provided $M_\xi \sim 10^{13}$ GeV- 10^{14} GeV. When $\xi(2, 2, 15)$ is made lighter than the GUT scale having such an

M_ξ (GeV)	M_P (GeV)	M_{GUT} (GeV)	α_G	v_ξ (MeV)
$10^{13.2}$	$10^{14.19}$	$10^{17.83}$	0.083	25-250
$10^{13.4}$	$10^{14.19}$	$10^{17.83}$	0.076	10-100
$10^{13.5}$	$10^{14.19}$	$10^{17.83}$	0.073	7-70
$10^{13.8}$	$10^{14.20}$	$10^{17.82}$	0.068	2-16
$10^{14.0}$	$10^{14.20}$	$10^{17.81}$	0.065	1-7

Table 5.11: Allowed solutions in the $SO(10)$ symmetry breaking chain shown in eq. (5.42) but with the scalar component $\xi(2, 2, 15) \subset 126_H$ lighter than the GUT scale and consistent with the determination of the induced VEV $v_\xi \sim (10 - 100)$ MeV needed to fit charged fermion masses at the GUT scale. For all solutions we have fixed $M_R^0 = 5$ TeV, $M_R^+ = 10$ TeV, and $M_C = 10^6$ GeV.

intermediate mass, $M_\xi = 10^{13.4}$ GeV, the precision gauge coupling is found to occur as shown in Fig. 5.12 but now with nearly two times larger GUT scale and larger GUT fine-structure constant than the minimal case. Our numerical solutions are shown in Tab. 5.11 where the Parity violating scale is close to the minimal case. It is interesting to note that the precision unification with $\xi(2, 2, 15) \subset 126_H$ at the intermediate scale is possible without upsetting low mass W_R , Z' , M_C and other mass scale predictions of the model. The fermion mass evolutions and the emerging value of M_D remain close to the value derived in Sec. 5.5.5. The unification pattern and model predictions including GUT-scale fermion mass fit are essentially unchanged when the second $126'_H$ is introduced with its Yukawa coupling f' and the component $\xi'(2, 2, 15) \subset 126'_H$ at the intermediate scale replacing $\xi(2, 2, 15) \subset 126_H$ and the latter is assigned its natural GUT scale mass. In this case the mass scales of the model give $v_{\xi'} = (10 - 100)$ MeV. As the additional threshold contributions to $\sin^2 \theta_W$ and M_P due to the super-heavy components of second $126'_H$ vanish [279–281], the only change that can occur is the GUT-scale threshold effects on M_{GUT} . However as the unification scale is close to the Plank scale with large proton lifetime prediction, this will not have any additional observable effects.

Thus, we have shown that the small induced VEV v_ξ or $v_{\xi'}$ needed for GUT scale fit to the charged fermion masses and prediction of M_D which is crucial for low-energy estimation of $0\nu 2\beta$ decay rate can be easily derived from the present $SO(10)$ structure. It is possible to have a diagonal structure or a general structure for the RH neutrino mass matrix M_N for which dominant contributions to $0\nu 2\beta$ decay, experimentally accessible lepton flavor violating decays, and non-unitarity and CP -violating effects have been discussed in Sec. 5.3 and Sec. 5.4.

5.5.6 Suppressed induced contribution to ν - S mixing

In our model the ν - S mixing term has been chosen to be vanishingly small in eq. (5.3). However, because of the presence of non-minimal Higgs fields including LH and RH doublets carrying $B - L = -1$, triplets carrying $B - L = -2$, two bi-doublets each with $B - L = 0$, and Parity odd singlet, it is necessary to evaluate if such a term can arise through the induced VEV of $\langle\chi_L\rangle$. We find that without taking recourse to any severe fine tuning of parameters, minimization of the scalar potential gives

$$\langle\chi_L\rangle \simeq K \frac{\langle\chi_R\rangle v}{M_P}, \quad (5.64)$$

where the ratio of parameters $K = \mathcal{O}(0.1 - .01)$ and $M_P \simeq 10^{14}$ GeV. When eq. (5.64) is used in the corresponding correction to the light neutrino mass predictions [291, 292], $m_\nu \simeq M_D \frac{\langle\chi_L\rangle}{\langle\chi_R\rangle}$, this gives $m_{\nu_{33}} \ll 0.001$ eV and negligible contributions to all the three light neutrino masses. With fine-tuning of parameters this contribution can be reduced further. Thus the predictions of the model carried out using eq. (5.3) are found to hold up to a very good approximation as the small induced contribution $\langle\chi_L\rangle$ does not affect the results substantially. Fine tuning of model parameters would result in further reduction of this contribution.

CHAPTER 6

Proton, rare kaon and $0\nu 2\beta$ -decays, light Z' , $n-\bar{n}$ oscillation, LFV

The conventional approach [56, 58, 269, 283, 284, 293, 294], to observable $n - \bar{n}$ oscillation through lepto-quark gauge boson in $SO(10)$ GUTs requires Pati-Salam intermediate gauge symmetry breaking at $M_C \sim 10^6$ GeV. The canonical seesaw mechanism is also constrained by this symmetry breaking scale. For the Dirac mass matrix M_D estimated from RG evolution and GUT scale constraint the canonical seesaw gives the light neutrino masses several orders larger than the neutrino oscillation data. In the previous chapter we evaded this difficulty through TeV scale gauged inverse seesaw mechanism while predicting experimentally verifiable W_R^\pm, Z' bosons. The proton lifetime predictions in the model were far beyond the accessible limit [295] in the foreseeable future. In the present work, adopting the view that we may have only a nonstandard TeV scale Z' gauge boson [88, 90, 91, 93, 94, 296] accessible to the LHC [274, 275] while W_R^\pm may be heavy and currently inaccessible. We show a class of non-SUSY $SO(10)$ models allow experimentally verifiable proton lifetime together with the predictions for the new contributions to neutrinoless double beta decay in the W_L-W_L channel, lepton flavor violating branching ratios, observable $n-\bar{n}$ oscillation, and lepto-quark gauge boson mediated rare kaon decays close to experimental limits [297] as discussed in the previous chapter. Although the proton lifetime prediction is brought closer to the ongoing search limits with GUT threshold effects in the minimal model, no such threshold effects are needed once we lower down the masses of bi-triplet (3,3,1) and/or di-quark Higgs scalars by one to two order from the symmetry breaking scales for lifetimes close to the Super-Kamiokande limit. The non-minimal extension of the model in previous chapter also shows similar behavior where bi-triplet scalar is made several orders smaller than Pati-Salam D -parity breaking scale. In this chapter we elaborate (i) Lepto-quark gauge boson mediated

rare kaon decay, (ii) Observable $n-\bar{n}$ oscillation mediated by di-quark Higgs scalar at TeV. We also show how the existing experimental limits on $0\nu 2\beta$ life-time [298–301] impose the lower bound on the lightest of the three heavy sterile neutrino masses, irrespective of the nature of hierarchy of light neutrino masses.

In Sec. 6.1 we discuss the specific $SO(10)$ symmetry breaking chain and study predictions of different physically relevant mass scales emerging as solutions to renormalization group equations. In Sec. 6.2 we discuss predictions of proton lifetime accessible to ongoing search experiments. Lower bound on the lepto-quark gauge boson mediating rare-kaon decay is derived in Sec. 6.3 where mixing times for $n-\bar{n}$ oscillation are also predicted. In Sec. 6.4 we recapitulate the estimation of Dirac neutrino mass matrix from GUT-scale fit to the charged fermion masses, fits to the neutrino oscillation data, the model estimations of lepton flavor violating decay branching ratios and CP -violating parameter due to non-unitarity effects. In Sec. 6.5 we briefly discuss the model predictions of the dominant contributions to $0\nu 2\beta$ process and study variation of half-life as a function of sterile neutrino masses. The cancellations among the light neutrino and sterile contribution to effective mass, leading to ultra large $0\nu 2\beta$ -decay lifetime, are also discussed in in this Section. In Sec. 6.6 we extend the model presented in chapter 5 to rectify the large proton lifetime prediction of the model. In the Appendix E we derive analytic formulas for GUT threshold effects on $\ln(M_P/M_Z)$ and $\ln(M_{GUT}/M_Z)$.

6.1 Precision gauge coupling unification and mass scales

With a right structure of new physics beyond the SM, the non-SUSY $SO(10)$ GUT breaks through Pati-Salam symmetries occurring in two intermediate regimes: once between the high parity breaking scale M_P and the GUT scale M_{GUT} and, for the second time, without parity between the $SU(4)_C$ breaking scale M_C and M_P as

$$\begin{aligned}
 SO(10) & \xrightarrow[54_H]{M_{GUT}} G_{224D} \xrightarrow[210_H]{M_P} G_{224} \\
 & \xrightarrow[210_H]{M_R^+} G_{2113} \xrightarrow[126_H+16_H]{M_R^0} G_{213} \xrightarrow[10_H]{M_Z} G_{13}
 \end{aligned} \tag{6.1}$$

This symmetry breaking closely follows the symmetry breaking discussed in Sec. 5.5.1. The only difference in the scheme is that the intermediate LR symmetry is absent from the scenario and the W_R^\pm gauge bosons reside at Pati-Salam breaking scale.

Thus the scalar multiplet $(1, 1, 15)_H^0 \subset 210_H$ do not survive until the Pati-Salam breaking scale and gets integrated out at GUT scale only.

The breaking of G_{224} gauge symmetry to G_{2113} is implemented by assigning VEV of order $M_C \sim 10^5 - 10^6$ GeV to the neutral component of the G_{224} sub-multiplet $(1, 3, 15) \subset 210_H$. This technique of symmetry breaking to examine the feasibility of observable $n-\bar{n}$ through the type of intermediate breaking $G_{224} \rightarrow G_{2113}$ was proposed at a time when neither the neutrino oscillation data, nor the precision CERN-LEP data were available [266, 293, 294]. The gauge symmetry G_{2113} that is found to survive down to the TeV scale leading to the low-mass extra Z' boson accessible to LHC. At this stage RH Majorana mass matrix $M_N = f \langle \Delta_R^0 \rangle$ is generated through the Higgs Yukawa interaction. The VEV of the neutral component of RH Higgs doublet $\xi_R(1, 2, 4)$ under G_{224} symmetry contained in 16_H of $SO(10)$ is used to generate the N - S mixing mass term needed for extended seesaw mechanism. For the sake of fermion mass fit at the GUT, scale we utilize two Higgs doublets for $\mu \geq 5$ TeV. Out of these two, the up type doublet $\phi_u \subset 10_{H_1}$ contributes to Dirac masses for up quarks and neutrinos, and the down type doublet $\phi_d \subset 10_{H_2}$ contributes to masses of down type quarks and charged leptons. We will see later in this work how the induced VEV of the sub-multiplet $\xi(2, 2, 15) \subset 126_H$ [32, 295] naturally available in this model plays a crucial role in splitting quark and lepton masses at the GUT scale and determining the value of M_D . In one interesting scenario, the GUT scale fit to fermion masses and mixings results in the diagonal structure of RH neutrino mass matrix near the TeV scale which is accessible for verification at LHC energies.

Using extended survival hypothesis [268, 269] the Higgs scalars responsible for spontaneous symmetry breaking and their contributions to β -function coefficients up to two-loop order are given in Tab. B.3. One set of allowed solutions for mass scales and GUT-scale fine-structure constant is

$$\begin{aligned} M_R^0 &= 5 \text{ TeV}, \quad M_\Delta = M_C = 10^{5.5} - 10^{6.5} \text{ GeV}, \\ M_P &= 10^{13.45} \text{ GeV}, \quad M_{GUT} = 10^{16.07} \text{ GeV}, \quad \alpha_G = 0.0429. \end{aligned} \quad (6.2)$$

where M_Δ represents the degenerate mass of diquark Higgs scalars contained in $\Delta_R(1, 3, \bar{10}) \subset 126_H$.

The renormalization group evolution of gauge couplings is shown in Fig. 6.1 exhibiting precision unification.

We have noted that when $M_\Delta < M_C$, there is a small decrease in the unification scale that is capable of reducing the proton lifetime predictions by a factor 3 – 5.

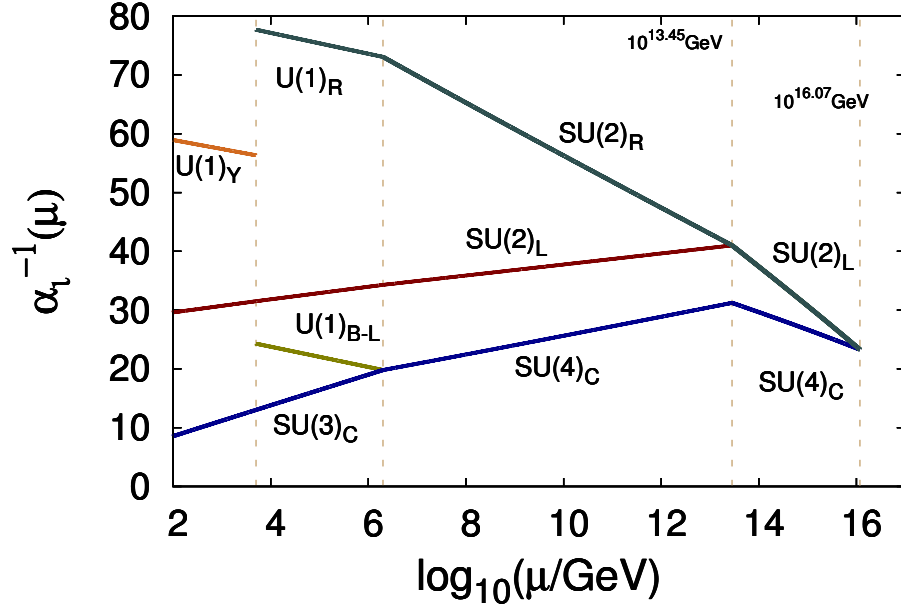


Figure 6.1: The gauge coupling unification for the breaking scheme given in eq. (6.1) and the scalar particle spectrum as given in Tab. B.3.

One example of this solution is,

$$\begin{aligned}
 M_R^0 &= 5 \text{ TeV}, \quad M_\Delta = 10^4 \text{ GeV}, \quad M_C = 10^6 \text{ GeV}, \\
 M_P &= 10^{12.75} \text{ GeV}, \quad M_{GUT} = 10^{15.92} \text{ GeV}, \quad \alpha_G = 0.0429.
 \end{aligned}
 \tag{6.3}$$

It is interesting to note that the present LHC bound on the diquark Higgs scalar mass [302] is

$$(M_\Delta)_{\text{expt.}} \geq 3.75 \text{ TeV}.
 \tag{6.4}$$

As discussed in the context of $n-\bar{n}$ oscillation in Sec. 6.3, our model accommodates a TeV scale di-quark with observable mixing time. But substantial decrease in the unification scale and the corresponding decrease in proton lifetime is possible when the bi-triplet Higgs scalar $\Theta_H(3, 3, 1) \subset 54_H$ is lighter than the GUT scale by a factor ranging from $\frac{1}{15} - \frac{1}{25}$. These solutions are discussed in the following section.

6.2 Low mass Z' boson and proton decay

6.2.1 Low-mass Z' boson

In the solutions of RGEs with precision unification, we have found that $g_{(B-L)} = 0.72 - 0.75$ and $g_{1R} = 0.40 - 0.42$ in the range of values $M_R^0 = v_{B-L} = 3 - 10 \text{ TeV}$.

This predicts the mass of the Z' boson in the range

$$M_{Z'} = 1.75 - 6.1 \text{ TeV}, \quad (6.5)$$

whereas the current experimental bound from LHC is $(M_{Z'})_{\text{expt.}} \geq 2.5 \text{ TeV}$. Thus, if such a Z' boson in the predicted mass range of the present model exists, it is likely to be discovered by the ongoing searches at the LHC.

6.2.2 Proton lifetime for $p \rightarrow e^+\pi^0$ decay

The formula for the proton-decay width [151,157,303] is discussed in Sec. 4.2.1. From eq. (4.4) we see that

$$\Gamma^{-1}(p \rightarrow e^+\pi^0) \propto \left(\frac{M_{GUT}^4}{g_G^4} \right) \frac{1}{|A_L|^2 R}. \quad (6.6)$$

where R , A_L are defined there. In this model, the product of the short distance with the long distance renormalization factor $A_L = 1.25$ turns out to be $A_R \simeq A_L A_{SL} \simeq A_L A_{SR} \simeq 3.20$. Then using the the two-loop value of the unification scale and the GUT coupling from eq. (6.2) gives

$$\tau_p(p \rightarrow e^+\pi^0) \simeq 5.05 \times 10^{35} \text{ yrs} \quad (6.7)$$

whereas the solution of RGEs corresponding to eq. (6.3) gives

$$\tau_p(p \rightarrow e^+\pi^0) \simeq 1.05 \times 10^{35} \text{ yrs}. \quad (6.8)$$

For comparison we note the current experimental search limit from Super-Kamiokande is [84–87]

$$(\tau_p)_{\text{Super-K}} \geq 1.4 \times 10^{34} \text{ yrs}. \quad (6.9)$$

A second generation underground water Cherenkov detector being planned at Hyper-Kamiokande in Japan is expected to probe higher limits through its 5.6 Megaton year exposure leading to the partial lifetime [87]

$$(\tau_p)_{\text{Hyper-K}} \geq 1.3 \times 10^{35} \text{ yrs}. \quad (6.10)$$

if actual decay event is not observed within this limit. Thus our model prediction in eq. (6.8) barely within the planned Hyper-K limit although this the prediction in

eq. (6.7) nearly 4 times larger than this limit.

If the proton decay is observed closer to the current or planned experimental limits, it would vindicate the long standing fundamental hypothesis of grand unification. On the other hand proton may be much more stable and its lifetime may not be accessible even to Hyper K. experimental search program. These possibilities are addressed below.

6.2.3 GUT scale and proton life-time reduction through bi-triplet scalar

We note that the present estimation of the GUT scale can be significantly lowered so as to bring the proton-lifetime prediction closer to the current Super-K. limit if the the Higgs scalar bi-triplet $\Theta_H(3, 3, 1) \subset 54_H$ of $SO(10)$ is near the Parity violating intermediate scale. For example in Fig. 6.2, we have shown how in this model only the unification scale is lowered while keeping the other physical mass scales unchanged as in eq. (6.2) for a value of $M_{331} = 9 \times 10^{13}$ GeV.

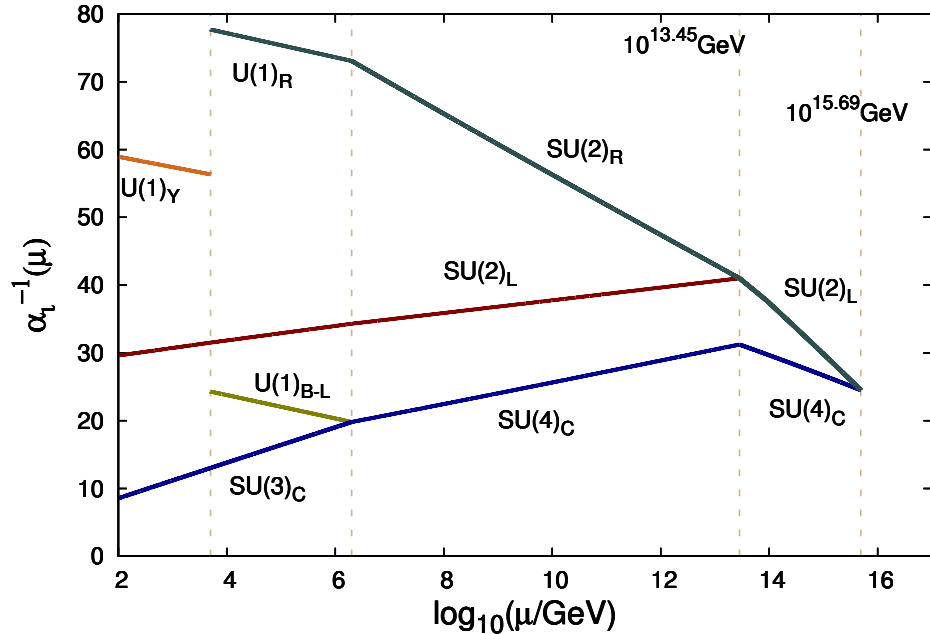


Figure 6.2: Same as Fig. 6.1 but with the Higgs scalar bi-triplet acquiring mass $M_{(3,3,1)} = 9 \times 10^{13}$ GeV.

In Tab. 6.1 we have presented various allowed values of the GUT scale and the proton life-time for different combinations of the di-quark Higgs scalar masses M_Δ contained in $\Delta_R(1, 3, \bar{10}) \subset 126_H$ which mediate $n-\bar{n}$ oscillation process. Even for

M_Δ (GeV)	M_P (GeV)	$M_{(3,3,1)}$ (GeV)	M_G (GeV)	α_G^{-1}	τ_p (years)
$10^{4.0}$	$10^{12.73}$	$10^{14.00}$	$10^{15.57}$	22.37	4.65×10^{33}
$10^{4.0}$	$10^{12.73}$	$10^{14.50}$	$10^{15.66}$	22.08	1.03×10^{34}
$10^{4.0}$	$10^{12.73}$	$10^{15.00}$	$10^{15.75}$	21.79	2.32×10^{34}
$10^{4.0}$	$10^{12.73}$	$10^{15.92}$	$10^{15.92}$	21.22	1.05×10^{35}
$10^{4.5}$	$10^{12.89}$	$10^{14.00}$	$10^{15.60}$	23.16	6.58×10^{33}
$10^{4.5}$	$10^{12.89}$	$10^{14.50}$	$10^{15.69}$	22.88	1.47×10^{34}
$10^{4.5}$	$10^{12.89}$	$10^{15.50}$	$10^{15.87}$	22.19	7.26×10^{34}
$10^{4.5}$	$10^{12.89}$	$10^{15.95}$	$10^{15.95}$	22.01	1.49×10^{35}
$10^{5.0}$	$10^{13.05}$	$10^{14.00}$	$10^{15.62}$	23.94	8.45×10^{33}
$10^{5.0}$	$10^{13.05}$	$10^{14.50}$	$10^{15.71}$	23.66	1.89×10^{34}
$10^{5.0}$	$10^{13.05}$	$10^{15.50}$	$10^{15.89}$	23.08	9.44×10^{34}
$10^{5.0}$	$10^{13.05}$	$10^{15.98}$	$10^{15.98}$	22.79	2.11×10^{35}

Table 6.1: Proton decay lifetime predictions for different combination of bi-triplet scalar mass $M_{(3,3,1)}$ and the average di-quark scalar mass M_Δ .

at the bi-triplet mass $M_{GUT}/15$ we note a reduced value of the unification scale at $M_{GUT} = 10^{15.63}$ GeV and the corresponding proton lifetime at $\tau_p = 4.6 \times 10^{33}$ yrs when $M_\Delta \sim 10^4$ GeV. The estimated lifetimes without including the GUT-threshold effects is found to be in the range $\tau_p = 4.6 \times 10^{33}$ yrs to 2.1×10^{35} yrs, most of which are between the Super-K and the Hyper-K limits.

An important source of uncertainty on τ_p in GUTs is known to be due to GUT-threshold effects as illustrated in the following sub-section.

6.2.4 Estimation of GUT-threshold effects

That there could be significant threshold effects on the unification scale arising out of heavy and super-heavy particle masses was pointed out especially in the context grand desert models [304–306] and in intermediate scale $SO(10)$ models [82, 83, 92, 163, 224–226, 307–310].

In order to examine how closer to or farther from the current experimental bound our model predictions could be, we have estimated the major source of uncertainty on proton lifetime due to GUT threshold effects in $SO(10)$ with intermediate scales [82, 83] taking into account the contributions of the super-heavy (SH) components

in $54_H, 126_H, 210_H, 10_{H_1}$ and 10_{H_2} in the case of the minimal model

$$\begin{aligned}
210_H &\supset \Sigma_1(2, 2, 10) + \Sigma_2(2, 2, \overline{10}) + \Sigma_3(2, 2, 6) + \Sigma_4(1, 1, 15), \\
54_H &\supset S_1(1, 1, 20) + S_2(3, 3, 1) + S_3(2, 2, 6), \\
126_H &\supset \Delta_1(1, 1, 6), \quad 10_{H_i} \supset H_i(1, 1, 6), i = 1, 2,
\end{aligned} \tag{6.11}$$

where the quantum numbers on the right-hand side (RHS) are under the gauge group G_{224} and the components have super-heavy masses around the GUT scale. It was shown in refs. [224–226] that when G_{224D} occurs as intermediate symmetry, all loop corrections due to super-heavy masses $m_{SH} \geq M_P$ cancels out from the predictions of $\sin^2 \theta_W$ and also from M_P obtained as solutions of RGEs for gauge couplings while the GUT threshold effect on the unification scale due to the super-heavy scalar masses assumes an analytically simple form. As outlined in the Appendix E, even in the presence of two more intermediate symmetries below M_P , analogous formulas on the GUT-threshold effects are also valid

$$\Delta \ln \left(\frac{M_{GUT}}{M_Z} \right) = \frac{\lambda_{2L}^U - \lambda_{4C}^U}{6(a_{2L}''' - a_{4C}''')} \tag{6.12}$$

where a_i''' is one-loop beta function coefficients in the range $\mu = M_P - M_{GUT}$ for the gauge group G_{224D} . In eq.(6.12)

$$\lambda_i^U = b_i^V + \Sigma_{SH} b_i^{SH} \ln \left(\frac{M_{SH}}{M_{GUT}} \right), i = 2L, 2R, 4C \tag{6.13}$$

$b_i^V = \text{tr}(\theta_i^V)^2$ and $b_i^{SH} = \text{tr}(\theta_i^{SH})^2$ where θ_i^V (θ_i^{SH}) are generators of the gauge group G_{224D} in the representations of super-heavy gauge bosons (Higgs scalars). The one-loop coefficients for various SH components in eq. (6.11) contributing to threshold effects are [82]

$$\begin{aligned}
b_{2L}^V &= b_{2R}^V = 6, \quad b_{4C}^V = 4, \quad b_i^{\Sigma_4} = (0, 0, 4) \\
b_i^{\Sigma_1} &= b_i^{\Sigma_2} = (10, 10, 12), \quad b_i^{\Sigma_3} = b_i^{S_3} = (6, 6, 4), \\
b_i^{S_1} &= (0, 0, 16), \quad b_i^{S_2} = (12, 12, 0), \quad b_i^{H_{1,2}} = b_i^{\Delta_1} = (0, 0, 2),
\end{aligned} \tag{6.14}$$

where we have projected out the would-be Goldstone components from S_3 leading to

$$\lambda_{2L}^U - \lambda_{4C}^U = 2 - 6\eta_{210} - 2\eta_{54} - 2\eta_{126} - 4\eta_{10}, \tag{6.15}$$

with $\eta_X = \ln(M_X/M_{GUT})$, and we have made the assumption that all super-heavy

scalars belonging to a particular $SO(10)$ representation have mass of same order, say $M_{\Sigma_i} \in (10M_{210}, M_{210}/10) : (i = 1 - 4)$, for 210_H and so on for other representations [83]. Utilizing the model coefficients $a_{2L}''' = 44/3$ and $a_{4C}''' = 16/3$, and using eq. (6.15) in eq. (6.12) gives

$$M_{GUT}/M_{GUT}^0 = 10^{(0.25 \ln \eta)/2.3025} \quad (6.16)$$

where $\eta = 10(1/10)$ depending upon our assumption that SH components are 10 (1/10) times heavier (lighter) than the GUT scale. By applying these GUT-threshold effects to the solutions of RGE in eq. (6.3), we obtain

$$\begin{aligned} M_{GUT} &= 10^{15.92 \pm 0.25} \text{GeV}, \\ \tau_p(p \rightarrow e^+ \pi^0) &\simeq 5.05 \times 10^{35 \pm 1.0 \pm 0.34} \text{yrs} \end{aligned} \quad (6.17)$$

where the first uncertainty is due to GUT threshold effects, and the second uncertainty derived in Appendix E.2, is due to the 1σ level uncertainties in the experimental values of $\sin^2 \theta_W(M_Z)$ and $\alpha_S(M_Z)$. It is clear from eq. (6.17) that our prediction covers wider range of values in proton lifetime prediction including value few times larger than the current Super-K limit.

Similarly each of the numerical values in the last column of Tab. 6.1 is modified by this additional uncertainty factor of $10^{\pm 1 \pm 0.32}$ in the estimated lifetimes.

6.3 Rare kaon decay and $n-\bar{n}$ oscillation

In this section we discuss the model predictions on rare kaon decays mediated by lepto-quark gauge bosons of $SU(4)_C$ that occurs as a part of Pati-Salam intermediate gauge symmetry $SU(2)_L \times SU(2)_R \times SU(4)_C$ which breaks spontaneously at the mass scale $\mu = M_R^\pm = M_C$. The lepto-quark Higgs scalar contribution to the rare decay process is suppressed in this model due to the natural values of their masses at $M_C = 10^6$ GeV and smaller Yukawa couplings.

6.3.1 Rare kaon decay $K_L \rightarrow \mu \bar{e}$

Earlier several attempts have been made to derive lower bound on the lepto-quark gauge boson mass [47, 279, 280]. In this subsection we update the existing latest lower bound on the $SU(4)_C$ lepto-quark gauge boson mass [279] using the improved measurement on the branching ratio and improved renormalization group running of gauge couplings due to the running VEVs and the additional presence of G_{2113} gauge

symmetry in between G_{224} and the SM gauge symmetries. Experimental searches on rare kaon decays in the channel $K_L \rightarrow \mu^\pm e^\mp$ have limited its branching ratio with the upper bound [297]

$$Br(K_L \rightarrow \mu\bar{e})_{\text{expt.}} \equiv \frac{\Gamma(K_L \rightarrow \mu^\pm e^\mp)}{\Gamma(K_L \rightarrow \text{all})} < 4.7 \times 10^{-12} \quad (6.18)$$

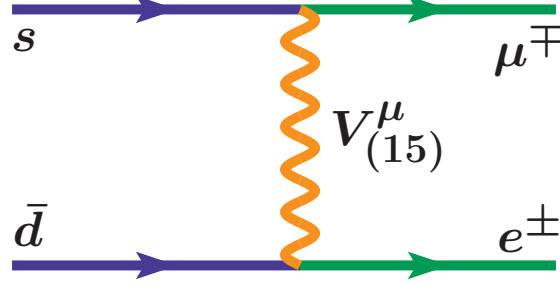


Figure 6.3: Feynman diagram for rare kaon decays $K_L^0 \rightarrow \mu^\pm e^\mp$ mediated by a heavy lepto-quark gauge boson of $SU(4)_C$ gauge symmetry.

The lepto-quark gauge bosons of $SU(4)_C$ in the adjoint representation $(1, 1, 15)$ under G_{224} mediate rare kaon decay $K_L \rightarrow \mu^\pm e^\mp$ whose Feynman diagram is shown in the Fig. 6.3. Analytic formulas for the corresponding branching ratio is [279, 280],

$$Br(K_L \rightarrow \mu\bar{e}) = \frac{4\pi^2 \alpha_s^2(M_C) m_K^4 R}{G_F^2 \sin^2 \theta_C m_\mu^2 (m_s + m_d)^2 M_C^4}, \quad (6.19)$$

where the factor R includes renormalization effects on the quark masses m_d or m_s from $\mu = M_C$ down to $\mu = \mu_0 = 1$ GeV through the G_{2113} , the SM and the $SU(3)_C$ gauge symmetries.

Noting that the down quark or the strange quark mass satisfies the following renormalization group equations,

$$m_{d,s}(M_C) = \frac{m_{d,s}(\mu_0)}{\eta_{\text{em}}} R_{2113} R_{213}^{(6)} R_{213}^{(5)} R_{QCD}^{(5)} R_{QCD}^{(4)} R_{QCD}^{(3)} \quad (6.20)$$

where

$$R_{2113} = \prod_i \left(\frac{\alpha_i(M_C)}{\alpha_i(M_R^0)} \right)^{-C_1^i/2a_i^{(1)}}, \quad i = 2L, 1R, B-L, 3C,$$

$$R_{213}^{(6)} = \prod_i \left[\frac{\alpha_i(M_R^0)}{\alpha_i(m_t)} \right]^{-C_2^i/2a_i^{(2)}}, \quad R_{213}^{(5)} = \prod_i \left[\frac{\alpha_i(m_t)}{\alpha_i(M_Z)} \right]^{-C_2^i/2a_i^{(3)}}, \quad i = 2L, Y, 3C,$$

$$\begin{aligned}
R^{(5)}_{QCD} &= \left[\frac{\alpha_S(M_Z)}{\alpha_S(m_b)} \right]^{-4/a^{(4)}}, & R^{(4)}_{QCD} &= \left[\frac{\alpha_S(m_b)}{\alpha_i(m_c)} \right]^{-4/a^{(5)}} \\
R^{(3)}_{QCD} &= \left[\frac{\alpha_S(m_c)}{\alpha_S(\mu^0)} \right]^{-4/a^{(6)}}, & &
\end{aligned} \tag{6.21}$$

where the input parameters used in above eq. (6.21) are: $C_1^i = (0, 0, 1/4, 8)$, $C_2^i = (0, -1/5, 8)$ and the one-loop beta-coefficients relevant for our present work are $a_i^{(1)} = (-3, 57/12, 37/8, -7)$, $a_i^{(2)} = (-19/6, 41/10, -7)$, $a_i^{(3)} = (-23/6, 103/30, -23/3)$, $a^{(4)} = -23/3$, $a^{(5)} = -25/3$, $a^{(6)} = -9$. Now we can obtain the renormalization factor in eq. (6.19)

$$R = \left[R_{2113} R_{213}^{(6)} R_{213}^{(5)} R_{QCD}^{(5)} R_{QCD}^{(4)} R_{QCD}^{(3)} \right]^{-2}. \tag{6.22}$$

Using eq.(6.21) and eq.(6.22) and eq.(6.18), we derive the following inequality,

$$F_L(M_C, M_R^0) > \left[\frac{4\pi^2 m_K^4 R_p}{G_F^2 \sin^2 \theta_C m_\mu^2 (m_s + m_d)^2} \times 10^{11.318} \right]^{1/4}, \tag{6.23}$$

where

$$\begin{aligned}
F_L(M_C, M_R^0) &= M_C \alpha_S^{-\frac{3}{14}}(M_C) \alpha_Y^{-\frac{1}{82}}(M_{R^0}) \left[\frac{\alpha_{B-L}(M_C)}{\alpha_{B-L}(M_{R^0})} \right]^{-\frac{1}{74}} \alpha_Y^{\frac{1}{82}}(m_t) \alpha_C^{-\frac{2}{7}}(m_t), \\
R_p &= \left[R_{213}^{(5)} R_{QCD}^{(5)} R_{QCD}^{(4)} R_{QCD}^{(3)} \right]^{-2}.
\end{aligned} \tag{6.24}$$

In Fig. 6.4 the function $F_L(M_C, M_R^0)$ in the LHS of eq. (6.23) is plotted against M_C for a fixed value of $M_R^0 = 5$ TeV, where the Horizontal lines represent the RHS of the same equation including uncertainties in the parameters. Thus, for the purpose of this numerical estimation, keeping M_R^0 fixed at any value between 5 – 10 TeV, we vary M_C until the LHS of eq. (6.23) equals its RHS.

For our computation at $\mu_0 = 1$ GeV, we use the inputs $m_K = 0.4976$ GeV, $m_d = 4.8_{-0.3}^{+0.7}$ MeV, $m_s = 95 \pm 5$ MeV, $m_\mu = 105.658$ MeV, $G_F = 1.166 \times 10^{-5}$ GeV⁻², and $\sin \theta_C = 0.2254 \pm 0.0007$, $m_b = 4.18 \pm 0.03$ GeV, $m_c = 1.275 \pm 0.025$ GeV, $m_t = 172$ GeV. At $\mu = M_Z$ we have used $\sin^2 \theta_W = 0.23166 \pm 0.00012$, $\alpha_S = 0.1184 \pm 0.0007$, $\alpha^{-1} = 127.9$ and utilized eq. (6.18)–eq. (6.24). With $M_{R^0} = 5$ TeV and $M_{Z'} \simeq 1.2$ TeV, the existing experimental upper bound on $Br(K_L \rightarrow \mu^\mp e^\pm)$ gives the lower bound on the G_{224} symmetry breaking scale

$$M_C > (1.932_{-0.074}^{+0.082}) \times 10^6 \text{ GeV}. \tag{6.25}$$

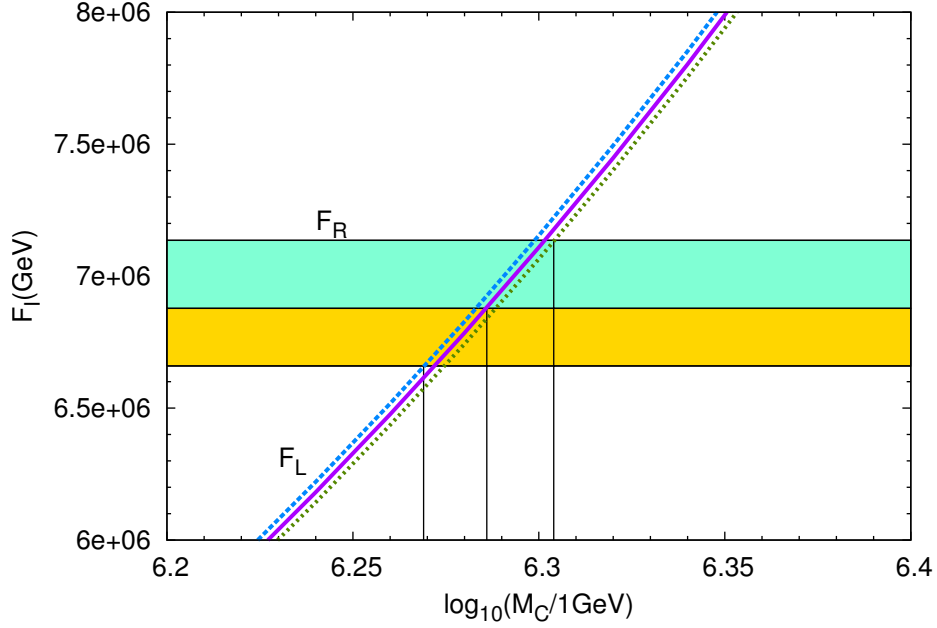


Figure 6.4: Graphical representation of the method for numerical solution of the lower bound on M_C . The horizontal lines are the RHS of the inequality (6.23) whereas the curve represents the LHS. The colored horizontal bands are due to uncertainties in the input parameters.

Noting from Fig. 6.1 that in our model $\alpha_S(M_C) = 0.0505$, we get from eq. (6.25) as rare-kaon decay constraint on the $SU(4)_C$ lepto-quark gauge boson mass

$$M_{\text{lepto}} > (1.539^{+0.065}_{-0.059}) \times 10^6 \text{ GeV}. \quad (6.26)$$

where the uncertainty is due to the the existing uncertainties in the input parameters. From the derived solutions to RGEs for gauge couplings this lower bound on the lepto-quark gauge boson mass is easily accommodated in our model.

6.3.2 Neutron-antineutron oscillation

Here we discuss the prospect of this model predictions for experimentally observable $n-\bar{n}$ oscillation while satisfying the rare kaon decay constraint by fixing the G_{224} symmetry breaking scale at $M_C \sim 2 \times 10^6$ GeV as derived in eq. (6.25). The Feynman diagrams for the $n-\bar{n}$ oscillation processes are shown in left- and right-panel of Fig. 6.5 where $\Delta_{u^c u^c}$, $\Delta_{d^c d^c}$, and $\Delta_{u^c d^c}$ denote different di-quark Higgs scalars contained in

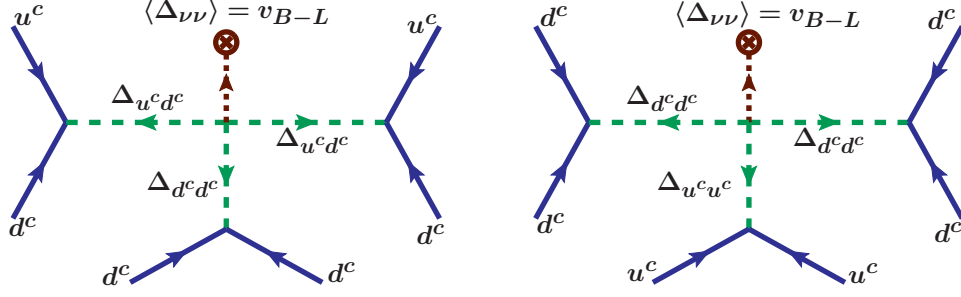


Figure 6.5: Feynman diagrams for neutron-antineutron oscillation mediated by two $\Delta_{u^c d^c}$ and one $\Delta_{d^c d^c}$ di-quark Higgs scalars (left-panel), and two $\Delta_{d^c d^c}$, one $\Delta_{u^c u^c}$ di-quark Higgs scalars (right-panel).

$\Delta_R(1, 3, \overline{10}) \subset 126_H$. The amplitude for these two diagrams can be written as [311]

$$\text{Amp}_{n\bar{n}}^{(a)} = \frac{f_{11}^3 \lambda v_{B-L}}{M_{\Delta_{u^c d^c}}^4 M_{\Delta_{d^c d^c}}^2}, \quad \text{Amp}_{n\bar{n}}^{(b)} = \frac{f_{11}^3 \lambda v_{B-L}}{M_{\Delta_{d^c d^c}}^4 M_{\Delta_{u^c u^c}}^2}, \quad (6.27)$$

where $f_{11} = f_{\Delta_{u^c d^c}} = f_{\Delta_{d^c d^c}} = f_{\Delta_{u^c u^c}}$ from the $SO(10)$ invariance and the quartic coupling between different di-quark Higgs scalar has its natural value i.e. $\mathcal{O}(0.1) - \mathcal{O}(1)$.

The n - \bar{n} mixing mass element $\delta m_{n\bar{n}}$ and the di-baryon number violating amplitude $W_{(B=2)} = \text{Amp}^{(a)} + \text{Amp}^{(b)}$ are related up to a factor depending upon combined effects of hadronic and nuclear matrix element effects

$$\delta m_{n\bar{n}} = (10^{-4} \text{ GeV}^6) \cdot W_{B=2}. \quad (6.28)$$

The experimentally measurable mixing time $\tau_{n\bar{n}}$ is just the inverse of $\delta m_{n\bar{n}}$

$$\tau_{n\bar{n}} = \frac{1}{\delta m_{n\bar{n}}}. \quad (6.29)$$

With $v_{B-L} = 5 \text{ TeV}$ in the degenerate case, when all di-quark Higgs scalars have identical masses $M_{\Delta} = 10^5 \text{ GeV}$, the choice of the parameters $f_{11} \simeq \lambda \sim \mathcal{O}(0.1)$ gives $\tau_{n\bar{n}} = 6.58 \times 10^9 \text{ sec}$. As described below our $SO(10)$ model can fit all charged fermion masses and CKM mixings at the GUT scale with two kinds of structures: (i) only one 126_H , and (ii) two Higgs representations 126_H and $126'_H$. In the minimal case the Yukawa coupling f of 126_H to fermions has a diagonal structure,

$$f = \text{diag}(0.0236, -0.38, 1.5), \quad (6.30)$$

f_{11}	λ	$M_{\Delta_{ucdc}}$ (GeV)	$M_{\Delta_{dcdc}}$ (GeV)	$\tau_{n\bar{n}}$ (secs)
0.1	0.1	10^5	10^5	6.6×10^9
0.0236	0.1	10^5	10^5	2.5×10^{13}
0.0236	1.0	10^5	10^5	2.5×10^{14}
0.1	0.1	10^4	10^5	6.6×10^9
0.0236	1.0	10^4	10^5	2.5×10^{13}
0.0236	1.0	10^5	10^4	2.5×10^{13}

Table 6.2: Predictions for n - \bar{n} oscillation mixing time as a function of allowed couplings and masses of di-quark Higgs scalars in the model described in the text.

which gives through eq. (6.27), eq. (6.28), and eq. (6.29)

$$\tau_{n\bar{n}} = 10^8 - 10^{10} \text{secs.} \quad (6.31)$$

This model prediction is accessible to ongoing search experiments [312]. However, the GUT scale fit to the fermion masses can be successfully implemented without constraining the f values when a second $126'_H$ is present at the GUT scale with all its component at M_U except $\xi'(2, 2, 15)$ being around the M_P scale. Then using $f_{11} = 0.1 - 0.01$, the estimated value turns out to be

$$\tau_{n\bar{n}} \sim 10^9 - 10^{13} \text{sec.} \quad (6.32)$$

Out of this the mixing time in the range $10^9 - 10^{10}$ sec can be probed by ongoing experiment [312].

6.4 Dirac neutrino mass matrix, neutrino parameter fitting and lepton flavor violation

The Dirac neutrino mass near the TeV scale forms an essential ingredient in the estimations of inverse seesaw contribution to light neutrino masses and mixings as well as the LFV and LNV processes in this model in addition to predicting leptonic CP -violation through non-unitarity effects. Since the procedure for determination of M_D has been discussed in Sec. 5.5.5 [295], we recap it here in the context of the present model. In order to obtain the Dirac neutrino mass matrix M_D and the RH Majorana mass matrix M_N near TeV scale, at first the PDG values [313] of fermion masses at the electroweak scale are extrapolated to the GUT scale using the

RGEs for fermion masses in the presence of the SM for $\mu = M_Z - 5$ TeV, and from $\mu = 5 - 1000$ TeV using the RGEs in the presence of G_{2113} symmetry [186, 246]. From $\mu = 5 - 1000$ TeV, RGEs have two Higgs doublets $\Phi_1 \subset 10_{H_1}$ and $\Phi_2 \subset 10_{H_2}$ in the presence of G_{2113} symmetry [246]. For mass scale $\mu \geq 10^6$ GeV till the GUT scale the fermion mass RGEs in the presence of the G_{224} and G_{224D} symmetries [288] should be exploited. The new estimations of the parameters are not very different from the estimations in Sec. 5.5.5, therefore we continue our study with the predictions in eq. (4.19) - eq. (5.49), eq. (5.55) - eq. (5.58) and eq. (5.61).

In the presence of three singlet fermions S_i , ($i = 1, 2, 3$), the inverse seesaw mechanism [143, 144, 246, 295, 314] is implemented through the $SO(10)$ invariant Yukawa Lagrangian

$$\mathcal{L}_{\text{Yuk}} = Y^a 16.16.10_H^a + f 16.16.126_H^\dagger + y_\chi 16.1.16_H^\dagger + \mu_S 1.1 \quad (6.33)$$

which gives rise to the G_{2113} invariant interaction near the TeV scale [246, 295] where $\chi_R(1, 1/2, -1, 1) \subset 16_H$ generates the N - S mixing term giving

$$\mathcal{L}_{\text{Yuk}} = Y^{\ell\bar{L}} N_R \Phi_1 + f N_R^c N_R \Delta_R + F \bar{N}_R S \chi_R + S^T \mu_S S + \text{h.c.} \quad (6.34)$$

This Lagrangian gives rise to the 9×9 neutral fermion mass matrix after electroweak symmetry breaking. This mass matrix is given in eq. (5.3). The diagonalization of this matrix can be followed from Sec. 5.1.2 and Appendix D.

Although the N - S mixing matrix M in general can be non diagonal, we have assumed it to be diagonal partly to reduce the unknown parameters. The LFV bounds, as listed in and column C0 of Tab. 5.1, constrain the diagonal elements. Noting that for diagonal M , $\eta_{\alpha\beta} = \frac{1}{2} \sum_{k=1}^3 (M_{D_{\alpha k}} M_{D_{\beta k}}^*) / M_k^2$. The possible CP -phases of the elements of $\eta_{\alpha\beta}$ ($= \phi_{\alpha\beta}$) are not yet constrained. The knowledge of M_D matrix given in eq. (5.11) and saturation of the lower bound on $|\eta_{\tau\tau}| = 2.7 \times 10^{-3}$ leads to the relation, eq. (5.13), between diagonal elements of M . The above relation can give the lower bounds on the diagonal elements of matrix M . The partial degenerate and degenerate cases have also been discussed in the text below eq. (5.13) of the Sec. 5.1.3. Diagonalizing the light neutrino mass matrix using the PMNS matrix $m_\nu = U_\nu \hat{m}_\nu U_\nu^T$ and from the light neutrino mass formula (5.6) we can find the μ_S matrix as in eq. (5.14) and estimated in Tab. 5.2 and Tab. 5.3 for normal and inverted hierarchies of light neutrinos. Both of the above mentioned tables comprise various possible choices of elements of M .

The dominant lepton flavor violating contributions coming through the exchange

of heavy sterile neutrinos (S) and heavy RH neutrinos (N_R) are discussed in Sec. 5.4 and the branching ratios for LFV and CP -violation contributions are listed in Tab. 5.8 and Tab. 5.9 respectively.

6.5 Contributions to neutrinoless double beta decay in $W_L - W_L$ channel

In the generic inverse seesaw, there is only one small lepton number violating scale μ_S and the lepton number is conserved in the $\mu_S = 0$ limit leading to vanishing non-standard contribution to the $0\nu 2\beta$ transition amplitude. On the contrary, in the extended seesaw under consideration, there can be a dominant contributions from the exchanges of heavy sterile neutrinos [295]. The main thrust of our discussion will be the new contribution arising from exchange of heavy sterile neutrinos S_i with Majorana mass $M_S = \mu_S - M(1/M_N)M^T$ as explained in Sec. 5.1.2. Although, the dominance of sterile neutrino exchange was estimated very approximately in Sec. 5.3, its interference with quasi-degenerate light neutrino contribution was ignored. Also no bound on the lightest sterile neutrino mass was discussed. So, this section is a detailed extension of Sec. 5.3 in view of diagonal M_N as estimated in eq. (5.58). The high-light of the present analysis include scattered plot of effective mass parameter against the lightest active neutrino mass in the theory, plot of combined effective mass parameter against lightest sterile neutrino mass, scattered plots of half life against lightest sterile neutrino mass and functional plot of half life against lightest sterile neutrino mass in different cases. Because of heavy mass of W_R boson in this theory, the RH current contributions are insignificant. The standard and new contributions in the $W_L^- - W_L^-$ channel are shown in Fig. 5.2 and Fig. 5.3.

As we know now, RH neutrinos are necessarily heavier than the sterile fermion masses because of the underlying constraint imposed by the extended see-saw mechanism, contributions from RH neutrino mediation, in all $W_L^- - W_L^-$, $W_L^- - W_R^-$ and $W_R^- - W_R^-$ channels are orders less than due to sterile mediation. Since right handed gauge bosons, W_R , do not appear below Pati-Salam scale, contributions from $W_L^- - W_R^-$ and $W_R^- - W_R^-$ channel are redundant. Therefore, we ignore RH neutrino contribution and consider only the combined effective mass due to the light neutrino and the sterile fermion exchanges in the $W_L - W_L$ channel, which is expressed as

$$m_{ee}^{\text{eff}} = \sum \mathcal{N}_{ei}^2 m_{\nu_i} + p^2 \sum_i \frac{(\mathcal{V}_{ei}^{\nu S})^2}{\hat{M}_{S_i}}. \quad (6.35)$$

The two Majorana phases, α_1, α_2 , of the light neutrino sector are inside $\mathcal{N} \equiv \mathcal{V}^{\nu\nu}$, see eq.(5.9). From eq.(5.10) we note that $(\mathcal{V}_{ej}^{\nu S}) \simeq (M_D/M)_{ej}$. The sterile contribution in eq.(6.35) depends on Dirac neutrino mass matrix, Dirac $N - S$ mixing matrix M and Majorana $N - N$ matrix M_N . In Sec.5.3 and in the second item of Sec.5.5.5.2 we observed that mass of sterile (M_S) is a good parameter to see the variance of BSM $0\nu\beta\beta$ contribution. A sample of mixing matrix elements for prediction of $0\nu\beta\beta$ amplitude are given below

$$\begin{aligned} \mathcal{N}_{e1} &= 0.8143 - 0.0008i, & \mathcal{N}_{e2} &= 0.5588 + 0.0002i, & \mathcal{N}_{e3} &= 0.1270 + 0.0924i, \\ \mathcal{V}_{e1}^{\nu S} &= 0.00054i, & \mathcal{V}_{e2}^{\nu S} &= 0.00005 + 0.00032i, & \mathcal{V}_{e3}^{\nu S} &= 0.00023 + 0.00009i \end{aligned} \quad (6.36)$$

for $M_N = \text{diag}(115, 1785, 7500)$ GeV, $M = \text{diag}(40, 300, 1661)$ GeV and M_D matrix as given in eq.(5.61). For this combination of matrices M_D , M and M_N , we get sterile masses $M_S = (12.5, 49, 346)$ GeV.

In Fig.6.6 we have presented the effective mass parameter for $0\nu\beta\beta$ decay as a function of lightest neutrino mass. The yellow band in the left-panel represents the Heidelberg-Moscow (HM) evidence corresponding to measured half-life $T_{1/2}^{0\nu}(^{76}\text{Ge}) = 2.23_{-0.31}^{+0.44} \times 10^{25}$ yrs at 68% C.L. In the right-panel it represents the combined bound from KamLAND-Zen and EXO-200 experiments corresponding to $T_{1/2}^{0\nu}(^{136}\text{Xe}) = 3.4 \times 10^{25}$ yrs at 90% C.L. This band, instead of single line, is due to uncertainty in nuclear matrix elements as listed in Tab.5.4. The effective mass predictions for normal and inverted hierarchy of light neutrinos which are known to be far below the current experimental bounds are also shown in the left- and the right-panels. The vertical lines to the right of each figure represent experimental bound on sum of active neutrino masses. The slanted hammer shaped region corresponds mainly to QD region of neutrino masses.

The scattered dots in this figure are effective mass due to sterile neutrino exchange in the $W_L^- - W_L^-$ channel. The nuclear matrix elements and phase space factors are taken from the Tab.5.4. Nuclear matrix elements for the respective isotopes are allowed to vary in the range as given in the table. The diagonal elements of M have been obtained from non-unitarity constraint as discussed in Sec.4.5 and Sec.5.1.3. For a fixed values of $M_1 = 55$ GeV, we get almost a fixed value of $M_{S1} \simeq 22$ GeV. The spread of scatted points is due to uncertainty in nuclear matrix elements and allowed variance of elements $M_2 \in [250, 550]$, and $M_3 \in [1600, 2500]$ GeV. For values of M_{S1} smaller (larger) than 22 GeV the central region of the scattered points shifts upwards (downwards). Thus, we find that even without the quasi-degeneracy assumption on

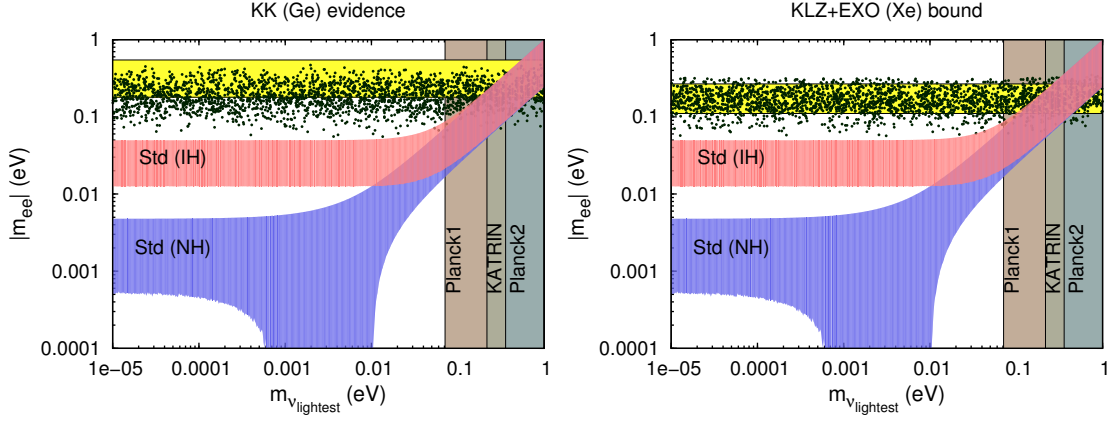


Figure 6.6: Effective mass as a function of the lightest active neutrino mass. The blue and the red bands correspond to normal and inverted hierarchy, respectively. The vertical bands are from the bounds on the sum of light neutrino masses given by Planck1, Planck2, and KATRIN experiments. The horizontal yellow band in the left panel corresponds to HM claim with $T_{1/2}^{0\nu}({}^{76}\text{Ge}) = 2.23_{-0.31}^{+0.44} \times 10^{25}$ yrs at 68% C.L. and that in the right-panel corresponds to the KamLAND-Zen and EXO-200 combined bound $T_{1/2}^{0\nu}({}^{136}\text{Xe}) = 3.4 \times 10^{25}$ yrs at 90% C.L. The scattered points are sterile neutrino contributions to the effective mass.

the light neutrino masses, it is possible to explain current experimental bounds or any future data, close to experimental limits, by the sterile neutrino dominance. As the standard and sterile contributions to effective mass parameter have opposite signs, as well as there are various phases, there is the possibility of cancellation between the two terms. This behavior of the combined contribution will also be discussed here.

Saturation of the Plank1 bound on the sum of the three light neutrino masses at 0.23 eV [315] combined with neutrino oscillation data gives $(m_1, m_2, m_3) = (0.0712, 0.0717, 0.0870)$ eV, or $(m_1, m_2, m_3) = (0.0820, 0.0824, 0.0655)$ eV. The maximum possible contribution of such light neutrinos alone to the effective mass which is shown by the solid-blue horizontal line is way below the HM data or far from the combined bound from KamLAND-Zen and EXO-200 experiments. The light neutrino contributions of IH and NH type are even smaller as shown by the dot-dashed and the dashed horizontal lines in this figure whereas the combined effective mass parameters including sterile neutrino contributions are represented by the corresponding slanting curves. A dip in the solid-blue curve that includes contribution of light neutrino masses of Planck1 type hierarchy occurs at $M_{S_1} \simeq 26$ GeV for $\langle p^2 \rangle = -(130\text{MeV})^2$, but the corresponding dip in the dot-dashed curve that includes contribution of IH type neutrinos is found to occur at $M_{S_1} \simeq 30$ GeV. Please note that here neutrino

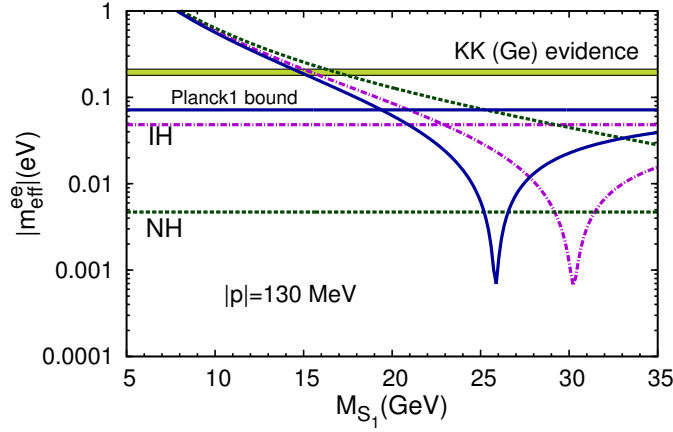


Figure 6.7: Effective mass as a function of lightest sterile neutrino mass. The green band corresponds to the effective mass corresponding to HM experiment. Horizontal lines are the standard effective masses in the NH, IH, and saturation of Planck1 pattern of light neutrino masses in the absence of any Majorana phase. The solid, dashed, and the dotted curves are for light-neutrino masses corresponding to saturation of Planck1 bound, IH, and NH patterns. We have used $\langle p^2 \rangle = -(130 \text{ MeV})^2$.

oscillation parameters are such that active light neutrinos produce maximum contribution to effective mass. We have also noted that the cancellation between the light neutrino and sterile neutrino contributions occurs at still larger value of $M_{S_1} \geq 40$ GeV. This cancellation phenomenon with increasing values of dip positions for decreasing values of light neutrino masses as evidenced in Planck1, IH, and NH cases is clearly understood by our formulas given in eq.(6.35). Being inversely proportional to M_{S_i} , the sterile neutrino contribution decreases for increasing mass eigenvalues and the dip region appears when the sterile neutrino contribution is comparable to the contribution due to the light neutrinos of a given type of hierarchy.

We also note the occurrence of a stringent bound on the mass of the lightest sterile neutrino $M_{S_1} \gtrsim 15$ GeV from the crossing region of the HM experimental band. This bound on M_{S_1} is for Planck1 bound on sum of neutrino masses and occurs for smallest allowed value of $|p| = 130$ MeV and large values of $(M_{S_2}, M_{S_3}) = (160, 758)$ GeV so that the contributions of the latter two masses are negligible. For larger values of $|p|$, the bound on M_{S_1} will be larger. We will discuss this issue later in this section in the context of half-life predictions for $0\nu\beta\beta$ -decay where peaks are expected to appear.

The cancellation among the light neutrino and sterile neutrino contributions is more prominent in the quasi-degenerate case as shown in Fig.6.8 where the horizontal overlapping dark region shows that, in the absence of both the Majorana phases, the contribution of light quasi-degenerate neutrinos alone with common mass $m_\nu =$

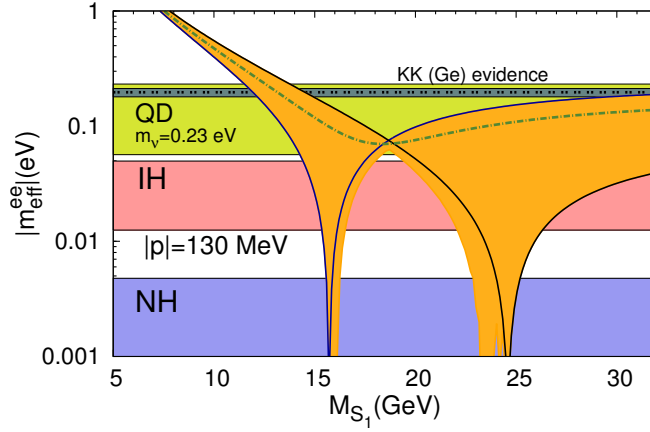


Figure 6.8: Predicted variation of combined effective mass parameter for $0\nu\beta\beta$ decay as a function of lightest sterile neutrino mass M_{S_1} . The horizontal blue, red and green bands of effective masses are generated for the NH, IH, and the QD type of light neutrinos, respectively when all the Majorana phases are scanned. The horizontal dark-green band, with double-dot line in the middle, represents the HM data. The orange band is quasi-degenerate light + sterile neutrino contribution for fixed $\mathcal{M}_{0\nu}^\nu = 6.64$ and $|p| = 130$ MeV.

0.23 eV can explain the HM data with nuclear matrix element $M_{0\nu}^\nu = 6.64$. On the other hand, in the presence of sterile neutrinos, the two contributions cancel out for certain allowed values of parameters giving much smaller value of the resultant effective mass for certain values of M_{S_1} . In the Fig.6.8, the first dip in the effective mass occurs at $M_{S_1} \simeq 15.8$ GeV for zero Majorana phases of light-neutrinos. This behavior is shown by the solid-blue curve. The dip in the region $M_{S_1} \simeq 25$ GeV occurs when each of the two Majorana phases in the light neutrino sector is $\pi/2$. The orange band shown in the Fig.6.8 spans over all the possible values of the two Majorana phases between $0 - 2\pi$. We have shown one case by the dot-dashed green curve which corresponds to Majorana phase $\alpha_1 = \pi/4$. We have noted that for larger values of $|p|$, the cancellation and the dip regions shift towards higher values of M_{S_1} .

From the Fig.6.7 and the Fig.6.8 it is clear that for agreement with the current experimental data on the effective mass parameter, the lightest sterile neutrino mass should be constrained with the following lower bounds

$$\begin{aligned}
 M_{S_1} &\geq 11.7 \text{ GeV, QD } (m_\nu = 0.23\text{eV}), \\
 &\geq 14.5 \text{ GeV, Plank1}, \\
 &\geq 14.5 \text{ GeV, IH}, \\
 &\geq 16.3 \text{ GeV, NH}.
 \end{aligned} \tag{6.37}$$

6.5.1 Half-life and bound on sterile neutrino mass

We present the expression for half-life of $0\nu\beta\beta$ decay as a function of sterile neutrino masses and other parameters in the theory. We then show by means of scattered plots or otherwise, how the current experimental bounds limit the lightest sterile neutrino mass.

Using results discussed in previous sections, the inverse half-life is presented in terms of η - parameters and others including the nuclear matrix elements [254, 261, 295, 316]

$$[T_{1/2}^{0\nu}]^{-1} = G_{01}^{0\nu} |\mathcal{M}_\nu^{0\nu}|^2 \eta_\nu + \frac{\mathcal{M}_N^{0\nu}}{\mathcal{M}_\nu^{0\nu}} \eta_S|^2. \quad (6.38)$$

where the dimensionless particle physics parameters are

$$\eta_\nu = \sum_i \frac{(\mathcal{V}_{ei}^{\nu\nu})^2 m_i}{m_e}, \quad \eta_S = \sum_i \frac{(\mathcal{V}_{ei}^{\nu S})^2 m_p}{M_{S_i}} \quad (6.39)$$

In eq.(6.39), m_e (m_i)= mass of electron (light neutrino), and m_p = proton mass. In eq.(6.38), $G_{01}^{0\nu}$ is the the phase space factor and, besides different particle parameters, it contains the nuclear matrix elements due to different chiralities of the hadronic weak currents such as $\mathcal{M}_\nu^{0\nu}$ involving left-left chirality in the standard contribution. Explicit numerical values of these nuclear matrix elements discussed in ref. [254, 261, 295, 316] are given in Table. 5.4.

In terms of effective mass parameter, the inverse half-life for $0\nu\beta\beta$ decay is

$$[T_{1/2}^{0\nu}]^{-1} = \frac{\Gamma_{0\nu\beta\beta}}{\ln 2} = G_{0\nu} \left| \frac{\mathcal{M}_\nu^{0\nu}}{m_e} \right|^2 \times |m_{ee}^{\text{eff}}|^2, \quad (6.40)$$

$$m_{ee}^{\text{eff}} = m_{ee}^\nu + m_{ee}^S,$$

where $G_{0\nu}$ contains the phase space factors, m_e is the electron mass, and \mathcal{M}_ν is the nuclear matrix element and the effective mass parameters are

$$m_{ee}^\nu = \mathcal{N}_{ei}^2 m_{\nu_i} \quad , \quad m_{ee}^S = p^2 \frac{(\mathcal{V}_{ei}^{\nu S})^2}{\hat{M}_{S_i}}, \quad (6.41)$$

where

$$\begin{aligned} |\langle p^2 \rangle| &= |m_e m_p \mathcal{M}_N^{0\nu} / \mathcal{M}_\nu^{0\nu}| = [(130 - 277) \text{ MeV}]^2 ; \quad {}^{76}\text{Ge}, \\ &= [(140 - 230) \text{ MeV}]^2 ; \quad {}^{136}\text{Xe}. \end{aligned} \quad (6.42)$$

For direct prediction of half-life as a function of heavy sterile neutrino masses and its comparison with experimental data of ongoing search experiments, we write the total half life, including light neutrino contribution, as

$$T_{1/2}^{0\nu} = \mathcal{K}_{0\nu}^{-1} \times \frac{M_{N_1}^2 M_{S_1}^4}{|\langle p^2 \rangle|^2 (M_{D_{e1}})^4} \left[\left| 1 + \mathbf{a} \frac{M_{S_1}^2}{M_{S_2}^2} + \mathbf{b} \frac{M_{S_1}^2}{M_{S_3}^2} - \delta \right| \right]^{-2}, \quad (6.43)$$

where $K_{0\nu} = G_{0\nu} \left| \frac{\mathcal{M}_{\nu}^{0\nu}}{m_e} \right|^2$ and

$$\mathbf{a} = \frac{M_{D_{e2}}^2 M_{N_1}}{M_{D_{e1}}^2 M_{N_2}}, \quad \mathbf{b} = \frac{M_{D_{e3}}^2 M_{N_1}}{M_{D_{e1}}^2 M_{N_3}}, \quad \delta = \frac{m_{ee}^\nu M_{N_1} M_{S_1}^2}{M_{D_{e1}}^2 |p^2|}. \quad (6.44)$$

The light-neutrino contribution has entered through the quantity δ in the eq.(6.43). Using the predicted value of M_D from eq.(5.61) and derived values of heavy RH Majorana neutrino mass matrix, $M_N = \text{diag}(115, -1785, 7500)$ GeV from the GUT-scale fit to the fermion masses we obtain from eq.(6.44)

$$\mathbf{a} = -1.187 + i 0.395, \quad \mathbf{b} = -3.782 - i 3.346. \quad (6.45)$$

For different values of the diagonal matrix $M = \text{diag}(M_1, M_2, M_3)$ consistent with the non-unitarity constraint eq.(4.36), and the $M_N = \text{diag}(115, -1785, 7500)$ GeV we can get M_S . The difference in leading order values of $\hat{M}_{S_i} = -M_i^2/M_{N_i}$ and exact numerical calculation by diagonalizing 9×9 \mathcal{M}_ν matrix is given in Tab. 6.3. where the values obtained by direct diagonalization of \mathcal{M}_ν matrix are denoted as M_S . It is clear from eq.(6.43) that the half-life is a function of three mass eigenvalues M_{S_1} , M_{S_2} and M_{S_3} while all other parameters are known. This calls for a scattered plot for half life as discussed below. It is evident from eq.(6.43) that for $M_{S_3} \gg M_{S_2} \gg M_{S_1}$, a $\log(T_{1/2})$ vs $\log(M_{S_1})$ would exhibit a linear behavior.

Including the contribution of light neutrinos with NH patterns of masses, we have shown the scattered plot of half-life as a function of lightest sterile neutrino mass M_{S_1} and compared it with experimental data from ^{76}Ge (left-panel) and ^{136}Xe (right panel) as shown in Fig.6.9. Including the the contribution of light neutrinos with IH patterns of masses, the scattered plots are shown in the left-panel and the right panel of Fig.6.10. Including contributions of light neutrinos with QD pattern ($m_\nu = 0.23$ eV) of masses, the scattered plots for half life are shown in Fig.6.11.

The spread of points show the uncertainty in nuclear matrix elements, light neutrino Majorana phases and M_{S_2}, M_{S_3} . Since NH and IH predictions for half-life are

M (GeV)	$ \hat{M}_S $ (GeV)	M_S (GeV) [NH]
(20, 550, 2500)	(3.48, 169, 833)	(3.38, 156, 758)
(25, 550, 2500)	(5.43, 169, 833)	(5.20, 156, 758)
(30, 550, 2500)	(7.82, 169, 833)	(7.35, 156, 758)
(35, 550, 2500)	(10.6, 169, 833)	(9.81, 156, 758)
(40, 550, 2500)	(13.9, 169, 833)	(12.5, 156, 758)
(45, 550, 2500)	(17.6, 169, 833)	(15.5, 156, 758)
(50, 550, 2500)	(21.7, 169, 833)	(18.7, 156, 758)
(55, 550, 2500)	(26.3, 169, 833)	(22.1, 156, 758)
(60, 550, 2500)	(31.3, 169, 833)	(25.6, 156, 758)
(65, 550, 2500)	(36.7, 169, 833)	(29.3, 156, 758)
(70, 550, 2500)	(42.6, 169, 833)	(33.1, 156, 758)
(75, 550, 2500)	(48.9, 169, 833)	(37.0, 156, 758)

Table 6.3: Eigenvalues of sterile neutrino mass matrix for different allowed $N - S$ mixing matrix elements.

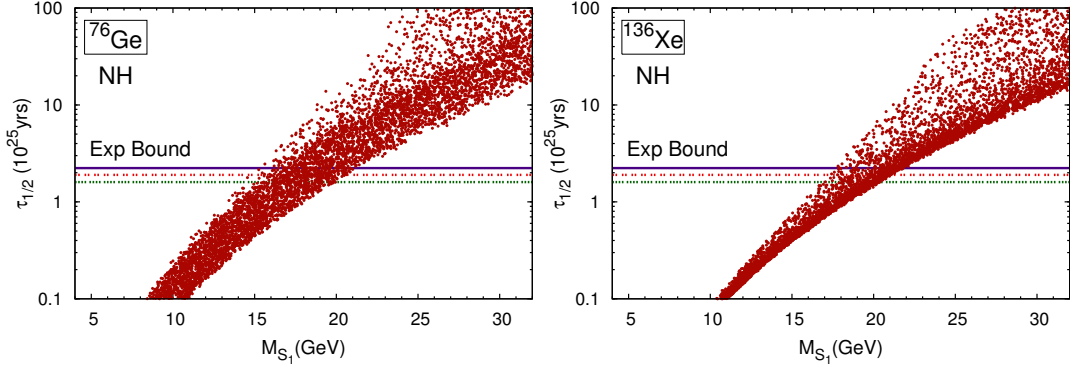


Figure 6.9: Scattered plot of half-life due to NH type light neutrino and heavy sterile neutrino exchange contributions in the $W_L - W_L$ channel as a function of lightest sterile mass. Left (right) panel corresponds to the nuclear matrix elements and phase space factor of ^{76}Ge (^{136}Xe). Details of various parameters is given in the text. The solid horizontal lines indicate the HM evidence.

very large compare to current experimental bound, the spread near the horizontal lines are mainly due to uncertainty in nuclear matrix element. While the spread in the dots is over a much wider region for $M_{S_1} > 15$ GeV in the QD case. This is because QD contribution themselves are of the order of experimental bound. This Majorana phases play major role in deciding the half-life of $0\nu 2\beta$ -decay. For certain phase there can be cancellation between the light neutrino and the sterile neutrino contributions, while for the same M_{S_1} but for different Majorana phase contribution can be constrictive. To analyse this aspect more vividly we have plotted the half-life as a function of M_{S_1} as shown in Fig. 6.12, which can be understood easily using

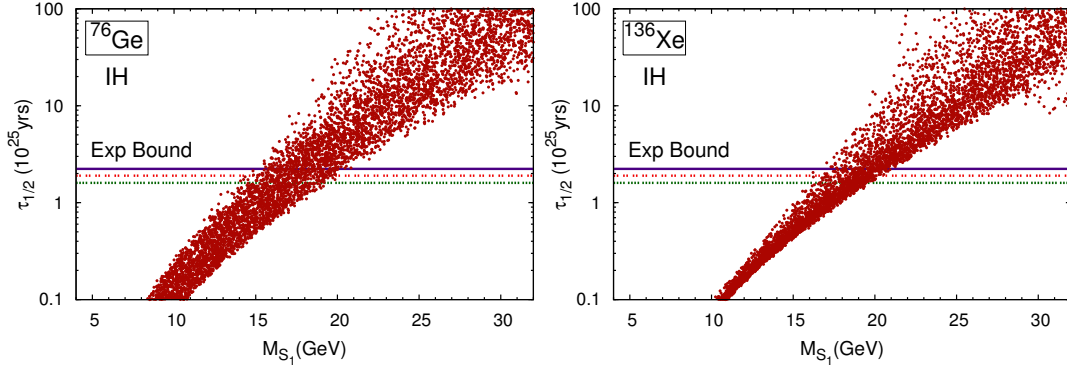


Figure 6.10: Same as Fig.6.9 but for inverted hierarchy of light neutrino masses.

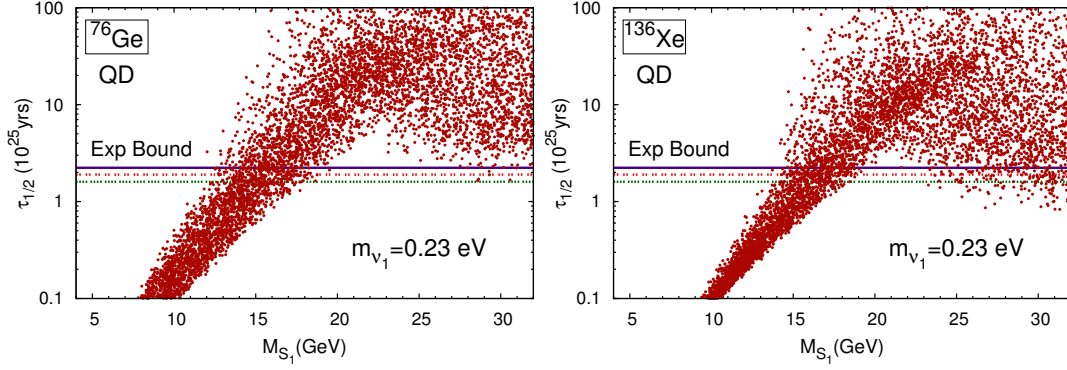


Figure 6.11: Same as Fig.6.9 and Fig.6.10 but for quasi-degenerate light neutrino masses with $m_\nu = 0.23$ eV.

eq. (6.43).

In Fig. 6.12 we note that for $M_{S_1} \sim 15.8$ GeV and zero Majorana masses the half-life diverges, while if the two Majorana phases are $\pi/2$ each the life time is close to experimental reach. On the other hand, if $M_{S_1} \simeq 25$ then for zero Majorana phases the half-life is close to experiment while for Majorana phases $\pi/2$ each the light and sterile contributions cancel, giving infinitely large half-life.

From the Fig.6.9, Fig.6.10, and Fig.6.11, it is clear that the ^{76}Ge data gives the following bounds on the lightest sterile neutrino mass,

$$\begin{aligned}
 M_{S_1} &\geq 15.5 \pm 3.5 \text{ GeV, QD,} \\
 &\geq 18.0 \pm 3.0 \text{ GeV, IH,} \\
 &\geq 18.5 \pm 3.0 \text{ GeV, NH.}
 \end{aligned} \tag{6.46}$$

whereas from the ^{136}Xe data, the bounds are

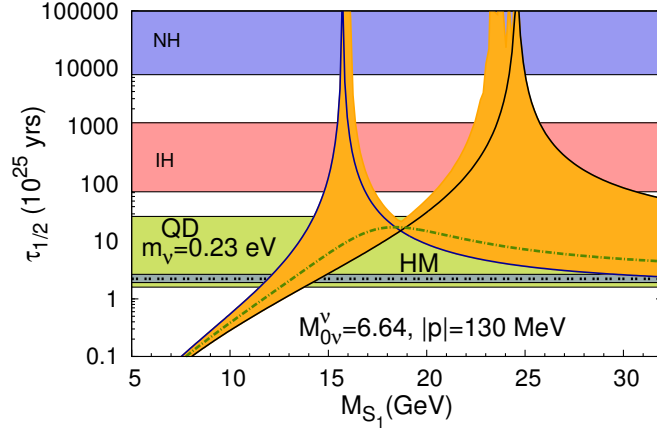


Figure 6.12: Predicted variation of half-life as a function of lightest sterile neutrino mass M_{S_1} . The blue, red and green bands have been generated taking the normal, inverted and quasi-degenerate patterns of light neutrino masses, respectively when all the Majorana phases are scanned and sterile neutrino contributions are switched off. The orange band is the combined contribution with fixed nuclear matrix element, $\mathcal{M}_{0\nu}^V = 6.64$ and $|p| = 130$ MeV.

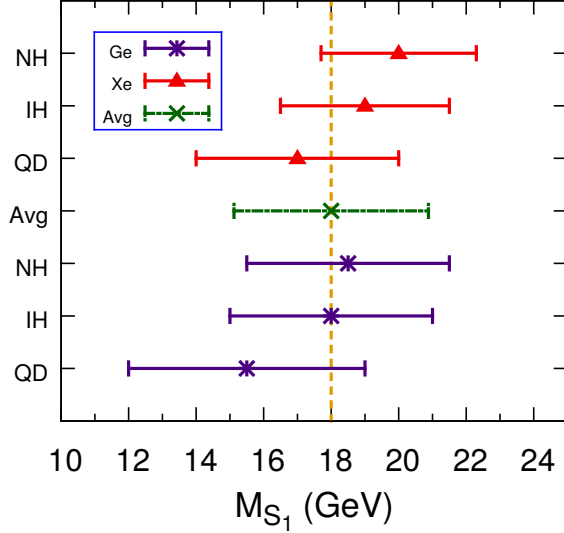


Figure 6.13: Mass bounds for the lightest sterile neutrino mass M_{S_1} obtained from scattered plots of half-life for different light-neutrino mass hierarchies and their comparison with experimental data for ^{76}Ge and ^{136}Xe isotopes cited in the text. The horizontal dashed-green line represents the average value $\overline{M}_{S_1} \geq 18.0 \pm 2.9$ GeV. The vertical dashed-red line passing through the average is to guide the eye.

$$\begin{aligned}
 M_{S_1} &\geq 17.0 \pm 3.0 \text{ GeV, QD,} \\
 &\geq 19.0 \pm 2.0 \text{ GeV, IH,} \\
 &\geq 20.0 \pm 2.3 \text{ GeV, NH.}
 \end{aligned} \tag{6.47}$$

For all QD cases used to obtain mass bounds, we have used the common mass of light neutrinos $m_\nu = 0.23$ eV. We find that the bounds obtained from effective mass plots and the half-life plots are in agreement as expected. These bounds are also depicted in Fig. 6.13.

6.6 Rectifying the large τ_p problem of low energy LR model using light bi-triplet mass

b_i	b_{ij}	b_i	b_{ij}
$\begin{pmatrix} 2 \\ 2 \\ 0 \end{pmatrix}$	$\begin{pmatrix} 56 & 48 & 0 \\ 48 & 58 & 0 \\ 0 & 0 & 0 \end{pmatrix}$	$\begin{pmatrix} 5 \\ 5 \\ 16/3 \end{pmatrix}$	$\begin{pmatrix} 65 & 45 & 240 \\ 45 & 65 & 240 \\ 48 & 48 & 896/3 \end{pmatrix}$

Table 6.4: The one and two loop beta coefficients for $(3, 3, 1)$ and $(2, 2, 15)$ scalar representation under the PS symmetry.

The large proton lifetime prediction of the model presented in Chapter 5 can be rectified by a simple extension of the model. We use bi-triplet scalar $(3, 3, 1) \subset 54_H$ and allow its mass from GUT scale to Pati-Salam symmetry breaking scale ($\sim 10^6$), similar to the procedure we followed in Sec. 4.2.2. Super-heavy bi-doublet $\zeta(2, 2, 15)$ is allowed to stay at D -preserving Pati-Salam symmetry breaking scale. One and two loop beta coefficients for the $(3, 3, 1)$ and $(2, 2, 15)$ scalars are listed in Tab. 6.4. The rest of the beta coefficients are same as give in Tab. B.2 [295].

The minimal content of the model discussed in Chapter 5 failed to give proton decay predictions. This deficiency of the model can be eradicated by introduction of a bi-triplet $(3, 3, 1)$ scalar at some lower energies. Introduction of such a scalar requires additional fine tuning since it doesn't follow the *extended survival hypothesis*. The bi-triplet at the energy scale $10^{7.1} - 10^{8.5}$ GeV brings down the unification scale close to the experimentally reachable region. The unification scale dependence on bi-triplet scalar mass. For $M_{(3,3,1)} = 10^{7.3}$ GeV gauge coupling unification is depicted in the left panel of Fig. 6.14. In the right panel of the same figure dependence of unification scale and proton lifetime on bi-triplet is exhibited. The light-blue and the green bands in the right figure correspond to the current limit and future reach of Hyper-K experiment, respectively. Exact numerical values of lifetime and unification scales vs bi-triplet masses are also given in Tab. 6.5. Recent excess observed in searches of W_R gauge boson at CMS [317] at 1.9 TeV to 2.4 TeV has prospects of being

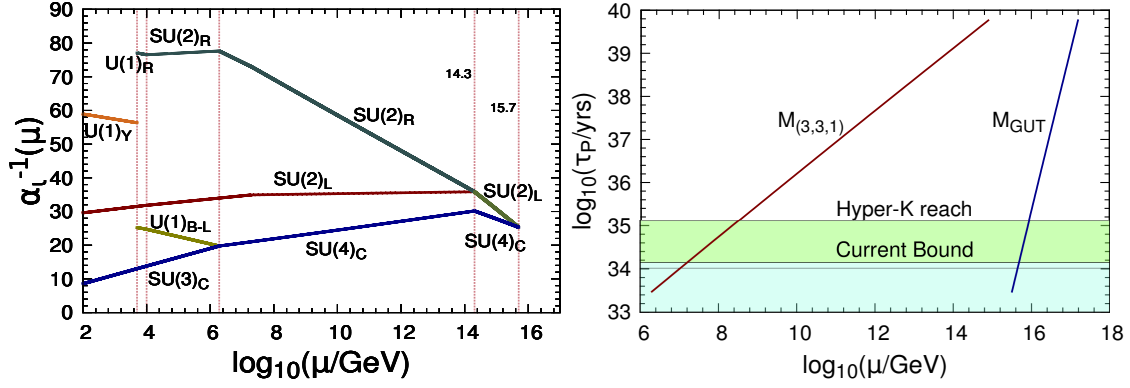


Figure 6.14: Left panel: Two loop gauge coupling unification for $M_{(3,3,1)} = 10^{7.3}$ GeV. The multiplet $\xi_{(2,2,15)}$ appears at Pati-Salam D -parity breaking scale. The Pati-Salam, left-right and G_{2113} symmetry breaking scales are at $M_C \sim 10^{6.28}$ GeV, $M_R^+ \sim 10$ TeV and $M_R^0 \sim 5$ TeV, respectively. Right panel: The bi-triplet mass dependence of proton life-time. Parameters are same as used for generating the Tab. 6.5.

$\log_{10} \frac{M_{(3,3,1)}}{\text{GeV}}$	$\log_{10} \frac{M_G}{\text{GeV}}$	α_G	A_{SR}	$\log_{10} \frac{\tau_P}{\text{Yrs}}$
7.0	15.6408	0.0391987	2.77194	33.996
7.2	15.6804	0.039409	2.78914	34.1444
7.5	15.7399	0.0397315	2.81533	34.3672
8.0	15.8389	0.0402809	2.85983	34.7377
8.5	15.9377	0.040849	2.90553	35.1069
9.0	16.0365	0.0414368	2.95254	35.4758
10	16.2338	0.0426775	3.05085	36.2109

Table 6.5: Bi-triplet mass dependence of the unification scale and proton life-time. The Pati-Salam, left-right and G_{2113} symmetry breaking scales are at $M_C \sim 10^{6.28}$ GeV, $M_R^+ \sim 10$ TeV and $M_R^0 \sim 5$ TeV, respectively. The Pati-Salam D -parity breaking scale remains at $M_P \sim 10^{14.3}$ GeV. The parameter $A_L \sim 1.25$ is used.

explained within the low energy LR model discussed in Chapter 5 [318]. Thus, in case of confirmation of W_R gauge boson at LHC, the model presented in Chapter 5, with an intermediate mass scale bi-triplet scalar, may emerge as most promising non-SUSY $SO(10)$ GUT model.

Conclusion

In this thesis we have investigated the prospects of experimentally reachable beyond standard model physics in TeV-scale inverse seesaw motivated non-SUSY $SO(10)$ grand unification framework. The TeV-scale inverse seesaw mechanism can be successfully implemented with a low-mass Z' gauge boson, which can be accessible at LHC and planned accelerators. The inverse seesaw scenario for explaining light neutrino masses and mixings may emerge from particular textures of 9×9 neutrino mass matrix. In the minimal scenario (Chapter 4) the light neutrinos are accompanied by three Majorana pairs of quasi-Dirac type heavy neutrinos. These pairs of BSM neutrinos have mass difference of keV scale. In the extended inverse seesaw texture (Chapters 5 and 6) three of the six BSM neutrinos acquire masses in type-I seesaw fashion and are called sterile neutrinos. The remaining three get the masses close to the largest mass scale present in the the seesaw structure. The scalar rep $16_H \subset SO(10)$ is the essential part of model giving inverse seesaw. The scalar $126_H \subset SO(10)$ is required to generate the extended inverse seesaw and to explain the fermion masses at GUT scale using only renormalizable term in Yukawa Lagrangian. The unification theories based on $SO(10)$ gauge group are particularly interesting because $SO(10)$ is smallest simple, anomaly free Lie group which unifies matter besides interactions. All the SM fermions of one generation plus a right handed neutrino can be accommodated in the irreducible 16-dim representation. Since $SO(10)$ is a larger group, its spontaneous symmetry breaking to SM may pass through various intermediate symmetries. Once intermediate symmetries are present in the theory, gauge couplings unify nicely without any requirement of supersymmetry.

In the Chapter 1 we motivated the need to study non-SUSY unification models with experimentally reachable BSM predictions. We also presented the schema of investigation, briefly. In Chapter 2 we recapitulated the SM and its ineptitude in

explaining various BSM phenomena. In Chapter 3 we motivated and briefly discussed the $SU(5)$ and $SO(10)$ GUT prototypes. We also briefly described the conventional seesaw mechanisms (type-I, II and III) which can explain small neutrino masses very naturally. In Chapter 4 we have investigated the prospects of inducing TeV-scale inverse seesaw mechanism for neutrino masses in a non-SUSY $SO(10)$ GUT model which passes through two intermediate symmetries (G_{2213} at $\sim 10^{11}$ GeV and G_{2113} at \sim TeV) to reach to SM. A $SO(10)$ singlet fermion (S) per generation is introduced to get TeV scale inverse seesaw. A TeV scale Z' boson acquires mass through spontaneous breaking of $U(1)_R \times U(1)_{B-L}$ gauge symmetries in to $U(1)_Y$ generated through the Higgs representation 16_H . The right-handed neutrino (N) and sterile (S) mixing matrix M is also generated through the VEV of RH doublet Higgs $[(1, -1/2, 1/2, 1) \subset (1, 2, 1/2, 1)]$ of LR model contained in 16_H . The left-right symmetry is restored at the intermediate energy scale.

The Dirac neutrino mass matrix M_D at seesaw scale (M_R^0) is the necessary input to estimate lepton number and lepton flavor violating contributions, non-unitarity effects as well as leptonic CP -violation. This matrix has been explicitly computed using the associated renormalization group equations in the presence of G_{2213} and G_{2113} intermediate gauge symmetries via bottom-up and top-down iterative approach, and by implementing the unification model constraint on the fermion masses at GUT scale. The matrix M is estimated using the current non-unitarity experimental constraint ($\eta_{\tau\tau}$). The predominant Dirac mass matrix together with TeV scale heavy neutrino masses give the branching ratio predictions only few orders less than the current bounds. The branching ratio $\text{Br}(\mu \rightarrow e\gamma)$ prediction for the non-degenerate right-handed neutrino masses (first and second generation acquiring ~ 50 GeV mass) are one order closer to experimental bounds, compared to predictions in degenerate scenario. In degenerate M_i scenario, branching ratios show at most a factor of three variations from the corresponding SUSY $SO(10)$ predictions. For the non-unitarity matrix element $\eta_{\mu\tau}$ an important model prediction is its enhanced phase $\delta_{\mu\tau}$ larger by two to four orders in non-degenerate case. This may play a dominant role in the experimental detection of the non-unitary CP -violation effects at neutrino factories.

Interestingly, the two-loop prediction on proton lifetime in the minimal model turns out to be $[\tau_p(p \rightarrow e^+\pi^0)]=2 \times 10^{34}$ yrs. which increases by a factor of 2 when GUT threshold effects are included. While providing a possibility of verification of the underlying GUT hypothesis, this offers another opportunity for testing the minimal model by ongoing search experiments. We have also identified this model to be the best among all involving single or two-step breaking of $SO(10)$ to the TeV

scale gauge symmetry G_{2113} , which is essential for low mass Z' , TeV scale seesaw and prominent non-unitarity effects.

We have presented one such model where G_{2113} intermediate symmetry is replaced by G_{2213D} . We also show that fast proton decay problem of such models can be evaded by simple extensions in the particle content. A color octet scalar, below the GUT scale, can be an easy choice. The proton lifetime bounds put the constraints on the masses of these multiplets. If the actual proton lifetime is very-very large, accelerator reachable color octet scalar is also permissible.

In the Chapter 5 we have investigated in detail the prospects of TeV scale left-right gauge theory originated from $SO(10)$ grand unified theory. Extended inverse seesaw mechanism for neutrino masses and mixings was implemented for predicting dominant contributions to $0\nu 2\beta$ decay. The model also predicts experimentally accessible lepton flavor violating decays, non-unitarity and CP -violating effects, which is of the same order as predicted in the Chapter 4. The $n-\bar{n}$ oscillation and rare kaon decays are the other beyond standard model predictions due to Pati-Salam symmetry (G_{224}) restoration around 10^6 GeV. We have embedded the LR model successfully in non-SUSY Pati-Salam symmetry and $SO(10)$ GUT, predicting low mass W_R^\pm and Z' bosons near 1 – 10 TeV scale accessible to LHC and future accelerators. The unification of gauge couplings requires parity restoration under Pati-Salam symmetry near 10^{14} GeV.

The Dirac neutrino mass matrix M_D and heavy-sterile mass matrix M estimations follow the procedure discussed in Chapter 4. The induced VEV of the Pati-Salam sub-multiplet $\xi(2, 2, 15)$ of $126_H \subset SO(10)$ needed to fit the fermion masses at the GUT scale. It is found to emerge naturally within the specified $SO(10)$ structure while safeguarding the precision gauge coupling unification, and values of other mass scales. The W_R^\pm gauge bosons acquire masses at the $SU(2)_R$ to $U(1)_R$ breaking scale via a RH triplet $(1, 3, 0, 1) \subset 210_H$. The Z' gauge boson and RH Majorana neutrinos acquire masses due to spontaneous breaking of $U(1)_R \times U(1)_{B-L}$ symmetry to $U(1)_Y$ via the RH Higgs triplet $[(1, 1, -1, 1) \subset (1, 3, -1, 1)]$ of LR model contained in $\overline{126}_H$. The fermion mass fit in the model gives almost a diagonal structure of RH Majorana neutrino mass matrix M_N with specific eigenvalues accessible to accelerator searches. Even though M_N is of TeV scale and M_D is naturally dominant, the would-be large contribution to neutrino masses due to type-I seesaw cancels out. The type-II seesaw contribution is damped out because of large parity violating scale and the TeV scale $B-L$ breaking. Thus, the light left-handed neutrino masses and mixings adequately acquire the gauged inverse seesaw formula.

The low mass W_R^\pm and Z' bosons, $M_D \sim \mathcal{O}(m_{\text{up-quark}})$, and dominant contributions to $0\nu 2\beta$ decay are in concordance with the neutrino oscillation data for explaining tiny masses of light neutrinos. Due to presence of M_N in the neutrino mass matrix, the pseudo-Dirac nature of heavy neutrinos disappears. The type-I seesaw structure emerges for sterile neutrinos $M_S \sim \mu_S - MM_N^{-1}M^T$, and the heavy neutrinos get mass $\sim M_N$. The most dominant contributions to the $0\nu 2\beta$ decay comes from the W_L^- - W_L^- mediated channel through the light sterile neutrino exchange. The effective mass parameter contribution from this channel is $m_{\text{sterile}}^{ee} \propto M_N/M^4$. Thus, this contribution is extremely sensitive to N - S mixing term and hence to sterile neutrino masses. The sub-leading contributions, as in the W_L^- - W_R^- mediated channel due to the exchanges of light and heavy RH neutrinos, are found to be much smaller compared to the leading contributions. In addition to the large contribution to the $0\nu 2\beta$ rate, the predictions for LFV, non-unitarity and CP -violating effects are of the same order as predicted in the minimal model, and are accessible to ongoing searches. The details can be followed from Chapter 4. The prediction of W_R^\pm and Z' bosons in this model is further accompanied by observable n - \bar{n} oscillation with mixing time $\tau_{n\bar{n}} \simeq (10^8 - 10^{11})$ sec as well as lepto-quark gauge boson mediated rare kaon decay with $\text{Br}(K_L \rightarrow \mu\bar{e}) \simeq (10^{-9} - 10^{-11})$, accessible to ongoing experiments.

In the Chapter 6 we have shown that even if only the Z' boson is detected at LHC, a number of the predictions from the study in Chapter 5 are still applicable. We have a non-SUSY $SO(10)$ grand unification model which resembles the model in Chapter 5. But, the W_R^\pm gauge boson now reside at the Pati-Salam breaking scale, i.e., very far from the LHC reachable scale. Due to change in breaking scheme, scalars content of the model at various breaking scales also gets changed. This leads to change in the scale of unification.

Implementing the renormalization group analysis, we have derived the new lower bound on the lepto-quark gauge boson mass mediating rare kaon decays to be $M_{lepto} \geq (1.53 \pm 0.06) \times 10^6$ GeV which is easily accommodated in the GUT scenario. The unification constraint on gauge couplings of the $SO(10)$ model is found to permit di-quark Higgs scalar masses in the range 10 – 100 TeV. This leads to observable n - \bar{n} oscillation while satisfying flavor physics constraints [319] saturating the lepto-quark gauge boson mass bound. This suggests that the model is also simultaneously consistent with observable rare kaon decay by ongoing search experiments.

The dependence of $0\nu 2\beta$ life-time on lightest sterile neutrino mass is explored in various scatter plots. In the NH and IH scenarios of light neutrino masses, for the allowed range of unknown parameters in the model, predictions to $0\nu 2\beta$ life-

time close to current experimental bound give the lightest sterile neutrino mass $m_{S_1} \geq 14 \pm 4 \text{ GeV}$. In the QD case light neutrino contributions to $0\nu 2\beta$ effective mass are in competition with sterile contributions. Since the two contribution have opposite phases, sterile contributions may cancel with light neutrino contribution of some parameter space leading to infinitely large $0\nu 2\beta$ life-time. These observations are also present in the model discussed in Chapter 5.

The predicted proton-lifetime in the minimal structure of the model is found to be $\tau_p(p \rightarrow e^+\pi^0) \simeq 5.05 \times 10^{35 \pm 1.0 \pm 0.34} \text{ yrs}$ where the first (second) uncertainty is due to GUT-threshold effects (experimental errors). This lifetime is accessible to ongoing and planned experiments. We have noted significant reduction of the predicted lifetime, bringing the central value much closer to the current Super-K limit with $\tau_p(p \rightarrow e^+\pi^0) = 1.1 \times 10^{34} \text{ yrs} - 5.05 \times 10^{35} \text{ yrs}$ when the effect of a lighter bi-triplet Higgs contained in the representation $54_H \subset SO(10)$ is included. Thus, even though the model does not have low-mass RH W_R^\pm bosons in the accessible range of LHC, it is associated with interesting signatures on lepton flavor, lepton number and baryon number violations and rare kaon decays. The predicted values of these phenomena are in concordance with the predictions in the previous chapters.

Compared to the recent interesting proposal of refs. [320–322], although successful generation of baryon asymmetry of the universe has not been implemented so far in this model, we have one extra gauge boson accessible to LHC. Likewise, in our model the lepto-quark gauge boson mediated $K_L \rightarrow \mu\bar{e}$ is also accessible to ongoing search experiments. However, the new $B - L$ violating proton decay is predicted to be accessible in refs. [320–322], which in our case is $B - L$ conserving proton decay $p \rightarrow e^+\pi^0$. The type-I seesaw mechanism associated with high $B - L$ breaking scale is generally inaccessible to direct experimental tests, in our case the TeV-scale gauged inverse seesaw is directly verifiable. The predicted values of the RH neutrino masses are also accessible for verification at LHC.

APPENDIX **A**

Few remarks on $SU(n)$, and $SO(10)$ Algebra

A.1 Anomalies

It happens sometimes that a symmetry of Lagrangian gets broken by quantum effects, ie the symmetry of Lagrangian is not a symmetry of quantized theory. Anomalies appear in those symmetries involving both axial and vector currents, and reflect the impossibility of regularizing the quantum theory (the divergent loop) in a way which preserves symmetry. The grand unifications gauge groups, being non-abelian lie groups, are likely to meet triangular anomalies. We either choose a gauge group which is either anomaly free or we fix it by cancelling the anomaly as suggested by [323–325] where we find that all $SO(n)$ groups with $n \neq 6$ are anomaly free and all the $SU(n)$ groups with $n \geq 3$ are anomalous. For an example in $SU(5)$ GUTs the representation space chosen for cancelling anomaly are $\bar{5}$ and 10. While considering extension of such $SU(n)$ theories the cancellation of anomaly has to be taken care of. Here we list strength of anomaly for few representations of general $SU(n)$ and $SU(4)$ being isomorphic to $SO(6)$ it applies there as well.

A.1.1 Adler Anomalies for a $SU(n)$ representation

As described above all the $SU(n)$ groups with $n \geq 3$ are anomalous groups, we need to study the order of anomaly of the representations in general. Adler anomalies for left handed fermion representations of $SU(n)$ are as follows

- For totally antisymmetric left handed fermionic representation with m anti-symmetric indices, the anomaly is

$$A_a = \frac{(n-3)!(n-2m)}{(n-m-1)!(m-1)!} \quad (\text{A.1})$$

Young Tableaux	Dimension	Anomaly
\square	n	1
$\square \square$	$n(n+1)/2$	$n+4$
$\square \square \square$	$n(n+1)(n+2)/3!$	$(n+3)(n+6)/2$
$\begin{array}{c} \square \\ \square \end{array}$	$n(n-1)/2$	$n-4$
$\begin{array}{c} \square \\ \square \\ \square \end{array}$	$n(n-1)(n-2)/3!$	$(n-3)(n-6)/2$
$\begin{array}{cc} \square & \square \\ \square & \end{array}$	$(n+1)n(n-1)/3$	$(n-3)(n+3)$
$n-1 \left\{ \begin{array}{ccc} \square & \square & \square \\ \vdots & & \\ \square & & \end{array} \right.$	(n^2-1) Adj. rep.	0

Table A.1: Adler anomalies for few simple representations in $SU(n)$ gauge theories. All $SO(n)$, $n \neq 6$, theories are anomaly free. Anomalies for right-handed fermion representations and corresponding complex conjugate representation will change the sign.

- For totally symmetric left handed fermionic representation with m symmetric indices, the anomaly is

$$A_s = \frac{(n+m)!(n+2m)}{(n+2)!(m-1)!} \quad (\text{A.2})$$

For the two representations R_1 and R_2 , $A(R_1 + R_2) = A(R_1) + A(R_2)$ and $A(R_1 \otimes R_2) = D(R_1)A(R_2) + D(R_2)A(R_1)$ following the additive rule. Using these relations we can calculate anomaly due to a mixed representation. To complete this subsection we list few representations in Young tableaux form write their dimension and list anomaly in $SU(n)$ Lie group.

A.2 Quadratic Casimir and Dynkin index invariants in $SU(n)$

In a group $G = SU(n)$ group no of generators is $n^2 - 1$. We denote generators of this group in a specific representation R by $M_a(R)$. The quadratic Casimir invariance is defined as

$$\delta_{ij}C_2(R) = \sum_a \sum_k (M_a(R))_{ik}(M_a(R))_{kj} \quad (\text{A.3})$$

where $a = 1, 2, \dots, d_G$; $i, j, k = 1, 2, \dots, d_R$ and $d_G (= n^2 - 1)$, d_R are the dimensions of group G and representation R in the group, respectively. The Dynkin index invariance is defined as

$$\delta_{ab}T(R) = \text{Tr}[M_a(R)M_b(R)] \quad (\text{A.4})$$

Obviously $d_R C_2(R) = d_G T(R)$. The properties of Dynkin index invariance are

$$T(R^*) = T(R) \quad (\text{A.5})$$

$$T(R_1 + R_2) = T(R_1) + T(R_2) \quad (\text{A.6})$$

$$T(R_1 \otimes R_2) = d_{R_1}T(R_2) + d_{R_2}T(R_1) \quad (\text{A.7})$$

$$T(\square) = 1/2 \quad (\text{A.8})$$

$$T\left(\left\{\begin{array}{c} \square \\ \vdots \\ \square \end{array}\right\}_{m\text{-boxes}}\right) = \frac{1}{2} \frac{(n-2)!}{(m-1)!(n-m-1)!} \quad (\text{A.9})$$

$$T\left(\underbrace{\left[\begin{array}{ccc} \square & \dots & \square \end{array}\right]}_{m\text{-boxes}}\right) = \frac{1}{2} \frac{(n+m)!}{(n+1)!(m-1)!} \quad (\text{A.10})$$

Using the above properties we can calculate $C_2(R)$, $T(R)$ for any representation R . $C_2(G) = n$ is the quadratic Casimir for the adjoint representation. For a representation of $U(1)_X$ we have $C_2(G) = 0$, and $C_2(R) = T(R) = X^2$, where X is the appropriately normalized charge of the symmetry.

The best way to get the Dynkin indexes of a group $SU(n)$ is to first evaluate them for $SU(2)$ and then achieve rest iteratively. Like, the adjoint representation of $SU(2)$ can be easily estimated, $T(\text{Adj})_{SU(2)} = 2$. Now, since adjoint of $SU(n+1)$ can be decomposed into $SU(n)$ representations as as

$$\text{Adj}(n+1) = \begin{pmatrix} \text{Adj}(n) & n \\ \bar{n} & 1. \end{pmatrix} \quad (\text{A.11})$$

Therefore the Dynkin indexes are related as

$$\begin{aligned} T[Adj(n+1)] &= T[Adj(n)] + T[n] + T[\bar{n}] + T[1] \\ &= T[Adj(n)] + 1 \equiv n + 1. \end{aligned} \quad (\text{A.12})$$

Similarly for two index (anti)-symmetric representations we have

$$T[(n+1) \times (n+1)]_{(A)S} = T[n \times n]_{(A)S} + T[n]. \quad (\text{A.13})$$

We remember that two index antisymmetric and symmetric representations in $SU(2)$ are singlet and adjoint representations also and their Dynkin index $T(AS) = 0$ and $T(S) = 2$, respectively. Therefore

$$T[n \times n]_{(A)S} = (0)2 + (n-2)/2. \quad (\text{A.14})$$

A.3 Lorentz group

A point in four dimensional space-time manifold of Minkowski space is denoted by $x^\mu = (t, \vec{x})$, where the laws of physics are invariant under Lorentz group. Vectorial transformation in this group are denoted as $x'^\mu = \Lambda^\mu{}_\nu x^\nu$, leading to the quadratic form $x^2 = x^\mu x_\mu = \eta_{\mu\nu} x^\mu x^\nu$ invariant. Hence Lorentz group is a non-trivial real orthogonal group of 4×4 real orthogonal matrices obeying

$$\eta_{\mu\nu} \Lambda^\mu{}_\rho \Lambda^\nu{}_\sigma = \eta_{\rho\sigma} \equiv \Lambda^T \eta \Lambda = \eta \quad (\text{A.15})$$

with $\det(\Lambda) = +1$. The invariance of Lorentz symmetry can also be written as

$$x_\alpha x^\alpha = (\gamma_\mu x^\mu)(\gamma_\nu x^\nu) \quad (\text{A.16})$$

This requires that $\{\gamma_\mu, \gamma_\nu\} = 2\eta_{\mu\nu}$. This γ_μ defines a rank four Clifford algebra. It's obvious that $\gamma_0^2 = 1_4$ and $\gamma_i^2 = -1_4$. And $\gamma^\mu = \Lambda^\mu{}_\nu \gamma^\nu$ and $\gamma_\mu = \eta_{\mu\nu} \gamma^\nu$, $\text{tr}(\gamma^\mu) = 0$. First and second condition on γ_μ^2 requires the hermiticity condition as $\gamma_0 = \gamma_0^\dagger$ and $\gamma_i = -\gamma_i^\dagger$. Hence eigen values are either ± 1 or $\pm i$ and they occur in pair. We require the dimension of these matrices to be at least $2^2 \times 2^2$ as there are only three such γ matrices in 2×2 dimension i.e. Pauli matrices themselves, and higher dimensional matrices will be reducible. Hence we find that the dimension of fundamental representation is same as spinor representation, but their generators are

quite different. Out of different possible representation we write them in the form

$$\gamma_0 = \sigma_1 \otimes 1_2, \quad \gamma_k = i\sigma_2 \otimes \sigma_k \quad (\text{A.17})$$

known as Weyl representation. The Weyl basis has simple chiral projections. One more γ matrix we can define is the product of all four gamma matrices.

$$\gamma^5 = i\gamma^0\gamma^1\gamma^2\gamma^3 \quad (\text{A.18})$$

and the chiral projections are read as

$$\psi_{L/R} = \frac{1}{2} (1 \pm \gamma^5) \psi \quad (\text{A.19})$$

$$\gamma^0 = \begin{pmatrix} 0 & 1_2 \\ 1_2 & 0 \end{pmatrix}, \quad \gamma^k = \begin{pmatrix} 0 & \sigma^k \\ \sigma^k & 0 \end{pmatrix}, \quad \gamma^5 = \begin{pmatrix} 1_2 & 0 \\ 0 & -1_2 \end{pmatrix}, \quad \psi = \begin{pmatrix} \psi_L \\ \psi_R \end{pmatrix} \quad (\text{A.20})$$

where ψ_L and ψ_R are the left-handed and right-handed two-component Weyl spinors.

$$\gamma'^{\mu} = \Lambda^{\mu}_{\nu} \gamma^{\nu} \quad (\text{A.21})$$

generating the Clifford algebra for γ' matrices. Transformation of a 2^2 dimensional spinor under the above transformation of γ matrices is

$$\psi'(x') = S(\Lambda)\psi(x) \quad (\text{A.22})$$

γ^{μ} 's are $2^2 \times 2^2$ matrix forms of spinor representation hence transform like

$$\gamma'_{\mu} = S(\Lambda)\gamma_{\mu}S^{-1}(\Lambda) \quad (\text{A.23})$$

we construct the explicit form of the transformation matrix, $S(\Lambda) = e^{-\frac{i}{4}a_{\alpha\beta}\Sigma_{\alpha\beta}}$. Simplification of infinitesimal rotation gives

$$\Sigma_{\mu\nu} = \frac{i}{2} [\gamma_{\mu}, \gamma_{\nu}] \quad (\text{A.24})$$

The generators $\Sigma_{0,2}$ and $\Sigma_{1,3}$ can be simultaneously diagonalised therefore we define chirality operator as

$$\gamma_5 = i\Sigma_{02}\Sigma_{13} = i\gamma^0\gamma^1\gamma^2\gamma^3. \quad (\text{A.25})$$

One can easily verify the following properties of chirality operator

$$\gamma_5^\dagger = \gamma_5, \quad \text{tr}(\gamma_5) = 0, \quad \{\gamma_5, \gamma_\mu\} = 0, \quad \gamma_5^2 = 0, \quad [\gamma_5, \Sigma_{\mu\nu}] = 0. \quad (\text{A.26})$$

Thus a 4-dimensional spinor representation is reducible into two 2-dimensional representations. The generators of the reduced representations are $\frac{1}{2}(1 \pm \gamma_5)\Sigma_{\mu\nu}$. Charge conjugation operators can be found to be product $\gamma_0\gamma_2$ or $\gamma_1\gamma_3$.

A.3.1 Lorentz scalar and vector constructs

If ψ is a Dirac spinor

Lorentz Scalars

$$\begin{aligned} \bar{\psi}\psi &= \bar{\psi}^C\psi^C = \bar{\psi}_L\psi_R + \bar{\psi}_R\psi_L \\ \bar{\psi}^C\psi &= \psi_L^T C\psi_L + \psi_R^T C\psi_R \\ \bar{\psi}\psi^C &= \bar{\psi}_L C\bar{\psi}_L^T + \bar{\psi}_R C\bar{\psi}_R^T \end{aligned} \quad (\text{A.27})$$

Lorentz Vectors

$$\begin{aligned} \bar{\psi}\gamma_\mu\psi &= \bar{\psi}_L\gamma_\mu\psi_L + \bar{\psi}_R\gamma_\mu\psi_R \\ \bar{\psi}^C\gamma_\mu\psi &= \psi_L^T C\gamma_\mu C\bar{\psi}_L^T + \psi_R^T C\gamma_\mu C\bar{\psi}_R^T \\ \bar{\psi}^C\gamma_\mu\psi &= \psi_L^T C\gamma_\mu\psi_R + \psi_R^T C\gamma_\mu\psi_L \\ \bar{\psi}\gamma_\mu\psi^C &= \bar{\psi}_L\gamma_\mu C\bar{\psi}_R^T + \bar{\psi}_R\gamma_\mu C\bar{\psi}_L^T \end{aligned} \quad (\text{A.28})$$

where

$$\bar{\psi} = \psi^\dagger\gamma_0, \quad \psi^C = C\bar{\psi}^T, \quad \psi = \psi_L + \psi_R \quad (\text{A.29})$$

A.4 $SO(2n)$ Algebra

The special orthogonal group, $SO(2n)$ is a group of $2n \times 2n$ real orthogonal matrices, O obeying

$$O^T O = O O^T = \mathbf{1}, \quad \det(O) = +1 \quad (\text{A.30})$$

A real $2n$ -dimensional column vector x transforms as

$$x'_i = O_{ij}x_j; \quad i, j = 1, 2, \dots, 2n. \quad (\text{A.31})$$

such that

$$x'^T x' = (Ox)^T Ox = x^T O^T Ox = x^T x. \quad (\text{A.32})$$

The transformation matrix, O can be parametrized as

$$O(a) = \exp\left(\frac{i}{2}a_{ij}L_{ij}\right), \quad \text{such that } a_{ij} = -a_{ji} \quad (\text{A.33})$$

The real numbers a_{ij} are the rotation parameters and under the local symmetry transformation depend on space-time coordinate, and L_{ij} are $2n \times 2n$ linearly independent matrices and the generators of the group. Putting eq. (A.33) in the eq. (A.30) and eq. (A.31) we get

$$L_{ij}^T = -L_{ji}. \quad \text{and } (L_{ij})_{kl} = -i(\delta_{ik}\delta_{jl} - \delta_{il}\delta_{jk}); \quad 1 \leq k < l \leq 2n. \quad (\text{A.34})$$

which gives $\text{tr}(L_{ij}) = 0$ and the matrix is antisymmetric therefore it's easy to write the explicit form of generators. The generators L_{ij} have *zeros* everywhere except at the positions (i, j) and (j, i) , which are occupied by $-i$ and $+i$ respectively, and additionally we have $L_{ij} = -L_{ji} = L_{ij}^\dagger$. Therefore, the algebra of the real representation can be calculated using the definition of generators, eq. (A.34) as

$$[L_{ij}, L_{kl}] = -i(\delta_{jk}L_{il} + \delta_{il}L_{jk} - \delta_{ik}L_{jl} - \delta_{jl}L_{ik}) \quad (\text{A.35})$$

The higher rank tensors can be defined which transform as

$$A'_{i_1 i_2 \dots i_p} = O_{i_1 j_1} O_{i_2 j_2} \dots O_{i_p j_p} A_{j_1 j_2 \dots j_p} \quad (\text{A.36})$$

The invariants of the group are second rank δ_{ij} and $2n^{\text{th}}$ rank Levi-Civita tensor. The later can be proved using the definition of determinant, ie.

$$\det(O) = \frac{1}{2n!} \epsilon_{i_1 i_2 \dots i_{2n}} \epsilon_{j_1 j_2 \dots j_{2n}} O_{i_1 i_2 \dots i_{2n}, j_1 j_2 \dots j_{2n}} \quad (\text{A.37})$$

A higher rank tensor is reducible if it's contraction with Kroncker delta or Levi-Civita tensor gives a tensor of lower rank. The dimensionality of second rank anti-symmetric tensor and second rank symmetric traceless tensor are $n(2n-1)$ and $[n(2n+1)-1]$. Their transformation follow the definition of eq. (A.36) for two indices. The dimension of second rank antisymmetric tensor, which is also the adjoint representation of the group, is same as the number of generators. Therefore, the transformation of Lorentz-vectors under $SO(2n)$ adjoint representation follow the similar properties

with additional Lorentz index on gauge boson.

A.4.1 $SO(2n)$ spinor representation

Similar to the Lorentz algebra in Minkowski space, the invariant quadratic form of $SO(2n)$ symmetry is given by eq. (A.32). The quadratic form as square of linear form can be written as

$$x_1^2 + x_2^2 + \cdots + x_{2n}^2 = (x_1\Gamma_1 + x_2\Gamma_2 \cdots + x_{2n}\Gamma_{2n})^2 \quad (\text{A.38})$$

if

$$\{\Gamma_i, \Gamma_j\} = 2\delta_{ij}\mathbf{1}; \quad i, j = 1, 2, \dots, 2n \quad (\text{A.39})$$

This $2n$ rank Clifford algebra gives

$$\Gamma_i^2 = \mathbf{1} \quad (\text{no sum}), \quad \text{and} \quad \text{tr}(\Gamma_i) = 0 \quad (\text{A.40})$$

We can prove by explicit iterative construction that “there exist $2n$ Hermitian matrices Γ_i , $i = 1, 2, \dots, 2n$, which are $2^n \times 2^n$ and satisfy the $2n$ rank Clifford algebra” [326]. Thus from eq. (A.40) we see that their eigenvalues are $+1$ and -1 which come in pair.

The invariance of linear term, $\sum_i x_i \Gamma_i$ demands the transformation of Γ as

$$\Gamma_i \rightarrow \Gamma'_i = O_{ij}\Gamma_j. \quad (\text{A.41})$$

The transformation of $SO(2n)$ spinor is written as

$$\Psi(x) \rightarrow \Psi'(x') = S(O)\Psi(x) \quad \text{and} \quad \Gamma'_i = S(O)\Gamma_i S^{-1}(O) = O_{ij}\Gamma_j. \quad (\text{A.42})$$

where Ψ is a 2^n dimensional spinor. The Γ 's follow the same Clifford algebra. The explicit form of the transformation matrix

$$S(O) = \exp\left(\frac{i}{2}a_{ij}\Sigma_{ij}\right). \quad (\text{A.43})$$

Here Σ_{ij} are the generators in the spinorial basis. Putting $S(O)$ in eq. (A.42) and using $O_{ij} = \delta_{ij} + a_{ij}$ we get

$$\Sigma_{ij} = \frac{i}{4}[\Gamma_i, \Gamma_j] \quad (\text{A.44})$$

These antisymmetric ($\Sigma_{ij} = -\Sigma_{ji}$) and Hermitian ($\Sigma_{ij} = \Sigma_{ij}^\dagger$) generators satisfy the

$SO(2n)$ Lie algebra

$$[\Sigma_{ij}, \Sigma_{kl}] = -i(\delta_{ik}\Sigma_{jl} - \delta_{il}\Sigma_{jk} - \delta_{jk}\Sigma_{il} + \delta_{jl}\Sigma_{ik}), \quad (\text{A.45})$$

which is the usual commutation relation of $SO(2n)$ generators in real representation, eq. (A.35). The cartan subalgebra consist of n generators, say

$$\text{Cartan subalgebra} = [\Sigma_{12}, \Sigma_{34}, \dots, \Sigma_{2n-12n}] \quad (\text{A.46})$$

We can write, analogous to γ_5 in Dirac theory, the group chirality operator using the Cartan subalgebra

$$\Gamma_{\text{P}} \equiv \prod_{i=1}^n \Sigma_{2i-12i} = (-1)^n \Gamma_1 \Gamma_2 \dots \Gamma_{2n} \quad (\text{A.47})$$

with the properties

$$\Gamma_{\text{P}}^2 = \mathbf{1}, \quad \Gamma_{\text{P}} = \Gamma_{\text{P}}^\dagger, \quad \text{tr}(\Gamma_{\text{P}}) = 0, \quad [\Gamma_{\text{P}}, \Sigma_{ij}] = 0, \quad \{\Gamma_{\text{P}}, \Gamma_i\} = 0. \quad (\text{A.48})$$

Thus since $\Gamma_{\text{P}} \neq \text{const.}\mathbf{1}$ and $[\Gamma_{\text{P}}, S(O)] = 0$, Schurs lemma suggests that 2^n representation is reducible, and $\Gamma_{\text{P}}^2 = \mathbf{1}$ and $\text{tr}(\Gamma_{\text{P}}) = 0$ suggest that this representation can reduce as $2^n = 2^{n-1} \oplus 2^{n-1}$ with opposite eigenvalues. Using the projection operator

$$\Gamma_{\pm} \equiv \frac{1 \pm \Gamma_{\text{P}}}{2} \quad (\text{A.49})$$

we get

$$\Psi_{\pm} = \Gamma_{\pm} \Psi. \quad (\text{A.50})$$

Demanding the condition

$$\Psi^T B \Psi = \text{invariance} \Leftrightarrow \Psi^C = B \Psi^* \quad (\text{A.51})$$

we get $\Sigma^T B + B \Sigma = 0$ leading to two possible solutions

$$B = \prod_i^n \Gamma_{2i} \quad \text{and} \quad B = \prod_i^n \Gamma_{2i-1}. \quad (\text{A.52})$$

A.4.2 Bilinears and invariant constructs

From $\Psi'(x') = S(O)\Psi(x)$ and unitarity of $S(O)$, $S^{-1}(O) = S^\dagger(O)$ we immediately get bilinear structure

$$\Psi^\dagger\Psi \quad \text{Scalar} \quad (\text{A.53})$$

$$\Psi^\dagger\Gamma_i\Psi \quad \text{Vector} \quad (\text{A.54})$$

$$\Psi^\dagger\Gamma_i\Gamma_j\Psi \quad 2^{\text{nd}} \text{ rank tensor} \quad (\text{A.55})$$

$$\Psi^\dagger\Gamma_{i_1}\Gamma_{i_2}\dots\Gamma_{i_r}\Psi \quad r^{\text{th}} \text{ rank tensor} \quad (\text{A.56})$$

Where $r \leq n$. An antisymmetric combinations of these bilinears can be extracted out by choosing the antisymmetric combinations of Γ matrices, $\Gamma_{[i_1}\Gamma_{i_2}\dots\Gamma_{i_r]}$. These bilinears can be decomposed in terms of irreducible representations using the projection operator Γ_\pm such that $\Psi = \Psi_+ + \Psi_-$. The surviving odd and even rank antisymmetric tensors would be

$$\Psi_\pm^\dagger\Gamma_{[i_1}\Gamma_{i_2}\dots\Gamma_{i_r]}\Psi_\mp; \quad r - \text{odd} \quad (\text{A.57})$$

$$\Psi_\pm^\dagger\Gamma_{[i_1}\Gamma_{i_2}\dots\Gamma_{i_r]}\Psi_\pm; \quad r - \text{even}. \quad (\text{A.58})$$

For $r = n$ they will form complex and real self dual and antiself dual. We assign left-handed and right-handed CP -conjugate chirality to Ψ_+ and Ψ_- respectively. To incorporate the Lorentz symmetry we insert γ^0 and $\gamma^0\gamma^\mu$ to make them Lorentz scalar and vectors respectively. Thus the scalar and vector couplings of these bispinors look like

$$\begin{aligned} \mathcal{K}_{ab} \bar{\Psi}_{\pm a}\Gamma_{[i_1}\Gamma_{i_2}\dots\Gamma_{i_r]}\Psi_{\mp b}\Phi_{i_1i_2\dots i_r}^{(\text{asym})}; \quad r - \text{odd} \\ \mathcal{K}'_{ab} \bar{\Psi}_{\pm a}\gamma^\mu\Gamma_{[i_1}\Gamma_{i_2}\dots\Gamma_{i_r]}\Psi_{\pm b}V_{\mu i_1i_2\dots i_r}^{(\text{asym})}; \quad r - \text{even}, \end{aligned} \quad (\text{A.59})$$

respectively. Here a, b are generation indices, μ is Lorentz index, $\mathcal{K}, \mathcal{K}'$ are coupling constants, and Φ, V are Lorentz scalar and vectors of $SO(2n)$ antisymmetric (asym) tensors of rank r . The symmetries of $\mathcal{K}, \mathcal{K}'$ are decided by the properties of γ and Γ matrices.

The demand for invariance of term constructed by Ψ^T and Ψ in eq. (A.51) can be trivially implemented for writing bilinears using Ψ^T and Ψ . Now vector and scalar

couplings are

$$\begin{aligned}
\mathcal{K}_{ab} & \Psi^T_{\pm a} C B^T \Gamma_{[i_1 \Gamma_{i_2} \dots \Gamma_{i_r}]} \Psi_{\pm b} \Phi_{i_1 i_2 \dots i_r}^{(\text{asym})} ; & r - \text{even} \\
\mathcal{K}'_{ab} & \Psi^T_{\pm a} C \gamma^\mu B^T \Gamma_{[i_1 \Gamma_{i_2} \dots \Gamma_{i_r}]} \Psi_{\mp b} V_{\mu i_1 i_2 \dots i_r}^{(\text{asym})} ; & r - \text{odd},
\end{aligned} \tag{A.60}$$

for n -even, and for n -odd ($r - \text{even}$) \leftrightarrow ($r - \text{odd}$) in the eq. (A.60). A detailed discussion on $SO(2n)$ group with GUT orientation can be found in [123, 327].

APPENDIX B

Decomposition of representations and beta coefficients

B.1 One and two loop beta function coefficients for RG evolution of gauge couplings

Model	Symmetry	a_i	b_{ij}
I, I'	G_{213}	$\begin{pmatrix} -19/6 \\ 41/10 \\ -7 \end{pmatrix}$	$\begin{pmatrix} 199/50 & 27/10 & 44/5 \\ 9/10 & 35/6 & 12 \\ 11/10 & 9/2 & -26 \end{pmatrix}$
I, I'	G_{2113}	$\begin{pmatrix} -3 \\ 53/12 \\ 33/8 \\ -7 \end{pmatrix}$	$\begin{pmatrix} 8 & 1 & 3/2 & 12 \\ 3 & 17/4 & 15/8 & 12 \\ 9/2 & 15/8 & 65/16 & 4 \\ 9/2 & 3/2 & 1/2 & -26 \end{pmatrix}$
I	G_{2213}	$\begin{pmatrix} -8/3 \\ -13/6 \\ 17/4 \\ -7 \end{pmatrix}$	$\begin{pmatrix} 37/3 & 6 & 3/2 & 12 \\ 6 & 143/6 & 9/4 & 12 \\ 9/2 & 27/4 & 37/8 & 4 \\ 9/2 & 9/2 & 1/2 & -26 \end{pmatrix}$
I'	G_{2213D}	$\begin{pmatrix} -13/6 \\ -13/6 \\ 17/4 \\ -7 \end{pmatrix}$	$\begin{pmatrix} 143/6 & 6 & 9/4 & 12 \\ 6 & 143/6 & 9/4 & 12 \\ 27/4 & 27/4 & 23/4 & 4 \\ 9/2 & 9/2 & 1/2 & -26 \end{pmatrix}$

Table B.1: One-loop and two-loop beta function coefficients for gauge coupling evolutions in Model-I and Model-I' described in Sec. 4.1. The second Higgs doublet mass assumed at 1 TeV.

Group G_I	Higgs content	a_i	b_{ij}
$G_{1_Y 2_L 3_C}$	$\Phi(\frac{1}{2}, 2, 1)_{10}$	$\begin{pmatrix} 41/10 \\ -19/6 \\ -7 \end{pmatrix}$	$\begin{pmatrix} 199/50 & 27/10 & 44/5 \\ 9/10 & 35/6 & 12 \\ 11/10 & 9/2 & -26 \end{pmatrix}$
$G_{1_{B-L} 1_R 2_L 3_C}$	$\Phi_1(0, \frac{1}{2}, 2, 1)_{10}$ $\oplus \Phi_2(0, -\frac{1}{2}, 2, 1)_{10'}$ $\oplus \Delta_R(-1, 1, 1, 1)_{126}$ $\oplus \chi_R(-\frac{1}{2}, \frac{1}{2}, 1, 1)_{16}$	$\begin{pmatrix} 37/8 \\ 57/12 \\ -3 \\ -7 \end{pmatrix}$	$\begin{pmatrix} 209/16 & 63/8 & 9/4 & 4 \\ 63/8 & 33/4 & 3 & 12 \\ 3/2 & 1 & 8 & 12 \\ 1/2 & 3/2 & 9/2 & -26 \end{pmatrix}$
$G_{1_{B-L} 2_L 2_R 3_C}$	$\Phi_1(0, 2, 2, 1)_{10}$ $\oplus \Phi_2(0, 2, 2, 1)_{10'}$ $\oplus \Delta_R(-2, 1, 3, 1)_{126}$ $\oplus \chi_R(-1, 1, 2, 1)_{16}$ $\oplus \Sigma_R(0, 1, 3, 1)_{210}$	$\begin{pmatrix} 23/4 \\ -8/3 \\ -3/2 \\ -7 \end{pmatrix}$	$\begin{pmatrix} 253/8 & 9/2 & 171/4 & 4 \\ 3/2 & 37/3 & 6 & 12 \\ 57/4 & 6 & 263/6 & 12 \\ 1/2 & 9/2 & 9/2 & -26 \end{pmatrix}$
$G_{2_L 2_R 4_C}$	$\Phi_1(2, 2, 1)_{10}$ $\oplus \Phi_2(2, 2, 1)_{10'}$ $\oplus \Delta_R(1, 3, \overline{10})_{126}$ $\oplus \chi_R(1, 2, \overline{4})_{16}$ $\oplus \Sigma_R(1, 3, 15)_{210}$ $\oplus \sigma'(1, 1, 15)_{210}$	$\begin{pmatrix} -8/3 \\ 29/2 \\ -14/3 \end{pmatrix}$	$\begin{pmatrix} 37/3 & 6 & 45/2 \\ 6 & 1103/3 & 1275/2 \\ 9/2 & 255/2 & 288 \end{pmatrix}$
$G_{2_L 2_R 4_C D}$	$\Phi_1 \oplus \Phi_2 \oplus \Delta_R$ $\oplus \Delta_L(3, 1, 10)_{126}$ $\oplus \chi_L(2, 1, 4)_{16}$ $\oplus \Sigma_L(3, 1, 15)_{210}$ $\oplus \chi_R \oplus \Sigma_R \oplus \sigma'$	$\begin{pmatrix} 29/3 \\ 29/3 \\ 2/3 \end{pmatrix}$	$\begin{pmatrix} 1103/3 & 6 & 1275/2 \\ 6 & 1103/3 & 1275/2 \\ 255/2 & 255/2 & 3673/6 \end{pmatrix}$

Table B.2: One and two loop beta coefficients for different gauge coupling evolutions for the model described in Sec. 5.5. The second Higgs doublet is assumed at $\mu \geq 10$ TeV.

Group G_I	Higgs content	a_i	b_{ij}
G_{1Y2L3C}	$\Phi(\frac{1}{2}, 2, 1)_{10}$	$\begin{pmatrix} 41/10 \\ -19/6 \\ -7 \end{pmatrix}$	$\begin{pmatrix} 199/50 & 27/10 & 44/5 \\ 9/10 & 35/6 & 12 \\ 11/10 & 9/2 & -26 \end{pmatrix}$
$G_{1B-L1R2L3C}$	$\Phi_1(0, \frac{1}{2}, 2, 1)_{10}$ $\oplus \Phi_2(0, -\frac{1}{2}, 2, 1)_{10'}$ $\oplus \Delta_R(-1, 1, 1, 1)_{126}$ $\oplus \chi_R(-\frac{1}{2}, \frac{1}{2}, 1, 1)_{16}$	$\begin{pmatrix} 37/8 \\ 57/12 \\ -3 \\ -7 \end{pmatrix}$	$\begin{pmatrix} 209/16 & 63/8 & 9/4 & 4 \\ 63/8 & 33/4 & 3 & 12 \\ 3/2 & 1 & 8 & 12 \\ 1/2 & 3/2 & 9/2 & -26 \end{pmatrix}$
G_{2L2R4C}	$\Phi_1(2, 2, 1)_{10}$ $\oplus \Phi_2(2, 2, 1)_{10'}$ $\oplus \Delta_R(1, 3, \overline{10})_{126}$ $\oplus \chi_R(1, 2, \overline{4})_{16}$ $\oplus \sigma_R(1, 3, 15)_{210}$	$\begin{pmatrix} -8/3 \\ 29/3 \\ -16/3 \end{pmatrix}$	$\begin{pmatrix} 37/3 & 6 & 45/2 \\ 6 & 1103/3 & 1275/2 \\ 9/2 & 255/2 & 736/3 \end{pmatrix}$
$G_{2L2R4CD}$	$\Phi_1 \oplus \Phi_2 \oplus \Delta_R$ $\oplus \Delta_L(3, 1, 10)_{126}$ $\oplus \chi_R \oplus \sigma_R$ $\oplus \chi_L(2, 1, 4)_{16}$ $\oplus \sigma_L(3, 1, 15)_{210}$ $\oplus \xi(2, 2, 15)_{126/126'}$	$\begin{pmatrix} 44/3 \\ 44/3 \\ 16/3 \end{pmatrix}$	$\begin{pmatrix} 1298/3 & 51 & 1755/2 \\ 51 & 1298/3 & 1755/2 \\ 351/2 & 351/2 & 1403/2 \end{pmatrix}$

Table B.3: One and two loop beta coefficients for different gauge coupling evolutions for the model described Sec. 6.1. The second Higgs doublet is taken at $\mu \geq 5$ TeV.

B.2 Decomposition of $SO(10)$ irreducible representations

Since we have been extensively using the decomposition of various $SO(10)$ representations in to it subgroups, and very often we required various scalar sub-multiplets at various scalars following extended survival hypothesis and residing in the symmetry at the corresponding scale, we would often require the decomposition table. We have borrowed the tables for various representations from a very good review on $SO(10)$ group theory by Fukuyama *et al* [124].

$(4_C, 2_L, 2_R)$	$(3_C, 2_L, 2_R, 1_{B-L})$	$(3_C, 2_L, 1_R, 1_{B-L})$	$(3_C, 2_L, 1_Y)$	$(5, 1_X)$
$(\mathbf{6}, \mathbf{1}, \mathbf{1})$	$(\mathbf{3}, \mathbf{1}, \mathbf{1}; -\frac{1}{3})$ $(\overline{\mathbf{3}}, \mathbf{1}, \mathbf{1}; \frac{1}{3})$	$(\mathbf{3}, \mathbf{1}; 0, -\frac{1}{3})$ $(\overline{\mathbf{3}}, \mathbf{1}; 0, \frac{1}{3})$	$(\mathbf{3}, \mathbf{1}; -\frac{1}{3})$ $(\overline{\mathbf{3}}, \mathbf{1}; \frac{1}{3})$	$(\mathbf{5}, 2)$ $(\overline{\mathbf{5}}, -2)$
$(\mathbf{1}, \mathbf{2}, \mathbf{2})$	$(\mathbf{1}, \mathbf{2}, \mathbf{2}; 0)$	$(\mathbf{1}, \mathbf{2}; \frac{1}{2}, 0)$ $(\mathbf{1}, \mathbf{2}; -\frac{1}{2}, 0)$	$(\mathbf{1}, \mathbf{2}; \frac{1}{2})$ $(\mathbf{1}, \mathbf{2}; -\frac{1}{2})$	$(\mathbf{5}, 2)$ $(\overline{\mathbf{5}}, -2)$

Table B.4: Decomposition of the representation **10**

$(4_C, 2_L, 2_R)$	$(3_C, 2_L, 2_R, 1_{B-L})$	$(3_C, 2_L, 1_R, 1_{B-L})$	$(3_C, 2_L, 1_Y)$	$(5, 1_X)$
$(\mathbf{4}, \mathbf{2}, \mathbf{1})$	$(\mathbf{3}, \mathbf{2}, \mathbf{1}; \frac{1}{6})$ $(\mathbf{1}, \mathbf{2}, \mathbf{1}; -\frac{1}{2})$	$(\mathbf{3}, \mathbf{2}; 0, \frac{1}{6})$ $(\mathbf{1}, \mathbf{2}; 0, -\frac{1}{2})$	$(\mathbf{3}, \mathbf{2}; \frac{1}{6})$ $(\mathbf{1}, \mathbf{2}; -\frac{1}{2})$	$(\mathbf{10}, -1)$ $(\overline{\mathbf{5}}, 3)$
$(\mathbf{4}, \mathbf{1}, \mathbf{2})$	$(\mathbf{3}, \mathbf{1}, \mathbf{2}; -\frac{1}{6})$ $(\mathbf{1}, \mathbf{1}, \mathbf{2}; \frac{1}{2})$	$(\mathbf{3}, \mathbf{1}; \frac{1}{2}, -\frac{1}{6})$ $(\overline{\mathbf{3}}, \mathbf{1}; -\frac{1}{2}, -\frac{1}{6})$ $(\mathbf{1}, \mathbf{1}; \frac{1}{2}, \frac{1}{2})$ $(\mathbf{1}, \mathbf{1}; -\frac{1}{2}, \frac{1}{2})$	$(\mathbf{3}, \mathbf{1}; \frac{1}{3})$ $(\overline{\mathbf{3}}, \mathbf{1}; -\frac{2}{3})$ $(\mathbf{1}, \mathbf{1}; 1)$ $(\mathbf{1}, \mathbf{1}; 0)$	$(\overline{\mathbf{5}}, 3)$ $(\mathbf{10}, -1)$ $(\mathbf{10}, -1)$ $(\mathbf{1}, -5)$

Table B.5: Decomposition of the representation **16**

$(4_C, 2_L, 2_R)$	$(3_C, 2_L, 2_R, 1_{B-L})$	$(3_C, 2_L, 1_R, 1_{B-L})$	$(3_C, 2_L, 1_Y)$	$(5, 1_X)$
$(\mathbf{1}, \mathbf{1}, \mathbf{3})$	$(\mathbf{1}, \mathbf{1}, \mathbf{3}; 0)$	$(\mathbf{1}, \mathbf{1}; 1, 0)$ $(\mathbf{1}, \mathbf{1}; 0, 0)$ $(\mathbf{1}, \mathbf{1}; -1, 0)$	$(\mathbf{1}, \mathbf{1}; 1)$ $(\mathbf{1}, \mathbf{1}; 0)$ $(\mathbf{1}, \mathbf{1}; -1)$	$(\mathbf{10}, 4)$ $(\mathbf{1}, 0)$ $(\overline{\mathbf{10}}, -4)$
$(\mathbf{1}, \mathbf{3}, \mathbf{1})$	$(\mathbf{1}, \mathbf{3}, \mathbf{1}; 0)$	$(\mathbf{1}, \mathbf{3}; 0, 0)$	$(\mathbf{1}, \mathbf{3}; 0)$	$(\mathbf{24}, 0)$
$(\mathbf{6}, \mathbf{2}, \mathbf{2})$	$(\mathbf{3}, \mathbf{2}, \mathbf{2}; -\frac{1}{3})$ $(\overline{\mathbf{3}}, \mathbf{2}, \mathbf{2}; \frac{1}{3})$	$(\mathbf{3}, \mathbf{2}; \frac{1}{2}, -\frac{1}{3})$ $(\mathbf{3}, \mathbf{2}; -\frac{1}{2}, -\frac{1}{3})$ $(\overline{\mathbf{3}}, \mathbf{2}; \frac{1}{2}, \frac{1}{3})$ $(\overline{\mathbf{3}}, \mathbf{2}; -\frac{1}{2}, \frac{1}{3})$	$(\mathbf{3}, \mathbf{2}; \frac{1}{6})$ $(\mathbf{3}, \mathbf{2}; -\frac{5}{6})$ $(\overline{\mathbf{3}}, \mathbf{2}; \frac{5}{6})$ $(\overline{\mathbf{3}}, \mathbf{2}; -\frac{1}{6})$	$(\mathbf{10}, 4)$ $(\mathbf{24}, 0)$ $(\mathbf{24}, 0)$ $(\overline{\mathbf{10}}, -4)$
$(\mathbf{15}, \mathbf{1}, \mathbf{1})$	$(\mathbf{1}, \mathbf{1}, \mathbf{1}; 0)$ $(\mathbf{3}, \mathbf{1}, \mathbf{1}; \frac{2}{3})$ $(\overline{\mathbf{3}}, \mathbf{1}, \mathbf{1}; -\frac{2}{3})$ $(\mathbf{8}, \mathbf{1}, \mathbf{1}; 0)$	$(\mathbf{1}, \mathbf{1}; 0, 0)$ $(\mathbf{3}, \mathbf{1}; 0, \frac{2}{3})$ $(\overline{\mathbf{3}}, \mathbf{1}; 0, -\frac{2}{3})$ $(\mathbf{8}, \mathbf{1}; 0, 0)$	$(\mathbf{1}, \mathbf{1}; 0)$ $(\mathbf{3}, \mathbf{1}; \frac{2}{3})$ $(\overline{\mathbf{3}}, \mathbf{1}; -\frac{2}{3})$ $(\mathbf{8}, \mathbf{1}; 0)$	$(\mathbf{24}, 0)$ $(\overline{\mathbf{10}}, -4)$ $(\mathbf{10}, 4)$ $(\mathbf{24}, 0)$

Table B.6: Decomposition of the representation **45**

$(4_C, 2_L, 2_R)$	$(3_C, 2_L, 2_R, 1_{B-L})$	$(3_C, 2_L, 1_R, 1_{B-L})$	$(3_C, 2_L, 1_Y)$	$(5, 1_X)$
$(1, 1, 1)$	$(1, 1, 1; 0)$	$(1, 1; 0, 0)$	$(1, 1; 0)$	$(24, 0)$
$(1, 3, 3)$	$(1, 3, 3; 0)$	$(1, 3; 1, 0)$ $(1, 3; 0, 0)$ $(1, 3; -1, 0)$	$(1, 3; 1)$ $(1, 3; 0)$ $(1, 3; -1)$	$(15, 4)$ $(24, 0)$ $(\overline{15}, -4)$
$(20', 1, 1)$	$(\overline{6}, 1, 1; \frac{2}{3})$ $(6, 1, 1; -\frac{2}{3})$ $(8, 1, 1; 0)$	$(\overline{6}, 1; 0, \frac{2}{3})$ $(6, 1; 0, -\frac{2}{3})$ $(8, 1; 0, 0)$	$(\overline{6}, 1; \frac{2}{3})$ $(6, 1; -\frac{2}{3})$ $(8, 1; 0)$	$(15, -4)$ $(15, 4)$ $(24, 0)$
$(6, 2, 2)$	$(3, 2, 2; -\frac{1}{3})$ $(\overline{3}, 2, 2; \frac{1}{3})$	$(3, 2; \frac{1}{2}, -\frac{1}{3})$ $(3, 2; -\frac{1}{2}, -\frac{1}{3})$ $(\overline{3}, 2; \frac{1}{2}, \frac{1}{3})$ $(\overline{3}, 2; -\frac{1}{2}, \frac{1}{3})$	$(3, 2; \frac{1}{6})$ $(3, 2; -\frac{5}{6})$ $(\overline{3}, 2; \frac{5}{6})$ $(\overline{3}, 2; -\frac{1}{6})$	$(15, 4)$ $(24, 0)$ $(24, 0)$ $(\overline{15}, -4)$

Table B.7: Decomposition of the representation **54**

$(4_C, 2_L, 2_R)$	$(3_C, 2_L, 2_R, 1_{B-L})$	$(3_C, 2_L, 1_R, 1_{B-L})$	$(3_C, 2_L, 1_Y)$	$(5, 1_X)$
$(1, 2, 2)$	$(1, 2, 2; 0)$	$(1, 2; \frac{1}{2}, 0)$ $(1, 2; -\frac{1}{2}, 0)$	$(1, 2; \frac{1}{2})$ $(1, 2; -\frac{1}{2})$	$(5, 2)$ $(\overline{5}, -2)$
$(10, 1, 1)$	$(1, 1, 1; -1)$ $(3, 1, 1; -\frac{1}{3})$ $(6, 1, 1; \frac{1}{3})$	$(1, 1; 0, -1)$ $(3, 1; 0, -\frac{1}{3})$ $(6, 1; 0, \frac{1}{3})$	$(1, 1; -1)$ $(3, 1; -\frac{1}{3})$ $(6, 1; \frac{1}{3})$	$(10, 6)$ $(5, 2)$ $(\overline{45}, -2)$
$(\overline{10}, 1, 1)$	$(1, 1, 1; 1)$ $(\overline{3}, 1, 1; \frac{1}{3})$ $(\overline{6}, 1, 1; -\frac{1}{3})$	$(1, 1; 0, 1)$ $(\overline{3}, 1; 0, \frac{1}{3})$ $(\overline{6}, 1; 0, -\frac{1}{3})$	$(1, 1; 1)$ $(\overline{3}, 1; \frac{1}{3})$ $(\overline{6}, 1; -\frac{1}{3})$	$(10, -6)$ $(\overline{5}, -2)$ $(45, 2)$
$(6, 3, 1)$	$(3, 3, 1; -\frac{1}{3})$ $(\overline{3}, 3, 1; \frac{1}{3})$	$(3, 3; 0, -\frac{1}{3})$ $(\overline{3}, 3; 0, \frac{1}{3})$	$(3, 3; -\frac{1}{3})$ $(\overline{3}, 3; \frac{1}{3})$	$(45, 2)$ $(\overline{45}, -2)$
$(6, 1, 3)$	$(3, 1, 3; -\frac{1}{3})$ $(\overline{3}, 1, 3; \frac{1}{3})$	$(3, 1; 1, -\frac{1}{3})$ $(3, 1; 0, -\frac{1}{3})$ $(3, 1; -1, -\frac{1}{3})$ $(\overline{3}, 1; 1, \frac{1}{3})$ $(\overline{3}, 1; 0, \frac{1}{3})$ $(\overline{3}, 1; -1, \frac{1}{3})$	$(3, 1; \frac{2}{3})$ $(3, 1; -\frac{1}{3})$ $(3, 1; -\frac{4}{3})$ $(\overline{3}, 1; \frac{4}{3})$ $(\overline{3}, 1; \frac{1}{3})$ $(\overline{3}, 1; -\frac{2}{3})$	$(10, 6)$ $(45, 2)$ $(\overline{45}, -2)$ $(45, 2)$ $(\overline{45}, -2)$ $(10, -6)$
$(15, 2, 2)$	$(1, 2, 2; 0)$ $(3, 2, 2; \frac{2}{3})$ $(\overline{3}, 2, 2; -\frac{2}{3})$ $(8, 2, 2; 0)$	$(1, 2; \frac{1}{2}, 0)$ $(1, 2; -\frac{1}{2}, 0)$ $(3, 2; \frac{1}{2}, \frac{2}{3})$ $(3, 2; -\frac{1}{2}, \frac{2}{3})$ $(\overline{3}, 2; -\frac{1}{2}, -\frac{2}{3})$ $(\overline{3}, 2; \frac{1}{2}, -\frac{2}{3})$ $(8, 2; \frac{1}{2}, 0)$ $(8, 2; -\frac{1}{2}, 0)$	$(1, 2; \frac{1}{2})$ $(1, 2; -\frac{1}{2})$ $(3, 2; \frac{7}{6})$ $(3, 2; \frac{1}{6})$ $(\overline{3}, 2; -\frac{7}{6})$ $(\overline{3}, 2; -\frac{1}{6})$ $(8, 2; \frac{1}{2})$ $(8, 2; -\frac{1}{2})$	$(45, 2)$ $(\overline{45}, -2)$ $(\overline{45}, -2)$ $(10, -6)$ $(45, 2)$ $(10, 6)$ $(45, 2)$ $(\overline{45}, -2)$

Table B.8: Decomposition of the representation **120**

$(4_C, 2_L, 2_R)$	$(3_C, 2_L, 2_R, 1_{B-L})$	$(3_C, 2_L, 1_R, 1_{B-L})$	$(3_C, 2_L, 1_Y)$	$(5, 1_X)$
$(\mathbf{6}, \mathbf{1}, \mathbf{1})$	$(\mathbf{3}, \mathbf{1}, \mathbf{1}; -\frac{1}{3})$ $(\overline{\mathbf{3}}, \mathbf{1}, \mathbf{1}; \frac{1}{3})$	$(\mathbf{3}, \mathbf{1}; 0, -\frac{1}{3})$ $(\overline{\mathbf{3}}, \mathbf{1}; 0, \frac{1}{3})$	$(\mathbf{3}, \mathbf{1}; -\frac{1}{3})$ $(\overline{\mathbf{3}}, \mathbf{1}; \frac{1}{3})$	$(\mathbf{5}, 2)$ $(\overline{\mathbf{45}}, -2)$
$(\overline{\mathbf{10}}, \mathbf{3}, \mathbf{1})$	$(\mathbf{1}, \mathbf{3}, \mathbf{1}; 1)$ $(\overline{\mathbf{3}}, \mathbf{1}, \mathbf{3}; \frac{1}{3})$ $(\overline{\mathbf{6}}, \mathbf{1}, \mathbf{3}; -\frac{1}{3})$	$(\mathbf{1}, \mathbf{3}; 0, 1)$ $(\overline{\mathbf{3}}, \mathbf{3}; 0, \frac{1}{3})$ $(\overline{\mathbf{6}}, \mathbf{3}; 0, -\frac{1}{3})$	$(\mathbf{1}, \mathbf{3}; 1)$ $(\overline{\mathbf{3}}, \mathbf{3}; \frac{1}{3})$ $(\overline{\mathbf{6}}, \mathbf{3}; -\frac{1}{3})$	$(\mathbf{15}, -6)$ $(\overline{\mathbf{45}}, -2)$ $(\mathbf{50}, 2)$
$(\mathbf{10}, \mathbf{1}, \mathbf{3})$	$(\mathbf{1}, \mathbf{1}, \mathbf{3}; -1)$ $(\mathbf{3}, \mathbf{1}, \mathbf{3}; -\frac{1}{3})$ $(\mathbf{6}, \mathbf{1}, \mathbf{3}; \frac{1}{3})$	$(\mathbf{1}, \mathbf{1}; 1, -1)$ $(\mathbf{1}, \mathbf{1}; 0, -1)$ $(\mathbf{1}, \mathbf{1}; -1, -1)$ $(\mathbf{3}, \mathbf{1}; 1, -\frac{1}{3})$ $(\mathbf{3}, \mathbf{1}; 0, -\frac{1}{3})$ $(\mathbf{3}, \mathbf{1}; -1, -\frac{1}{3})$ $(\mathbf{6}, \mathbf{1}; 1, \frac{1}{3})$ $(\mathbf{6}, \mathbf{1}; 0, \frac{1}{3})$ $(\mathbf{6}, \mathbf{1}; -1, \frac{1}{3})$	$(\mathbf{1}, \mathbf{1}; 0)$ $(\mathbf{1}, \mathbf{1}; -1)$ $(\mathbf{1}, \mathbf{1}; -2)$ $(\mathbf{3}, \mathbf{1}; \frac{2}{3})$ $(\mathbf{3}, \mathbf{1}; -\frac{1}{3})$ $(\mathbf{3}, \mathbf{1}; -\frac{4}{3})$ $(\mathbf{6}, \mathbf{1}; \frac{4}{3})$ $(\mathbf{6}, \mathbf{1}; \frac{1}{3})$ $(\mathbf{6}, \mathbf{1}; -\frac{2}{3})$	$(\mathbf{1}, 10)$ $(\overline{\mathbf{10}}, 6)$ $(\mathbf{50}, 2)$ $(\overline{\mathbf{10}}, 6)$ $(\mathbf{50}, 2)$ $(\overline{\mathbf{45}}, -2)$ $(\mathbf{50}, 2)$ $(\overline{\mathbf{45}}, -2)$ $(\mathbf{15}, -6)$
$(\mathbf{15}, \mathbf{2}, \mathbf{2})$	$(\mathbf{1}, \mathbf{2}, \mathbf{2}; 0)$ $(\mathbf{3}, \mathbf{2}, \mathbf{2}; \frac{2}{3})$ $(\overline{\mathbf{3}}, \mathbf{2}, \mathbf{2}; -\frac{2}{3})$ $(\mathbf{8}, \mathbf{2}, \mathbf{2}; 0)$	$(\mathbf{1}, \mathbf{2}; \frac{1}{2}, 0)$ $(\mathbf{1}, \mathbf{2}; -\frac{1}{2}, 0)$ $(\mathbf{3}, \mathbf{2}; \frac{1}{2}, \frac{2}{3})$ $(\mathbf{3}, \mathbf{2}; -\frac{1}{2}, \frac{2}{3})$ $(\overline{\mathbf{3}}, \mathbf{2}; -\frac{1}{2}, -\frac{2}{3})$ $(\overline{\mathbf{3}}, \mathbf{2}; \frac{1}{2}, -\frac{2}{3})$ $(\mathbf{8}, \mathbf{2}; \frac{1}{2}, 0)$ $(\mathbf{8}, \mathbf{2}; -\frac{1}{2}, 0)$	$(\mathbf{1}, \mathbf{2}; \frac{1}{2})$ $(\mathbf{1}, \mathbf{2}; -\frac{1}{2})$ $(\mathbf{3}, \mathbf{2}; \frac{7}{6})$ $(\mathbf{3}, \mathbf{2}; \frac{1}{6})$ $(\overline{\mathbf{3}}, \mathbf{2}; -\frac{7}{6})$ $(\overline{\mathbf{3}}, \mathbf{2}; -\frac{1}{6})$ $(\mathbf{8}, \mathbf{2}; \frac{1}{2})$ $(\mathbf{8}, \mathbf{2}; -\frac{1}{2})$	$(\mathbf{5}, 2)$ $(\overline{\mathbf{45}}, -2)$ $(\overline{\mathbf{45}}, -2)$ $(\mathbf{15}, -6)$ $(\mathbf{50}, 2)$ $(\overline{\mathbf{10}}, 6)$ $(\mathbf{50}, 2)$ $(\overline{\mathbf{45}}, -2)$

Table B.9: Decomposition of the representation $\overline{\mathbf{126}}$

$(4_C, 2_L, 2_R)$	$(3_C, 2_L, 2_R, 1_{B-L})$	$(3_C, 2_L, 1_R, 1_{B-L})$	$(3_C, 2_L, 1_Y)$	$(5, 1_X)$
$(1, 1, 1)$	$(1, 1, 1; 0)$	$(1, 1; 0, 0)$	$(1, 1; 0)$	$(1, 0)$
$(15, 1, 1)$	$(1, 1, 1; 0)$ $(\mathbf{3}, 1, 1; \frac{2}{3})$ $(\bar{\mathbf{3}}, 1, 1; -\frac{2}{3})$ $(8, 1, 1; 0)$	$(1, 1; 0, 0)$ $(\mathbf{3}, 1; 0, \frac{2}{3})$ $(\bar{\mathbf{3}}, 1; 0, -\frac{2}{3})$ $(8, 1; 0, 0)$	$(1, 1; 0)$ $(\mathbf{3}, 1; \frac{2}{3})$ $(\bar{\mathbf{3}}, 1; -\frac{2}{3})$ $(8, 1; 0)$	$(24, 0)$ $(\overline{10}, -4)$ $(10, 4)$ $(24, 0)$
$(6, 2, 2)$	$(\mathbf{3}, 2, 2; -\frac{1}{3})$ $(\bar{\mathbf{3}}, 2, 2; \frac{1}{3})$	$(\mathbf{3}, 2; \frac{1}{2}, -\frac{1}{3})$ $(\mathbf{3}, 2; -\frac{1}{2}, -\frac{1}{3})$ $(\bar{\mathbf{3}}, 2; \frac{1}{2}, \frac{1}{3})$ $(\bar{\mathbf{3}}, 2; -\frac{1}{2}, \frac{1}{3})$	$(\mathbf{3}, 2; \frac{1}{6})$ $(\mathbf{3}, 2; -\frac{5}{6})$ $(\bar{\mathbf{3}}, 2; \frac{5}{6})$ $(\bar{\mathbf{3}}, 2; -\frac{1}{6})$	$(10, 4)$ $(24, 0)$ $(24, 0)$ $(\overline{10}, -4)$
$(10, 2, 2)$	$(1, 2, 2; -1)$ $(\mathbf{3}, 2, 2; -\frac{1}{3})$ $(\bar{\mathbf{6}}, 2, 2; \frac{1}{3})$	$(1, 2; \frac{1}{2}, -1)$ $(1, 2; -\frac{1}{2}, -1)$ $(\mathbf{3}, 2; \frac{1}{2}, \frac{1}{3})$ $(\mathbf{3}, 2; -\frac{1}{2}, -\frac{1}{3})$ $(\bar{\mathbf{6}}, 2; \frac{1}{2}, \frac{1}{3})$ $(\bar{\mathbf{6}}, 2; -\frac{1}{2}, \frac{1}{3})$	$(1, 2; -\frac{1}{2})$ $(1, 2; -\frac{3}{2})$ $(\mathbf{3}, 2; \frac{1}{6})$ $(\mathbf{3}, 2; -\frac{5}{6})$ $(\bar{\mathbf{6}}, 2; \frac{5}{6})$ $(\bar{\mathbf{6}}, 2; -\frac{1}{6})$	$(\bar{5}, 8)$ $(40, 4)$ $(40, 4)$ $(75, 0)$ $(75, 0)$ $(40, -4)$
$(\overline{10}, 2, 2)$	$(1, 2, 2; 1)$ $(\bar{\mathbf{3}}, 2, 2; \frac{1}{3})$ $(\bar{\mathbf{6}}, 2, 2; -\frac{1}{3})$	$(1, 2; \frac{1}{2}, 1)$ $(1, 2; -\frac{1}{2}, 1)$ $(\bar{\mathbf{3}}, 2; \frac{1}{2}, \frac{1}{3})$ $(\bar{\mathbf{3}}, 2; -\frac{1}{2}, \frac{1}{3})$ $(\bar{\mathbf{6}}, 2; \frac{1}{2}, -\frac{1}{3})$ $(\bar{\mathbf{6}}, 2; -\frac{1}{2}, -\frac{1}{3})$	$(1, 2; \frac{3}{2})$ $(1, 2; \frac{1}{2})$ $(\bar{\mathbf{3}}, 2; \frac{5}{6})$ $(\bar{\mathbf{3}}, 2; -\frac{1}{6})$ $(\bar{\mathbf{6}}, 2; \frac{1}{6})$ $(\bar{\mathbf{6}}, 2; -\frac{5}{6})$	$(40, -4)$ $(5, -8)$ $(75, 0)$ $(40, -4)$ $(40, 4)$ $(75, 0)$
$(15, 3, 1)$	$(1, 3, 1; 0)$ $(\mathbf{3}, 3, 1; \frac{2}{3})$ $(\bar{\mathbf{3}}, 3, 1; -\frac{2}{3})$ $(8, 3, 1; 0)$	$(1, 3; 0, 0)$ $(\mathbf{3}, 3; 0, \frac{2}{3})$ $(\bar{\mathbf{3}}, 3; 0, -\frac{2}{3})$ $(8, 3; 0, 0)$	$(1, 3; 0)$ $(\mathbf{3}, 3; \frac{2}{3})$ $(\bar{\mathbf{3}}, 3; -\frac{2}{3})$ $(8, 3; 0)$	$(24, 0)$ $(40, -4)$ $(40, 4)$ $(75, 0)$
$(15, 1, 3)$	$(1, 1, 3; 0)$ $(\mathbf{3}, 1, 3; \frac{2}{3})$ $(\bar{\mathbf{3}}, 1, 3; -\frac{2}{3})$ $(8, 1, 3; 0)$	$(1, 1; 1, 0)$ $(1, 1; 0, 0)$ $(1, 1; -1, 0)$ $(\mathbf{3}, 1; 1, \frac{2}{3})$ $(\mathbf{3}, 1; 0, \frac{2}{3})$ $(\mathbf{3}, 1; -1, \frac{2}{3})$ $(\bar{\mathbf{3}}, 1; 1, -\frac{2}{3})$ $(\bar{\mathbf{3}}, 1; 0, -\frac{2}{3})$ $(\bar{\mathbf{3}}, 1; -1, -\frac{2}{3})$ $(8, 1; 1, 0)$ $(8, 1; 0, 0)$ $(8, 1; -1, 0)$	$(1, 1; 1)$ $(1, 1; 0)$ $(1, 1; -1)$ $(\mathbf{3}, 1; \frac{5}{3})$ $(\mathbf{3}, 1; \frac{2}{3})$ $(\mathbf{3}, 1; -\frac{1}{3})$ $(\bar{\mathbf{3}}, 1; \frac{1}{3})$ $(\bar{\mathbf{3}}, 1; -\frac{2}{3})$ $(\bar{\mathbf{3}}, 1; -\frac{5}{3})$ $(8, 1; 1)$ $(8, 1; 0)$ $(8, 1; -1)$	$(10, 4)$ $(75, 0)$ $(\overline{10}, -4)$ $(75, 0)$ $(40, -4)$ $(5, -8)$ $(\bar{5}, 8)$ $(40, 4)$ $(75, 0)$ $(40, 4)$ $(75, 0)$ $(40, -4)$

Table B.10: Decomposition of the representation **210**

Renormalization group evolution for Model-I

Each of the two $SO(10)$ models we have considered for inverse seesaw has two types of nonstandard gauge symmetries, G_{2213} or G_{2213D} and G_{2113} . Here we derive RGEs for running Yukawa and fermion mass matrices from which, following the earlier approach [186], we derive RGEs for the mass eigenvalues and mixing angles. We define the rescaled β -functions

$$16\pi^2\mu\frac{\partial F_i}{\partial\mu} = \beta_{F_i}. \quad (\text{C.1})$$

With G_{2113} symmetry the scalar field $\Phi_d(2, 1/2, 0, 1)$ through its VEV v_d gives masses to down quarks and charged leptons while $\Phi_u(2, -1/2, 0, 1)$ through its VEV v_u gives Dirac masses to up quarks and neutrinos. These fields are embedded into separate bi-doublets in the presence of G_{2213} and their vacuum structure has been specified in Sec. 4.3. We have derived the beta functions for RG evolution of Yukawa matrices (Y_i), fermion mass matrices (M_i), and the vacuum expectation values ($v_{u,d}$). The rescaled beta functions are given below in both cases,

G_{2113} **Symmetry:**

$$\begin{aligned} \beta_{Y_u} &= \left[\frac{3}{2}Y_uY_u^\dagger + \frac{1}{2}Y_dY_d^\dagger + T_u - \sum_i C_i^q g_i^2 \right] Y_u, \\ \beta_{Y_d} &= \left[\frac{3}{2}Y_dY_d^\dagger + \frac{1}{2}Y_uY_u^\dagger + T_d - \sum_i C_i^q g_i^2 \right] Y_d, \end{aligned}$$

$$\begin{aligned}
\beta_{Y_\nu} &= \left[\frac{3}{2} Y_\nu Y_\nu^\dagger + \frac{1}{2} Y_e Y_e^\dagger + T_u - \sum_i C_i^l g_i^2 \right] Y_\nu, \\
\beta_{Y_e} &= \left[\frac{3}{2} Y_e Y_e^\dagger + \frac{1}{2} Y_\nu Y_\nu^\dagger + T_d - \sum_i C_i^l g_i^2 \right] Y_e, \\
\beta_{M_u} &= \left[\frac{3}{2} Y_u Y_u^\dagger + \frac{1}{2} Y_d Y_d^\dagger - \sum_i \tilde{C}_i^q g_i^2 \right] M_u, \\
\beta_{M_d} &= \left[\frac{3}{2} Y_d Y_d^\dagger + \frac{1}{2} Y_u Y_u^\dagger - \sum_i \tilde{C}_i^q g_i^2 \right] M_d, \\
\beta_{M_D} &= \left[\frac{3}{2} Y_\nu u Y_\nu^\dagger + \frac{1}{2} Y_e Y_e^\dagger - \sum_i \tilde{C}_i^l g_i^2 \right] M_D, \\
\beta_{M_e} &= \left[\frac{3}{2} Y_e u Y_e^\dagger + \frac{1}{2} Y_\nu Y_\nu^\dagger - \sum_i \tilde{C}_i^l g_i^2 \right] M_e,
\end{aligned} \tag{C.2}$$

where the beta-functions for VEVs are

$$\begin{aligned}
\beta_{v_u} &= \left[\sum_i C_i^v g_i^2 - T_u \right] v_u, \\
\beta_{v_d} &= \left[\sum_i C_i^v g_i^2 - T_d \right] v_d,
\end{aligned} \tag{C.3}$$

with

$$T_u = \text{Tr}(3Y_u^\dagger Y_u + Y_\nu^\dagger Y_\nu), \quad T_d = \text{Tr}(3Y_d^\dagger Y_d + Y_e^\dagger Y_e). \tag{C.4}$$

The parameters occurring in these equations, and also in eq. (C.9) and eq. (C.10) given below are

$$\begin{aligned}
a &= \frac{3}{2}, \quad b = \frac{1}{2}, \quad a' = b' = 0, \\
C_i^q &= (9/4, 3/4, 1/4, 8), \quad C_i^l = (9/4, 3/4, 9/4, 0), \\
\tilde{C}_i^q &= (0, 0, 1/4, 8), \quad \tilde{C}_i^l = (0, 0, 9/4, 0), \quad C_i^v = (9/4, 3/4, 0, 0), \\
i &= 2L, 1R, BL, 3C.
\end{aligned} \tag{C.5}$$

G_{2213} Symmetry:

Following definitions of Sec. 4.3 in the presence of left-right symmetry, the rescaled beta functions for RGEs of the Yukawa and fermion mass matrices are

$$\begin{aligned}
\beta_{Y_u} &= (Y_u Y_u^\dagger + Y_d Y_d^\dagger) Y_u + Y_u (Y_u^\dagger Y_u + Y_d^\dagger Y_d) + T_u Y_u + \hat{T}_1 Y_d - \sum_i C_i^q g_i^2 Y_u, \\
\beta_{Y_d} &= (Y_d Y_d^\dagger + Y_u Y_u^\dagger) Y_d + Y_d (Y_d^\dagger Y_d + Y_u^\dagger Y_u) + T_d Y_d + \hat{T}_2 Y_u - \sum_i C_i^q g_i^2 Y_d, \\
\beta_{Y_\nu} &= (Y_\nu Y_\nu^\dagger + Y_e Y_e^\dagger) Y_\nu + Y_\nu (Y_\nu^\dagger Y_\nu + Y_e^\dagger Y_e) + T_u Y_\nu + \hat{T}_1 Y_e - \sum_i C_i^l g_i^2 Y_\nu, \\
\beta_{Y_e} &= (Y_e Y_e^\dagger + Y_\nu Y_\nu^\dagger) Y_e + Y_e (Y_e^\dagger Y_e + Y_\nu^\dagger Y_\nu) + T_d Y_e + \hat{T}_2 Y_\nu - \sum_i C_i^l g_i^2 Y_e, \\
\beta_{M_u} &= (Y_u Y_u^\dagger + Y_d Y_d^\dagger) M_u + M_u (Y_u^\dagger Y_u + Y_d^\dagger Y_d) - \sum_i \tilde{C}_i^q g_i^2 M_u + \hat{T}_1 \tan \beta M_d, \\
\beta_{M_d} &= (Y_d Y_d^\dagger + Y_u Y_u^\dagger) M_d + M_d (Y_d^\dagger Y_d + Y_u^\dagger Y_u) - \sum_i \tilde{C}_i^q g_i^2 M_d + \frac{\hat{T}_2}{\tan \beta} M_u, \\
\beta_{M_D} &= (Y_\nu Y_\nu^\dagger + Y_e Y_e^\dagger) M_D + M_D (Y_\nu^\dagger Y_\nu + Y_e^\dagger Y_e) - \sum_i \tilde{C}_i^l g_i^2 M_D + \hat{T}_1 \tan \beta M_e, \\
\beta_{M_e} &= (Y_e Y_e^\dagger + Y_\nu Y_\nu^\dagger) M_e + M_e (Y_e^\dagger Y_e + Y_\nu^\dagger Y_\nu) - \sum_i \tilde{C}_i^l g_i^2 M_e + \frac{\hat{T}_2}{\tan \beta} M_D, \quad (\text{C.6})
\end{aligned}$$

where the rescaled beta functions for VEVs β_{v_u}, β_{v_d} are the same as in eq. (C.3) with different coefficients C_i^v defined below and functions T_u and T_d are the same as in eq. (C.4). Other two traces entering in this case are

$$\begin{aligned}
\hat{T}_1 &= \text{Tr}(3Y_d^\dagger Y_u + Y_e^\dagger Y_\nu), \\
\hat{T}_2 &= \text{Tr}(3Y_u^\dagger Y_d + Y_\nu^\dagger Y_e). \quad (\text{C.7})
\end{aligned}$$

The parameters occurring in these equations and also in eq. (C.9) and eq. (C.10) given below are

$$\begin{aligned}
a &= b = 2, \quad a' = b' = 1, \\
C_i^q &= (9/4, 9/4, 1/4, 8), \quad C_i^l = (9/4, 9/4, 9/4, 0), \quad \tilde{C}_i^q = (0, 0, 1/4, 8), \\
\tilde{C}_i^l &= (0, 0, 9/4, 0), \quad C_i^v = (9/4, 9/4, 0, 0), \quad (i = 2L, 2R, BL, 3C). \quad (\text{C.8})
\end{aligned}$$

Then following the procedure described in [186], and using the definition of parameters in the two different mass ranges, given above we obtain RGEs for mass eigenvalues and elements of CKM mixing matrix $V_{\alpha\beta}$ which can be expressed in the

generalized form for both cases,

Mass Eigenvalues:

$$\begin{aligned}
\beta_{m_i} &= \left[-\sum_k \tilde{C}_k^{(q)} g_k^2 + ay_i^2 + 2b \sum_{j=d,s,b} |V_{uj}|^2 y_j^2 + a' \frac{\hat{T}_1 \tan \beta}{m_i} \sum_{j=d,s,b} |V_{uj}|^2 m_j \right] m_i, \\
&\text{where } i = u, c, t \\
\beta_{m_i} &= \left[-\sum_k \tilde{C}_k^{(q)} g_k^2 + ay_i^2 + 2b \sum_{j=u,c,t} |V_{dj}|^2 y_j^2 + b' \frac{\hat{T}_2}{\tan \beta m_i} \sum_{j=u,c,t} |V_{dj}|^2 m_j \right] m_i, \\
&\text{where } i = d, s, b \\
\beta_{m_i} &= \left[-\sum_k \tilde{C}_k^{(l)} g_k^2 + ay_i^2 + 2b \sum_{j=N_1, N_2, N_3} y_j^2 + b' \frac{\hat{T}_2}{\tan \beta m_i} \sum_{j=N_1, N_2, N_3} m_j \right] m_i, \\
&\text{where } i = e, \mu, \tau \\
\beta_{m_i} &= \left[-\sum_k \tilde{C}_k^{(l)} g_k^2 + ay_i^2 + a' \frac{\hat{T}_1 \tan \beta}{m_i} \sum_{j=e, \mu, \tau} m_j \right] m_i, \\
&\text{where } i = N_1, N_2, N_3.
\end{aligned} \tag{C.9}$$

CKM Matrix Elements:

$$\begin{aligned}
\beta_{V_{\alpha\beta}} &= \sum_{\gamma=u,c,t;\gamma \neq \alpha} \left[a' \frac{\hat{T}_1 \tan \beta}{m_\alpha - m_\gamma} (V \hat{M}_d V^\dagger)_{\alpha\gamma} + \frac{b}{v_d^2} \frac{m_\alpha^2 + m_\gamma^2}{m_\alpha^2 - m_\gamma^2} (V \hat{M}_d^2 V^\dagger)_{\alpha\gamma} \right] V_{\gamma\beta} \\
&- \sum_{\gamma=d,s,b;\gamma \neq \beta} V_{\alpha\gamma} \left[b' \frac{\hat{T}_2}{\tan \beta (m_\gamma - m_\alpha)} (V^\dagger \hat{M}_u V)_{\gamma\beta} \right. \\
&\left. + \frac{b}{v_u^2} \frac{m_\gamma^2 + m_\beta^2}{m_\gamma^2 - m_\beta^2} (V^\dagger \hat{M}_u^2 V)_{\gamma\beta} \right].
\end{aligned} \tag{C.10}$$

Then using third generation dominance, the beta functions for all the 9 elements are easily obtained for respective mass ranges where in addition to the parameters in the respective cases in eq. (C.5) and eq. (C.8), $a' = b' = 0$ in the mass range $M_{R^0} \rightarrow M_{R^+}$ with G_{2113} symmetry, but $a' = b' = 1$ in the mass range $M_{R^+} \rightarrow M_{GUT}$ with G_{2213} or G_{2213D} symmetry and, in the latter case, the nonvanishing traces $\hat{T}_{1,2}$ are easily evaluated in the mass basis.

APPENDIX D

Neutrino mass and mixings in inverse seesaw

D.1 Diagonalization of inverse and extended inverse seesaw

We present the recipe to decouple the large scale from the small scales in the mass matrix of inverse and extended inverse seesaw. The complete mass matrix for neutral particle is written in flavor basis $\{\nu_L, S_L, N_R^C\}$ as

$$\mathcal{M}_\nu = \begin{pmatrix} 0 & 0 & M_D \\ 0 & \mu_S & M \\ M_D^T & M^T & M_N \end{pmatrix} \quad (\text{D.1})$$

where all the elements of the matrix are themselves 3×3 matrices. To generate the tiny masses for light neutrinos, the elements of the matrix follow the hierarchy

$$\mu_S \ll M_D < M \ll M_N. \quad (\text{D.2})$$

When the $\overline{126}_H$ scalar is absent from the theory the matrix M_N is absent and the structure is minimal inverse seesaw matrix giving pseudo-Dirac nature to heavy states.

The flavor basis to mass basis transformation and the diagonalization of the above

mass matrix is achieved through a unitary matrix (\mathcal{V}) such that

$$|\psi\rangle_f = \mathcal{V}^* |\psi\rangle_m \quad (\text{D.3})$$

$$\text{or, } \begin{pmatrix} \nu_\alpha \\ S_\beta \\ N_\gamma^C \end{pmatrix} = \begin{pmatrix} \mathcal{V}_{\alpha i}^{\nu\hat{\nu}} & \mathcal{V}_{\alpha j}^{\nu\hat{S}} & \mathcal{V}_{\alpha k}^{\nu\hat{N}} \\ \mathcal{V}_{\beta i}^{S\hat{\nu}} & \mathcal{V}_{\beta j}^{S\hat{S}} & \mathcal{V}_{\beta k}^{S\hat{N}} \\ \mathcal{V}_{\gamma i}^{N\hat{\nu}} & \mathcal{V}_{\gamma j}^{N\hat{S}} & \mathcal{V}_{\gamma k}^{N\hat{N}} \end{pmatrix}^* \begin{pmatrix} \hat{\nu}_i \\ \hat{S}_j \\ \hat{N}_k^C \end{pmatrix} \quad (\text{D.4})$$

$$\text{and } \mathcal{V}^\dagger \mathcal{M}_\nu \mathcal{V}^* = \hat{\mathcal{M}}_\nu = \text{diag}(\hat{m}_{\nu_i}, \hat{m}_{S_j}, \hat{m}_{N_k}) \quad (\text{D.5})$$

where subscripts f, m denote the flavor and mass basis, respectively. Also, \mathcal{M}_ν is the complex symmetric mass matrix in flavor basis with α, β, γ running over three generations of three species ν, S, N_R^C in flavor state whereas $\hat{\mathcal{M}}_\nu$ is the diagonal mass matrix with $(i, j, k = 1, 2, 3)$ running over corresponding mass states.

By mapping our problem to the type-I seesaw analysis of [242] we make the close correspondence with the recipe followed there for our inverse seesaw case. Due to larger structure, we require to implement the mechanism more than once. The neutrino mass matrix in the type-I form [242] is

$$\mathcal{M}_\nu = \begin{pmatrix} \mathcal{M}_\mathcal{L} & \mathcal{M}_\mathcal{D}^T \\ \mathcal{M}_\mathcal{D} & \mathcal{M}_\mathcal{R} \end{pmatrix}. \quad (\text{D.6})$$

For the two case:

(i) $M_N = 0$

$$\mathcal{M}_\mathcal{L} = 0_{3 \times 3}, \quad \mathcal{M}_\mathcal{D} = \begin{pmatrix} 0 \\ M_D^T \end{pmatrix}_{6 \times 3}, \quad \mathcal{M}_\mathcal{R} = \begin{pmatrix} \mu_S & M \\ M^T & 0 \end{pmatrix}_{6 \times 6}, \quad (\text{D.7})$$

(ii) $M_N \neq 0$

$$\mathcal{M}_\mathcal{L} = \begin{pmatrix} 0 & 0 \\ 0 & \mu_s \end{pmatrix}_{6 \times 6}, \quad \mathcal{M}_\mathcal{D} = \begin{pmatrix} M_D^T & M^T \end{pmatrix}_{3 \times 6}, \quad \mathcal{M}_\mathcal{R} = M_N. \quad (\text{D.8})$$

The complete block diagonalization is achieved in two steps by recursively integrating out the heavier modes as

$$\mathcal{W}_1^\dagger \mathcal{M}_\nu \mathcal{W}_1^* = \hat{\mathcal{M}}'_\nu \quad \& \quad \mathcal{W}_2^\dagger \hat{\mathcal{M}}'_\nu \mathcal{W}_2^* = \hat{\mathcal{M}}_\nu \quad (\text{D.9})$$

where $\hat{\mathcal{M}}'_\nu$ is the block diagonalised 9×9 matrix after integrating out the heaviest mode and $\hat{\mathcal{M}}_\nu$ is the block diagonalised 9×9 matrix after integrating out the next

heaviest mode. The transformation matrices \mathcal{W}_1 can be written as a general unitary matrix in the form

$$\mathcal{W}_1^* = \begin{pmatrix} \sqrt{1 - \mathcal{B}\mathcal{B}^\dagger} & \mathcal{B} \\ -\mathcal{B}^\dagger & \sqrt{1 - \mathcal{B}^\dagger\mathcal{B}} \end{pmatrix} \quad (\text{D.10})$$

where for the case (i) \mathcal{B} is a 3×6 matrix and for the case (ii) \mathcal{B} is a 6×3 dimensional.

$$\sqrt{1 - \mathcal{B}\mathcal{B}^\dagger} = 1 - \frac{1}{2}\mathcal{B}\mathcal{B}^\dagger - \frac{1}{8}(\mathcal{B}\mathcal{B}^\dagger)^2 - \frac{1}{16}(\mathcal{B}\mathcal{B}^\dagger)^3 - \dots \quad (\text{D.11})$$

$$\mathcal{B} = \sum_i \mathcal{B}_i, \quad \mathcal{O}(\mathcal{M}_{\mathcal{R}}^{-i}) \quad (\text{D.12})$$

At the leading order it looks like

$$\sqrt{1 - \mathcal{B}\mathcal{B}^\dagger} = \mathbf{1} - \frac{1}{2}\mathcal{B}_1\mathcal{B}_1^\dagger - \frac{1}{2}(\mathcal{B}_1\mathcal{B}_2^\dagger + \mathcal{B}_2\mathcal{B}_1^\dagger) - \dots \quad (\text{D.13})$$

$$\begin{aligned} \mathcal{B}_1^\dagger &= \mathcal{M}_{\mathcal{R}}^{-1}\mathcal{M}_{\mathcal{D}} \\ \mathcal{B}_2^\dagger &= \mathcal{M}_{\mathcal{R}}^{-1}\mathcal{M}_{\mathcal{R}}^{*-1}\mathcal{M}_{\mathcal{D}}^*\mathcal{M}_{\mathcal{L}} \\ &= 0, \text{ if } \mathcal{M}_{\mathcal{L}} = 0 \end{aligned} \quad (\text{D.14})$$

The inverse of matrix $\mathcal{M}_{\mathcal{R}}$ in eq. D.7 is

$$\mathcal{M}_{\mathcal{R}}^{-1} = \begin{pmatrix} 0 & (M^T)^{-1} \\ M^{-1} & -M^{-1}\mu_S(M^{-1})^T \end{pmatrix} \quad (\text{D.15})$$

Hence for case (i):

$$\mathcal{B}_1^\dagger \simeq \begin{pmatrix} (M^{-1})^T M_D^T \\ -M^{-1}\mu_S(M^{-1})^T M_D^T \end{pmatrix} \quad (\text{D.16})$$

and for case (ii):

$$\mathcal{B}_1^\dagger = \begin{pmatrix} M_D M_N^{-1} \\ M M_N^{-1} \end{pmatrix}^T \quad (\text{D.17})$$

$$\sqrt{1 - \mathcal{B}\mathcal{B}^\dagger} \sim \mathbf{1} - \frac{1}{2}\mathcal{B}_1\mathcal{B}_1^\dagger \quad (\text{D.18})$$

Leaving the $\mathcal{O}(\mu_S^2)$ terms we get

$$(i) \quad \mathcal{B}_1 \mathcal{B}_1^\dagger \sim [M_D M^{-1} (M_D M^{-1})^\dagger]^T \quad (D.19)$$

$$(ii) \quad \mathcal{B}_1 \mathcal{B}_1^\dagger \sim \begin{pmatrix} (M_D M_N^{-1})^* (M_D M_N^{-1})^T & (M_D M_N^{-1})^* (M M_N^{-1})^T \\ (M M_N^{-1})^* (M_D M_N^{-1})^T & (M M_N^{-1})^* (M M_N^{-1})^T \end{pmatrix} \quad (D.20)$$

$$= \begin{pmatrix} (M_D M_N^{-1}) (M_D M_N^{-1})^\dagger & (M_D M_N^{-1}) (M M_N^{-1})^\dagger \\ (M M_N^{-1}) (M_D M_N^{-1})^\dagger & (M M_N^{-1}) (M M_N^{-1})^\dagger \end{pmatrix}^T \quad (D.21)$$

Therefore, if M is a real matrix for case (i) we get

$$(i) \quad \sqrt{1 - \mathcal{B}\mathcal{B}^\dagger} \sim \mathbf{1} - \frac{1}{2} \left(M_D M^{-2} M_D^\dagger \right)^T \quad (D.22)$$

$$(ii) \quad \sqrt{1 - \mathcal{B}\mathcal{B}^\dagger} \sim \mathbf{1} - \frac{1}{2} \begin{pmatrix} (M_D M_N^{-1}) (M_D M_N^{-1})^\dagger & (M_D M_N^{-1}) (M M_N^{-1})^\dagger \\ (M M_N^{-1}) (M_D M_N^{-1})^\dagger & (M M_N^{-1}) (M M_N^{-1})^\dagger \end{pmatrix}^T \quad (D.23)$$

Light and heavy neutrino mass matrices as listed in [242]

$$\begin{aligned} m_l &= \mathcal{M}_\mathcal{L} - \mathcal{M}_\mathcal{D}^T \mathcal{M}_\mathcal{R}^{-1} \mathcal{M}_\mathcal{D} \\ &\quad - \frac{1}{2} (\mathcal{M}_\mathcal{D}^T \mathcal{M}_\mathcal{R}^{-1} \mathcal{M}_\mathcal{R}^* \mathcal{M}_\mathcal{D}^* \mathcal{M}_\mathcal{L} + \mathcal{M}_\mathcal{L} \mathcal{M}_\mathcal{D}^\dagger \mathcal{M}_\mathcal{R}^* \mathcal{M}_\mathcal{R}^{-1} \mathcal{M}_\mathcal{D}) - \dots \\ m_H &= \mathcal{M}_\mathcal{R} + \frac{1}{2} (\mathcal{M}_\mathcal{D} \mathcal{M}_\mathcal{D}^\dagger \mathcal{M}_\mathcal{R}^* \mathcal{M}_\mathcal{R}^{-1} + \mathcal{M}_\mathcal{R}^* \mathcal{M}_\mathcal{D}^* \mathcal{M}_\mathcal{D}^T) + \dots \end{aligned} \quad (D.24)$$

Putting $\mathcal{M}_\mathcal{R}$ and $\mathcal{M}_\mathcal{D}$ from eq. D.7 and eq. D.8 in this expression gives

$$(i) \quad m_l \simeq M_D M_R^{-1} \mu_S [M_D M_R^{-1}]^T \quad (D.25)$$

$$m_H \simeq \begin{pmatrix} \mu_S & M \\ M^T & 0 \end{pmatrix} + \dots \quad (D.26)$$

$$(ii) \quad m_l \simeq \begin{pmatrix} 0 & 0 \\ 0 & \mu_S \end{pmatrix} - \begin{pmatrix} M_D M_N^{-1} M_D^T & M_D M_N^{-1} M^T \\ M M_N^{-1} M_D^T & M M_N^{-1} M^T \end{pmatrix} \quad (D.27)$$

$$m_H \simeq M_N + \dots \quad (D.28)$$

where m_l is light mass matrix and the m_H is the heavy element which is the remainder of whatever is getting integrated out. We also note that after this diagonalization the 9×9 matrix gets block diagonalised in to a 3×3 and a 6×6 . These 6×6 matrices can be further diagonalised using the similar technique. The above transformation matrix in dimensionless parameters $X = M_D M^{-1}$, $Y = M M_N^{-1}$, and $Z = M_D M_N^{-1}$

so that $Z = X \cdot Y \neq Y \cdot X$ and $y = M^{-1}\mu_S$, $z = M_N^{-1}\mu_S$, as

$$(i) \quad \mathcal{W}_1 = \begin{pmatrix} 1 - \frac{1}{2}XX^\dagger & X & Xy^T \\ -X^\dagger & 1 - \frac{1}{2}X^\dagger X & -X^\dagger Xy^T \\ -y^* X^\dagger & -y^* X^\dagger X & 1 - \frac{1}{2}y^* X^\dagger Xy^T \end{pmatrix} \quad (D.29)$$

$$(ii) \quad \mathcal{W}_1 = \begin{pmatrix} 1 - \frac{1}{2}ZZ^\dagger & -\frac{1}{2}ZY^\dagger & Z \\ -\frac{1}{2}YZ^\dagger & 1 - \frac{1}{2}YY^\dagger & Y \\ -Z^\dagger & -Y^\dagger & 1 - \frac{1}{2}(Z^\dagger Z + Y^\dagger Y) \end{pmatrix} \quad (D.30)$$

Thus

$$\mathcal{M}_\nu = \mathcal{W}_1 \begin{pmatrix} m_l & 0 \\ 0 & m_H \end{pmatrix} \mathcal{W}_1^T \quad (D.31)$$

In this block diagonalization process we see that in the case (i) the light neutrino acquire 3×3 structure and thus now can mimic the Majorana light neutrino mass matrix. The heavy mass matrix m_H is further diagonalized using the similar mechanism. The block diagonalization of the matrix in case (ii) integrates out the heaviest mass and the light state is 6×6 dimensional and further diagonalization.

From the above discussion, it is quite clear now that eventually the light neutrino eigenstates are decoupled from other in case (i), and eigenstates \mathcal{N}_i are decoupled from others in case (ii). The remaining mass matrices m_H in case (i) and m_l in case (ii) can be block diagonalized using another transformation matrix

$$\mathcal{W}_2^\dagger \begin{pmatrix} m_l & 0 \\ 0 & m_H \end{pmatrix} \mathcal{W}_2^* = \begin{pmatrix} m_\nu & 0 & 0 \\ 0 & m'_H & 0 \\ 0 & 0 & m''_H \end{pmatrix} \quad (D.32)$$

such that

$$(i) \quad \mathcal{W}_2 = \begin{pmatrix} 1 & 0 \\ 0 & \mathcal{S} \end{pmatrix} \quad (ii) \quad \mathcal{W}_2 = \begin{pmatrix} \mathcal{S} & 0 \\ 0 & 1 \end{pmatrix} \quad (D.33)$$

where \mathcal{S} are 6×6 matrices and \mathcal{W}_2 have the same dimension as \mathcal{M}_ν . In a simplified structure

$$-\mathcal{M}_{eff} = \begin{pmatrix} M_D Z^T & M_D Y^T \\ Y M_D^T & (M Y^T - \mu_S) \end{pmatrix} \quad (D.34)$$

Under the assumption at the beginning $Z \ll Y$, we immediately get the light

neutrino masses as

$$(i) \quad m_\nu \simeq M_D M^{-1} \mu_S (M_D M^{-1})^T \quad (D.35)$$

$$m'_H \simeq -M + \mu_S/2 \quad (D.36)$$

$$m''_H \simeq M + \mu_S/2 \quad (D.37)$$

$$(ii) \quad \begin{aligned} m_\nu &\simeq -M_D Z^T + M_D Y^T (M Y^T - \mu_S)^{-1} Y M_D^T \\ &\simeq -M_D Z^T + M_D Z^T + M_D M \mu_S (Z Y^{-1})^T \\ &\simeq M_D M^{-1} \mu_S (M_D M^{-1})^T \end{aligned} \quad (D.38)$$

$$m'_H \simeq \mu_S - M M_N^{-1} M^T \quad (D.39)$$

$$m''_H \simeq M_N. \quad (D.40)$$

Here we have made another assumption to get inverse seesaw, canceling the type-I seesaw, i.e $M Y^T \gg \mu_S$. We see that in addition to m'_H the m''_H is also almost diagonal if M and M_N are taken to be diagonal.

The transformation matrix S is

$$S^* = \begin{pmatrix} \sqrt{1 - \mathcal{A} \mathcal{A}^\dagger} & \mathcal{A} \\ -\mathcal{A}^\dagger & \sqrt{1 - \mathcal{A}^\dagger \mathcal{A}} \end{pmatrix} \quad (D.41)$$

such that

$$(i) \quad \mathcal{A} \simeq \frac{1}{\sqrt{2}} \mathbf{1}; \text{ for diagonal } M. \quad (D.42)$$

$$(ii) \quad \begin{aligned} \mathcal{A}^\dagger &\simeq (M Y^T - \mu_S)^{-1} Y M_D^T \\ &\simeq (1 + (M^T)^{-1} Y^{-1} \mu_S) X^T \simeq X^T. \end{aligned} \quad (D.43)$$

The 3×3 block diagonal mixing matrix \mathcal{W}_2 has the following form

$$\mathcal{W}_2 = \begin{pmatrix} S & \mathbf{0} \\ \mathbf{0} & \mathbf{1} \end{pmatrix} = \begin{pmatrix} 1 - \frac{1}{2} X X^\dagger & X & 0 \\ -X^\dagger & 1 - \frac{1}{2} X^\dagger X & 0 \\ 0 & 0 & 1 \end{pmatrix} \quad (D.44)$$

D.2 Complete diagonalization and physical neutrino masses

The block diagonal matrices m_ν , m_S and m_N can further be diagonalized to give physical masses for all neutral leptons by a unitary matrix \mathcal{U} as

$$\mathcal{U} = \begin{pmatrix} U_\nu & 0 & 0 \\ 0 & U_{H_1} & 0 \\ 0 & 0 & U_{H_2} \end{pmatrix}. \quad (\text{D.45})$$

where the unitary matrices U_ν , U_S and U_N satisfy

$$\begin{aligned} U_\nu^\dagger m_\nu U_\nu^* &= \hat{m}_\nu = \text{diag}(m_{\nu_1}, m_{\nu_2}, m_{\nu_3}), \\ U_{H_1}^\dagger m'_H U_{H_1}^* &= \hat{m}'_H = \text{diag}(m'_{H_1}, m'_{H_2}, m'_{H_3}), \\ U_{H_2}^\dagger m''_H U_{H_2}^* &= \hat{m}''_H = \text{diag}(m''_{H_1}, m''_{H_2}, m''_{H_3}) \end{aligned} \quad (\text{D.46})$$

For the sake of simplicity, in case (ii) we assume $m'_H = m_S$ and $m''_H = m_N$ and similarly $U_{H_1} = U_S$ and $U_{H_2} = U_N$.

Thus, the complete mixing matrix is

$$\begin{aligned} \text{(i) } \mathcal{V} &= \mathcal{W} \cdot \mathcal{U} = \mathcal{W}_1 \cdot \mathcal{W}_2 \cdot \mathcal{U} \\ &\simeq \begin{pmatrix} 1 - \frac{1}{2} X X^\dagger & -\frac{1}{2} X & X y^T \\ -X^\dagger & 1 - \frac{1}{2} X^\dagger X & -X^\dagger X y^T \\ -y^* X^\dagger & -y^* X^\dagger X & 1 - \frac{1}{2} y^* X^\dagger X y^T \end{pmatrix} \begin{pmatrix} 1 & 0 & 0 \\ 0 & \frac{1}{\sqrt{2}} \mathbf{1} & \frac{1}{\sqrt{2}} \mathbf{1} \\ 0 & -\frac{1}{\sqrt{2}} \mathbf{1} & \frac{1}{\sqrt{2}} \mathbf{1} \end{pmatrix} \\ &\quad \times \begin{pmatrix} U_\nu & 0 & 0 \\ 0 & U_{H_1} & 0 \\ 0 & 0 & U_{H_2} \end{pmatrix} \\ &\simeq \begin{pmatrix} 1 - \frac{1}{2} X X^\dagger & \frac{1}{\sqrt{2}} X & \frac{1}{\sqrt{2}} X \\ -X^\dagger & \frac{1}{\sqrt{2}} (1 - \frac{1}{2} X^\dagger X) & \frac{1}{\sqrt{2}} (1 - \frac{1}{2} X^\dagger X) \\ -y^* X^\dagger & -\frac{1}{\sqrt{2}} (1 + y^* X^\dagger X) & \frac{1}{\sqrt{2}} (1 - y^* X^\dagger X) \end{pmatrix} \\ &\quad \times \begin{pmatrix} U_\nu & 0 & 0 \\ 0 & U_{H_1} & 0 \\ 0 & 0 & U_{H_2} \end{pmatrix} \end{aligned} \quad (\text{D.47})$$

and

$$\begin{aligned}
\text{(ii) } \mathcal{V} &= \mathcal{W} \cdot \mathcal{U} = \mathcal{W}_1 \cdot \mathcal{W}_2 \cdot \mathcal{U} \\
&\simeq \begin{pmatrix} 1 - \frac{1}{2}ZZ^\dagger & -\frac{1}{2}ZY^\dagger & Z \\ -\frac{1}{2}YZ^\dagger & 1 - \frac{1}{2}YY^\dagger & Y \\ -Z^\dagger & -Y^\dagger & 1 - \frac{1}{2}(Z^\dagger Z + Y^\dagger Y) \end{pmatrix} \\
&\times \begin{pmatrix} 1 - \frac{1}{2}XX^\dagger & X & 0 \\ -X^\dagger & 1 - \frac{1}{2}X^\dagger X & 0 \\ 0 & 0 & 1 \end{pmatrix} \times \begin{pmatrix} U_\nu & 0 & 0 \\ 0 & U_S & 0 \\ 0 & 0 & U_N \end{pmatrix} \\
&\simeq \begin{pmatrix} 1 - \frac{1}{2}XX^\dagger & X - \frac{1}{2}ZY^\dagger & Z \\ -X^\dagger & 1 - \frac{1}{2}(X^\dagger X + YY^\dagger) & Y - \frac{1}{2}X^\dagger Z \\ \frac{1}{2}Z^\dagger XX^\dagger + y^* X^\dagger & -Y^\dagger & 1 - \frac{1}{2}Y^\dagger Y \end{pmatrix} \\
&\times \begin{pmatrix} U_\nu & 0 & 0 \\ 0 & U_S & 0 \\ 0 & 0 & U_N \end{pmatrix} \tag{D.48}
\end{aligned}$$

Here the $\mathcal{V}_{N\nu}$ element is negligibly smaller than other elements in the matrix. Also $Z^\dagger XX^\dagger$ term, which is usually ignored with respect to $y^* X^\dagger$, can be larger of the two. The $U_{S,N}$ matrices are very close to unity while U_ν is the popular PMNS matrix.

APPENDIX E

Estimation of experimental and GUT-threshold uncertainties on the unification scale

E.1 Analytic formulas

In contrast to other intermediate gauge symmetries, $SO(10)$ model with G_{224D} intermediate symmetry was noted to have the remarkable property that GUT threshold corrections arising out of super-heavy masses or higher dimensional operators identically vanish on $\sin^2 \theta_W$ or the G_{224D} breaking scale [83, 224–226]. We show how this property can be ensured in this model with precision gauge coupling unification while predicting vanishing GUT-threshold corrections on M_P , analytically, but with non-vanishing finite corrections on M_{GUT} . We derive the corresponding GUT threshold effects in $SO(10)$ model with three intermediate symmetry breaking steps, G_{224D} , G_{224} , and G_{2113} between the GUT and the standard model whereas the uncertainties in the mass scales has been discussed in ref. [82] only with single intermediate breaking. The symmetry breaking chain under consideration is

$$SO(10) \xrightarrow[M_{GUT}]{a_i'''} G_{224D} \xrightarrow[M_P]{a_i''} G_{224} \xrightarrow[M_C]{a_i'} G_{2113} \xrightarrow[M_R^0]{a_i} G_{SM} \xrightarrow[M_Z]{} G_{13}, \quad (\text{E.1})$$

where a_i''' , a_i'' , a_i' , and a_i are, respectively, the one-loop beta coefficients for the gauge group $G_{2_L 2_R 4_C D}$, $G_{2_L 2_R 4_C}$, $G_{2_L 1_R 1_B - L 3_C}$, and $G_{SM} \equiv G_{2_L 1_Y 3_C}$.

Following the formalism used in ref. [82, 83], one can write the expressions for two different contributions of $\sin^2 \theta_W(M_Z)$, and $\alpha_s(M_Z)$:

$$\begin{aligned}
16\pi \left(\alpha_s^{-1} - \frac{3}{8} \alpha_{\text{em}}^{-1} \right) &= \mathcal{A}_P \ln \left(\frac{M_P}{M_Z} \right) + \mathcal{A}_U \ln \left(\frac{M_{GUT}}{M_Z} \right) \\
&+ \mathcal{A}_C \ln \left(\frac{M_C}{M_Z} \right) + \mathcal{A}_0 \ln \left(\frac{M_R^0}{M_Z} \right) + f_M^U, \quad (\text{E.2})
\end{aligned}$$

where,

$$\begin{aligned}
\mathcal{A}_0 &= (8a_{3C} - 3a_{2L} - 5a_Y) - (8a'_{3C} - 3a'_{2L} - 3a'_{1R} - 2a'_{B-L}), \\
\mathcal{A}_C &= (8a'_{3C} - 3a'_{2L} - 3a'_{1R} - 2a'_{B-L}) - (6a''_{4C} - 3a''_{2L} - 3a''_{2R}), \\
\mathcal{A}_P &= (6a''_{4C} - 3a''_{2L} - 3a''_{2R}) - (6a'''_{4C} - 6a'''_{2L}), \\
\mathcal{A}_U &= (6a'''_{4C} - 6a'''_{2L}), \\
f_M^U &= \lambda_{2L}^U - \lambda_{4C}^U.
\end{aligned}$$

Similarly,

$$\begin{aligned}
16\pi \alpha_{\text{em}}^{-1} \left(\sin^2 \theta_W - \frac{3}{8} \right) &= \mathcal{B}_P \ln \left(\frac{M_P}{M_Z} \right) + \mathcal{B}_U \ln \left(\frac{M_{GUT}}{M_Z} \right) \\
&+ \mathcal{B}_C \ln \left(\frac{M_C}{M_Z} \right) + \mathcal{B}_0 \ln \left(\frac{M_R^0}{M_Z} \right) + f_\theta^U, \quad (\text{E.3})
\end{aligned}$$

with

$$\begin{aligned}
\mathcal{B}_0 &= (5a_{2L} - 5a_Y) - (5a'_{2L} - 3a'_{1R} - 2a'_{B-L}), \\
\mathcal{B}_C &= (5a'_{2L} - 3a'_{1R} - 2a'_{B-L}) - (5a''_{2L} - 3a''_{2R} - 2a''_{4C}), \\
\mathcal{B}_P &= (5a''_{2L} - 3a''_{2R} - 2a''_{4C}) - (2a'''_{2L} - 2a'''_{4C}), \\
\mathcal{B}_U &= (2a'''_{2L} - 2a'''_{4C}), \\
f_\theta^U &= \frac{1}{3} (\lambda_{4C}^U - \lambda_{2L}^U).
\end{aligned}$$

It is well known that threshold effects at intermediate scales are likely to introduce discontinuities in the gauge couplings thereby destroying possibilities of precision unification. This fact has led us to restrict the model with vanishing intermediate scale threshold corrections by assuming relevant sub-multiplets to have masses exactly equal to their respective intermediate scales which is applicable to the intermediate scales M_R^0 , M_R^+ , and M_C in the present work.

Denoting $\mathcal{C}_0 = 16\pi \left(\alpha_s^{-1} - \frac{3}{8} \alpha_{\text{em}}^{-1} \right)$, and $\mathcal{C}_1 = 16\pi \alpha_{\text{em}}^{-1} \left(\sin^2 \theta_W - \frac{3}{8} \right)$, one can

rewrite the eq. (E.2), and eq. (E.3) for M_P and M_{GUT} as

$$\begin{aligned}\mathcal{D}_0 &= \mathcal{A}_P \ln \left(\frac{M_P}{M_Z} \right) + \mathcal{A}_U \ln \left(\frac{M_{GUT}}{M_Z} \right) \\ &= \mathcal{C}_0 - \mathcal{A}_C \ln \left(\frac{M_C}{M_Z} \right) - \mathcal{A}_0 \ln \left(\frac{M_R^0}{M_Z} \right) - f_M^U,\end{aligned}\quad (\text{E.4})$$

$$\begin{aligned}\mathcal{D}_1 &= \mathcal{B}_P \ln \left(\frac{M_P}{M_Z} \right) + \mathcal{B}_U \ln \left(\frac{M_{GUT}}{M_Z} \right) \\ &= \mathcal{C}_1 - \mathcal{B}_C \ln \left(\frac{M_C}{M_Z} \right) - \mathcal{B}_0 \ln \left(\frac{M_R^0}{M_Z} \right) - f_\theta^U.\end{aligned}\quad (\text{E.5})$$

A formal solution for these two sets of eqns. (E.4), and (E.5),

$$\ln \left(\frac{M_{GUT}}{M_Z} \right) = \frac{\mathcal{D}_1 \mathcal{A}_P - \mathcal{D}_0 \mathcal{B}_P}{\mathcal{B}_U \mathcal{A}_P - \mathcal{A}_U \mathcal{B}_P}, \quad (\text{E.6})$$

$$\ln \left(\frac{M_P}{M_Z} \right) = \frac{\mathcal{D}_0 \mathcal{B}_U - \mathcal{D}_1 \mathcal{A}_U}{\mathcal{B}_U \mathcal{A}_P - \mathcal{A}_U \mathcal{B}_P}. \quad (\text{E.7})$$

In the present work, we derive two types of uncertainties in the mass scales of $SO(10)$ model i.e., the first one comes from low energy parameters taken from their experimental errors and another one arising from the threshold corrections accounting the theoretical uncertainties in the mass scales due to heavy Higgs fields present at GUT scale. These two categories are presented below:

E.2 Uncertainties due to experimental errors in $\sin^2 \theta_W$ and α_s

In eqns. (E.4) and (E.5) the low energy parameters are contained in \mathcal{C}_0 and \mathcal{C}_1 . As a result, we have got further simplified relations relevant for experimental uncertainties, i.e, $\Delta(\mathcal{D}_0) = \Delta(\mathcal{C}_0)$ and $\Delta(\mathcal{D}_1) = \Delta(\mathcal{C}_1)$, and hence,

$$\begin{aligned}\Delta \ln \left(\frac{M_{GUT}}{M_Z} \right) \Big|_{\text{expt.}} &= \frac{\Delta(\mathcal{C}_1) \mathcal{A}_P - \Delta(\mathcal{C}_0) \mathcal{B}_P}{\mathcal{B}_U \mathcal{A}_P - \mathcal{A}_U \mathcal{B}_P} \\ &= \frac{[(16\pi) \alpha_{\text{em}}^{-1} (\delta \sin^2 \theta_W)] \mathcal{A}_P - \left[-\frac{(16\pi)}{\alpha_s^2} (\delta \alpha_s) \right] \mathcal{B}_P}{\mathcal{B}_U \mathcal{A}_P - \mathcal{A}_U \mathcal{B}_P},\end{aligned}\quad (\text{E.8})$$

$$\begin{aligned}
\Delta \ln \left(\frac{M_P}{M_Z} \right) \Big|_{\text{expt.}} &= \frac{\Delta (\mathcal{C}_0) \mathcal{B}_U - \Delta (\mathcal{C}_1) \mathcal{A}_U}{\mathcal{B}_U \mathcal{A}_P - \mathcal{A}_U \mathcal{B}_P} \\
&= \frac{\left[-\frac{(16\pi)}{\alpha_s^2} (\delta \alpha_s) \right] \mathcal{B}_U - [(16\pi) \alpha_{\text{em}}^{-1} (\delta \sin^2 \theta_W)] \mathcal{A}_U}{\mathcal{B}_U \mathcal{A}_P - \mathcal{A}_U \mathcal{B}_P}, \quad (\text{E.9})
\end{aligned}$$

where, the errors in the experimental values on electroweak mixing angle $\sin^2 \theta_W$ and strong coupling constant α_s as $\sin^2 \theta_W = 0.23102 \mp 0.00005$, $\alpha_s = 0.118 \pm 0.003$ giving $\delta \alpha_s = \pm 0.003$ and $\delta \sin^2 \theta_W = \mp 0.00005$.

E.3 Uncertainties in M_U with vanishing correction on M_P

In the present work, we have considered minimal set of Higgs fields belonging to a larger $SO(10)$ Higgs representation implying other Higgs fields which do not take part in symmetry breaking will automatically present at GUT scale. Since we can not determine the masses of these heavy Higgs bosons and, hence, they introduce uncertainty in other mass scales M_P and M_{GUT} via renormalization group equations resulting source of GUT threshold uncertainty in our predictions for proton life time. For this particular model, the GUT threshold corrections to D -parity breaking scale and unification mass scale is presented below

$$\begin{aligned}
\Delta \ln \left(\frac{M_U}{M_Z} \right) \Big|_{\text{GUT Th.}} &= \frac{\Delta (\mathcal{D}_1) \mathcal{A}_P - \Delta (\mathcal{D}_0) \mathcal{B}_P}{\mathcal{B}_U \mathcal{A}_P - \mathcal{A}_U \mathcal{B}_P} \\
&= \frac{-f_M^U}{6 (a_{2L}''' - a_{4C}''')}, \quad (\text{E.10})
\end{aligned}$$

$$\begin{aligned}
\Delta \ln \left(\frac{M_P}{M_Z} \right) \Big|_{\text{GUT Th.}} &= \frac{\Delta (\mathcal{D}_0) \mathcal{B}_U - \Delta (\mathcal{D}_1) \mathcal{A}_U}{\mathcal{B}_U \mathcal{A}_P - \mathcal{A}_U \mathcal{B}_P} \\
&= \frac{\mathcal{B}_U f_M^U - \mathcal{A}_U f_\theta^U}{24 (a_{2L}'' - a_{4C}'') (a_{2L}'' - a_{4C}'')} = 0. \quad (\text{E.11})
\end{aligned}$$

The last step resulting in vanishing GUT-threshold correction analytically follows by using expressions for $f_M^U, f_\theta^U, \mathcal{B}_U$ and \mathcal{A}_U derived in Sec E.1. This was proved in ref. [226]

Bibliography

- [1] H. Weyl, “Electron and gravitation. 1. (in german),” *Z.Phys.*, vol. 56, pp. 330–352, 1929.
- [2] C.-N. Yang and R. L. Mills, “Conservation of Isotopic Spin and Isotopic Gauge Invariance,” *Phys.Rev.*, vol. 96, pp. 191–195, 1954.
- [3] S. Glashow, “Partial Symmetries of Weak Interactions,” *Nucl.Phys.*, vol. 22, pp. 579–588, 1961.
- [4] J. S. Schwinger, “A Theory of the Fundamental Interactions,” *Annals Phys.*, vol. 2, pp. 407–434, 1957.
- [5] F. Englert and R. Brout, “Broken Symmetry and the Mass of Gauge Vector Mesons,” *Phys.Rev.Lett.*, vol. 13, pp. 321–323, 1964.
- [6] P. W. Higgs, “Broken Symmetries and the Masses of Gauge Bosons,” *Phys.Rev.Lett.*, vol. 13, pp. 508–509, 1964.
- [7] A. Salam, “Weak and Electromagnetic Interactions,” *Conf.Proc.*, vol. C680519, pp. 367–377, 1968.
- [8] S. Weinberg, “A Model of Leptons,” *Phys.Rev.Lett.*, vol. 19, pp. 1264–1266, 1967.
- [9] D. J. Gross and F. Wilczek, “Ultraviolet Behavior of Nonabelian Gauge Theories,” *Phys.Rev.Lett.*, vol. 30, pp. 1343–1346, 1973.
- [10] H. D. Politzer, “Reliable Perturbative Results for Strong Interactions?,” *Phys.Rev.Lett.*, vol. 30, pp. 1346–1349, 1973.

- [11] L. H. L. Brown, M. Dresden and M. Riordan, eds., *The Rise of the Standard Model - A History of Particle Physics from 1964 to 1979*. Cambridge: Cambridge University Press, 1997.
- [12] G. 't Hooft, "Renormalization of Massless Yang-Mills Fields," *Nucl.Phys.*, vol. B33, pp. 173–199, 1971.
- [13] G. 't Hooft, "Renormalizable Lagrangians for Massive Yang-Mills Fields," *Nucl.Phys.*, vol. B35, pp. 167–188, 1971.
- [14] G. 't Hooft and M. Veltman, "Regularization and Renormalization of Gauge Fields," *Nucl.Phys.*, vol. B44, pp. 189–213, 1972.
- [15] F. Jegerlehner, "Renormalizing the standard model," *Conf.Proc.*, vol. C900603, pp. 476–590, 1990.
- [16] E. Kraus, "The Renormalization of the electroweak standard model to all orders," *Annals Phys.*, vol. 262, pp. 155–259, 1998.
- [17] G. Aad *et al.*, "Observation of a new particle in the search for the standard model higgs boson with the atlas detector at the lhc," *Phys.Lett.*, vol. B716, pp. 1–29, 2012.
- [18] S. Chatrchyan *et al.*, "Observation of a new boson at a mass of 125 GeV with the CMS experiment at the LHC," *Phys.Lett.*, vol. B716, pp. 30–61, 2012.
- [19] G. Altarelli, "Theoretical Models of Neutrino Mixing: Recent Developments," pp. 377–396, 2009.
- [20] G. Altarelli, "Status of Neutrino Masses and Mixing in 2010," *PoS*, vol. HRMS2010, p. 022, 2010.
- [21] G. Altarelli, "Perspectives in Neutrino Physics," pp. 383–391, 2011.
- [22] E. Ma, "Verifiable radiative seesaw mechanism of neutrino mass and dark matter," *Phys.Rev.*, vol. D73, p. 077301, 2006.
- [23] R. Mohapatra, S. Antusch, K. Babu, G. Barenboim, M.-C. Chen, *et al.*, "Theory of neutrinos: A White paper," *Rept.Prog.Phys.*, vol. 70, pp. 1757–1867, 2007.
- [24] R. Mohapatra, "Neutrino mass and unification," *Prog.Part.Nucl.Phys.*, vol. 64, pp. 307–312, 2010.

- [25] S. Raby, T. Walker, K. Babu, H. Baer, A. Balantekin, *et al.*, “DUSEL Theory White Paper,” 2008.
- [26] E. Ma, “Neutrino Mass: Mechanisms and Models,” 2009.
- [27] E. Ma, “Neutrino Mass Seesaw Version 3: Recent Developments,” *AIP Conf.Proc.*, vol. 1116, pp. 239–246, 2009. XIII Mexican School of Particles and Fields, San Carlos, Sonora, Mexico, Oct 2008.
- [28] H. Hettmansperger, M. Lindner, and W. Rodejohann, “Phenomenological Consequences of sub-leading Terms in See-Saw Formulas,” *JHEP*, vol. 1104, p. 123, 2011.
- [29] G. Senjanovic, “Neutrino mass: From LHC to grand unification,” *Riv.Nuovo Cim.*, vol. 034, pp. 1–68, 2011.
- [30] C. Aulakh and R. N. Mohapatra, “Implications of Supersymmetric SO(10) Grand Unification,” *Phys.Rev.*, vol. D28, p. 217, 1983; CCNY-HEP-82-4-REV, CCNY-HEP-82-4.
- [31] T. E. Clark, T.-K. Kuo, and N. Nakagawa, “A SO(10) SUPERSYMMETRIC GRAND UNIFIED THEORY,” *Phys. Lett.*, vol. B115, p. 26, 1982.
- [32] K. Babu and R. Mohapatra, “Predictive neutrino spectrum in minimal SO(10) grand unification,” *Phys.Rev.Lett.*, vol. 70, pp. 2845–2848, 1993.
- [33] C. S. Aulakh, B. Bajc, A. Melfo, G. Senjanovic, and F. Vissani, “The Minimal supersymmetric grand unified theory,” *Phys.Lett.*, vol. B588, pp. 196–202, 2004.
- [34] C. S. Aulakh and A. Girdhar, “SO(10) MSGUT: Spectra, couplings and threshold effects,” *Nucl.Phys.*, vol. B711, pp. 275–313, 2005.
- [35] B. Bajc, A. Melfo, G. Senjanovic, and F. Vissani, “The Minimal supersymmetric grand unified theory. 1. Symmetry breaking and the particle spectrum,” *Phys.Rev.*, vol. D70, p. 035007, 2004.
- [36] C. S. Aulakh, K. Benakli, and G. Senjanovic, “Reconciling supersymmetry and left-right symmetry,” *Phys.Rev.Lett.*, vol. 79, pp. 2188–2191, 1997.
- [37] C. S. Aulakh, A. Melfo, and G. Senjanovic, “Minimal supersymmetric left-right model,” *Phys.Rev.*, vol. D57, pp. 4174–4178, 1998.

- [38] C. S. Aulakh, A. Melfo, A. Rasin, and G. Senjanovic, “Seesaw and supersymmetry or exact R-parity,” *Phys.Lett.*, vol. B459, pp. 557–562, 1999.
- [39] M. Cvetič and J. C. Pati, “ $N = 1$ Supergravity Within the Minimal Left-right Symmetric Model,” *Phys.Lett.*, vol. B135, p. 57, 1984.
- [40] R. Kuchimanchi and R. Mohapatra, “No parity violation without R-parity violation,” *Phys.Rev.*, vol. D48, pp. 4352–4360, 1993.
- [41] C. S. Aulakh and S. K. Garg, “MSGUT : From bloom to doom,” *Nucl.Phys.*, vol. B757, pp. 47–78, 2006.
- [42] C. S. Aulakh, “MSGUTs from germ to bloom: Towards falsifiability and beyond,” 2005.
- [43] C. S. Aulakh and S. K. Garg, “The New Minimal Supersymmetric GUT : Spectra, RG analysis and Fermion Fits,” *Nucl. Phys.*, vol. B857, pp. 101–142, 2012.
- [44] C. S. Aulakh and S. K. Garg, “The New Minimal Supersymmetric GUT : Spectra, RG analysis and fitting formulae,” 2006.
- [45] P. B. Dev and R. Mohapatra, “TeV Scale Inverse Seesaw in SO(10) and Leptonic Non-Unitarity Effects,” *Phys.Rev.*, vol. D81, p. 013001, 2010.
- [46] J. C. Pati and A. Salam, “Unified Lepton-Hadron Symmetry and a Gauge Theory of the Basic Interactions,” *Phys.Rev.*, vol. D8, pp. 1240–1251, 1973.
- [47] J. C. Pati and A. Salam, “Lepton Number as the Fourth Color,” *Phys.Rev.*, vol. D10, pp. 275–289, 1974.
- [48] R. Mohapatra and J. C. Pati, “A Natural Left-Right Symmetry,” *Phys.Rev.*, vol. D11, p. 2558, 1975.
- [49] R. N. Mohapatra and J. C. Pati, “Left-Right Gauge Symmetry and an Isoconjugate Model of CP Violation,” *Phys.Rev.*, vol. D11, pp. 566–571, 1975.
- [50] H. Georgi and S. Glashow, “Unity of All Elementary Particle Forces,” *Phys.Rev.Lett.*, vol. 32, pp. 438–441, 1974.
- [51] H. Georgi, H. R. Quinn, and S. Weinberg, “Hierarchy of Interactions in Unified Gauge Theories,” *Phys.Rev.Lett.*, vol. 33, pp. 451–454, 1974.

- [52] H. Georgi, “The State of the Art - Gauge Theories. (Talk),” *AIP Conf.Proc.*, vol. 23, pp. 575–582, 1975.
- [53] A. De Rujula, H. Georgi, and S. Glashow, “Hadron Masses in a Gauge Theory,” *Phys.Rev.*, vol. D12, pp. 147–162, 1975.
- [54] H. Fritzsch and P. Minkowski, “Unified Interactions of Leptons and Hadrons,” *Annals Phys.*, vol. 93, pp. 193–266, 1975.
- [55] G. Senjanovic and R. N. Mohapatra, “Exact Left-Right Symmetry and Spontaneous Violation of Parity,” *Phys.Rev.*, vol. D12, p. 1502, 1975.
- [56] D. Chang, R. Mohapatra, and M. Parida, “Decoupling Parity and $SU(2)_R$ Breaking Scales: A New Approach to Left-Right Symmetric Models,” *Phys.Rev.Lett.*, vol. 52, p. 1072, 1984.
- [57] D. Chang, R. Mohapatra, and M. Parida, “A New Approach to Left-Right Symmetry Breaking in Unified Gauge Theories,” *Phys.Rev.*, vol. D30, p. 1052, 1984.
- [58] D. Chang, R. Mohapatra, J. Gipson, R. Marshak, and M. Parida, “Experimental Tests of New $SO(10)$ Grand Unification,” *Phys.Rev.*, vol. D31, p. 1718, 1985.
- [59] P. Minkowski, “ $\mu \rightarrow e\gamma$ at a Rate of One Out of 1-Billion Muon Decays?,” *Phys.Lett.*, vol. B67, p. 421, 1977.
- [60] T. Yanagida, “Horizontal symmetry and masses of neutrinos,” *Conf.Proc.*, vol. C7902131, pp. 95–99, 1979.
- [61] M. Gell-Mann, P. Ramond, and R. Slansky, “Complex Spinors and Unified Theories,” *Conf.Proc.*, vol. C790927, pp. 315–321, 1979.
- [62] S. Glashow, “The Future of Elementary Particle Physics,” *NATO Adv.Study Inst.Ser.B Phys.*, vol. 59, p. 687, 1980.
- [63] R. N. Mohapatra and G. Senjanovic, “Neutrino Mass and Spontaneous Parity Violation,” *Phys.Rev.Lett.*, vol. 44, p. 912, 1980.
- [64] R. N. Mohapatra and G. Senjanovic, “Neutrino Masses and Mixings in Gauge Models with Spontaneous Parity Violation,” *Phys.Rev.*, vol. D23, p. 165, 1981.

- [65] M. Magg and C. Wetterich, “Neutrino Mass Problem and Gauge Hierarchy,” *Phys.Lett.*, vol. B94, p. 61, 1980.
- [66] G. Lazarides, Q. Shafi, and C. Wetterich, “Proton Lifetime and Fermion Masses in an SO(10) Model,” *Nucl.Phys.*, vol. B181, pp. 287–300, 1981.
- [67] J. Schechter and J. Valle, “Neutrino Masses in $SU(2) \times U(1)$ Theories,” *Phys.Rev.*, vol. D22, p. 2227, 1980.
- [68] B. Brahmachari and R. Mohapatra, “Unified explanation of the solar and atmospheric neutrino puzzles in a minimal supersymmetric SO(10) model,” *Phys.Rev.*, vol. D58, p. 015001, 1998.
- [69] T. Fukuyama and N. Okada, “Neutrino oscillation data versus minimal supersymmetric SO(10) model,” *JHEP*, vol. 0211, p. 011, 2002.
- [70] N. Oshimo, “Antisymmetric Higgs representation in SO(10) for neutrinos,” *Phys.Rev.*, vol. D66, p. 095010, 2002.
- [71] B. Bajc, G. Senjanovic, and F. Vissani, “b - tau unification and large atmospheric mixing: A Case for noncanonical seesaw,” *Phys.Rev.Lett.*, vol. 90, p. 051802, 2003.
- [72] H. Goh, R. Mohapatra, and S. Nasri, “SO(10) symmetry breaking and type II seesaw,” *Phys.Rev.*, vol. D70, p. 075022, 2004.
- [73] R. Mohapatra and M. K. Parida, “Type II Seesaw Dominance in Non-supersymmetric and Split Susy SO(10) and Proton Life Time,” *Phys.Rev.*, vol. D84, p. 095021, 2011.
- [74] A. Melfo, A. Ramirez, and G. Senjanovic, “Type II see-saw dominance in SO(10),” *Phys.Rev.*, vol. D82, p. 075014, 2010.
- [75] G. Altarelli and G. Blankenburg, “Different SO(10) Paths to Fermion Masses and Mixings,” *JHEP*, vol. 1103, p. 133, 2011.
- [76] P. Bhupal Dev, R. Mohapatra, and M. Severson, “Neutrino Mixings in SO(10) with Type II Seesaw and θ_{13} ,” *Phys.Rev.*, vol. D84, p. 053005, 2011.
- [77] S. Bertolini, T. Schwetz, and M. Malinsky, “Fermion masses and mixings in SO(10) models and the neutrino challenge to SUSY GUTs,” *Phys.Rev.*, vol. D73, p. 115012, 2006.

- [78] W. J. Marciano and G. Senjanovic, “Predictions of Supersymmetric Grand Unified Theories,” *Phys.Rev.*, vol. D25, p. 3092, 1982.
- [79] U. Amaldi, W. de Boer, and H. Furstenau, “Comparison of grand unified theories with electroweak and strong coupling constants measured at LEP,” *Phys.Lett.*, vol. B260, pp. 447–455, 1991.
- [80] P. Langacker and M.-x. Luo, “Implications of precision electroweak experiments for M_t , ρ_0 , $\sin^2 \theta_W$ and grand unification,” *Phys.Rev.*, vol. D44, pp. 817–822, 1991.
- [81] N. Deshpande, E. Keith, and P. B. Pal, “Implications of LEP results for SO(10) grand unification,” *Phys.Rev.*, vol. D46, pp. 2261–2264, 1993.
- [82] R. Mohapatra and M. Parida, “Threshold effects on the mass scale predictions in SO(10) models and solar neutrino puzzle,” *Phys.Rev.*, vol. D47, pp. 264–272, 1993.
- [83] D.-G. Lee, R. Mohapatra, M. Parida, and M. Rani, “Predictions for proton lifetime in minimal nonsupersymmetric SO(10) models: An update,” *Phys.Rev.*, vol. D51, pp. 229–235, 1995.
- [84] H. Nishino *et al.*, “Search for Nucleon Decay into Charged Anti-lepton plus Meson in Super-Kamiokande I and II,” *Phys.Rev.*, vol. D85, p. 112001, 2012.
- [85] J. L. Raaf, “Recent Nucleon Decay Results from Super-Kamiokande,” *Nucl.Phys.Proc.Suppl.*, vol. 229-232, p. 559, 2012.
- [86] J. Hewett, H. Weerts, R. Brock, J. Butler, B. Casey, *et al.*, “Fundamental Physics at the Intensity Frontier,” 2012.
- [87] K. Babu, E. Kearns, U. Al-Binni, S. Banerjee, D. Baxter, *et al.*, “Baryon Number Violation,” 2013.
- [88] P. Langacker, “The Physics of Heavy Z' Gauge Bosons,” *Rev.Mod.Phys.*, vol. 81, pp. 1199–1228, 2009.
- [89] P. Langacker, “The Physics of New $U(1)'$ Gauge Bosons,” *AIP Conf.Proc.*, vol. 1200, pp. 55–63, 2010.
- [90] M. Parida and A. Raychaudhuri, “Low Mass Parity Restoration, Weak Interaction Phenomenology and Grand Unification,” *Phys.Rev.*, vol. D26, p. 2364, 1982.

- [91] M. Parida and C. Hazra, “Left-right Symmetry, K_L, K_S Mass Difference and a Possible New Formula for Neutrino Mass,” *Phys.Lett.*, vol. B121, p. 355, 1983.
- [92] M. Parida and C. Hazra, “Superheavy Higgs Scalar Effects in Effective Gauge Theories From SO(10) Grand Unification With Low Mass Right-handed Gauge Bosons,” *Phys.Rev.*, vol. D40, pp. 3074–3085, 1989.
- [93] O. Eboli, J. Gonzalez-Fraile, and M. Gonzalez-Garcia, “Present Bounds on New Neutral Vector Resonances from Electroweak Gauge Boson Pair Production at the LHC,” *Phys.Rev.*, vol. D85, p. 055019, 2012.
- [94] A. Falkowski, C. Grojean, A. Kaminska, S. Pokorski, and A. Weiler, “If no Higgs then what?,” *JHEP*, vol. 1111, p. 028, 2011.
- [95] P. Langacker, “The standard model and beyond,” 2009.
- [96] G. Altarelli, “The Standard model and beyond,” *Nucl. Phys. B - Proceedings Supplements*, vol. 75, no. 1–2, pp. 37 – 45, 1999.
- [97] F. Capozzi, G. Fogli, E. Lisi, A. Marrone, D. Montanino, *et al.*, “Status of three-neutrino oscillation parameters, circa 2013,” 2013.
- [98] G. Fogli, E. Lisi, A. Marrone, A. Melchiorri, A. Palazzo, *et al.*, “Observables sensitive to absolute neutrino masses. II,” *Phys.Rev.*, vol. D78, p. 033010, 2008.
- [99] J. e. a. Beringer, “Review of Particle Physics, 2012-2013. Review of Particle Properties,” *Phys. Rev. D*, vol. 86, no. 1, p. 010001, 2012. The 2012 edition of Review of Particle Physics is published for the Particle Data Group as article 010001 in volume 86 of Physical Review D. This edition should be cited as: J. Beringer et al. (Particle Data Group), Phys. Rev. D 86, 010001 (2012).
- [100] A. Sakharov, “Violation of CP Invariance, c Asymmetry, and Baryon Asymmetry of the Universe,” *Pisma Zh.Eksp.Teor.Fiz.*, vol. 5, pp. 32–35, 1967.
- [101] A. G. Cohen, D. Kaplan, and A. Nelson, “Progress in electroweak baryogenesis,” *Ann.Rev.Nucl.Part.Sci.*, vol. 43, pp. 27–70, 1993.
- [102] M. Quiros, “Field theory at finite temperature and phase transitions,” *Helv.Phys.Acta*, vol. 67, pp. 451–583, 1994.
- [103] V. Rubakov and M. Shaposhnikov, “Electroweak baryon number nonconservation in the early universe and in high-energy collisions,” *Usp.Fiz.Nauk*, vol. 166, pp. 493–537, 1996.

- [104] M. S. Carena, M. Quiros, and C. Wagner, “Electroweak baryogenesis and Higgs and stop searches at LEP and the Tevatron,” *Nucl.Phys.*, vol. B524, pp. 3–22, 1998.
- [105] G. Sigl, “Ultrahigh-energy cosmic rays: A Probe of physics and astrophysics at extreme energies,” *Science*, vol. 291, pp. 73–79, 2001.
- [106] D. Jones, “Two Loop Diagrams in Yang-Mills Theory,” *Nucl.Phys.*, vol. B75, p. 531, 1974.
- [107] D. Jones, “The Two Loop beta Function for a $G(1) \times G(2)$ Gauge Theory,” *Phys.Rev.*, vol. D25, p. 581, 1982.
- [108] A. Dighe, D. Ghosh, K. M. Patel, and S. Raychaudhuri, “Testing Times for Supersymmetry: Looking Under the Lamp Post,” *Int.J.Mod.Phys.*, vol. A28, p. 1350134, 2013.
- [109] P. Langacker, “Grand Unified Theories and Proton Decay,” *Phys.Rept.*, vol. 72, p. 185, 1981.
- [110] L.-F. Li, “Group Theory of the Spontaneously Broken Gauge Symmetries,” *Phys.Rev.*, vol. D9, pp. 1723–1739, 1974.
- [111] V. Elias, S. Eliezer, and A. Swift, “Comment on ‘Group Theory of the Spontaneously Broken Gauge Symmetries’,” *Phys.Rev.*, vol. D12, p. 3356, 1975.
- [112] R. N. Mohapatra, *Unification and Supersymmetry: The Frontiers of Quark-Lepton Physics*. New York: Springer, 2002.
- [113] G. G. Ross, *Grand Unified Theories*. New York: Frontiers in Physics, Westview Press, 1984.
- [114] H. Georgi, *Lie Algebras In Particle Physics: From Isospin To Unified Theories*. New York: Frontiers in Physics, Westview Press, 1999.
- [115] B. Bajc, “Grand unification and proton decay,” 2011. Lectures given in ICTP summer school on Particle Physics.
- [116] S. Dimopoulos and H. Georgi, “Softly Broken Supersymmetry and SU(5),” *Nucl.Phys.*, vol. B193, p. 150, 1981.
- [117] N. Sakai, “Naturalness in Supersymmetric Guts,” *Z.Phys.*, vol. C11, p. 153, 1981.

- [118] B. Bajc and G. Senjanovic, “Seesaw at LHC,” *JHEP*, vol. 0708, p. 014, 2007.
- [119] B. Bajc, M. Nemevsek, and G. Senjanovic, “Probing seesaw at LHC,” *Phys.Rev.*, vol. D76, p. 055011, 2007.
- [120] P. Fileviez Perez, “Renormalizable adjoint SU(5),” *Phys.Lett.*, vol. B654, pp. 189–193, 2007.
- [121] R. N. Mohapatra and B. Sakita, “SO(2n) Grand Unification in an SU(N) Basis,” *Phys.Rev.*, vol. D21, p. 1062, 1980.
- [122] P. Nath and R. M. Syed, “Analysis of couplings with large tensor representations in SO(2N) and proton decay,” *Phys.Lett.*, vol. B506, pp. 68–76, 2001.
- [123] C. S. Aulakh and A. Girdhar, “SO(10) a la Pati-Salam,” *Int.J.Mod.Phys.*, vol. A20, pp. 865–894, 2005.
- [124] T. Fukuyama, A. Ilakovac, T. Kikuchi, S. Meljanac, and N. Okada, “SO(10) group theory for the unified model building,” *J.Math.Phys.*, vol. 46, p. 033505, 2005.
- [125] R. Slansky, “Group Theory for Unified Model Building,” *Phys.Rept.*, vol. 79, pp. 1–128, 1981.
- [126] J. M. Gipson and R. Marshak, “Intermediate Mass Scales in the New SO(10) Grand Unification in the One Loop Approximation,” *Phys.Rev.*, vol. D31, p. 1705, 1985.
- [127] S. Bertolini, L. Di Luzio, and M. Malinsky, “Intermediate mass scales in the non-supersymmetric SO(10) grand unification: A Reappraisal,” *Phys.Rev.*, vol. D80, p. 015013, 2009.
- [128] H. Georgi and D. V. Nanopoulos, “Ordinary Predictions from Grand Principles: T Quark Mass in O(10),” *Nucl.Phys.*, vol. B155, p. 52, 1979.
- [129] S. M. Barr, “A New Symmetry Breaking Pattern for SO(10) and Proton Decay,” *Phys.Lett.*, vol. B112, p. 219, 1982.
- [130] K. Babu and E. Ma, “Symmetry Breaking in SO(10): Higgs Boson Structure,” *Phys.Rev.*, vol. D31, p. 2316, 1985.
- [131] M. Yasue, “How to break SO(10) VIA $SO(4) \times SO(6)$ down to $SU(2)_L \times SU(3)_C \times U(1)$,” *Phys.Lett.*, vol. B103, p. 33, 1981.

- [132] D. Chang and A. Kumar, “Symmetry Breaking of SO(10) by 210-dimensional Higgs Boson and the Michel’s Conjecture,” *Phys.Rev.*, vol. D33, p. 2695, 1986.
- [133] M. Yasue, “Symmetry Breaking of SO(10) and Constraints on Higgs Potential. 1. Adjoint (45) and Spinorial (16),” *Phys.Rev.*, vol. D24, p. 1005, 1981.
- [134] F. Buccella, J. P. Derendinger, S. Ferrara, and C. A. Savoy, “Patterns of Symmetry Breaking in Supersymmetric Gauge Theories,” *Phys. Lett.*, vol. B115, p. 375, 1982.
- [135] K. S. Babu and S. M. Barr, “Supersymmetric SO(10) simplified,” *Phys. Rev.*, vol. D51, pp. 2463–2470, 1995.
- [136] C. S. Aulakh, B. Bajc, A. Melfo, A. Rasin, and G. Senjanovic, “SO(10) theory of R-parity and neutrino mass,” *Nucl.Phys.*, vol. B597, pp. 89–109, 2001.
- [137] F. Buccella, H. Ruegg, and C. A. Savoy, “Spontaneous Symmetry Breaking in O(10),” *Phys. Lett.*, vol. B94, p. 491, 1980.
- [138] G. Anastaze, J. P. Derendinger, and F. Buccella, “INTERMEDIATE SYMMETRIES IN THE SO(10) MODEL WITH (16+16) + 45 HIGGSES,” *Z. Phys.*, vol. C20, pp. 269–273, 1983.
- [139] S. Bertolini, L. Di Luzio, and M. Malinsky, “On the vacuum of the minimal nonsupersymmetric SO(10) unification,” *Phys. Rev.*, vol. D81, p. 035015, 2010.
- [140] S. Weinberg, “Baryon and Lepton Nonconserving Processes,” *Phys.Rev.Lett.*, vol. 43, pp. 1566–1570, 1979.
- [141] R. Foot, H. Lew, X. He, and G. C. Joshi, “Seesaw Neutrino Masses Induced by a Triplet of Leptons,” *Z.Phys.*, vol. C44, p. 441, 1989.
- [142] P. Bhupal Dev and R. Mohapatra, “Electroweak Symmetry Breaking and Proton Decay in SO(10) SUSY-GUT with TeV W(R),” *Phys.Rev.*, vol. D82, p. 035014, 2010.
- [143] R. Mohapatra, “Mechanism for Understanding Small Neutrino Mass in Superstring Theories,” *Phys.Rev.Lett.*, vol. 56, pp. 561–563, 1986.
- [144] R. Mohapatra and J. Valle, “Neutrino Mass and Baryon Number Nonconservation in Superstring Models,” *Phys.Rev.*, vol. D34, p. 1642, 1986.

- [145] S. Bertolini, L. Di Luzio, and M. Malinsky, “Seesaw Scale in the Minimal Renormalizable SO(10) Grand Unification,” *Phys.Rev.*, vol. D85, p. 095014, 2012.
- [146] L. Lavoura, “On the renormalization group analysis of gauge groups containing $U(1) \times U(1)$ factors,” *Phys.Rev.*, vol. D48, pp. 2356–2359, 1993.
- [147] F. del Aguila, G. Coughlan, and M. Quiros, “Gauge Coupling Renormalization With Several U(1) Factors,” *Nucl.Phys.*, vol. B307, p. 633, 1988.
- [148] F. del Aguila, M. Masip, and M. Perez-Victoria, “Physical parameters and renormalization of $U(1)_a \times U(1)_b$ models,” *Nucl.Phys.*, vol. B456, pp. 531–549, 1995.
- [149] K. Nakamura *et al.*, “Review of particle physics,” *J.Phys.*, vol. G37, p. 075021, 2010.
- [150] C. Amsler *et al.*, “Review of Particle Physics,” *Phys.Lett.*, vol. B667, pp. 1–1340, 2008.
- [151] P. Nath and P. Fileviez Perez, “Proton stability in grand unified theories, in strings and in branes,” *Phys.Rept.*, vol. 441, pp. 191–317, 2007.
- [152] H. Nishino *et al.*, “Search for Proton Decay via $p \rightarrow e^+\pi^0$ and $p \rightarrow \mu^+\pi^0$ in a Large Water Cherenkov Detector,” *Phys.Rev.Lett.*, vol. 102, p. 141801, 2009.
- [153] K. Abe, T. Abe, H. Aihara, Y. Fukuda, Y. Hayato, *et al.*, “Letter of Intent: The Hyper-Kamiokande Experiment — Detector Design and Physics Potential —,” 2011.
- [154] B. A. Dobrescu, K. Kong, and R. Mahbubani, “Leptons and photons at the LHC: Cascades through spinless adjoints,” *JHEP*, vol. 0707, p. 006, 2007.
- [155] Y. Bai and B. A. Dobrescu, “Heavy octets and Tevatron signals with three or four b jets,” *JHEP*, vol. 1107, p. 100, 2011.
- [156] M. K. Parida, P. K. Sahu, and K. Bora, “Flavor unification, dark matter, proton decay and other observable predictions with low-scale S_4 symmetry,” *Phys.Rev.*, vol. D83, p. 093004, 2011.
- [157] M. K. Parida, “Radiative Seesaw in SO(10) with Dark Matter,” *Phys.Lett.*, vol. B704, pp. 206–210, 2011.

- [158] M. Lindner, M. A. Schmidt, and A. Y. Smirnov, “Screening of Dirac flavor structure in the seesaw and neutrino mixing,” *JHEP*, vol. 0507, p. 048, 2005.
- [159] S. K. Kang and C. Kim, “Extended double seesaw model for neutrino mass spectrum and low scale leptogenesis,” *Phys.Lett.*, vol. B646, pp. 248–252, 2007.
- [160] J. R. Ellis, D. V. Nanopoulos, and K. A. Olive, “Flipped heavy neutrinos: From the solar neutrino problem to baryogenesis,” *Phys.Lett.*, vol. B300, pp. 121–127, 1993.
- [161] S. K. Majee, M. K. Parida, and A. Raychaudhuri, “Neutrino mass and low-scale leptogenesis in a testable SUSY SO(10) model,” *Phys.Lett.*, vol. B668, pp. 299–302, 2008.
- [162] M. K. Parida and A. Raychaudhuri, “Inverse see-saw, leptogenesis, observable proton decay and $\Delta_R^{\pm\pm}$ in SUSY SO(10) with heavy W_R ,” *Phys.Rev.*, vol. D82, p. 093017, 2010.
- [163] S. K. Majee, M. K. Parida, A. Raychaudhuri, and U. Sarkar, “Low intermediate scales for leptogenesis in SUSY SO(10) GUTs,” *Phys.Rev.*, vol. D75, p. 075003, 2007.
- [164] F. Deppisch, T. Kosmas, and J. Valle, “Enhanced $\mu \rightarrow e$ - conversion in nuclei in the inverse seesaw model,” *Nucl.Phys.*, vol. B752, pp. 80–92, 2006.
- [165] F. Deppisch and J. Valle, “Enhanced lepton flavor violation in the supersymmetric inverse seesaw model,” *Phys.Rev.*, vol. D72, p. 036001, 2005.
- [166] J. Garayoa, M. Gonzalez-Garcia, and N. Rius, “Soft leptogenesis in the inverse seesaw model,” *JHEP*, vol. 0702, p. 021, 2007.
- [167] C. Arina, F. Bazzocchi, N. Fornengo, J. Romao, and J. Valle, “Minimal supergravity sneutrino dark matter and inverse seesaw neutrino masses,” *Phys.Rev.Lett.*, vol. 101, p. 161802, 2008.
- [168] F. Bazzocchi, D. Cerdeno, C. Munoz, and J. Valle, “Calculable inverse-seesaw neutrino masses in supersymmetry,” *Phys.Rev.*, vol. D81, p. 051701, 2010.
- [169] M. Gavela, T. Hambye, D. Hernandez, and P. Hernandez, “Minimal Flavour Seesaw Models,” *JHEP*, vol. 0909, p. 038, 2009.

- [170] M. Malinsky, T. Ohlsson, Z.-z. Xing, and H. Zhang, “Non-unitary neutrino mixing and CP violation in the minimal inverse seesaw model,” *Phys.Lett.*, vol. B679, pp. 242–248, 2009.
- [171] M. Hirsch, T. Kernreiter, J. Romao, and A. Villanova del Moral, “Minimal Supersymmetric Inverse Seesaw: Neutrino masses, lepton flavour violation and LHC phenomenology,” *JHEP*, vol. 1001, p. 103, 2010.
- [172] F. Bazzocchi, “Minimal Dynamical Inverse See Saw,” *Phys.Rev.*, vol. D83, p. 093009, 2011.
- [173] M. Catano, R. Martinez, and F. Ochoa, “Neutrino masses in a 331 model with right-handed neutrinos without doubly charged Higgs bosons via inverse and double seesaw mechanisms,” *Phys.Rev.*, vol. D86, p. 073015, 2012.
- [174] M. Hirsch, W. Porod, L. Reichert, and F. Staub, “Phenomenology of the minimal supersymmetric $U(1)_{B-L} \times U(1)_R$ extension of the standard model,” *Phys.Rev.*, vol. D86, p. 093018, 2012.
- [175] X.-G. He and E. Ma, “Seesaw Options for Three Neutrinos,” *Phys.Lett.*, vol. B683, pp. 178–182, 2010.
- [176] A. Abada, D. Das, and C. Weiland, “Enhanced Higgs Mediated Lepton Flavour Violating Processes in the Supersymmetric Inverse Seesaw Model,” *JHEP*, vol. 1203, p. 100, 2012.
- [177] A. Abada, D. Das, A. Vicente, and C. Weiland, “Enhancing lepton flavour violation in the supersymmetric inverse seesaw beyond the dipole contribution,” *JHEP*, vol. 1209, p. 015, 2012.
- [178] P. Bhupal Dev, S. Mondal, B. Mukhopadhyaya, and S. Roy, “Phenomenology of Light Sneutrino Dark Matter in cMSSM/mSUGRA with Inverse Seesaw,” *JHEP*, vol. 1209, p. 110, 2012.
- [179] S. Khalil, “TeV-scale gauged B-L symmetry with inverse seesaw mechanism,” *Phys.Rev.*, vol. D82, p. 077702, 2010.
- [180] S. Khalil, H. Okada, and T. Toma, “Right-handed Sneutrino Dark Matter in Supersymmetric B-L Model,” *JHEP*, vol. 1107, p. 026, 2011.
- [181] P.-H. Gu and U. Sarkar, “Leptogenesis with Linear, Inverse or Double Seesaw,” *Phys.Lett.*, vol. B694, pp. 226–232, 2010.

- [182] G. 'tHooft, “Naturalness, chiral symmetry, and spontaneous chiral symmetry breaking. (lecture iii),” 1980. Recent developments in Gauge theories, Cargese (Plenum Press, New York).
- [183] E. Ma, “Inverse Seesaw Neutrino Mass from Lepton Triplets in the U(1)(Sigma) Model,” *Mod.Phys.Lett.*, vol. A24, pp. 2491–2495, 2009.
- [184] D. Ibanez, S. Morisi, and J. Valle, “Inverse tri-bimaximal type-III seesaw and lepton flavor violation,” *Phys.Rev.*, vol. D80, p. 053015, 2009.
- [185] E. Ma, “Radiative inverse seesaw mechanism for nonzero neutrino mass,” *Phys.Rev.*, vol. D80, p. 013013, 2009.
- [186] C. Das and M. Parida, “New formulas and predictions for running fermion masses at higher scales in SM, 2 HDM, and MSSM,” *Eur.Phys.J.*, vol. C20, pp. 121–137, 2001.
- [187] S. Antusch, J. P. Baumann, and E. Fernandez-Martinez, “Non-Standard Neutrino Interactions with Matter from Physics Beyond the Standard Model,” *Nucl.Phys.*, vol. B810, pp. 369–388, 2009.
- [188] S. Antusch, M. Blennow, E. Fernandez-Martinez, and J. Lopez-Pavon, “Probing non-unitary mixing and CP-violation at a Neutrino Factory,” *Phys.Rev.*, vol. D80, p. 033002, 2009.
- [189] S. Antusch, C. Biggio, E. Fernandez-Martinez, M. Gavela, and J. Lopez-Pavon, “Unitarity of the Leptonic Mixing Matrix,” *JHEP*, vol. 0610, p. 084, 2006.
- [190] D. Forero, S. Morisi, M. Tortola, and J. Valle, “Lepton flavor violation and non-unitary lepton mixing in low-scale type-I seesaw,” *JHEP*, vol. 1109, p. 142, 2011.
- [191] E. Fernandez-Martinez, M. Gavela, J. Lopez-Pavon, and O. Yasuda, “CP-violation from non-unitary leptonic mixing,” *Phys.Lett.*, vol. B649, pp. 427–435, 2007.
- [192] K. Kanaya, “Neutrino Mixing in the Minimal SO(10) Model,” *Prog.Theor.Phys.*, vol. 64, p. 2278, 1980.
- [193] J. Kersten and A. Y. Smirnov, “Right-Handed Neutrinos at CERN LHC and the Mechanism of Neutrino Mass Generation,” *Phys.Rev.*, vol. D76, p. 073005, 2007.

- [194] M. Malinsky, T. Ohlsson, and H. Zhang, “Non-unitarity effects in a realistic low-scale seesaw model,” *Phys.Rev.*, vol. D79, p. 073009, 2009.
- [195] G. Altarelli and D. Meloni, “CP violation in neutrino oscillations and new physics,” *Nucl.Phys.*, vol. B809, pp. 158–182, 2009.
- [196] F. del Aguila and J. Aguilar-Saavedra, “Electroweak scale seesaw and heavy Dirac neutrino signals at LHC,” *Phys.Lett.*, vol. B672, pp. 158–165, 2009.
- [197] F. del Aguila, J. Aguilar-Saavedra, and J. de Blas, “Trilepton signals: the golden channel for seesaw searches at LHC,” *Acta Phys.Polon.*, vol. B40, pp. 2901–2911, 2009.
- [198] A. van der Schaaf, “Muon physics at a neutrino factory,” *J.Phys.*, vol. G29, pp. 2755–2762, 2003.
- [199] K. Abe *et al.*, “Indication of Electron Neutrino Appearance from an Accelerator-produced Off-axis Muon Neutrino Beam,” *Phys.Rev.Lett.*, vol. 107, p. 041801, 2011.
- [200] F. An *et al.*, “Observation of electron-antineutrino disappearance at Daya Bay,” *Phys.Rev.Lett.*, vol. 108, p. 171803, 2012.
- [201] P. Adamson *et al.*, “Improved search for muon-neutrino to electron-neutrino oscillations in MINOS,” *Phys.Rev.Lett.*, vol. 107, p. 181802, 2011.
- [202] J. Ahn *et al.*, “Observation of Reactor Electron Antineutrino Disappearance in the RENO Experiment,” *Phys.Rev.Lett.*, vol. 108, p. 191802, 2012.
- [203] G. Fogli, E. Lisi, A. Marrone, D. Montanino, A. Palazzo, *et al.*, “Global analysis of neutrino masses, mixings and phases: entering the era of leptonic CP violation searches,” *Phys.Rev.*, vol. D86, p. 013012, 2012.
- [204] T. Schwetz, M. Tortola, and J. Valle, “Global neutrino data and recent reactor fluxes: status of three-flavour oscillation parameters,” *New J.Phys.*, vol. 13, p. 063004, 2011.
- [205] D. Forero, M. Tortola, and J. Valle, “Global status of neutrino oscillation parameters after Neutrino-2012,” *Phys.Rev.*, vol. D86, p. 073012, 2012.
- [206] A. Ilakovac and A. Pilaftsis, “Flavor violating charged lepton decays in seesaw-type models,” *Nucl.Phys.*, vol. B437, p. 491, 1995.

- [207] J. Adam *et al.*, “New constraint on the existence of the $\mu^+ \rightarrow e^+\gamma$ decay,” *Phys.Rev.Lett.*, vol. 110, no. 20, p. 201801, 2013.
- [208] B. Aubert *et al.*, “Searches for Lepton Flavor Violation in the Decays $\tau^\pm \rightarrow e^\pm\gamma$ and $\tau^\pm \rightarrow \mu^\pm\gamma$,” *Phys.Rev.Lett.*, vol. 104, p. 021802, 2010.
- [209] F. Joaquim and A. Rossi, “Phenomenology of the triplet seesaw mechanism with Gauge and Yukawa mediation of SUSY breaking,” *Nucl.Phys.*, vol. B765, pp. 71–117, 2007.
- [210] Y. Kuno, “PRISM/PRIME,” *Nucl.Phys.Proc.Suppl.*, vol. 149, pp. 376–378, 2005.
- [211] C. H. Albright and S. M. Barr, “Explicit SO(10) supersymmetric grand unified model for the Higgs and Yukawa sectors,” *Phys.Rev.Lett.*, vol. 85, pp. 244–247, 2000.
- [212] C. H. Albright and S. M. Barr, “Construction of a minimal Higgs SO(10) SUSY GUT model,” *Phys.Rev.*, vol. D62, p. 093008, 2000.
- [213] S. Barr, “Overview of SUSY GUT models of neutrino mixing,” *Int.J.Mod.Phys.*, vol. A18, pp. 3971–3979, 2003.
- [214] C. H. Albright and S. Barr, “Leptogenesis in the type III seesaw mechanism,” *Phys.Rev.*, vol. D69, p. 073010, 2004.
- [215] S. Blanchet, P. B. Dev, and R. Mohapatra, “Leptogenesis with TeV Scale Inverse Seesaw in SO(10),” *Phys.Rev.*, vol. D82, p. 115025, 2010.
- [216] F. Gursev, P. Ramond, and P. Sikivie, “A Universal Gauge Theory Model Based on E_6 ,” *Phys.Lett.*, vol. B60, p. 177, 1976.
- [217] E. Ma, “Particle Dichotomy and Left-Right Decomposition of E(6) Superstring Models,” *Phys.Rev.*, vol. D36, p. 274, 1987.
- [218] S. Glashow, “in grand unification. proceedings, 5th workshop, providence, usa, 1974,” 1984. edited by K. Kang (World Scientific, Singapore, 1985).
- [219] C. Cauet, H. Pas, S. Wiesenfeldt, C. Cauet, H. Pas, *et al.*, “Trinification, the Hierarchy Problem and Inverse Seesaw Neutrino Masses,” *Phys.Rev.*, vol. D83, p. 093008, 2011.

- [220] S. Heinemeyer, E. Ma, M. Mondragon, and G. Zoupanos, “Finiteness in $SU(3)^3$ models,” *Fortsch.Phys.*, vol. 58, pp. 729–732, 2010.
- [221] S. Heinemeyer, E. Ma, M. Mondragon, and G. Zoupanos, “Finite $SU(3)^3$ model,” *AIP Conf.Proc.*, vol. 1200, pp. 568–571, 2010.
- [222] E. Ma, “Dark Left-Right Model: CDMS, LHC, etc,” *J.Phys.Conf.Ser.*, vol. 315, p. 012006, 2011.
- [223] V. V. Dixit and M. Sher, “The Futility of High Precision $SO(10)$ Calculations,” *Phys.Rev.*, vol. D40, p. 3765, 1989.
- [224] M. Parida and P. Patra, “Useful theorem on vanishing threshold contribution to $\sin^2(\theta_W)$ in a class of grand unified theories,” *Phys.Rev.Lett.*, vol. 66, pp. 858–861, 1991.
- [225] M. Parida and P. Patra, “Theorem on vanishing multiloop radiative corrections to $\sin^2(\theta_W)$ in grand unified theories at high mass scales,” *Phys.Rev.Lett.*, vol. 68, pp. 754–756, 1992.
- [226] M. Parida, “Vanishing corrections on intermediate scale and implications for unification of forces.,” *Phys.Rev.*, vol. D57, pp. 2736–2742, 1998.
- [227] T. Kibble, G. Lazarides, and Q. Shafi, “Walls Bounded by Strings,” *Phys.Rev.*, vol. D26, p. 435, 1982.
- [228] T. Lee and C.-N. Yang, “Question of Parity Conservation in Weak Interactions,” *Phys.Rev.*, vol. 104, pp. 254–258, 1956.
- [229] H. Klapdor-Kleingrothaus, A. Dietz, L. Baudis, G. Heusser, I. Krivosheina, *et al.*, “Latest results from the Heidelberg-Moscow double beta decay experiment,” *Eur.Phys.J.*, vol. A12, pp. 147–154, 2001.
- [230] C. Arnaboldi *et al.*, “Results from a search for the 0 neutrino beta beta-decay of Te-130,” *Phys.Rev.*, vol. C78, p. 035502, 2008.
- [231] C. Aalseth *et al.*, “The IGEX Ge-76 neutrinoless double beta decay experiment: Prospects for next generation experiments,” *Phys.Rev.*, vol. D65, p. 092007, 2002.
- [232] J. Argyriades *et al.*, “Measurement of the Double Beta Decay Half-life of Nd-150 and Search for Neutrinoless Decay Modes with the NEMO-3 Detector,” *Phys.Rev.*, vol. C80, p. 032501, 2009.

- [233] I. Abt, M. F. Altmann, A. Bakalyarov, I. Barabanov, C. Bauer, *et al.*, “A New Ge-76 double beta decay experiment at LNGS: Letter of intent,” 2004.
- [234] S. Schonert *et al.*, “The GERmanium Detector Array (GERDA) for the search of neutrinoless beta beta decays of Ge-76 at LNGS,” *Nucl.Phys.Proc.Suppl.*, vol. 145, pp. 242–245, 2005.
- [235] C. Arnaboldi *et al.*, “CUORE: A Cryogenic underground observatory for rare events,” *Nucl.Instrum.Meth.*, vol. A518, pp. 775–798, 2004.
- [236] H. Klapdor-Kleingrothaus, I. Krivosheina, A. Dietz, and O. Chkvorets, “Search for neutrinoless double beta decay with enriched ^{76}Ge in Gran Sasso 1990–2003,” *Phys.Lett.*, vol. B586, pp. 198–212, 2004.
- [237] H. Klapdor-Kleingrothaus and I. Krivosheina, “The evidence for the observation of $0\nu\beta\beta$ decay: The identification of $0\nu\beta\beta$ events from the full spectra,” *Mod.Phys.Lett.*, vol. A21, pp. 1547–1566, 2006.
- [238] H. Klapdor-Kleingrothaus, A. Dietz, H. Harney, and I. Krivosheina, “Evidence for neutrinoless double beta decay,” *Mod.Phys.Lett.*, vol. A16, pp. 2409–2420, 2001.
- [239] H. Klapdor-Kleingrothaus, A. Dietz, and I. Krivosheina, “Neutrinoless double beta decay: Status of evidence,” *Found.Phys.*, vol. 32, pp. 1181–1223, 2002.
- [240] E. Majorana, “Theory of the Symmetry of Electrons and Positrons,” *Nuovo Cim.*, vol. 14, pp. 171–184, 1937.
- [241] E. Witten, “New Issues in Manifolds of SU(3) Holonomy,” *Nucl.Phys.*, vol. B268, p. 79, 1986.
- [242] W. Grimus and L. Lavoura, “The Seesaw mechanism at arbitrary order: Disentangling the small scale from the large scale,” *JHEP*, vol. 0011, p. 042, 2000.
- [243] M. Hirsch, H. Klapdor-Kleingrothaus, and O. Panella, “Double beta decay in left-right symmetric models,” *Phys.Lett.*, vol. B374, pp. 7–12, 1996.
- [244] M. Mitra, G. Senjanovic, and F. Vissani, “Neutrinoless Double Beta Decay and Heavy Sterile Neutrinos,” *Nucl.Phys.*, vol. B856, pp. 26–73, 2012.
- [245] M. Parida and S. Patra, “Left-right models with light neutrino mass prediction and dominant neutrinoless double beta decay rate,” *Phys.Lett.*, vol. B718, pp. 1407–1412, 2013.

- [246] R. Lal Awasthi and M. K. Parida, “Inverse Seesaw Mechanism in Nonsymmetric SO(10), Proton Lifetime, Nonunitarity Effects, and a Low-mass Z’ Boson,” *Phys.Rev.*, vol. D86, p. 093004, 2012.
- [247] G. Fogli, E. Lisi, A. Marrone, A. Palazzo, and A. Rotunno, “Evidence of $\theta_{13} > 0$ from global neutrino data analysis,” *Phys.Rev.*, vol. D84, p. 053007, 2011.
- [248] R. N. Mohapatra, “Limits on the Mass of the Right-handed Majorana Neutrino,” *Phys.Rev.*, vol. D34, p. 909, 1986.
- [249] M. Doi and T. Kotani, “Neutrinoless modes of double beta decay,” *Prog.Theor.Phys.*, vol. 89, pp. 139–160, 1993.
- [250] K. Muto, E. Bender, and H. Klapdor, “Effects of Ground State Correlations on 2 Neutrino Beta Beta Decay Rates and Limitations of the Qrpa Approach,” *Z.Phys.*, vol. A334, pp. 177–186, 1989.
- [251] M. Hirsch, K. Muto, T. Oda, and H. Klapdor-Kleingrothaus, “Nuclear structure calculations of $\beta^+\beta^+$, β^+/EC and EC/EC decay matrix elements,” *Z.Phys.*, vol. A347, pp. 151–160, 1994.
- [252] J. Gomez-Cadenas, J. Martin-Albo, M. Mezzetto, F. Monrabal, and M. Sorel, “The Search for neutrinoless double beta decay,” *Riv.Nuovo Cim.*, vol. 35, pp. 29–98, 2012.
- [253] J. Lopez-Pavon, S. Pascoli, and C.-f. Wong, “Can heavy neutrinos dominate neutrinoless double beta decay?,” *Phys.Rev.*, vol. D87, no. 9, p. 093007, 2013.
- [254] M. Doi, T. Kotani, and E. Takasugi, “Double beta Decay and Majorana Neutrino,” *Prog.Theor.Phys.Suppl.*, vol. 83, p. 1, 1985.
- [255] F. Simkovic, G. Pantis, J. Vergados, and A. Faessler, “Additional nucleon current contributions to neutrinoless double beta decay,” *Phys.Rev.*, vol. C60, p. 055502, 1999.
- [256] A. Faessler, A. Meroni, S. Petcov, F. Simkovic, and J. Vergados, “Uncovering Multiple CP-Nonconserving Mechanisms of $\beta\beta$ -Decay,” *Phys.Rev.*, vol. D83, p. 113003, 2011.
- [257] G. Pantis, F. Simkovic, J. Vergados, and A. Faessler, “Neutrinoless double beta decay within QRPA with proton - neutron pairing,” *Phys.Rev.*, vol. C53, pp. 695–707, 1996.

- [258] K. Muto, E. Bender, and H. Klapdor, “Nuclear Structure Effects on the Neutrinoless Double Beta Decay,” *Z.Phys.*, vol. A334, pp. 187–194, 1989.
- [259] J. Suhonen and O. Civitarese, “Weak-interaction and nuclear-structure aspects of nuclear double beta decay,” *Phys.Rept.*, vol. 300, pp. 123–214, 1998.
- [260] J. Kotila and F. Iachello, “Phase space factors for double- β decay,” *Phys.Rev.*, vol. C85, p. 034316, 2012.
- [261] J. Barry and W. Rodejohann, “Lepton number and flavour violation in TeV-scale left-right symmetric theories with large left-right mixing,” *JHEP*, vol. 1309, p. 153, 2013.
- [262] S. Das, F. Deppisch, O. Kittel, and J. Valle, “Heavy Neutrinos and Lepton Flavour Violation in Left-Right Symmetric Models at the LHC,” *Phys.Rev.*, vol. D86, p. 055006, 2012.
- [263] M. Brooks *et al.*, “New limit for the family number nonconserving decay $\mu^+ \rightarrow e^+\gamma$,” *Phys.Rev.Lett.*, vol. 83, pp. 1521–1524, 1999.
- [264] T. G. Rizzo and G. Senjanovic, “Grand Unification and Parity Restoration at Low-energies. 2. Unification Constraints,” *Phys.Rev.*, vol. D25, p. 235, 1982.
- [265] T. G. Rizzo and G. Senjanovic, “Can There Be Low Intermediate Mass Scales in Grand Unified Theories?,” *Phys.Rev.Lett.*, vol. 46, p. 1315, 1981.
- [266] D. Chang, R. Mohapatra, and M. Parida, “New Mechanism for Baryon Generation in SO(10) Models With Low Mass $W(r)$ Boson,” *Phys.Lett.*, vol. B142, p. 55, 1984.
- [267] M. Blanke, A. J. Buras, K. Gemmler, and T. Heidsieck, “ $\Delta_F = 2$ observables and $B \rightarrow X_q \gamma$ decays in the Left-Right Model: Higgs particles striking back,” *JHEP*, vol. 1203, p. 024, 2012.
- [268] F. del Aguila and L. E. Ibanez, “Higgs Bosons in SO(10) and Partial Unification,” *Nucl.Phys.*, vol. B177, p. 60, 1981.
- [269] R. N. Mohapatra and G. Senjanovic, “Higgs Boson Effects in Grand Unified Theories,” *Phys.Rev.*, vol. D27, p. 1601, 1983.
- [270] G. Beall, M. Bander, and A. Soni, “Constraint on the Mass Scale of a Left-Right Symmetric Electroweak Theory from the K(L) K(S) Mass Difference,” *Phys.Rev.Lett.*, vol. 48, p. 848, 1982.

- [271] A. Maiezza, M. Nemevsek, F. Nesti, and G. Senjanovic, “Left-Right Symmetry at LHC,” *Phys.Rev.*, vol. D82, p. 055022, 2010.
- [272] D. Guadagnoli and R. N. Mohapatra, “TeV Scale Left Right Symmetry and Flavor Changing Neutral Higgs Effects,” *Phys.Lett.*, vol. B694, pp. 386–392, 2011.
- [273] S. Bertolini, J. O. Eeg, A. Maiezza, and F. Nesti, “New physics in ϵ' from gluomagnetic contributions and limits on Left-Right symmetry,” *Phys.Rev.*, vol. D86, p. 095013, 2012.
- [274] G. Aad *et al.*, “Search for heavy neutrinos and right-handed W bosons in events with two leptons and jets in pp collisions at $\sqrt{s} = 7$ TeV with the ATLAS detector,” *Eur.Phys.J.*, vol. C72, p. 2056, 2012.
- [275] S. Chatrchyan *et al.*, “Search for heavy neutrinos and W[R] bosons with right-handed couplings in a left-right symmetric model in pp collisions at $\sqrt{s} = 7$ TeV,” *Phys.Rev.Lett.*, vol. 109, p. 261802, 2012.
- [276] J. Beringer *et al.*, “Review of Particle Physics (RPP),” *Phys.Rev.*, vol. D86, p. 010001, 2012.
- [277] F. del Aguila, J. de Blas, and M. Perez-Victoria, “Electroweak Limits on General New Vector Bosons,” *JHEP*, vol. 1009, p. 033, 2010.
- [278] K. Arisaka, L. Auerbach, S. Axelrod, J. Belz, K. Biery, *et al.*, “Improved upper limit on the branching ratio $\text{Br}(K_L^0 \rightarrow \mu^\pm e^\mp)$,” *Phys.Rev.Lett.*, vol. 70, pp. 1049–1052, 1993.
- [279] M. Parida and B. Purkayastha, “New lower bound on $SU(4)_C$ gauge boson mass from CERN LEP measurements and $K_L \rightarrow \mu e$,” *Phys.Rev.*, vol. D53, pp. 1706–1708, 1996.
- [280] N. Deshpande and R. Johnson, “EXPERIMENTAL LIMIT ON $SU(4)_C$ GAUGE BOSON MASS,” *Phys.Rev.*, vol. D27, p. 1193, 1983.
- [281] S. Dimopoulos, S. Raby, and G. L. Kane, “Experimental Predictions from Technicolor Theories,” *Nucl.Phys.*, vol. B182, pp. 77–103, 1981.
- [282] M. Baldo-Ceolin, P. Benetti, T. Bitter, F. Bobisut, E. Calligarich, *et al.*, “A New experimental limit on neutron - anti-neutron oscillations,” *Z.Phys.*, vol. C63, pp. 409–416, 1994.

- [283] R. N. Mohapatra and R. Marshak, “Local $B - L$ Symmetry of Electroweak Interactions, Majorana Neutrinos and Neutron Oscillations,” *Phys.Rev.Lett.*, vol. 44, pp. 1316–1319, 1980.
- [284] R. Mohapatra, “Neutron-Anti-Neutron Oscillation: Theory and Phenomenology,” *J.Phys.*, vol. G36, p. 104006, 2009.
- [285] K. Babu, J. C. Pati, and P. Rastogi, “Lepton flavor violation within a realistic $SO(10)/G_{(224)}$ framework,” *Phys.Lett.*, vol. B621, pp. 160–170, 2005.
- [286] B. Bajc, A. Melfo, G. Senjanovic, and F. Vissani, “Yukawa sector in non-supersymmetric renormalizable $SO(10)$,” *Phys.Rev.*, vol. D73, p. 055001, 2006.
- [287] H. Goh, R. Mohapatra, and S.-P. Ng, “Minimal SUSY $SO(10)$ model and predictions for neutrino mixings and leptonic CP violation,” *Phys.Rev.*, vol. D68, p. 115008, 2003.
- [288] T. Fukuyama and T. Kikuchi, “Renormalization group equation of quark lepton mass matrices in the $SO(10)$ model with two Higgs scalars,” *Mod.Phys.Lett.*, vol. A18, p. 719, 2003.
- [289] M. Parida and A. Usmani, “Quark-lepton Yukawa unification at lower mass scales,” *Phys.Rev.*, vol. D54, pp. 3663–3666, 1996.
- [290] N. Deshpande and E. Keith, “Predictive fermion mass matrix ansatzes in non-supersymmetric $SO(10)$ grand unification,” *Phys.Rev.*, vol. D50, pp. 3513–3528, 1994.
- [291] S. Barr, “A Different seesaw formula for neutrino masses,” *Phys.Rev.Lett.*, vol. 92, p. 101601, 2004.
- [292] S. Barr and B. Kyae, “A General analysis of corrections to the standard see-saw formula in grand unified models,” *Phys.Rev.*, vol. D70, p. 075005, 2004.
- [293] M. Parida, “Matter - antimatter oscillations in grand unified theories with high unification masses,” *Phys.Rev.*, vol. D27, p. 2783, 1983.
- [294] M. Parida, “Natural mass scales for observable matter - antimatter oscillations in $SO(10)$,” *Phys.Lett.*, vol. B126, p. 220, 1983.
- [295] R. L. Awasthi, M. Parida, and S. Patra, “Neutrino masses, dominant neutrinoless double beta decay, and observable lepton flavor violation in left-right

models and SO(10) grand unification with low mass W_R, Z_R bosons,” *JHEP*, vol. 1308, p. 122, 2013.

- [296] T. Han, P. Langacker, Z. Liu, and L.-T. Wang, “Diagnosis of a New Neutral Gauge Boson at the LHC and ILC for Snowmass 2013,” 2013.
- [297] D. Ambrose *et al.*, “New limit on muon and electron lepton number violation from $K_L \rightarrow \mu^\pm e^\mp$ decay,” *Phys.Rev.Lett.*, vol. 81, pp. 5734–5737, 1998.
- [298] H. Klapdor-Kleingrothaus, I. Krivosheina, and I. Titkova, “Theoretical investigation of pulse shapes of double beta events in a Ge-76 detector, their dependence on particle physics parameters, and their separability from background gamma events,” *Mod.Phys.Lett.*, vol. A21, pp. 1257–1278, 2006.
- [299] M. Auger *et al.*, “Search for Neutrinoless Double-Beta Decay in ^{136}Xe with EXO-200,” *Phys.Rev.Lett.*, vol. 109, p. 032505, 2012.
- [300] A. Gando *et al.*, “Limit on Neutrinoless $\beta\beta$ Decay of Xe-136 from the First Phase of KamLAND-Zen and Comparison with the Positive Claim in Ge-76,” *Phys.Rev.Lett.*, vol. 110, no. 6, p. 062502, 2013.
- [301] M. Agostini *et al.*, “Results on neutrinoless double beta decay of ^{76}Ge from GERDA Phase I,” *Phys.Rev.Lett.*, vol. 111, p. 122503, 2013.
- [302] S. Chatrchyan *et al.*, “Search for narrow resonances and quantum black holes in inclusive and b -tagged dijet mass spectra from pp collisions at $\sqrt{s} = 7$ TeV,” *JHEP*, vol. 1301, p. 013, 2013.
- [303] S. Bertolini, L. Di Luzio, and M. Malinsky, “Light color octet scalars in the minimal SO(10) grand unification,” *Phys.Rev.*, vol. D87, no. 8, p. 085020, 2013.
- [304] S. Weinberg, “Effective Gauge Theories,” *Phys.Lett.*, vol. B91, p. 51, 1980.
- [305] L. J. Hall, “Grand Unification of Effective Gauge Theories,” *Nucl.Phys.*, vol. B178, p. 75, 1981.
- [306] P. Langacker and N. Polonsky, “Uncertainties in coupling constant unification,” *Phys.Rev.*, vol. D47, pp. 4028–4045, 1993.
- [307] R. Mohapatra, “A Theorem on the threshold corrections in grand unified theories,” *Phys.Lett.*, vol. B285, pp. 235–237, 1992.

- [308] M. Rani and M. Parida, “Confronting LEP data, proton lifetime and small neutrino masses by threshold effects in SO(10) with $SU(2)_L \times U(1)_R \times SU(4)_C$ intermediate breaking,” *Phys.Rev.*, vol. D49, pp. 3704–3710, 1994.
- [309] M. Parida, “Heavy Particle Effects in Grand Unified Theories With Fine Structure Constant Matching,” *Phys.Lett.*, vol. B196, pp. 163–169, 1987.
- [310] M. Parida and B. Cajee, “High scale perturbative gauge coupling in R-parity conserving SUSY SO(10) with larger proton lifetime,” *Eur.Phys.J.*, vol. C44, pp. 447–457, 2005.
- [311] K. Babu, P. Bhupal Dev, E. C. Fortes, and R. Mohapatra, “Post-Sphaleron Baryogenesis and an Upper Limit on the Neutron-Antineutron Oscillation Time,” *Phys.Rev.*, vol. D87, no. 11, p. 115019, 2013.
- [312] K. S. Ganezer, “The search for $n - \bar{n}$ oscillations at super-kamiokande i,” 2007. Workshop on $(B - L)$ violation, Lawrence Berkeley Laboratory.
- [313] W. Yao *et al.*, “Review of Particle Physics,” *J.Phys.*, vol. G33, pp. 1–1232, 2006.
- [314] D. Wyler and L. Wolfenstein, “Massless Neutrinos in Left-Right Symmetric Models,” *Nucl.Phys.*, vol. B218, p. 205, 1983.
- [315] P. Ade *et al.*, “Planck 2013 results. XVI. Cosmological parameters,” 2013.
- [316] J. Vergados, “The Neutrinoless double beta decay from a modern perspective,” *Phys.Rept.*, vol. 361, pp. 1–56, 2002.
- [317] V. Khachatryan *et al.*, “Search for heavy neutrinos and W bosons with right-handed couplings in proton-proton collisions at $\sqrt{s} = 8$ TeV,” *Eur.Phys.J.*, vol. C74, no. 11, p. 3149, 2014.
- [318] F. F. Deppisch, T. E. Gonzalo, S. Patra, N. Sahu, and U. Sarkar, “Signal of Right-Handed Charged Gauge Bosons at the LHC?,” *Phys.Rev.*, vol. D90, no. 5, p. 053014, 2014.
- [319] E. C. F. S. Fortes, K. Babu, and R. Mohapatra, “Flavor Physics Constraints on TeV Scale Color Sextet Scalars,” 2013.
- [320] K. Babu and R. Mohapatra, “Coupling Unification, GUT-Scale Baryogenesis and Neutron-Antineutron Oscillation in SO(10),” *Phys.Lett.*, vol. B715, pp. 328–334, 2012.

- [321] K. Babu and R. Mohapatra, “B-L Violating Nucleon Decay and GUT Scale Baryogenesis in SO(10),” *Phys.Rev.*, vol. D86, p. 035018, 2012.
- [322] K. Babu and R. Mohapatra, “B-L Violating Proton Decay Modes and New Baryogenesis Scenario in SO(10),” *Phys.Rev.Lett.*, vol. 109, p. 091803, 2012.
- [323] H. Georgi and S. L. Glashow, “Gauge theories without anomalies,” *Phys.Rev.*, vol. D6, p. 429, 1972.
- [324] J. Banks and H. Georgi, “Comment on Gauge Theories Without Anomalies,” *Phys.Rev.*, vol. D14, pp. 1159–1160, 1976.
- [325] S. Okubo, “Gauge Groups Without Triangular Anomaly,” *Phys.Rev.*, vol. D16, p. 3528, 1977.
- [326] F. Wilczek and A. Zee, “Families from Spinors,” *Phys.Rev.*, vol. D25, p. 553, 1982.
- [327] R. M. Syed, “Couplings in SO(10) grand unification,” 2005.